Charles University in Prague
First Faculty of Medicine

Study programme: Biomedicine
Study field: Biochemistry a patobiochemistry

Mgr. Ladislav Kuchař

Tandemová hmotnostní spektrometrie sfingolipidů s aplikací pro metabolické studie a diagnostiku sfingolipidos

Tandem mass spectrometry of sphingolipids with application for metabolic studies and diagnosis of sphingolipidoses

Ph.D. Thesis

Supervisor: RNDr. Jana Ledvinová, CSc.
Consultant: RNDr. Befekadu Asfaw, CSc.

Prague, 2013

Prohlášení:

Prohlašuji, že jsem závěrečnou práci zpracoval samostatně a že jsem řádně uvedl a citoval všechny použité prameny a literaturu. Současně prohlašuji, že práce nebyla využita k získání jiného nebo stejného titulu

Souhlasím s trvalým uložením elektronické verze mé práce v databázi systému meziuniverzitního projektu Theses.cz za účelem soustavné kontroly podobnosti kvalifikačních prací.

V Praze, 9.10.2013

Ladislav Kuchař

Podpis

Identifikační záznam:

KUCHAŘ, Ladislav. *Tandemová hmotnostní spektrometrie sfingolipidů s aplikací pro metabolické studie a diagnostiku sfingolipidos. [Tandem mass spectrometry of sphingolipids with application for metabolic studies and diagnosis of sphingolipidoses]*. Praha, 2013. 202 s., 8 příl. Disertační práce (PhD). Univerzita Karlova v Praze, 1. lékařská fakulta, Ústav dědičných metabolických poruch 1. LF UK. Vedoucí závěrečné práce Ledvinová, Jana

Klíčová slova:

tandemová hmotnostní spektrometrie, hmotnostní spektrometrie, sfingolipid, lipidomika, lysosom, lysosomální střádává onemocnění, sfingolipidosy, enzymologie, enzym, immobilizace

Key words:

tandem mass spectrometry, mass spectrometry, sphingolipid, lipidomics, lysosome, lysosomal storage disorders, sphingolipidoses, enymology, enzyme, immobilization

Acknowledgements

RNDr. Jana Ledvinová, Ph.D. my supervisor, for her excellent scientific competence and for her untiring encouragement throughout this work and for her support during the years of my postgraduate studies.

RNDr. Befekadu Asfaw, Ph.D., for his excellent scientific competence, continuous interest in my work and for useful practical advices.

Ing. Helena Poupětová, for her excellent scientific competence, ,continuous interest in my work and for useful practical advices.

All people at the Institute of Inherited Metabolic Disorders for creating a pleasant and stimulating working atmosphere and for interest in my research.

Prof. RNDr. František Tureček, Ph.D. for his excellence in mass spectrometry and advices which pushed forward my interest and knowledge of and knowledge of mass spectometry further

Ass. Prof. RNDr. Zuzana Bílková, Ph.D. for her scientific excellence and cooperation on enzyme immobilization on solid particels which is important part of this thesis

I would like to dedicate this work to Prof. Milan Elleder, M.D., Ph.D., (* 1938 – † 2011) former director of the Institute for Inherited Metabolic Disorders for making this work possible and for his excellent scientific attitudes stimulating my interest in science and beyond

Also, I would like to dedicate this work to my family, especially to my wife, for continuous support, love and understanding during my postgraduate studies.

This work was supported by the grant project GAUK 19509 from the Grant Agency of the Charles University in Prague, research projects MSM 0021620806 and PRVOUK-P24/LF1/3 from the Ministry of Education and Youth of the Czech Republic, Grant IGA MZ NT/14015, NT/12239, NS/10342, RVO-VFN64165 and MZOVFN2005 from the Ministry of Health of the Czech Republic, and by the grant 303/03H065 from the Grant Agency of the Czech Republic, grants SVV266504 and SVV262502 from the Charles University in Prague

Abstrakt

V posledních letech se hmotnostní spektrometrie (MS) stala dominantní technologií používanou při lipidomické analýze a silně ovlivnila výzkum a diagnostiku onemocnění lipidního metabolismu jako např. lysosomální střádavá onemocnění (LSD) charakterisovaná poruchami funkcí lysosomů. Soubor poruch lysosomální degradace sfingolipidů (SFL) přísluší ke skupině sfingolipidos. Tento stav má vážné až fatální klinické důsledky.

Prvotním cílem práce bylo zavedení kvantitativní a kvalitativní analýzy SFL pro výzkum a diagnostiku LSD. Na jejím počátku bylo třeba připravit semisynthesou lipidní hmotnostně značené standardy pomocí imobilizované sfingolipid ceramid N-deacylasy. Zavedené metody kvantitativní analysy byly posléze použity k průkazu zvýšené exkrece močových SFL u LSD s charakteristickým střádáním v ledvinách. Vyhodnocení SFL vylučovaných močí prokázalo svůj význam při diferenciální diagnostice deficitu prosaposinu a saposinu B kdy rutinní enzymologie selhává. MS navíc umožňuje sledování jednotlivých molekulárních druhů SFL (isoforem), jenž vedlo ke zjištění, že u některých LSD se jejich profil v moči mění. To následně vedlo k vývoji nové screeningové metody v suchém vzorku moče založeném na vyhodnocování profilu isoforem. Další aplikací MS byla analýza pitevních vzorků tkání nebo buněk u nevyjasněných případů. Fabryho choroba a prosaposinový deficit byly prokázány také analýzou pitevních vzorků ledvin a myokardu, což potvrdilo praktický význam takového postupu. V myokardu pacienta s Fabryho chorobou bylo také prokázáno zvýšení toxického lyso-SFL. MS vyhodnocení SFL v placentě podpořilo nálezy imunohistochemické analýzy a společně ukázalo na specifickou roli apikálního pólu placentálních endothelií. MS analýza se ukázala užitečná nejen při analýze metabolitů, ale též při měření aktivit lysosomálních enzymů, neboť umožňuje používání přirozených substrátů na rozdíl od fluorimetrických metod. Použitím MS se nám podařilo prokázat nulovou aktivitu β-glukocerebrosidasy v kožních fibroblastech pacienta s Gaucherovou chorobou typu II se závažným "collodion baby" fenotypem. Možnost používat hmotnostně značené substráty při dynamických metabolických experimentech namísto běžně užívaných radioaktivních lipidů byla testována v kulturách kožních fibroblastů pacientů s GM1 gangliosidosou. Bylo prokázáno, že hmotnostně značené substráty jsou vhodnou náhradou radioaktivních analogů, což přispívá k eliminaci rizik při práci s radioaktivními sloučeninami.

V rámci této disertační práce bylo zavedeno široké spektrum metod, které byly otestovány při určování metabolických profilů SFL za normálních a patologických stavů. Naše zjištění potvrdila, že MS lipidomika přináší novou, vyšší úroveň citlivosti analýzy i množství dalších detailních informací. Sledování metabolického osudu jednotlivých molekul může přispět k lepšímu pochopení molekulárních mechanismů onemocnění.

Abstract

In recent years, mass spectrometry (MS) become the dominant technology in lipidomic analysis and widely influenced research and diagnosis of diseases of lipid metabolism, e.g. lysosomal storage disorders (LSD) characterized by impairment of the lysosomal functions. Defects in lysosomal processing of sphingolipids SFL belong to the category of sphingolipidoses. This condition has severe and even fatal clinical outcome.

The primary aim of this work was to establish quantitative and qualitative methods of SFL analysis useful for research and diagnosis of LSD. At first, semisynthesis of mass labeled lipid standards utilizing immobilized sphingolipid ceramide N-deacylase was performed. Established methods of quantitative analysis were then used to prove the increased excretion of urinary SFL in LSD with characteristic storage in the kidney. Determination of excreted urinary SFL was found useful for differential diagnosis of prosaposin and saposin B deficiences for which routine enzymology is failing. MS also enabled monitoring of individual molecular species (isoforms) of SFL, which led to the finding that their urinary pattern is changing in some LSD. This resulted in the development of new screening method in dry urinary samples based on isoform profile evaluation. Another MS application referred to analysis of autoptic tissues or cell samples in unresolved cases. Fabry disease and prosaposin deficiency were proved in the autoptic kidney and myocardium which showed the usefulness of this procedure. In the myocardium of Fabry patient, the increase of toxic compound, lyso-SFL was also demonstrated. MS determination of placental SFL supported immunohistochemical analysis and thus pointed to the specific features of placental endothelial apical pole. In addition to metabolites, MS was found very useful for determination of activities of lysosomal enzymes because of use of natural substrates in contrast to fluorimetric methods. Using MS, we were able to demonstrate zero β-glucocerebrosidase activity in skin fibroblasts of Gaucher type II patient with severe collodion baby phenotype. The possibility to use the mass labeled substrates in dynamic metabolic experiments instead of conventional radioactive ones was tested in cultured skin fibroblasts from patients with GM1 gangliosidosis. Mass labeled substrates were found suitable substitutes eliminating the working risk with radioactive compounds.

While working on this Ph.D. thesis, the wide range of methods has been introduced and tested to determine metabolomic profiles of SFL under normal and pathological conditions. Our findings have confirmed that lipidomic MS brings a new, high level of sensitivity and more detailed information. Monitoring of metabolic fate of individual molecules can contribute to better understanding of the molecular mechanisms of the disease.

CONTENT

Abreviations

ABC	ATP Binding Cassette
AGAL	α-galactosidase A
API	air pressure ionization
ARSA	Arylsulphatase A
BMP	bis(monoacylglycerol)phosphate
BSA	bovine serum albumine
CDH	ceramidedihexoside
Cer	ceramide
CerS	ceramide synthase
CERT	ceramide transfer protein
CID	collision induced dissociation
CMH	ceramidemonohexoside
Da	dalton
DBS	dry blood spot
DEAE	diethylaminoethanol
DESI	desorption electrospray ionization
diGalCer	digalactosylceramide
EE	early endosome
ER	endopasmatic reiculum
ESI	electrospray ionization
eV	electron volt
FAPP2	four-phosphate adaptor protein 2
FIA	flow injection analysis
GalGlcCer	lactosylceramide
Gb3Cer	globotriaosylceramide

Gb4Cer	globotetraosylceramide
GlcCer	glucosylceramide
GLTP	glycolipid transfer protein
GM1	ganglioside GM1
GM2	ganglioside GM2
GM3	ganglioside GM3
GSL	glycosphingolipids
ILV	intraluminal vesicle
IPN	isoform profile number
IST	internal standard
LacCer	lactosylceramide
LE	late endosome
LSD	lysosomal storage disorders
MALDI	matrix assisted laser desorption ionization
MLD	metachromatic leukodystrophy
MMB	magnetic macroporous bead
MS	mass spectrometry
MS/MS	tandem mass spectrometry
MSI	mass spectrometry imaging
PAPS	3‘-phosphoadenosin 5‘-phosphosulfate
pSap	prosaposin (precursor of saposins)
pSap-d/ Psap-d	prosaposin deficiency
RF	radiofrequency
Sap	saposin (A-D)
SapB-d	saposin B deficiency
SCDase	sphingolipid ceramide N-deacylase

SFL	sphingolipids
SIMS	secondary ion mass spectrometry
SPG	sialylparagloboside
UDP	uridine diphosphate
V-ATPase	Vacuolar-type H^+-ATPase

1. Introduction

A. Sphingolipid biochemistry and pathobiochemistry

1.1 Brief history of sphingolipids

Term sphingolipid (SFL) is derived from amino alcohol backbone sphingosine. Name of mysterious Egyptian Sphinx reflected enigmatic physical and chemical behaviour of sphingosine.

Early history of SFL is connected with J. L. W. Thudichum and his famous book A Treatise on the chemical constitution of the brain (Bailliere, Tindall and Cox, London,1884) (Yamakawa T., 1996). Thudichum analyzed chemical composition of brain tissue and described Leibrich's "Protagon" as a mixture of lecithins, cephalins and myelins. He also identified sphingomyelins, sulfatides and cerebrosides in the brain and wrote: "they are of fundamental importance and all further developments in chemical neurology must start from them as a basis" and "When the normal composition of brain shall be known to the uttermost item, then pathology can begin its search for abnormal compounds or derangements of quantities" (Cyberlipid, 2013). Correct structure of sphingosine was later proposed by H.E. Carter in 1947 (Carter H. E. et al., 1947).

The other milestones in the history of SFL fall into the 1930s until the 1970s: isolation and characterization of sulfatides, sphingomyelin, neuraminic acid (later named sialic acid), structure and nomenclature of gangliosides, description of glycolipids responsible for ABO antigenic activity, etc (Kuhn R. and Wiegandt H., 1963; Yamakawa T. et al., 1962; Yamakawa T., 1996). History of sphingolipid research continues as a part of lipidomics untill these days (www.lipidmaps.org).

From the historical background, the important role of sphingolipid research is clearly visible in many biochemical and also medical fields. History also confirmed that new approaches in analysis together with understanding of basic principles of sphingolipid biochemistry and pathobiochemistry can help to find new analytical strategies and practical applications in clinical medicine and research. These aspects represent the major topics of the next chapters of my PhD thesis.

1.2 Nomenclature of sphingolipids

Nomenclature of SFL and glycosphingolipids (GSL) is based on IUPAC and IUMB rules (Chester M. A., 1998). Nevertheless, for some SFL historical (trivial) terminology is still used.

1.2.1 Sphingoid bases and ceramides

Sphingoid bases or sphingoids are long-chain aliphatic aminoalcohols. Basic chemical structure is represented by "dihydrosphingosine" which is [(2S,3R)-2-aminooctadecane-1,3-diol] and is referred as sphinganine or sphingosine, [(2S,3R)-2-aminooctadec-4-ene-1,3-diol], sphing-4-enine both with carbon chain length of 18.

Homologes with different chain length are named using root chemical name of the parent carbohydrate e.g. 20 carbon length homologue name is icosasphinganine (Chester M. A., 1998).

There is also used "short" abbreviation for sphingoids consisting from one letter and two numbers. For example, abbreviation d18:1 refers to the most abundant sphingoid - sphingosine. Letter d (like di-) refers to two hydroxyl groups and numbers represent chain-length of 18 carbons with 1 double bond (Chester M. A., 1998).

1.2.2 Trivial Names

Trivial names are used in some cases such as cerebrosides for brain β-galactosylceramides. Other trivial names consist of oligosaccharide name in combination with ceramide e.g. (LacCer) for GalGlcCer. Historically persisting nomenclature of gangliosides is simplified system invented by Svennerholm (Svennerholm L., 1963) which is widely accepted. Names consists of letter G for gangliosides followed by number of sialic acid residues, M for mono- D for di- and so on. The last number in the name identifies position of ganglioside from the start to the front of chromatogram. Sphingomyelin (N-acyl-sphing-4-enine-1-phosphocholine) is trivial name of phosphosphingolipid with phosphocholine group bound to the primary hydroxy group of sphingoid in the ceramide (Chester M. A., 1998).

1.2.3 Semisystematic names

They are used for GSL with larger oligosaccharide chains. The names are composed of: (root name)(root size)osylceramide e.g. globotetraosylceramide for GalNAcGalGalGlcCer. Root structures and their symbols are shown in Tab. 1.

Tab. 1 Root names and structures (Chester M. A., 1998)

Root	Symbol	Root structure
		IV III II I
ganglio	Gg	Galβ3GalNAcβ4Galβ4Glc-
lacto [1]	Lc	Galβ3GlcNAcβ3Galβ4Glc-
neolacto [2]	nLc	Galβ4GlcNAcβ3Galβ4Glc-
globo	Gb	GalNAcβ3Galα4Galβ4Glc-
isoglobo [2]	iGb	GalNAcβ3Galα3Galβ4Glc-
mollu	Mu	GlcNAcβ2Manα3Manβ4Glc-
arthro	At	GalNAcβ4GlcNAcβ3Manβ4Glc-

[1] Lacto as used here should not be confused with lactose.

[2] Note: The prefix "iso" is used here to denote a (1→3) vs (1→4) difference in the linkage position between the monosaccharide residues III and II, while the term "neo" denotes such a difference [(1→4) vs (1→3)] between residues IV and III. This scheme should be used also in other cases where such positional isomers occur, and only in such cases.

1.2.4 Systematic names

The oligosaccharide structure is described in detail by systematic names. The systematic names of GSL use the specific symbols for position of glycosidic bonds and anomeric configurations are represented by brackets between bonded monosaccharides. There are also short forms omitting the number of the anomeric carbon but retain possition of glycosidic bond. Example is shown in the Fig. 1.

α-D-Galp-(1→3)-α-D-Galp- (extended form)
or
Gal(α1−3)Gal(α- (condensed form)
or
Galα3Galα- or Galα-3Galα- (short form).

Fig. 1 Systematic names forms (Chester M. A., 1998)

Roman number is used for gangliosides and sulfatides to describe in their names the saccharide with attached sialic acid or sulfate group. Upper index number represents the carbon to which the groups are bonded (Fig. 2).

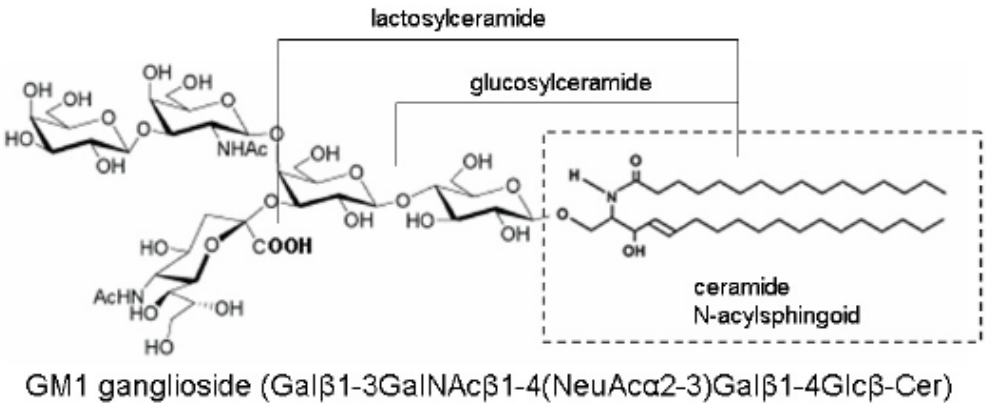

Fig. 2 Structure of GM1 ganglioside and systematic name
IV^3-A-N-glycoloylneuraminosyl-II^3-A-N-acetylneuraminosylgangliotetraosylceramide
IV^3-A-Neu5Gc,II^3-A-Neu5Ac-Gg_4Cer.

1.2.5 Specific nomenclature of the ceramide part of sphingolipids used in mass spectrometry

For some purposes, description of the ceramide part of sphingolipid or ceramide itself is based on short abreviated form of both sphingoid and fatty acid. For example ceramide consisted from sphingosine a palmitic acid can be abbreviated as Cer(d18:1,16:0), similarly sphingolipid with tetrasaccharide oligosaccharide and ceramide with 20 carbons chain length sphingoid and nervoic acid is referred as Gb4Cer(d20:0,24:1). This system of SFL nomenclature is commonly used e.g. in mass spectrometry because it determines the molecular weight of the molecule and also specifies the fragments acquired during the tandem mass spectrometric (MS/MS) analysis (Ii T. et al., 1995)

1.3 Chemical and biological functions and properties of sphingolipids

Hydrophobic ceramide represents the core structure of each sphingolipid. It is responsible for their participation on the generation of micellar and later membranous structures (Goni F. M. and Alonso A., 2006; Masserini M. and Ravasi D., 2001; Ulrich-

Bott B. and Wiegandt H., 1984; Westerlund B. and Slotte J. P., 2009). Ceramides itself are immiscible with water especially those with longer fatty acids in molecule (Goni F. M. and Alonso A., 2006). Fatty acids bound in ceramide are responsible for the shape of the ceramide molecule which secondarily influences their properties and functions. Hydrophilic structures of the ceramide can create H-bonds with nitrogen of the amide bond which is leading to lancet shape of the whole sphingolipid molecule (Goni F. M. and Alonso A., 2006; Grosch S. et al., 2012; Masserini M. and Ravasi D., 2001; Westerlund B. and Slotte J. P., 2009).

Sphingolipids play many different biological roles like participation on building of biological membranes (Goni F. M. and Alonso A., 2006). Hydrophilic parts of the lipids protruding outside of the membrane were later associated with SFL roles in adhesion, recognition, differentiation and antigenic function (Hakomori S. I., 2008; Lahiri S. and Futerman A. H., 2007; Schnaar R. L. et al., 2009). Changes in GSL oligosaccharide were found to participate in the oncogenic differentiation (Hakomori S., 1981; Hakomori S., 1998). Interconversion of SFL can modulate the membrane properties e.g. ceramides can cluster into the microdomains with different properties. Membrane modulation can also lead to permeabilization of membrane and induction of apoptosis (Goni F. M. and Alonso A., 2006; Grosch S. et al., 2012; Masserini M. and Ravasi D., 2001; Westerlund B. and Slotte J. P., 2009). Nowadays, the role of SFL as signal molecules is well known and theory of "sphingolipid rheostat" has been postulated (Lahiri S. and Futerman A. H., 2007; Maceyka M. et al., 2009; Maceyka M. et al., 2012; Stevenson C. E. et al., 2011; Takabe K. et al., 2008). Sphingolipids are also connected with immune response e.g. they play their role behind autoimmune reactions in sclerosis multiplex (Godfrey D. I. and Rossjohn J., 2011; Kanter J. L. et al., 2006; Kolter T. et al., 2005).

1.4 Biosynthesis of sphingolipids

1.4.1 Biosynthesis of ceramides

De novo biosythesis of ceramides takes place in the lumen of endoplasmatic reticulum (ER) and begins with condensation of L-serine and palmitoyl-CoA catalyzed by serine palmitoyl-CoA transferase. Condensation reaction produces 3-ketosphinganine which is

then enzymaticaly reduced by 3-ketosphinganine reductase and NADP cofactor to sphinganine. Sphinganine is coupled with Acyl-CoA via amide bond by action of ceramidesynthase (CerS) to produce dihydroceramide. which is then processed by dihydroceramidedesaturase on ceramide (Futerman A. H., 2006; Lahiri S. and Futerman A. H., 2007; Levy M. and Futerman A. H., 2010; Neumann S. and van Meer G., 2008; Wennekes T. et al., 2009). In contrast, the recycling pathway of degraded complex SFL produces sphing-4-enine which condensates with Acyl-CoA to directly form ceramide (Kitatani K. et al., 2008).

1.4.1.1 Ceramide synthases and isoforms of sphingolipids

Ceramide synthases are important group of enzymes responsible for coupling sphingoid bases with fatty acyl-CoA. Nowadays, six different CerS are known (Tab. 2). They are exposing different specificity toward fatty acyl-CoA and almost the same specificity toward sphingoid bases. Ceramid synthases are thus responsible for biosynthesis of different molecular species of ceramides (isoforms) (Laviad E. L. et al., 2008; Levy M. and Futerman A. H., 2010). Their specificity and tissue expression is summarized in Tab. 2.

Tab. 2 Human ceramid synthases (Levy M. and Futerman A. H., 2010)

Name	Chromosomal location	Gene size (base pairs)	Protein size (Da)	Tissue mRNA expression profile[a]	Acyl chain-length specificity
CerS1	19p12	25,837	39,536	Brain, skeletal muscle, testis <4 molecules per nanogram of total RNA	C18
CerS2	1q21.2	9,792	44,876	Kidney, liver 30–40 molecules RNA per nanogram of total RNA	C20–C26
CerS3	15q26.3	144,326	46,217	Testis, skin <20 molecules per nanogram of total RNA	C22–C26
CerS4	19p13.2	53,046	46,399	Low expression levels in all tissues, more in skin, leukocytes, heart, liver <8 molecules per nanogram of total RNA	C18–C20
CerS5	12q13.3	37,565	45,752	Low expression levels in all tissues <2 molecules per nanogram of total RNA	C16
CerS6	2q24.3	318,394	44,890	Low expression levels in all tissues <3 molecules per nanogram of total RNA	C14 and C16

1.4.2 Compartmentalization of biosynthesis of glycosphingolipids

1.4.2.1 Transport proteins

Specific proteins are required for SFL transportation between compartments and inner and outer layers of membrane bilayer (van Meer G., 2011). The system includes:

- transport proteins - FAPP2, CERT, GLTP, ABC family proteins
- flipases responsible for lipid flipping between inner and outer layers of membrane bilayer e.g. ABC family proteins

1.4.2.2 Endoplasmatic reticulum - galactosylceramide and sulfatide

Galactosylceramide is synthesized in lumen of ER after spontaneous ceramide flipping across the ER membrane (van Meer G., 2011; Wennekes T. et al., 2009). Galactose is transferred from UDP-Gal to ceramide by ceramide galactosyltransferase. Produced galactosyl ceramide is precursor for biosythesis of galactosylceramide-3-sulfate (sulfatide) by action of PAPS galactosylceramide: sulpho transferase. 3‘-phosphoadenosin 5‘-phosphosulfate (PAPS) is donor of sulfate group for biosynthesis (Wennekes T. et al., 2009).

1.4.2.3 Golgi aparatus - glucosylceramide, lactosylceramide and complex neutral glycosphingolipids

Ceramide is transported to cis-golgi by vesicular transport where glucosylceramide is synthesized on cytosolic side from UDP-Glc and ceramide by glucosylceramidesynthase. Synthesized glucosylceramide is then transported to the site of lactosylceramide biosynthesis by FAPP2 protein (D'Angelo G. et al., 2007; D'Angelo G. et al., 2012; Levine T. P., 2007; Wennekes T. et al., 2009). Translocation of glucosylceramide to golgi lumen is possibly provided also by FAPP2 protein (Wennekes T. et al., 2009). Lactosylceramide is then synthesized from UDP-Gal and glucosylceramide by galactosyl transferase I enzyme. Lactosylceramide is a precursor of various GSL series (Tab. 1) e.g. gangliosides from ganglioserie (Wennekes T. et al., 2009).

1.4.2.4 Gangliosides

Biosynthesis of gangliosides is maintained by enzymes either with high or low substrate specificity (Fig. 3). Enzymes with high substrate specificity synthesize starting substrates of different gangliosides branches called 0, a, b and c. Enzymes with small substrate specificity synthesize more complex gangliosides of each branch. They possibly create multienzyme complexes which contribute to regulation of gangliosides biosynthesis and also explain synthesis of GM1a ganglioside from GM3 ganglioside with only trace amount of GM2 ganglioside produced in mammals (Sandhoff K. and Kolter T., 2003).

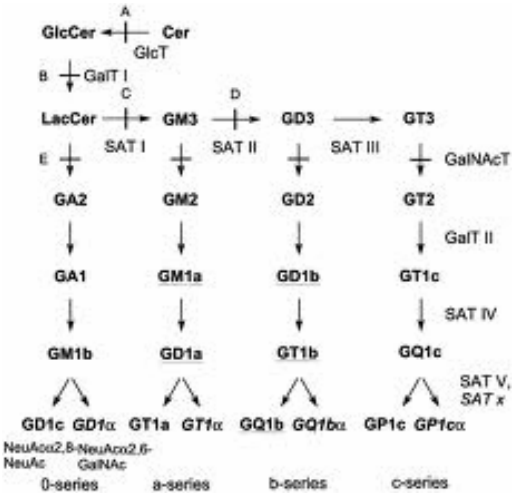

Fig. 3 Biosynthesis of complex gangliosides (Sandhoff K. and Kolter T., 2003)

1.4.2.5 Sphingomyelin

Ceramide is transported by CERT protein and by vesicular transport to trans-golgi network (Futerman A. H., 2006; Wennekes T. et al., 2009). Ceramide is there reoriented to golgi lumen by fliping. Sphingomyelin is then synthesized by sphingomyelin synthetase 1 which transfer phosphocholine from phosphatidylcholine to ceramide (Wennekes T. et al., 2009).

1.5 Degradation of sphingolipids

Catabolism of SFL takes place in the endosomal/lysosomal compartment of the cell. Lysosomes are called "stomach of the cell" where SFL are degraded to their building blocks (Huotari J. and Helenius A., 2011; Kolter T. and Sandhoff K., 2010; Kolter T., 2011) (Fig. 4).

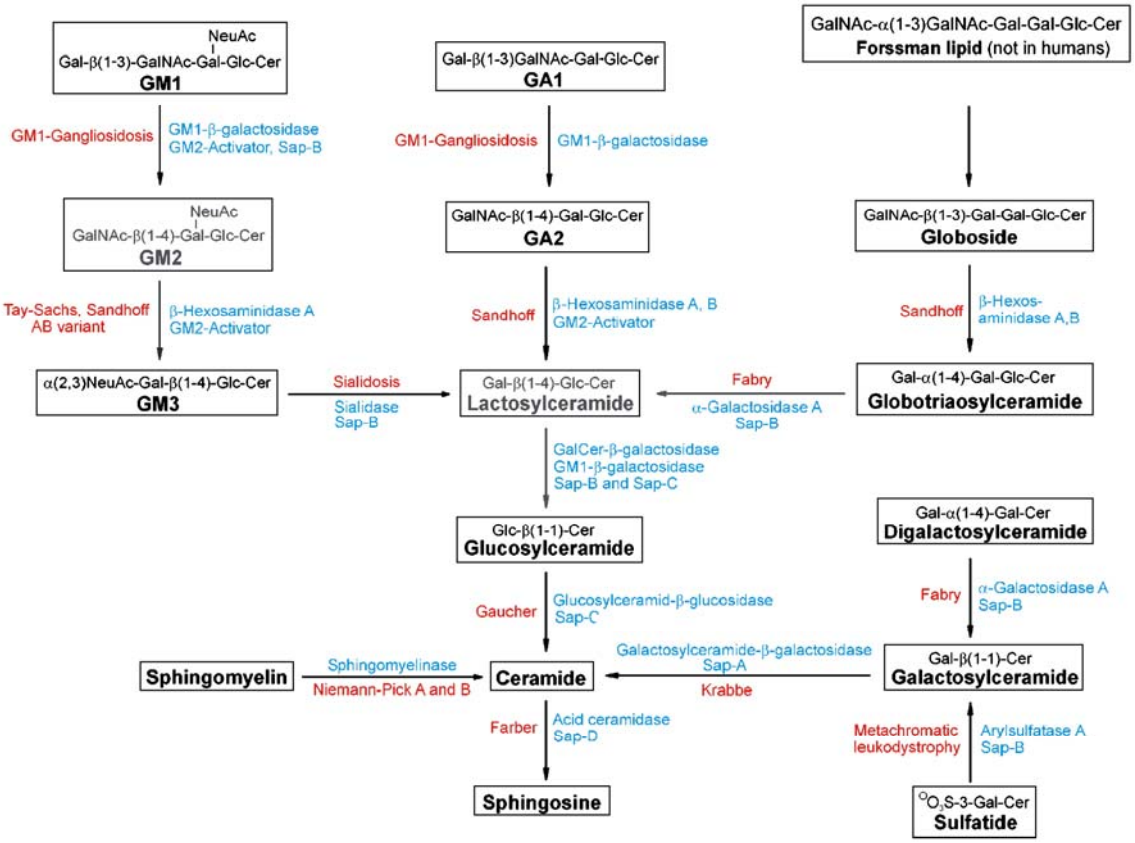

Fig. 4 Degradation pathways of selected sphingolipids and defects of individual catabolic steps. Sphingolipid hydrolases, their activators (Saps) and corresponding disorders are marked (Schulze H. et al., 2009)

Lysosomes are thus responsible for recycling of lipids which is important for cell homeostasis (Huotari J. and Helenius A., 2011; Kolter T. and Sandhoff K., 2010).

1.5.1 Endosomes

Endosomes are generated during endocytosis by regulated budding of the cytoplasmatic membrane. Clathrin and caveolin are most common proteins involved in the process.

Endosomes have characteristic evolutionary stages when they begin as early endosomes (EE) after membrane budding and terminate as late endosome (LE) before fusion with lysosome. Transformation of EE to LE has some characteristic events Fig. 5 (Huotari J. and Helenius A., 2011).

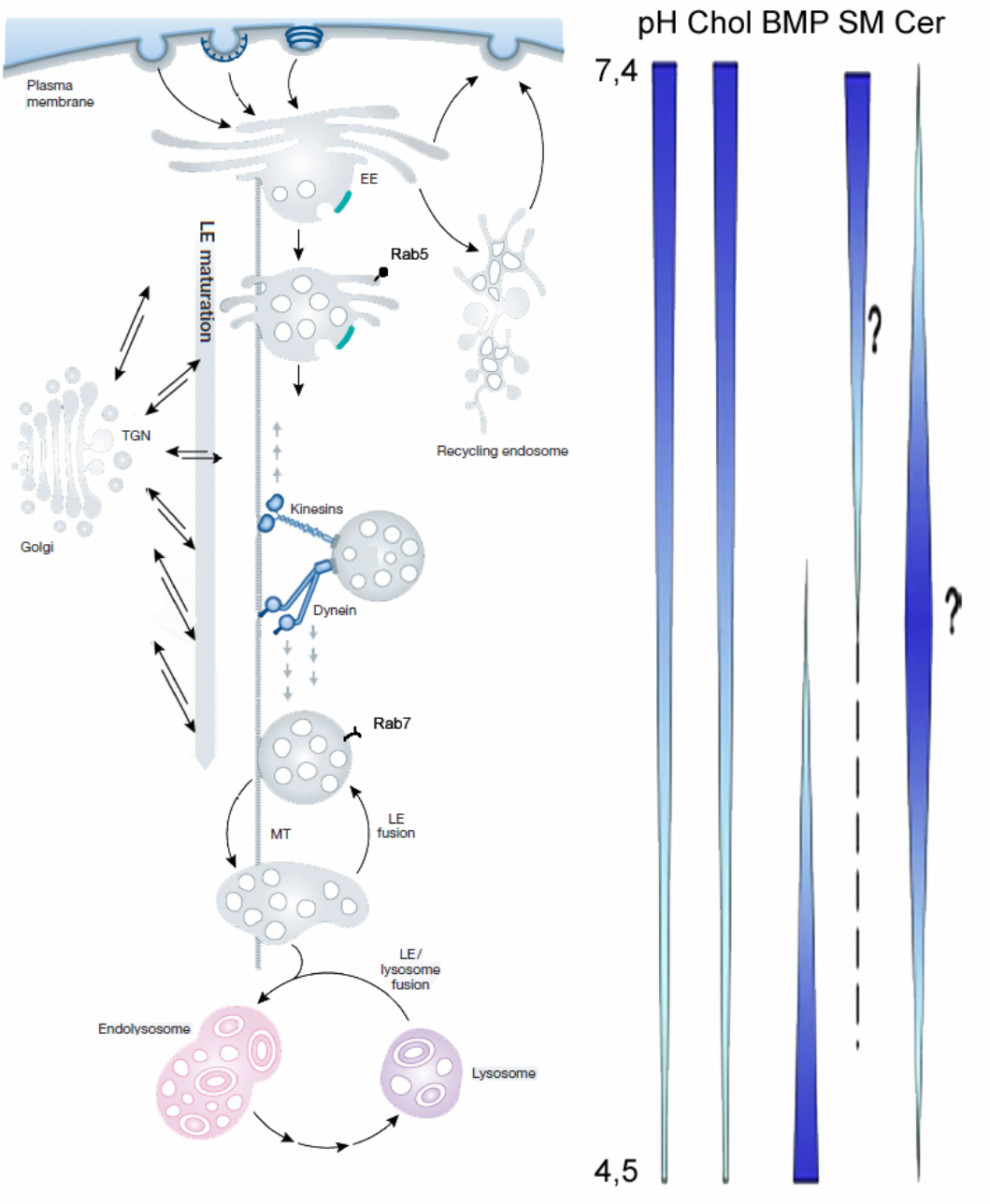

Fig. 5 The endosome/lysosome system. (Huotari J. and Helenius A., 2011; Kolter T. and Sandhoff K., 2010)

EE - Early Endosome, LE - Late Endosome, MT - Microtubules, TGN - trans-Golgi Network, Chol - cholesterol, Cer - Ceramide, BMP - bis(monoacylglacerol)phosphate, SM - sphingomyelin

1.5.2 Lysosomes

Macromolecules selected and sorted in endosomes are finally degraded in lysosomes. Lysosomal catabolism process is maintained by variety of acidic hydrolases in low internal pH of lysosomes generated by specific V-ATPase. Thick glycocalyx layer composed of N-glycosylated glycoproteins rich on repeated lactosamine residues on the intralysosomal membrane keeps lysosomal integrity and protects it from degradation by their own hydrolases (Huotari J. and Helenius A., 2011; Kolter T. and Sandhoff K., 2010).

Lysosomal degradation of SFL takes place on intralysosomal membraneous vesicles originating from intraluminal vesicle (ILV) of endosomes. These vesicles have specific composition to generate negative charge on their surface required for docking of positively charged acidic hydrolases. Negative charge is generated by high concentration of bis(monoacylglycerol)phosphate (BMP) and partially by phosphatidylinositol-3,5-bisphosphate (Kolter T. and Sandhoff K., 2010).

Intralysosomal degradation of macromolecules (e.g. SFL) to primary building blocks is followed by their transport out of the lysosomes and reutilization in the cell (Kolter T. and Sandhoff K., 2010).

1.5.3 Catabolism of sphingolipids with short oligosaccharide chain

Glycosphingolipids are degraded by sequential cleavage of sacharides from nonreducing oligosaccharide end by specific acid hydrolases (Fig.4). Glycosphingolipids with short oligosaccharide chains having four or less saccharide units require the protein activator (Saposins, GM2-activator) for their mobilization from the membrane and degradation (Kolter T. and Sandhoff K., 2010; Kolter T., 2011; Sandhoff K. et al., 2001).

1.5.3.1 Sphingolipid activator proteins

Sphingolipid activator proteins, saposins (Saps) are protein cofactors of lysosomal acid hydrolases facilitating solubilization of hydrophobic lipid substrates and acting as enzyme activators. (Kolter T. and Sandhoff K., 2010; Kolter T., 2011; Sandhoff K. et al., 2001).

Prosaposin (pSap) is 70kDa glycoprotein precursor of 4 saposins – Sap-A, Sap-B, Sap-C and Sap-D which are formed in lysosomes. Prosaposin gene is located on 10q22.1. (Kolter T. and Sandhoff K., 2010; Kolter T., 2011; Sandhoff K. et al., 2001).

Sap-B was the first described member of the Sap family formerly named "sulfatide activator protein" required for degradation of the sulfatides. Later on, Sap-B was found to act also in degradation of Gb3Cer and diGalCer. It has the shape of hair pin with open and closed-conformations. The open conformation is supposed to interact directly with the membrane, to promote a reorganization of the lipid alkyl chains, and to extract the lipid ligand, which is accompanied by a change to the closed conformation. The substrate is then mobilized and exposed to the enzyme in a water-soluble activator-lipid complex. (Kolter T. and Sandhoff K., 2010; Kolter T., 2011; Sandhoff K. et al., 2001).

1.6 Lysosomal storage disorders

Defects in genes of lysosomal acid hydrolases, protein activators and some other lysosomal proteins (e.g. NPC1 and NPC2 proteins) lead to disorders know as lysosomal storage disorders (LSD). Nowadays about 50 of these severe diseases are known. They are characterized by deficient lysosomal processing of substrates which leads to their intralysosomal accumulation. Impairments of related pathways are also known e.g impaired calcium homeostatsis, oxidative stress, autophagy, inflamamation, altered lipid trafficking (Vitner E. B. et al., 2010). Defects in lysosomal processing of SFL belong to the category of sphingolipidoses (Kolter T. and Sandhoff K., 2010; Kolter T., 2011). This study is focused on the following disorders:

1.6.1 Prosaposin deficiency (OMIM 611721) (Sandhoff K. et al., 2001)

http://omim.org/entry/611721

Genetics: mutation in prosaposin gene located on 10q22.1

Biochemistry: deficient activity of acid hydrolases requiring saposins for their function which leads to accumulation of sphigolipids with short oligosaccharide chain

Inheritance: autosomal recessive.

Clinical phenotype: severe neurovisceral disease (e.g. white matter abnormalities, hepatosplenomegaly) with early death.

Diagnosis: prosaposin gene analysis, multiple SFL increased in urine, in skin fibroblasts, in tissues (autopsy samples). Dynamic metabolic experiments in fibroblast cultures (loading tests) give evidence of blocks in degradative pathways of SFL.

1.6.2 Sap-B deficiency (OMIM 249900) (Sandhoff K. et al., 2001)

http://omim.org/entry/249900

Genetics: mutation in Sap-B region of prosaposin gene which affects the function of the Sap-B only.

Biochemistry: deficient activity of α-Galactosidase A and Arylsulfatase A, impairment in degradation of Gb3Cer, diGalCer and sulfatides.

Inheritance: autosomal recessive.

Clinical phenotype: similar to juvenile metachromatic leukodystrophy (MLD) with some exceptions. Life expectancy depends on the onset of the disorder and is similar to MLD.

Diagnosis: prosaposin gene analysis, several SFL increased in urine and fibroblasts. Dynamic metabolic experiments in fibroblast cultures (loading tests) give evidence of blocks in degradative pathways of SFL.

1.6.3 Metachromatic leukodystrophy (OMIM 607574) (von Figura K. et al., 2001)

http://omim.org/entry/607574

Genetics: mutations in ARSA gene located on 22q13.33

Biochemistry: Deficiency of enzymatic activity of Arylsulfatase A and block in degradation of sulfatides. Pseudodeficiency of Arylsulfatase A with low enzyme activity and without clinical affection is described in 2% of European population

Inheritance: autosomal recessive

Clinical phenotype: severe neuronal disorder which affects central and peripheral nervous system, storage in some visceral organs (especially kidney), three clinical phenotypes

Diagnosis: leukodystrophic image of the central nervous system, reduced nerve conduction velocity in peripheral nervous system; urinary sulfatide analysis, confirmation of deficient enzyme activity and genotyping

1.6.4 Fabry disease (OMIM 300644) (Desnick R. J. et al., 2001)

http://omim.org/entry/300644

Genetics: AGAL gene mutations, localization Xq22.1,

Biochemistry: deficiency of the activity of α-galactosidase A , block of degradation of Gb3Cer, diGalCer and GSL with oligosaccharide determinants of blood group B antigens (Asfaw B. et al., 2002; Ledvinova J. et al., 1997)

Inheritance: X-linked type of inheritance, female are heterozygots and males hemizygots

Clinical phenotype: direct neuronal involvement is missing, later-onset of symptoms (e.g. cardiomyopathy with hyperthrophy of left ventricle, kidney involvement, angiokeratoma, parenthesis)

Diagnosis: enzymology and gene analysis, urinary Gb3Cer analysis

1.6.5 Treatment of lysosomal storage disorders

Treatment of LSD is based on restoration of substrate turnover. This can be achieved by three different approaches.

- Replacement of deficient enzyme (Platt F. M. and Lachmann R. H., 2009; Sakuraba H. et al., 2006)
    - Enzyme replacement therapy – utilizing recombinant enzymes infusions
    - Bone marrow transplantation – replacement of deficient microglia by healthy cells which secretes enzyme to extracellular space
    - Gene therapy – repairing of the defective gene
    - Stem cell therapy – similar to bone marrow transplantation
- Chemical chaperon therapy using subinhibition dose of enzyme inhibitor to stabilize the mutant enzyme protein to allow it pass through quality control

mechanisms and express its residual activity in lysosomes. Chaperones are small molecules which can pass blood brain barrier (Platt F. M. and Lachmann R. H., 2009).

- Substrate reduction therapy is based on inhibition of SFL biosynthesis to decrease turnover of substrates; usually targets biosynthesis of glucosylceramide (Platt F. M. and Lachmann R. H., 2009).

B. Mass spectrometry and tandem mass spectrometry

1.7 Mass spectrometry – Mass spectrometers

Mass spectrometry (MS) is analytical method based on measurement of mass to charge ratio of ions in gaseous state (Cole R. B., 2010; de Hoffman E. and Stroobant V., 2002; Dulcks T. and Juraschek R., 1999). Mass spectrometer consists of three fundamental parts: ionization device, mass analyzer and detector.

1.7.1 Ionization device

Ionization device in mass spectrometer is used to generate gaseous ions of analysed compounds. We can differentiate ionization devices according to some criteria (Cole R. B., 2010; de Hoffman E. and Stroobant V., 2002):

- Pressure at which ionization is achieved - vacuum or atmospheric pressure ionization (abbreviated as API). API devices such as electrospray can be directly coupled to separation techniques like HPLC or capillary electrophoresis.
- Pulse or continuos ionization is another criteria.
- Energy applied to analyte to generate ions differentiates ionization on hard and soft techniques. Hard ionization methods are characterized by high fragmentation of analytes during ionization process whereas soft ionization methods are producing mostly molecular ions.

Some of the ionization techniques are able to perform surface scan and are used for mass spectrometry imaging (MSI) e.g. MALDI, DESI, SIMS (McDonnell L. A. and Heeren R. M., 2007).

1.7.1.1 Electrospray ionization

Electrospray ionization abbreviated as ESI is one of the soft techniques for polar compounds ionization in liquid solvent which is passing through the metal capillary at flow rates up to 1 ml/min (Fig. 6). Ions are generated by application of strong electric field on the capillary tip which sorts ions on the solvent surface and creates excess charge. This leads to generation of the Taylor cone on the capillary tip which is then dispersed into the droplets (Cole R. B., 2010; de Hoffman E. and Stroobant V., 2002; Dulcks T. and Juraschek R., 1999; Kebarle P., 2000).

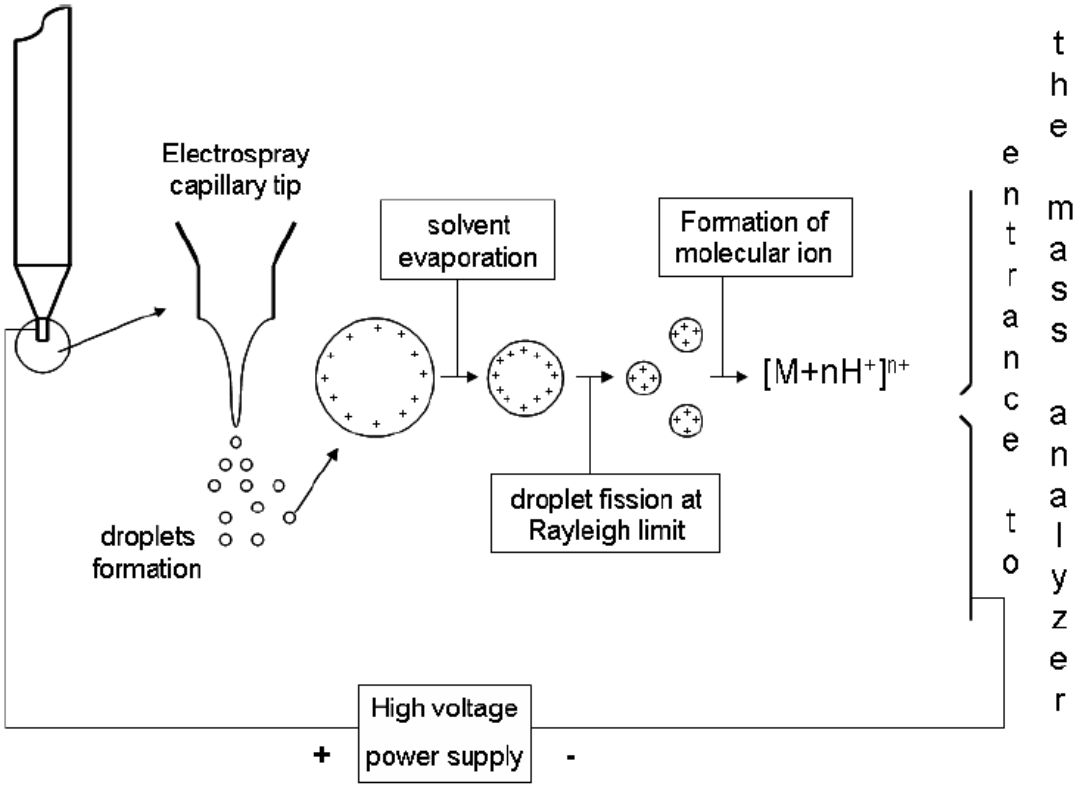

Fig. 6 Scheme of electrospray ionization process

Polarity of generated ions depends on the polarity of applied electric field. Cations are generated in the positive and anions in the negative ion mode (Cole R. B., 2010; de Hoffman E. and Stroobant V., 2002; Kebarle P., 2000).

Solvent of the droplets is evaporated and droplet shrinks in size which leads to accumulation of the surface charge. When the surface charge exceeds the surface tension then the droplet breaks forming secondary smaller droplets. This process is called Raileigh fission which is repeated until the gaseous ions are formed. Two theories of gaseous ions formation during ESI are postulated (Cech N. B. and Enke C. G., 2001; Cole R. B., 2010; Kebarle P., 2000).

- *Ion evaporation model* better matches formation of gaseous ions from small molecules which are formed in the moment when the ions are able leaving the droplet surface by repulsion force.
- *Charged residue model* better suits the formation of gaseous ions from large molecules such as proteins. Droplets undergo repetitive Raileigh fission to the point when droplet contains only one ion of analyte. In this point solvent is completely evaporated and gaseous ion is released.

Liquid surface of the formed droplets is limiting factor for gaseous ions formation and influences the analyte ionization efficiency. In some cases, ionization of analyte may be suppressed by other compounds. This is resulting in the matrix effect of co-eluted and co-ionized compounds on the signal of analyte. The matrix effect is recommended to measure prior to analysis (Cech N. B. and Enke C. G., 2001; Cole R. B., 2010; de Hoffman E. and Stroobant V., 2002; Kebarle P., 2000; Taylor P. J., 2005).

Mechanisms of electrospray ionization

Four different mechanisms describing the process of compound ionization in electrospray source were postulated (Cech N. B. and Enke C. G., 2001; Cole R. B., 2010; Kebarle P., 2000):

- Ionization through charge separation
- Adduct formation
- Ionization through gas-phase reaction

- Ionization through electrochemical oxidation or reduction

1.7.2 Mass analyzer

This part of mass spectrometer is used for evaluation of mass to charge ratio of analyzed gaseous ions. This is achieved by application of different physical principles and thus mass analyzers can be compared by their specific parameters e.g. resolution (de Hoffman E. and Stroobant V., 2002; Hu Q. et al., 2005; McLuckey S. A. and Wells J. M., 2001; Perry R. H. et al., 2008; Scigelova M. and Makarov A., 2006)

1.7.2.1 Quadrupole mass analyzer

Quandrupolar mass analyzer is working as ion filter which separates ions according to their mass to charge ratio. Quadrupole (Q) consists of four parallel rods with hyperbolic or cylindrical crossection (de Hoffman E. and Stroobant V., 2002; Douglas D. J., 2009; McLuckey S. A. and Wells J. M., 2001) (Fig. 7). Application of direct current together with radiofrequency voltage on the rods generates quadrupolar field which properties can be adjusted by changing direct curent voltage U and radiofrequency voltage amplitude V. Changing the properties of the quadrupolar field influences the ions trajectory when passing the quadrupole in the m/z dependent manner. The ion on the stable trajectory will pass through the quadrupole. On the other hand ions on the unstable trajectory will collide with the rods or will be rejected from the quadrupole (Fig. 7) (de Hoffman E. and Stroobant V., 2002; Douglas D. J., 2009).

Quadrupole is the low resolution mass analyzer which has usually unit resolving power and is able to distinguish the ions with difference ± 1m/z. Its main advantage is in the simple construction, low demand on vacuum, high scanning speed and possibility of real time separation of ions according to the m/z. These advantages made quadrupole one of the most widespread benchtop mass spectrometer for quantitative analyses (de Hoffman E. and Stroobant V., 2002; Douglas D. J., 2009; McLuckey S. A. and Wells J. M., 2001).

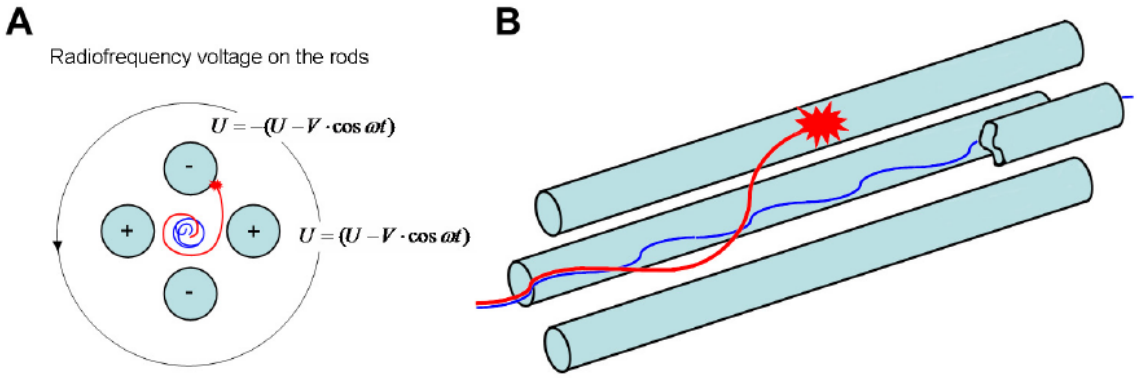

Fig. 7 Quadrupolar mass filter and the trajectories of two ions. Red line: an ion in an unstable region of the stability diagram on an unstable trajectory. Blue line: an ion in a stable region of the stability diagram passing the quadrupole on a stable trajectory. A) Section of the quadrupole illustrating radiofrequency voltage; B) Upper side view of the ion trajectories in the quadrupole.

1.8 Tandem mass spectrometry

Tandem mass spectrometry (MS/MS) uses the principle of two mass analyzes and fragmentation process which takes place between them. This two dimensional analytical technique can be performed in two ways (de Hoffman E. and Stroobant V., 2002; McLuckey S. A. and Wells J. M., 2001; Sleno L. and Volmer D. A., 2004)

- Tandem mass spectrometry in time is specific for instruments where the tandem analysis is performed in the same place which is characteristic for ion trap mass spectrometers.
- Mass spectrometry in space is done in two separated mass analyzers connected by collision cell e.g. tripplequadruple mass spectrometers.

A key feature of MS/MS is fragmentation of compounds after first mass spectrometric analysis. These fragments are then evaluated by second MS analysis. Fragmentation is based on the change in internal energy of the molecule and breaking its chemical bonds leading to generation of fragments. One of the ways how to fragment the ions is by collision induced dissociation (CID) (de Hoffman E. and Stroobant V., 2002; Jennings K. R., 2000; Sleno L. and Volmer D. A., 2004).

1.8.1 Collision induced dissociation

Process of CID is based on kinetic collisions of analyte ions (Precursor ions) with molecules of neutral gas (collision gas) in the collision cell (e.g. RF voltage quadrupole abbreviated by q). Kinetic energy of the collisions (collision energy) is transferred to the internal energy of analyte ion. If the increased internal energy is sufficient to break chemical bond then fragments of analyte (Product ions) are generated (de Hoffman E. and Stroobant V., 2002; Jennings K. R., 2000; Sleno L. and Volmer D. A., 2004).

Energy transfer of the collision is influenced by kinetic energy of precursor ions and MW of collision gas . We can discriminate the collisions based on their collision energy to low energy (1-100 eV) and to high energy (>1 keV) collisions (de Hoffman E. and Stroobant V., 2002; Sleno L. and Volmer D. A., 2004).

1.8.2 Scanning modes of tandem mass spectrometer

Tandem mass spectrometers are able to perform analyses as single MS instrument but have some specific MS/MS modes (de Hoffman E. and Stroobant V., 2002; Sleno L. and Volmer D. A., 2004).

MS scans

Mass range scan – mass spectrometer scans through the range of selected m/z.

Selected ion monitoring – mass spectrometer records signal intensity of selected ion(s) .

MS/MS scans

Product ions scan: This mode is used for evaluation of the product ions which are produced by CID from their selected precursors.

Precursor ions scan – This technique is reverse to the product ions scan and allows searching for precursor ions which share structural similarity based on selected product ion.

Neutral loss scan – MS/MS instruments are able to scan for ions producing neutral fragment in the process of CID.

Multiple reaction monitoring – First and second mass spectrometers scan selected pairs (transition pairs) of precursor and product ions. This technique is useful for selective and sensitive quantification because it maximizes duty cycle of the analysis.

1.9 Electrospray tandem mass analysis of sphingolipids: brief overview

Electrospray ionization can be used for the separation of SFL during the MS analysis. This can be achieved by selective intrasource ionization used e.g. in the shotgun lipidomics MS (Fig. 8) (Han X. and Gross R. W., 2005; Haynes C. A. et al., 2009).

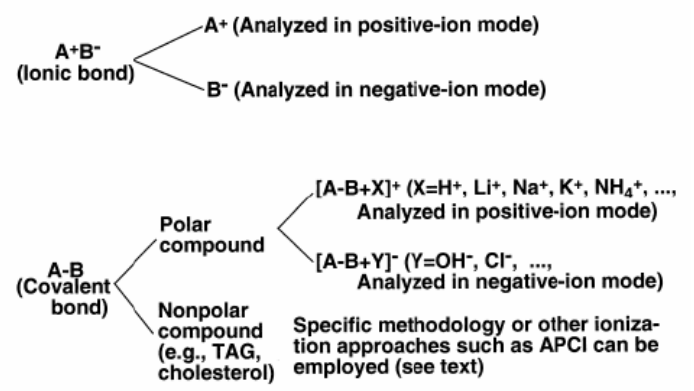

Fig. 8 Scheme of intrasource ionization strategies for shotgun lipidomics (Han X. and Gross R. W., 2003)

Different mechanisms of ion generation resulting in different forms of sphingolipid ions and their fragments can be used (Fig. 9) (Boscaro F. et al., 2002; Cech N. B. and Enke C. G., 2001; Han X. and Gross R. W., 2005; Haynes C. A. et al., 2009; Kebarle P., 2000; Mano N. et al., 1997; Olling A. et al., 1998).

It is also possible to use separation techniques prior the ESI-MS/MS analysis. Normal phase HPLC can be used for separation of SFL according to their hydrophilic part (Lipid groups separation - Fig. 10 D,C) whereas reverse phase HPLC can separate sphigolipid isoforms according to the hydrophobicity mostly by properties of the ceramide part of the molecule (Fig. 10 A,B) (Shaner R. L. et al., 2009).

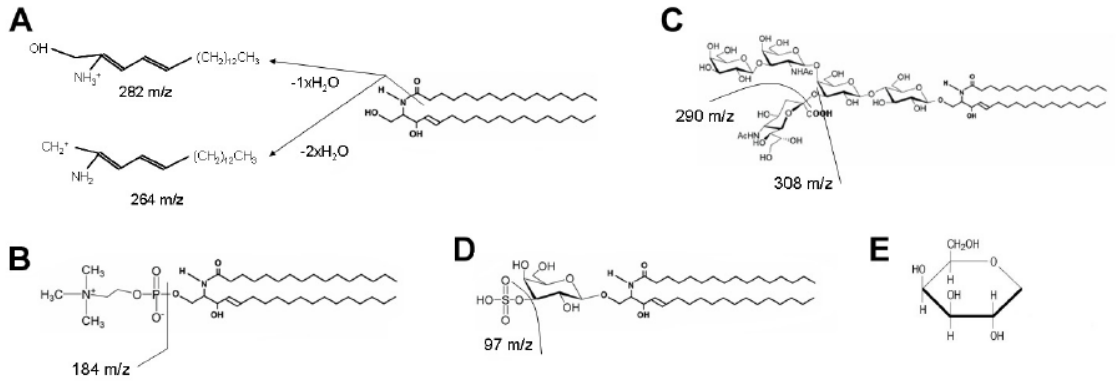

Fig. 9 Fragmentation of ceramide (A) and specific fragments of sphingomyelin (B), GM1 ganglioside (C) and sulfatides (D). Neutral fragment of hexose (galactose) is an example of fragmentation used in a neutral loss scan (E).

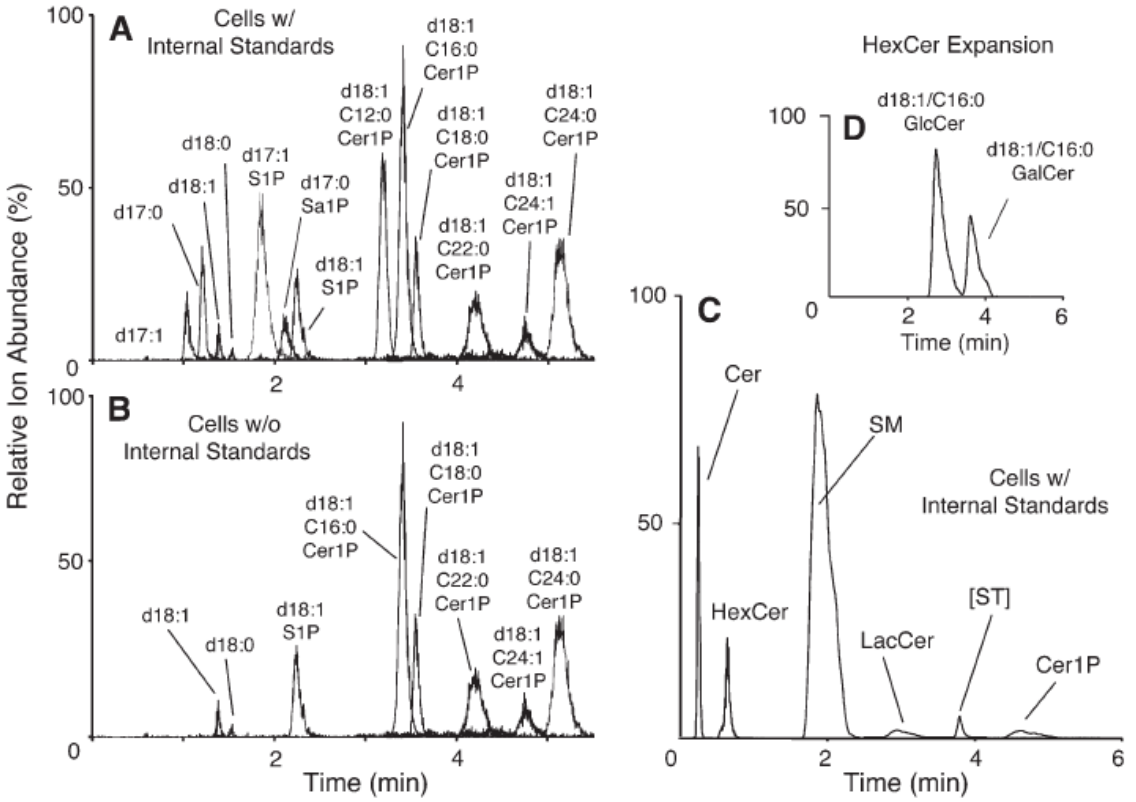

Fig. 10 HPLC separation of sphingolipids (Shaner R. L. et al., 2009) - elution profiles on reverse phase (A, B) and normal phase (C, D) chromatography. Shown are the elution of sphingoid bases and 1-phosphates and Cer1P in the single-phase extract of approximately (panel A) versus cells alone (panel B) The abbreviations identify the nature of the sphingoid base (e.g., S, sphingosine, d18:1; Sa, sphinganine, d18:0; and internal standards d17:1 and d17:0), the 1-phosphates (1P), and ceramide1-phosphates (Cer1P, designating the sphingoid base and amide-linked fatty acid). C: Elution of complex sphingolipids in the "lower phase extract" D: Separation of d18:1/C16:0-GlcCer and -GalCer standards

1.10 Quantitative analysis in the mass spectrometry

There are three major approaches for quantitative analysis which are based on the presumption that the measured signal express amount of analyte. It is required that the signal intensities have linear response in the measured range of concentrations. Nearly linear relationship between the relative intensities of molecular ions and the mass of individual lipids over a 10,000-fold dynamic range together with small experimental error makes this method ideal for selective and sensitive quantification (de Hoffman E. and Stroobant V., 2002; Han X. and Gross R. W., 2003; Han X. and Gross R. W., 2005).

- External calibration method
- Internal standard (IST) method is also based on the use of calibration curve. Analyte standards are mixed with known stable amount of the IST. The same amount of IST is added to the measured sample.. IST compensates for errors caused by sample preparation and by matrix effect. Internal standards are divided into three groups:
    - structural analogues labeled with stable isotopes
    - structural homologues
    - compounds from the same chemical family
- Isotopic dilution method

2. AIMS of the study

In recent years, increased interest in investigation of metabolism and biological functions of SFL has help to develop sensitive and accurate methods for their analysis. One of the leading analytical methods, tandem mass spectrometry (MS/MS), fulfils the requirements and provides high selectivity and sensitivity, even using crude lipid extracts and shotgun approach. Identification of various molecular species of individual sphingolipid classes in different biological material is an additional, but important, advantage.

This study focuses on the contribution of MS/MS to sphingolipidomics and its applications related to the laboratory research and diagnosis of inherited disorders of sphingolipid degradation. Outlines of the study include:

A. Selection and optimization of tandem mass spectrometry methods of sphingolipid analysis

- evaluation of fragmentation patterns and methods of qualitative and quantitative analysis of sphingolipids
- preparation of labeled sphingolipids containing atypical or mass labeled fatty acids

B. Analysis of sphingolipids in human urine for purposes of differencial diagnosis in lysosomal storage disorders

- to establish method for quantitative analysis of urinary SFL; optimization of methods for evaluating data and normalization of results
- to examine urinary sphingolipids as potential diagnostic markers in rare deficiences of saposin activators and other related LSD (Fabry disease and MLD)
- to search for new diagnostic markers of LSD: examination of the profiles of sphingolipid isoforms in urine

C. Analysis of sphingolipids in human cells and tissues in normal state and in lysosomal storage disorders

- analysis of sphingolipids and their deacylated derivatives in cells and tissues in selected LSD (Fabry disease, MLD, prosaposin and saposin B deficiencies)

D. *In vitro* and *in situ* enzymology of lysosomal storage disorders utilizing tandem mass spectrometry

- *In vitro* enzymology of LSD
- *In situ* examination of sphingolipid degradation pathways in living cells using mass labeled substrates

3. RESULTS AND DISCUSSION (A-D)

Laboratory methods and statistics are given in published articles that are listed in the Supplementary publications section of this PhD thesis. Link to relevant articles is always noted in references in the appropriate section of Results and discussion.

A. Selection and optimization of tandem mass spectrometry methods of sphingolipid analysis

The use of MS for the analysis of SFL requires reliable methodological background. This primarily needs selection of appropriate fragmentation reaction. The next crutial step is to choose suitable internal standards which often require laboratory preparation. For this purpose, we have developed a method of enzyme-catalyzed synthesis on the surface of solid nanoparticles and prepared several mass labeled sphingolipid analogs suitable as internal standards.

A.1 Biosynthesis of sphingolipids labeled by atypical fatty acid

In recent years, an enzymatic reaction catalyzed by sphingolipid ceramide N-deacylase (SCDase, EC 3.5.1.69) was found to be effective for the preparation of specific sphingolipid molecules (Fauler G. et al., 2005; Ito M. et al., 1995; Ito M. et al., 2000; Kita K. et al., 2001; Mills K. et al., 2002).

SCDase catalyses the conversion of GSL into lyso-derivatives (N-deacylated GSL, lyso-GSL) under acidic conditions (pH 5, detergent concentrations up to 0.8%) by splitting the amide bond between the sphingoid and fatty acid in the ceramide. Under modified conditions (pH 7, detergent concentrations up to 0.1%) the enzyme catalyses the reverse reaction, i.e., reacylation. The effectiveness of the condensation is influenced by the type of lyso-GSL and fatty acid (Ito M. et al., 1995; Ito M. et al., 2000; Kita K. et al., 2001).

SCDase is the most important and expensive component of the reaction mixture, so we looked for conditions that would enable us to reuse the enzyme, e.g., by utilizing the principle of enzyme immobilization on the surface of solid particles (Bilkova Z. et al., 2002; Bilkova Z. et al., 2005; Bilkova Z. et al., 2006; Korecka L. et al., 2008).

A carrier with superparamagnetic properties was chosen for the simple and gentle separation of products from the reaction mixture. Magnetic macroporous bead (MMB) cellulose was selected for its hydrophilic properties and high specific surface area, which provides maximum binding activity. The character of the particles and the chosen method of immobilisation resulted in a system with many advantages (Bilkova Z. et al., 2002; Bilkova Z. et al., 2005; Bilkova Z. et al., 2006; Korecka L. et al., 2008).

The standard procedure used for enzyme immobilisation was based on the creation of a Schiff base between the primary amino group of the enzyme and the aldehyde group of the activated MMB cellulose (Bilkova Z. et al., 2005; Korecka L. et al., 2005). The advantage is that the reactive aldehyde groups are formed on the solid phase, while the enzyme molecule is not affected by the oxidation. The resulting Schiff base is mildly reduced with cyanoborohydride to form a stable bond (Hermanson G. T., 1996). The prepared SCDase-activated MMB cellulose had a higher rate of substrate conversion for both the deacylation and reacylation reactions than the soluble enzyme using standard conditions (Kita K. et al., 2001). The optimal substrate ratio for synthesis was found 1:1 as shown in Tab. 3.

Tab. 3 The effects of different molar ratios of substrates on the formation of the C18:0 Gb_3Cer product. Reactions were catalyzed by the SCDase-activated MMB cellulose

Ratio lyso-Gb_3Cer/stearic acid	1:1	1:2	1:3	1:4
*lyso-Gb_3Cer**	143	216	219	310
*C18:0 Gb_3Cer**	1401	1478	1403	1307
synthesis (%)	**91**	**87**	**86**	**81**

*Evaluated by TLC densitometry in arbitrary units

Although soluble SCDase has been successfully applied to sphingolipid semisynthesis (Fauler G. et al., 2005; Kita K. et al., 2001; Mills K. et al., 2002; Mitsutake S. et al., 1997; Mitsutake S. et al., 1998) the reaction mixture contained considerable amount of contaminating fatty acids and the resulting product revealed very low isoform purity. This complicates the preparation of specific isoforms especially when different lots of commercial enzyme may contain varying amounts of contaminants. This is unacceptable for further studies where MS is used as analytical method.

To compare both methods of enzymatic semisynthesis, C17:0 GlcCer was prepared in bulk solution containing a soluble form of SCDase (Fig 11).. Mass spectra revealed a considerable amount of contaminants in the final product; the contaminants were identified as GlcCer isoforms with C16:0 and C18:0 fatty acids (see Fig. 11(A)). The total yield of GlcCer synthesis was 99% (data not shown), but only 36% of the lyso-GlcCer was converted into the requested C17:0 isoform. The remaining 63% of the product consisted of contaminating isoforms.

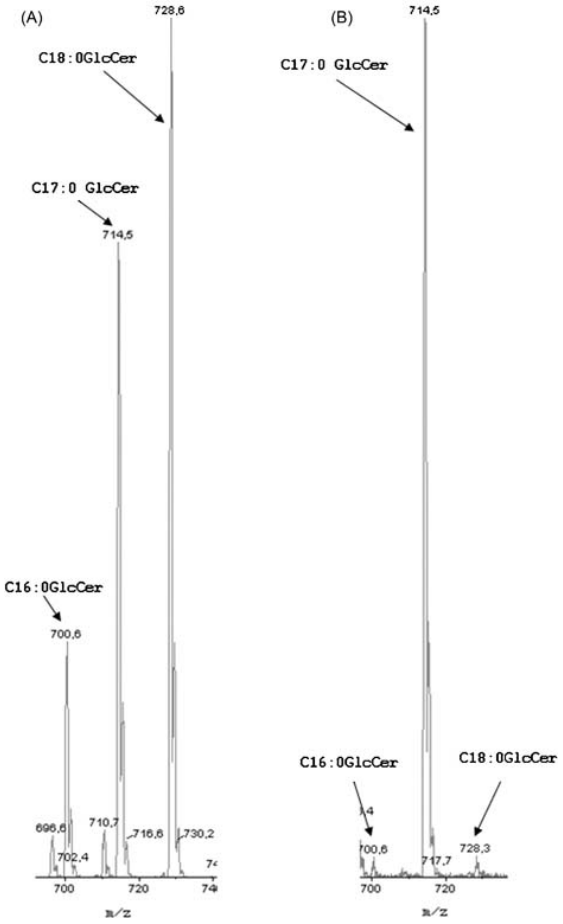

Fig. 11 ESI-MS/MS analysis of C18:0 and C16:0 isoform contaminants and comparison of the soluble and immobilized SCDase reaction products. Semisynthesis of C17:0 GlcCer using (A) soluble SCDase and (B) SCDase-activated MMB cellulose.

Using immobilized enzyme, 80% of lyso-SGalCer, 90% of lyso-GlcCer were acylated and converted into C17:0, SGalCer and GlcCer, respectively. Only trace amounts of contaminating isoforms (about 3% in both lipid preparations shown on Fig 11B and Fig

12) were detected. These fatty acid labeled SFL were then used as internal standards for MS quantitative analysis. Similarly, The C17:0 GM1 ganglioside was prepared from lyso-GM1 with 90% rate of conversion and 97% isoform purity.

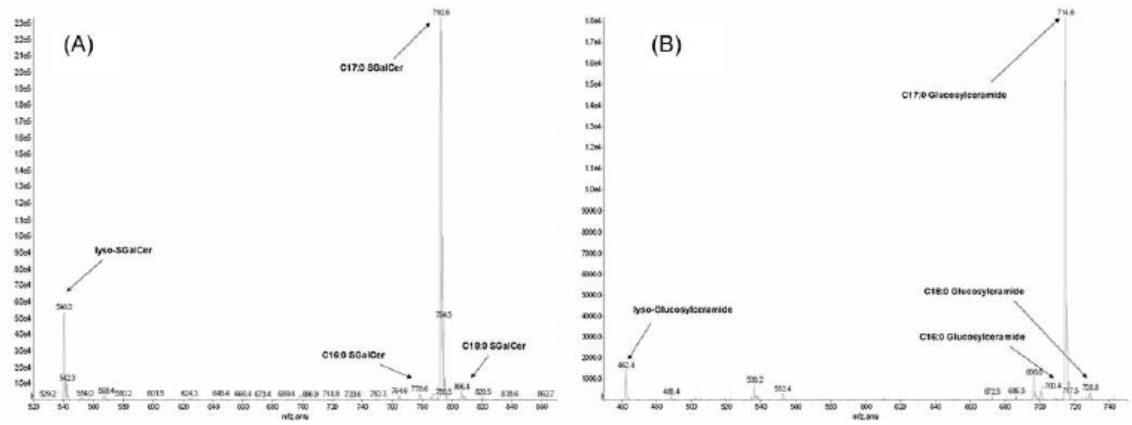

Fig. 12 ESI-MS/MS analysis of C17:0 sulfatide (A) and C17:0 glucosylceramide (B) prepared with the SCDase-activated MMB cellulose.

The great advantage of the SCDase-activated MMB cellulose was that did not show any decrease in activity after 15 reuses and was still active after 1.5 year of storage in the buffer.

In comparison with other methods, immobilized SCDase showed further advantages:

1. *using the soluble enzyme*, (Fauler G. et al., 2005) only 25% of lyso-Gb3Cer was converted into the pure Gb3Cer isoform and consumption of both, the enzyme and the product precursor was high

2. *chemical synthesis utilising lyso-sphingolipids* (Mills K. et al., 2005) and highly reactive acid chlorides can lead to non specific products due to side reaction with the hydroxyl groups of the oligosaccharide

3. *other procedures of organic synthesis* (Zhou X. et al., 2001) reactions have proved to be time consuming and giving small yields

Reference:

Supplementary publication A, Supplementary publication D

A.2 Set up of tandem mass spectrometry analysis of sphingolipids

The methodological scheme for MS/MS analysis of different classes of SFL was developed tested and optimized to get the most specific and sensitive analytical system.

The ionization of SFL by ESI can be done by different ionization strategies. One of them utitilizes neutral amonium salts which are added to the solution to facilitate the ionization of analytes. We have chosen ammonium formiate in the 5mM concentration which is a more efficient additive for generation of $[M+H]^+$ sphingolipid ions than ammonium acetate (Mano N. et al., 1997). Acidic SFL, e.g. sulfatides or gangliosides, have acidic groups that lose H^+ . We used pure methanol as convenient solvent to generate $[M-H]^-$ ions in negative ion mode by ionization through charge separation.

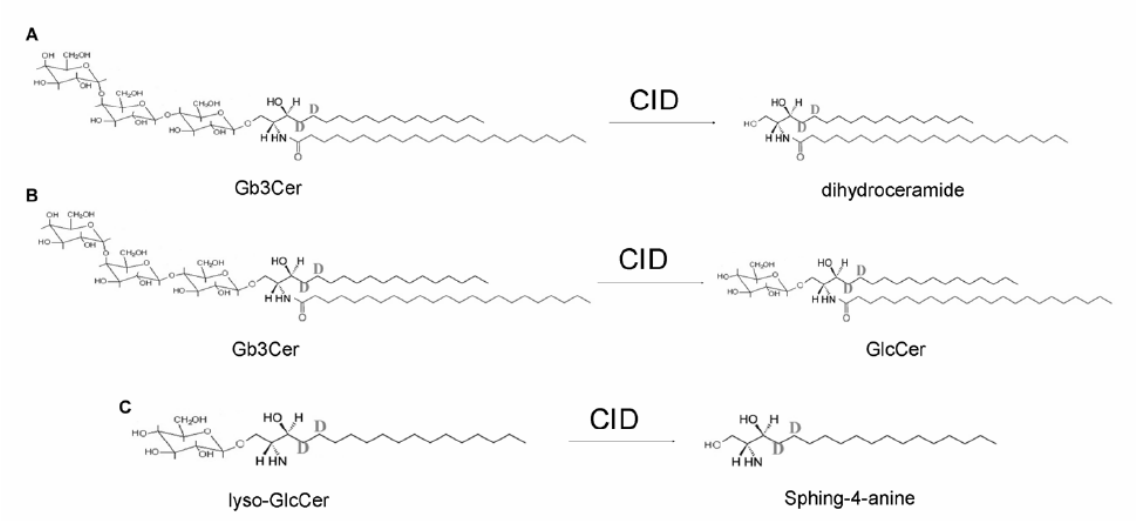

Fig. 13 Principle of neutral loss measurements of sphingolipids with deuterated dihydroceramide and sphinganine (sphing-4-anine) in the ceramide region of the molecule.

A) Complete loss of Gb3Cer oligosaccharide, B) Shortening of Gb3Cer oligosaccharide C) Neutral loss of saccharide part in lysoglycosphingolipids. CID – collision induced dissociation; Gb3Cer – globotriaosylceramide.

For further measurements we selected the most common fragment with 264 m/z which is derived from the ceramide with C18:1 sphingosine and the fragment with 282 m/z for deacylated derivatives (Gu M. et al., 1997; Lieser B. et al., 2003; Olling A. et al., 1998; Scherer M. et al., 2010). Other fragments were also occasionally used esp. for SFL with ionizable polar group like sphingomyelin, sulfatides etc. (Domon B. and Costello C. E.,

; Hsu F. F. et al., 1998; Hsu F. F. and Turk J., 2000; Ii T. et al., 1995; Kerwin J. L. et al., 1994; Murphy R. C. et al., 2001; Whitfield P. D. et al., 2001).

We found that for GSL containing dihydroceramide or sphinganine, generation of specific neutral fragment during CID is 5 times more effective than generation of 264 or 282 m/z fragments. (Fig. 13).

Reference:

Supplementary publication E

A.3 Quantification

Individual SFL are not represented by one specific molecule only, but they form a heterogeneous group of molecular types (isoforms) with various fatty acids and sphingoids with different molecular masses. Their profiles are usually cell- and tissue-specific (Fig. 14). This points to the importance of examination of isoform profiles before conducting a quantitative analysis.

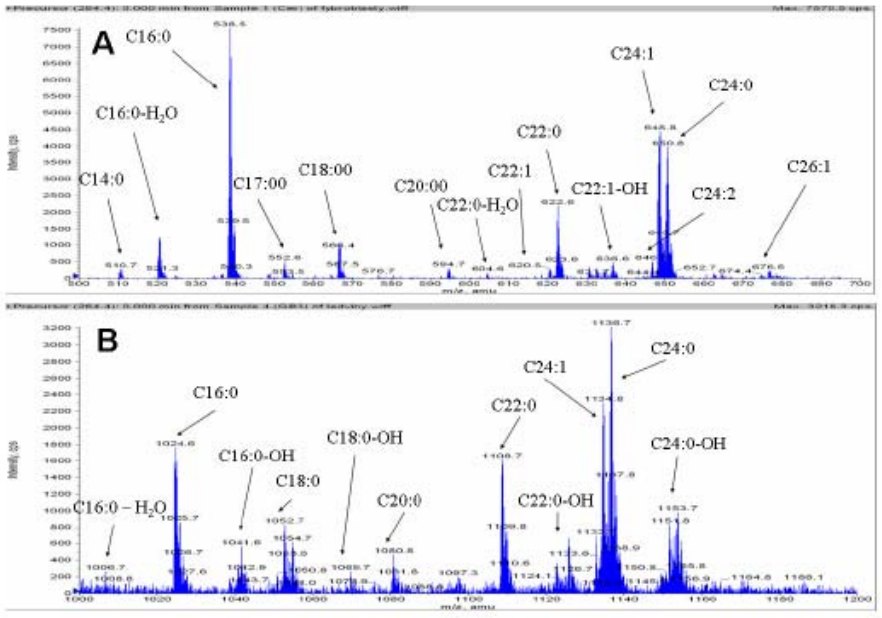

Fig. 14 Isoform profiles measured using precursor ion scans for different lipids and biological materials. Isoforms with different fatty acid chain lengths are identified. A) ceramides in skin fibroblasts, B) Gb3Cer in the kidney.

Quantification was done by single point calibration with an external lipid standard corrected by the signal ratio toward IST. The concentrations of lipid calibrators in external and internal standards were within the range of previously determined linear response. The concentrations of IST in the external calibration point and in the analyzed samples were the same (de Hoffman E. and Stroobant V., 2002).

Mono- and di- hexosyl SFL were quantified in one fraction because they are isobaric (have the same mass and product ions) and therefore indistinguishable by MS.

Reference:

Supplementary publication B, Supplementary publication E

B. Analysis of sphingolipids in human urine and its use for the differential diagnosis of lysosomal storage disorders

Laboratory diagnosis of LSD should be always focused on utilization of non invasive biological material. Therefore, we were interested in methods for analysis of SFL in the urine with a particular focus on the following:

- appropriate method of quantification of SFL in urine
- application for diagnosis of LSD with typically high excretion of specific SFL e.g. in Fabry disease and MLD
- application for LSD caused by the defects of protein activators (saposins) where routine laboratory enzymology fails
- examination of isoform profiles of specific urinary SFL as potential LSD biomarkers

B.1 Quantity of urinary sphingolipids

Urine is a non-invasive diagnostic material that is of practical importance in diagnosing lysosomal disorders where the storage of non-degraded substrate induces pathological processes in the kidney cells. These disorders are characterized by the massive excretion of specific SFL, e.g., Gb3Cer in Fabry disease (α-galactosidase A deficiency due to

mutations of the *GLA* gene) (Desnick R. J. et al., 2001); sulfatides in metachromatic leukodystrophy (arylsulfatase A deficiency due to mutations of the *ARSA* gene) (von Figura K. et al., 2001) and both lipids in prosaposin and saposin B defects (Sandhoff K. et al., 2001).

B.1.1 Pitfalls of the quantification of sphingolipids in urine

The normalization parameter commonly used for urinary metabolites is creatinine which, however, does not reflect the cellular origin of SFL. Therefore, concentration in urinary samples with creatinine level lower than 1 mM, are artificially inflated (Fig. 15A), which may lead to an incorrect diagnosis in patients (e.g., Fabry disease, prosaposin and saposin B deficiencies, and MLD). Regarding Fabry disease, this issue has already been pointed out (Forni S. et al., 2009).

Urinary volume was found more convenient normalization parameter (Fig. 15B). Another possibility is the concentration ratio of the analyzed compound to sphingomyelin representing a major sphingolipid of the cell membrane (Berna L. et al., 1999).

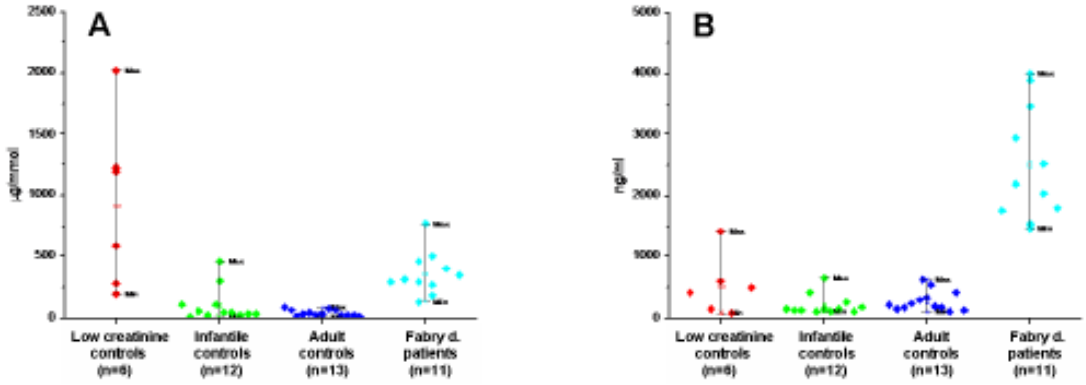

Fig. 15 Comparison of two methods of normalization of urinary Gb3Cer in four groups of samples: in controls with low creatinine (creatinine ≤1 mM), in infantile and adult controls with creatinine within a normal range (creatinine >1 mM-15 mM) and in Fabry patients.

Graph A clearly shows that controls with low creatinine values, are indistinguishable from patients with Fabry disease. This fact is usually not taken into account in the literature although low levels of creatinine are quite often found in newborns and young children. In contrast, urine volume as a normalization parameter more reliably distinguishes between controls and Fabry patients (graph B)

Reference:

Supplementary publication B, Supplementary publication E

B.1.2 Urinary sphingolipids in prosaposin and saposin-B deficient patients and in other sphingolipidoses

Results in Tab. 4 summarizes the quantity of urinary sphingolipids in patients 1 (pSap-d) and 2 (SapB-d) compared to findings in Fabry disease, MLD, and normal controls. The data were normalized relative to the concentration of sphingomyelin as a reference cellular sphingolipid.

Tab. 4 Urinary Sphingolipids in Patient 1 (pSap-d), Patient 2 (SapB-d) compared with MLD and Fabry patients and with controls (ESI-MS/MS determination)

	Lipid values[a] expressed as µg/100 µg sphingomyelin				
	Sulfatide	Globotriaosylceramide	Lactosyl- and digalactosylceramide	Monohexosylceramide (mainly glucosylceramide)	Ceramide
Patient 1 (pSap-d) 44-day-old	67[c]	208[c]	45[c]	26[c]	17[c]
Patient 2 (SapB-d) 50-month-old	145[c]	51[c]	35[c]	14[c]	6.3
Metachromatic leukodystrophy 1- to 5-year-old (n = 6)	120[c] 38[d]	8.8 3.3	14 5.3	6.2 1.7	3.8 1.1
Fabry disease males 24- to 54-year-old (n = 10)	6.8 2.5[d]	201[c] 102	35[e] 19	3.5 1.4	4.8 1.7
Infantile/late-infantile controls 0.5- to 12-year-old (n = 16)	14 5.2[d]	15 8.2	10.2 3.0	4.4 1.0	4.3 1.8
Adult controls males and females[b] 17- to 60-year-old (n = 12)	9.7 2.5[d]	21 14	16 6.1	4.4 1.4	5.8 2.8

[a]Mean of three determinations for patients 1 and 2. For the analytical reproducibility, see Patients and Methods Section.
[b]Fabry carrier status was excluded in control females molecularly.
[c]Statistical significance $P < 0.001$.
[d]Standard deviation.
[e]Statistical significance $P < 0.01$.

The percent distribution of the main urinary SFL is shown on Fig.16. This format, which allowed for a simple normalization of urinary lipid values in the absence of normalizing parameters, confirmed most of the findings summarized in Tab. 4. In normal controls sphingomyelin accounted for more than 60% of SFL, but in the patients, the proportion of sphingomyelin was considerably less due to the preponderance of other SFL. The combined percentages for sulfatide, Gb3Cer, dihexosylceramides, glucosylceramide, and ceramide was higher in the diseases studied than for controls, with pSap-d having the highest percentage, consistent with the unique urinary multiple sphingolipid elevations in this condition.

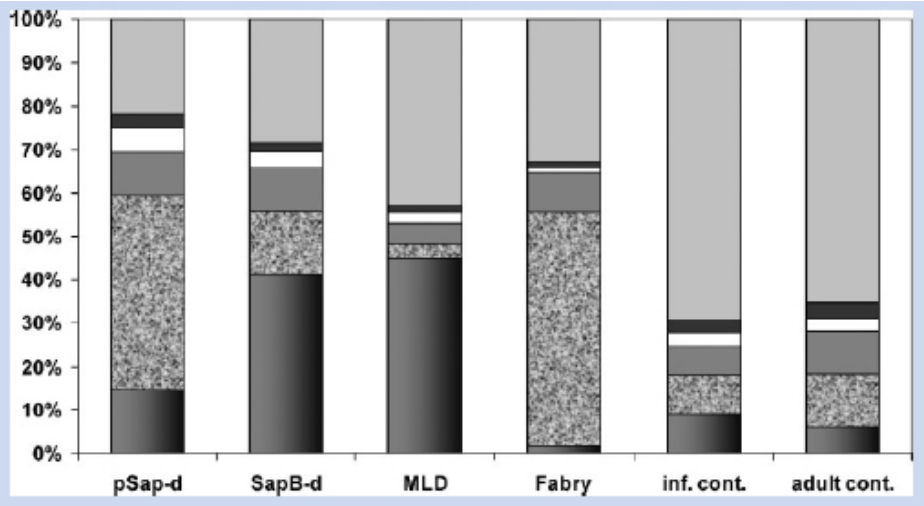

Fig. 16 Percent distribution of main urinary sphingolipids. Order of column sections from bottom to top: sulfatide (right edge dark), globotriaosylceramide (sand-like), dihexosylceramides (gray), glucosylceramide (light), ceramide (black), sphingomyelin (light gray). Columns: pSap-d, patient 1; SapB-d, patient 2; MLD, metachromatic leukodystrophy group (mean, Tab. 4); Fabry, Fabry disease group (mean, Tab. 4); inf. cont., infantile/late-infantile controls (mean, Tab. 4); adult cont., adult controls (mean, Tab. 4).

We have demonstrated for the first time the use of urinary sphingolipid analysis when diagnosing the rare pSap-d condition. We have also shown efficiency of this procedure when screening for SapB-d and other sphingolipidoses (Tab. 4). In particular, urinary lipid analysis by ESI-MS/MS done for the pSap-d neonate verified the complex urinary lipid changes in this condition and allowed quantification of individual sphingolipid classes. High increase in the concentration of Gb3Cer (within the range seen in adult Fabry disease) along with the increase in sulfatide, dihexosylceramides (LacCer and digalactosylceramide), GlcCer, and in ceramide has been demonstrated. The urinary concentration of LacCer/diGalCer fraction was also elevated in the SapB-d patient (Tab 4) due to digactosylceramide, another substrate of α-galactosidase A (EC 3.2.1.22) in synergic function with SapB (Bradova V. et al., 1993). Increase in multiple SFL, CDH, Gb3Cer and sulfatide in SapB-d has been reported previously using chromatographic methods (Li S. C. et al., 1985).

Reference:

Supplementary publication B, Supplementary publication E

B.2 Search for novel urinary sphingolipid biomarkers

B.2.1 Sphingolipid isoform profiles

Tandem mass spectrometry provides specific data that allow to examine patterns of molecular species and to monitor changes in their relative abundance related to the nature of the disease. It may strongly influence the clinical view in some diseases. Understanding these variations in relation to the disease may help to identify new categories of biomarkers (Paschke E. et al., 2011; Postle A. D., 2008).

For example, an analysis of urinary lipid extracts in the case of MLD showed significant differences in sulfatide isoform profiles (Fig 17, 18B); such differences were also evident in cases of pSap-d (Fig 17) and SapB-d (data not shown) We also found modified patterns of globotriaosylceramide species in the urine of Fabry patients (Fig. 18A).

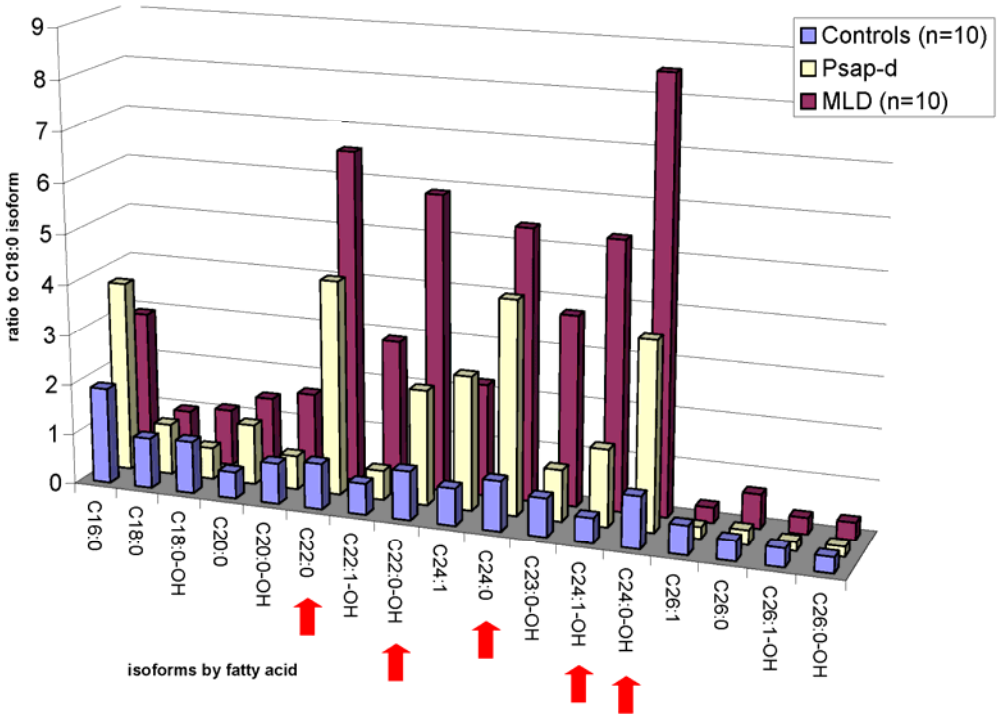

Fig. 17 Comparison of urinary isoform profiles from MLD and prosaposin deficiency (Psap-d) patients and controls. Arrows indicate components undergoing major changes.

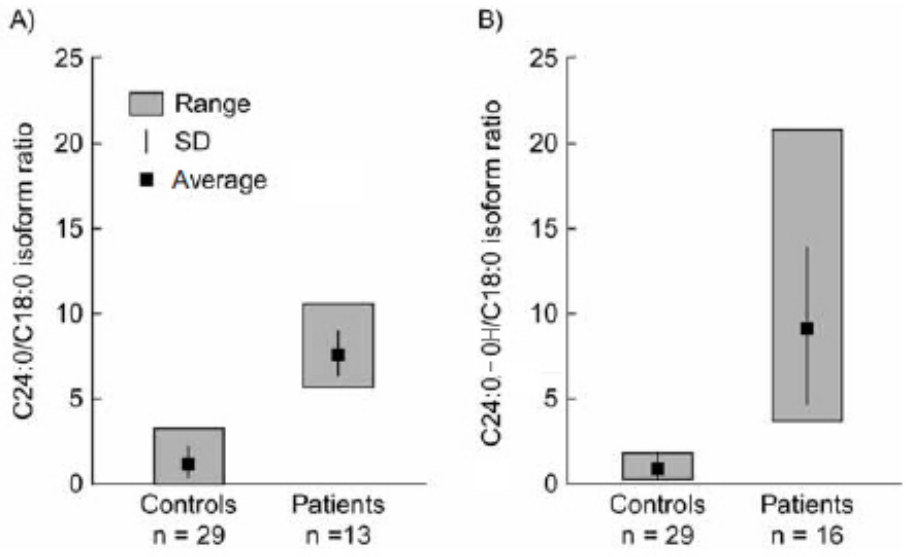

Fig. 18 Elevated excretion of major sphingolipid isoforms (A) C24:0 Gb3Cer in Fabry disease; (B) C24:0-OH sulfatide in MLD

Reference:

Supplementary publication C, Supplementary publication E, Supplementary publication F

B.2.2 Hypotesis explaining pathological changes in isoform patterns of urinary sulaftides

It is presumed that the exfoliated renal tubule epithelium cells affected by lysosomal storage are the primary source of excreted SFL in some LSD (Chatterjee S. et al., 1984; Iwamori M. and Moser H. W., 1975; von Figura K. et al., 2001; Warnock D. G. et al., 2010). In the absence of renal damage, the renal epithelium cells appear in the urinary sediment in only very small quantities (Chatterjee S. et al., 1986; Nguyen G. K. and Smith R., 2004).

We compared the sulfatide profiles in urine and in extracts of kidney homogenates from normal individuals and from the prosaposin deficient patient.

The pattern of sulfatide isoforms was similar in the healthy kidney and in the kidney affected by lysosomal storage (Fig. 19 A,B; purple highlighted bars).

In contrast, an altered urinary sulfatide profile (Fig. 19, blue bars) exactly corresponded to the sulfatide kidney profile ("indirect kidney biopsy"; (Desnick R. J. et al., 1970)) of

the prosaposin deficient patient. This can be taken as an indirect evidence for changes in the composition of cellular types in the urinary sediment - desquamated urothelial cells in healthy controls (Chatterjee S. et al., 1986) and lipid-laden renal tubule cells (Warnock D. G. et al., 2010) in patients with LSD .

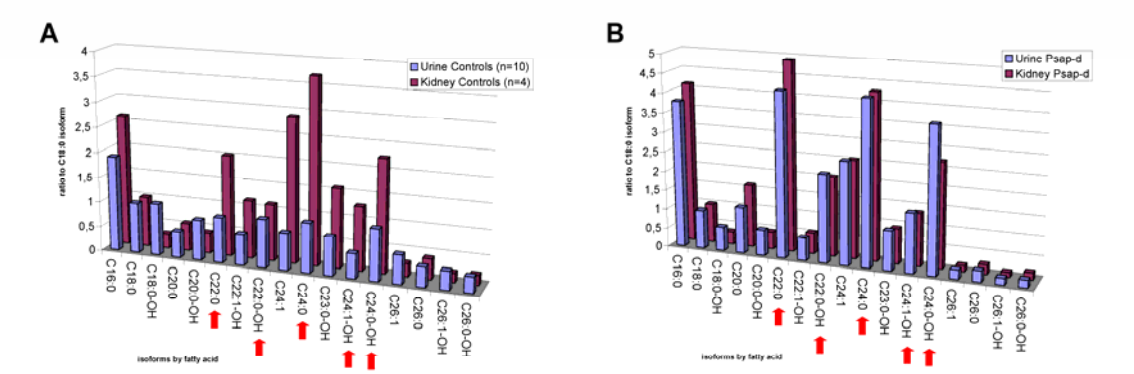

Fig. 19 Comparison of sulfatide isoform urinary and kidney profiles in controls (panel A) and the prosaposin deficiency (Psap-d) patient (panel B). The similarity of urinary and kidney profiles in Psap-d is obvious. Arrows indicate major changes in the isoform profiles.

The spectrum of the sulfatide isoforms in the kidney corresponds largely with the expression of CerS2 which is primarily expressed in the kidney cells and is specific for acylation of sphingoid base with C22 through C24 fatty acids (Laviad E. L. et al., 2008; Levy M. and Futerman A. H., 2010). These are the major molecular forms of kidney sulfatides and are elevated in urine of patients with MLD and prosaposin deficiency.

Reference:

Supplementary publication C

B.2.3 Tandem mass spectrometry profiling of urinary sulfatides bound to DEAE membrane and its diagnostic significance

Transportation of liquid biological material such as blood and urine is often quite complicated. Large sets of liquid samples, organization of a rapid transport from distant places and maintenance of required temperature pose a considerable burden and may lead to inaccuracies in the measured parameters. This can be overcome by preparation

of dry samples. As for the blood, the dry blood spots (DBS) have proved very useful for many different diagnostic applications including determination of activities of several lysosomal hydrolases (Turecek F. et al., 2007).

For diagnosis of sulfatidoses, we have introduced DEAE membrane (as a carrier of sulfatides) for preparation of dry urine samples, acting simultaneously as a tool of partial purification of sulfatides and enhancing sensitivity of the analysis. These are the key characteristics of the procedure which is being considered as a screening method for MLD because enzyme-based DBS analysis is still missing.

In an effort to simplify the analytical procedure and lower the cost, we sought to find the least variable component of the sulfatide spectrum for normalization of the signal of major elevated isoforms. Sulfatide C18:0 isoform was the most stable parameter percent wise and was used as an indigenous reference for calculating the isoform profile number (IPN), the disease marker. IPN represents the ratio of the summed SRM intensities of five elevated major urinary sulfatide isoforms (C22:0, C:22:0-OH, C24:0, C24:1-OH, and C24:0-OH) to C18:0 isoform. Selection of five MLD-related isoforms minimizes individual differences in collected samples in comparison with the previously reported analysis of Gb3Cer profile in urine of Fabry patients based on only one major elevated C24:0 isoform (Paschke E. et al., 2011). The use of the C18:0 reference isoform also helps to resolve the long-standing problem of suitable evaluation of urinary lipids which resulted from the use of inappropriate normalizing parameters (i.e. creatinine) (Forni S. et al., 2009).

We have shown that simple profiling of specifically increased sulfatide isoforms by calculating the IPN was able to reliably identify all patients with MLD and prosaposin deficiency, indicating no false negatives, and distinguished all controls, indicating no false positives (Fig. 20).

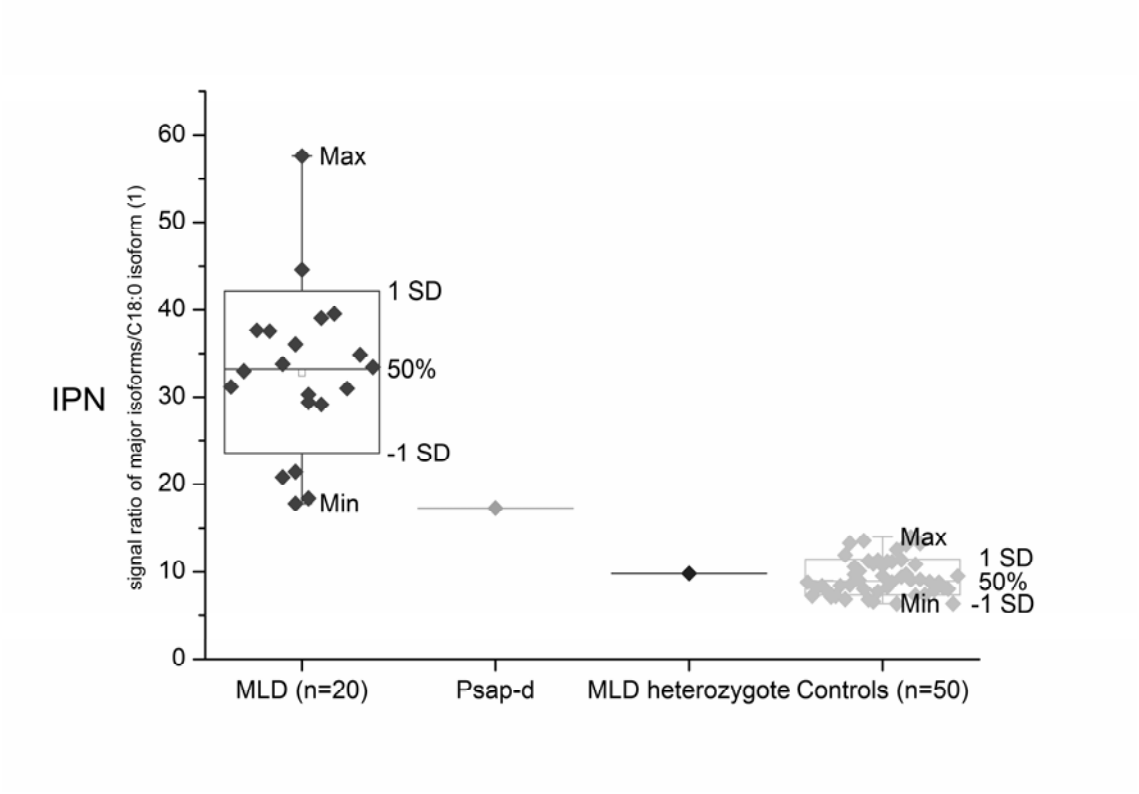

Fig. 20 Ratio of composed SRM intensities of major urinary isoforms to the SRM intensity of the intrinsic C18:0 reference (IPN) for MLD and prosaposin deficiency (Psap-d) patients, a heterozygote, and controls.

The stability of sulfatides captured on the DEAE membrane under different storage conditions was found sufficient, as the IPN value provided clear differentiation between the control group and MLD patients at any time point up to 100 days of storage (Tab. 5).

Samples are usually delivered to the analytical laboratory within one week after collection but even longer storage period had no negative impact on the outcome of the laboratory analysis and diagnosis.

Tab. 5 - Stability of sulfatides bound to DEAE membrane under different storage conditions evaluated by IPN

		Day						
		1	3	6	100	Avg	SD	CV%
C1	LT	7.69	6.73	8.06	6.07	7.14	0.91	12.71
	FR	7.30	8.28	8.03	6.40	7.50	0.84	11.24
C2	LT	9.51	10.05	8.44	7.78	8.95	1.03	11.46
	FR	8.50	8.34	9.55	8.80	8.80	0.54	6.12
C3	LT	8.62	9.86	10.26	6.79	8.88	1.56	17.57
	FR	11.04	8.62	9.98	8.55	9.55	1.19	12.50
MLD1	LT	48.86	51.69	40.40	43.16	46.03	5.16	11.22
	FR	36.42	37.19	48.27	35.53	39.35	5.98	15.20
MLD2	LT	32.33	20.63	25.30	20.50	24.69	5.56	22.53
	FR	31.22	28.20	30.62	34.63	31.17	2.65	8.51
MLD3	LT	27.07	29.83	20.99	27.70	26.40	3.79	14.37
	FR	21.76	24.20	24.32	24.99	23.82	1.42	5.95

IPN values are average of two measurements

C - Control; MLD - metachromatic leukodystrophy; LT - laboratory temperature; FR- storage in a freezer at -20 ^{o}C; values of IPN are in arbitrary units;

Reference:

Supplementary publication C

C. Analysis of sphingolipids in human cells and tissues in normal state and in lysosomal storage disorders

Sphingolipid analysis in tissues and cells may have the specific diagnostic application. Autopsy tissue analysis of SFL has been proved very useful for determining the postmortem diagnosis in many cases. Also sphingolipid composition of cultured skin fibroblasts can provide valid information on defects of degradative pathways in sphingolipidoses.

Some examples of analyses of archived human tissues and cells follow:

- SFL in skin fibroblasts
- Kidney SFL
- Myocardium Gb3Cer and its relation to lyso-Gb3Cer
- SFL in the placenta

C.1 Sphingolipids in skin fibroblasts

Cultured skin fibroblasts are not typical "storage cells," but the concentration of nondegraded SFL increases significantly in some of the LSD. Quantitification of SFL in the harvested pellet of skin fibroblasts thus can help in laboratory diagnosis of rare diseases e.g. defects of saposin activators (Table 6)

Tab. 6 Increased concentration of sphingolipids in cultured skin fibroblasts in patients with sphingolipid activator deficiencies (saposin B and prosaposin deficiencies) and in patients with defective enzyme proteins (Fabry and Niemann-Pick A disease).

	Cer	CMH	CDH	Gb3Cer	SM
Prosaposin def.	34,48	14,27	25,75	27,06	45,70
saposin B def.	6,87	1,44	1,86	21,36	107,33
Fabry disease	3,76	1,89	2,10	35,68	42,62
Nieman-Pick A	4,15	1,67	5,63	0,51	195,17
Control 1	6,21	3,25	5,17	0,52	68,28
Control 2	1,18	2,67	1,37	5,17	21,04

Values are in ng/µg of protein

Cer - ceramide; CDH – ceramidedihexoside, CMH – ceramidemonohexoside; SM – sphingomyelin; Gb3Cer - globotriaosylceramide

Reference:

Supplementary publication E

C.2 Sphingolipids of human kidney and myocardium

In some cases, postmortem analysis of autoptic tissues revealed a metabolic defect which was essential for genetic councelling in families. Here, we are showing two examples leading to a final diagnosis which was confirmed by DNA analysis later on.

The first example shows the accumulation of Gb3Cer in the kidneys of patients with Fabry disease and prosaposin deficiency (Tab. 7). These findings are in accordance with other authors (Aerts J. M. et al., 2008; Bradova V. et al., 1993; Desnick R. J. et al., 2001).

Tab. 7 Concentration of sphingolipids in the kidneys of Fabry male patient and in a case of prosaposin deficiency

	Cer	CMH	CDH	Gb3Cer	sulfatide	SM
Fabry disease	0,5	1,0	3,7	115,2	0,5	24,0
Prosaposin def.	39,1	23,9	49,8	57,6	39,6	125,8
Control (n=3)	11,2	0,7	3,2	10,2	1,1	57,9

Values are in ng/µg of protein, Control is represented by the mean value

Cer - ceramide; CDH – ceramidedihexoside, CMH – ceramidemonohexoside, SM – sphingomyelin; Gb3Cer - globotriaosylceramide

Second example demonstrates the storage of Gb3Cer and lyso-Gb3Cer (globotriaosylsphingosine) in the myocardium of Fabry patient (Fig. 21). The role of these derivates esp. that of lyso-Gb3Cer in the pathological process is still underrated. An elevated concentration of lyso-Gb3 encountered in plasma of symptomatic Fabry patients was found to inhibit residual α-galactosidase A activity and thus increase Gb3Cer concentration. Moreover, induction of smooth muscle cell proliferation in cell culture by low concentrations of lyso-Gb3 was reported (Aerts J. M. et al., 2008; Dekker N. et al., 2011). Another known effect is cell toxicity of lyso-SFL. It is assumed that the toxicity of lyso-GalCer has a major pathological effect in the Krabe disease (Suzuki K., 1998). Toxic effect of lyso-GlcCer in the cell culture of Gaucher neuroblastoma cells was also described (Schueler U. H. et al., 2003).

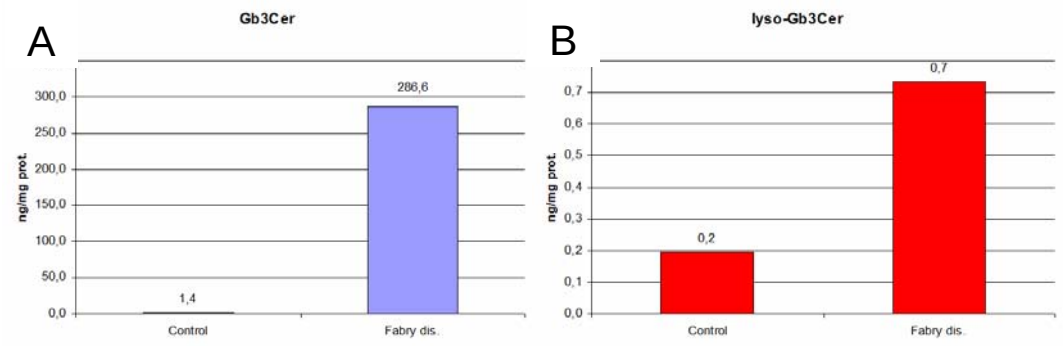

Fig. 21 Gb3Cer and lyso-Gb3Cer (globotriaosylsphingosine) in the myocardium of Fabry patient measured by FIA-ESI-MS/MS

A) Gb3Cer and B) lyso-Gb3Cer detected in the autoptic myocardium of Fabry patient compared to age-matched control.

Interestingly, it is not yet clear how deacylated derivatives are formed. Both hypotetical pathways, biosynthesis (Schueler U. H. et al., 2003) and deacylation (Yamaguchi Y. et al., 1994) are considered possible but not completely confirmed (Cox T. M. and Cachon-Gonzalez M. B., 2012).

Reference:

Supplementary publication E

C.3 Sphingolipids in human placenta

The study of the glycosphingolipid (GSL) profile of placental endothelial cells was induced by our engagement in studies of lysosomal storage of Gb3Cer in Fabry disease. Immunohistochemical detection of Gb3Cer in a sample of the placenta of Fabry heterozygote surprisingly showed strong staining of the villous capillaries but free of lysosomal storage. The same picture was found in placentas of healthy women. All placentas showed uniform distinct staining of vilous capillary endothelial cells for Gb3Cer, GM1 and GM3 gangliosides, cholesterol and caveolin 1 suggesting the presence of caveola-associated raft microdomains..

Comprehensive biochemical study of the GSL profile in normal placentas was done by tandem mass spectrometry and by TLC using specific detections to confirm the presence of immunohistochemically detected lipids. Gb3Cer and other frequently occurring neutral GSLs (ceramide mono- and dihexosides, globoside and GM3 ganglioside) were MS/MS proved (Tab. 8) which was consistent with previously published results (Jordan J. A. and DeLoia J. A., 1999; Mikami M. et al., 1993; Strasberg P. et al., 1989; Taki T. et al., 1988).

Gb3Cer was identified as the most abundant component of neutral GSL while GM3 was the major component of acidic sphingolipids. GM1 ganglioside formed one fraction with its positional isomer sialylparagloboside (IV^3NeuAc-nLc_4Cer (SPG) which is not discriminated by MS/MS because of isobaric character of both compounds.

The presence of GM1 ganglioside was confirmed by further analysis on the principle of its specific binding with cholera toxin B-subunit. This reaction was used for visualization after chromatografic separation of sialylated GSL on TLC plate and also for specific staining of tissue sections. Monosialylated tetrahexosylceramide fraction

contained SPG as a major component and traces of GM1 ganglioside (≤0.12% of the total fraction).

Gangliosides bearing ganglio-series backbone have not yet been demonstrated in the placenta. This is the first time that the detectable amount of GM1, a characteristic component of cellular membranes and their lipid domains (rafts) has been detected.

Positivity for GM1, GM3 and cholesterol in combination with caveolin 1 (see also (Lyden T. W. et al., 2002)) suggests the presence of caveola-associated microdomains (Pang H. et al., 2004; Parton R. G., 1994) at the apical pole of endothelial cells in the placental capillary network, unique with regard to their high levels of Gb3Cer.

The physiological significance of this finding is open for further studies, which may discover whether it is related to the clathrin-independent endocytosis (Mayor S. and Pagano R. E., 2007; Nichols B., 2003), to specific transport processes known to exist at this level (Solder E. et al., 2009; Takizawa T. et al., 2005) or to the regulation of the humoral control of the placental microcirculation (Tedde G. et al., 1990).

Tab. 8 GSL in human placenta (in pmol/nmol sphingomyelin)

	Gb4Cer	Gb3Cer	CDH	CMH	SPG + GM1	GM3
C1	12.8	27.1	27.8	22.7	7.0	51.9
C2	11.5	32.1	15.2	16.7	5.4	37.6
C3	19.1	20.4	15.1	20.2	4.3	50.1
C4	15.9	35.1	12.5	23.2	4.5	51.6
C5	13.5	35.3	16.0	19.2	N.Q.	N.Q.

C1-5, different normal human placentas; N.Q., not quantified. The MS/MS does not differentiate between GSL sugar moieties having the same mass. Therefore, glucosylceramide and galactosylceramide, lactosylceramide and digalactosylceramide, and SPG and GM1 are quantified as monohexosylceramides (CMH), dihexosylceramides (CDH), and SPG + GM1 fraction, respectively. Samples were measured in duplicates and values standardized to sphingomyelin, the major ubiquitous sphingolipid of the cell

Reference:

Supplementary publication D

D. *In vitro* and *in situ* enzymology of lysosomal storage disorders utilizing tandem mass spectrometry

Tandem mass spectrometry has wide applications in enzymology esp. in DBS screening for deficient activities of sphingolipid hydrolases (Turecek F. et al., 2007). We modified the DBS method for detemination of enzyme activities in cell homogenates i.e. skin fibroblasts. This would give us the opportunity to compare results obtained from *in vitro* measurements in cell homogenates and from the dynamic experiments on living cells *in situ* (loading tests). These tests are either performed with radiolabeled substrates or with mass labeled lipid compounds, the latter being then evaluated by MS/MS. Examples are following:

- *in vitro* determination of β-glucocerebrosidase activity using tandem mass spectrometry
- *in situ* dynamic metabolic experiments on acid β-galactosidase deficient cells (GM1 gangliosidosis): comparison of procedures of mass spectrometry and radiochemistry

D.1 Tandem mass spectrometry applications for *in vitro* enzymology of lysosomal storage disorders diagnosis

Enzymology, in combination with MS/MS, is useful for LSD screening and for evaluations of enzyme activities in biological material, in general (Kasper D. C. et al., 2010; Li Y. et al., 2004; Spacil Z. et al., 2011; Turecek F. et al., 2007). One possible application is measurement of residual β-galactocerebrosidase activity in cultured skin fibroblasts from patients with Gaucher disease. Assay is based on glucosylceramide with C12:0 fatty acid as a natural enzyme substrate.

We modified Turecek´s method (Turecek F. et al., 2007) by addition of inactivated bovine serum albumin (BSA) to the reaction mixture to stabilize the enzyme and used this procedure to determine residual enzyme activities in Gaucher patients including the most severe form "collodion baby phenotype" (Fig 22). Measurable residual enzyme activities were found in all Gaucher types (I and II) in contrast to zero activity in fibroblasts from Gaucher Type II-collodion baby phenotype. This is in concordance

with published observations when only arteficial substrate was used (Finn L. S. et al., 2000).

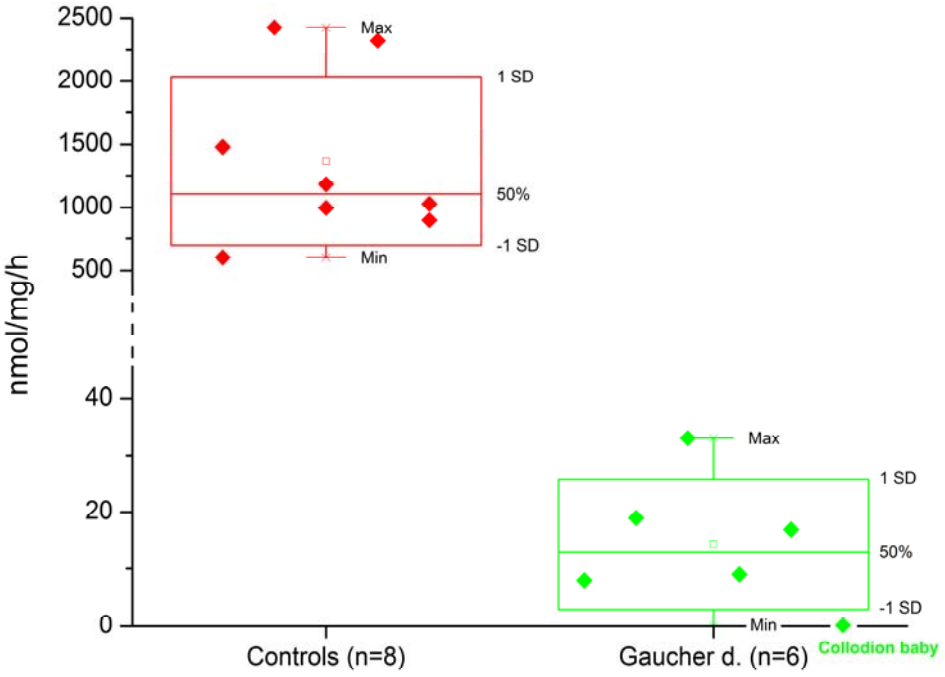

Fig. 22 *In vitro* activity of lysosomal acid β-glucocerebrosidase in Gaucher and control fibroblasts measured with natural substrate C12:0 glucosylceramide. The reaction product was analyzed by FIA-ESI-MS/MS

Reference:

Supplementary publication E

D.2 *In situ* enzymatic analysis for monitoring the sphingolipid degradation pathways by tandem mass spectrometry

Loading experiments in cell cultures (also called feeding experiments) are frequently used to track the metabolic fate of labeled exogenous compounds in living model systems (Asfaw B. et al., 1998; Asfaw B. et al., 2002; Leinekugel P. et al., 1992; Martin O. C. and Pagano R. E., 1994; Porter M. T. et al., 1971; Schwarzmann G. et al., 1983; Sonderfeld S. et al., 1985). The main advantage of such experiments is that they assess the entire aparatus of living cells, including any nonenzymatic cofactors e.g. like

saposins. It can give important diagnostic information in those LSD which are not detectable by routine enzymology.

We compared the methods utilizing radioisotope and mass labeled substrates in loading experiments on fibroblasts with genetic variants of the ß-galactosidase deficiency. Both methods using either [^{3}H]GM1 ganglioside or C18:0-D3 analogue, clearly revealed defect in β-galactosidase function (Fig. 23).

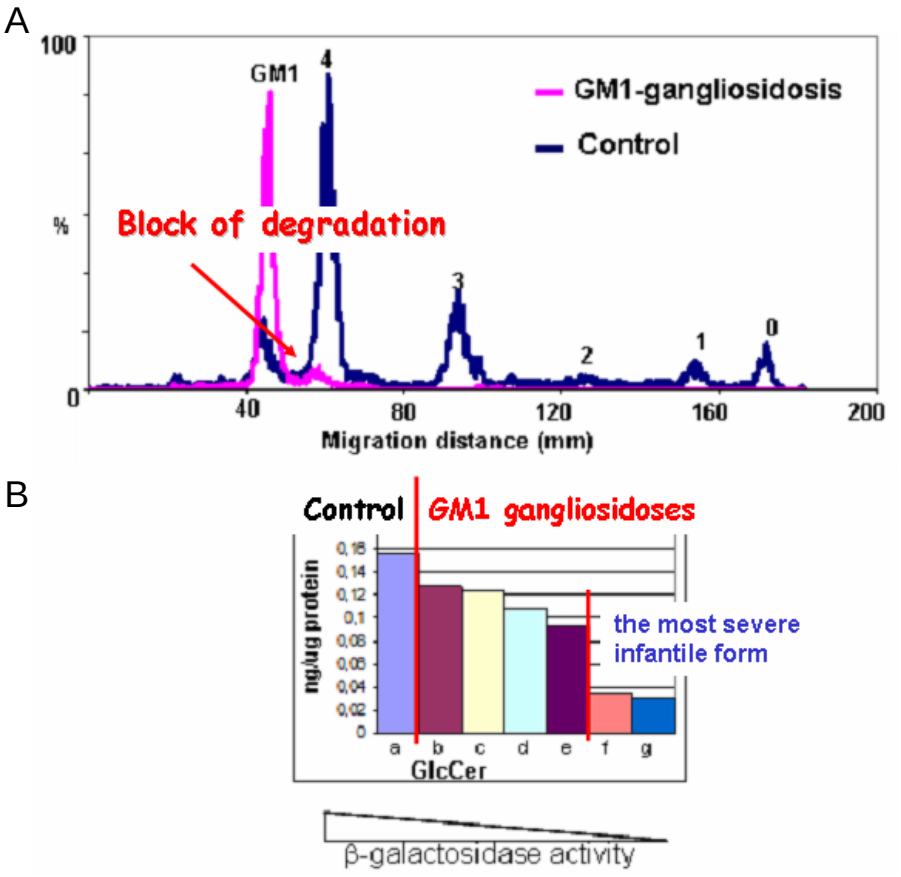

Fig. 23 *In situ* degradation of GM1 ganglioside by skin fibroblasts from control and β-galactosidase deficient patients (different variants of GM1 gangliosidosis).

(A) Degradation pattern of [^{3}H]GM1 ganglioside in control and β-galactosidase-deficient cells evaluated by HPTLC and radioscanner. Degradation products are represented by peaks: 0(ceramide), 1(monohexosylceramide), 2(dihexosylceramide), 3 (GM3 ganglioside) 4 (GM2 ganglioside)

(B) MS/MS quantification of GlcCer product formed from stable isotope-labeled GM1ganglioside precursor (C18:0-D_3);

Clinical GM1 gangliosidosis phenotypes: a-control, b-adult GM1 gangliosidosis, c-Morquio B, d-adult GM1 gangliosidosis/Morquio B, e-juvenile GM1 gangliosidosis, f-infantile GM1 gangliosidosis, and g-infantile GM1 gangliosidosis

Tandem mass spectrometry facilitates accurate quantification of lipids and the results correlate better with the clinical and biochemical phenotypes of individual cases. Moreover, the procedure used to prepare cellular lipids for MS/MS analysis is simple and relatively fast. Unlike radioisotope assays (Asfaw B. et al., 1998), it does not require separation during the pre-analytical phase. Finally, mass labeled substrates can replace radioactive analogues in many cases and thus contribute to the safety and simplification of analytical work.

On the other hand, the experiments with radiolabeled glycolipid substrates reveal the entire metabolic pattern of one specific compound (Fig 23 A) making thus possible to identify relevant metabolites for targeted MS/MS analysis (example Fig.23B)

Reference:

Supplementary publication E

4. CONCLUSIONS (A-D)

This study presents wide range of MS/MS applications in sphingolipid biochemistry and pathobiochemistry focused on LSD. Outputs of the main studied areas are following:

A. Selection and optimization of tandem mass spectrometry methods of sphingolipid analysis

A.1 Optimization of procedures of sphingolipids analysis by mass spectrometry

Ionization and fragmentation reactions for MS/MS analysis of SFL were selected and tested and procedures were optimized. For GSL containing dihydroceramide or sphinganine, new method of MS/MS analysis has been developed based on the important finding that they preferentially lose neutral (oligo)sacharide fragment during CID which is 5 times more effective than production of common fragments with 264 or 282 m/z.

A.2 Biosynthesis of sphingolipid isoforms labeled by specific fatty acids

Enzymatic semisynthesis of specific molecular types of SFL has been developed. Sphingolipid ceramide N-deacylase covalently immobilized on the porous magnetic cellulose catalyzed reverse conversion of corresponding lysoderivatives into fully acylated sphingolipid molecules containing C17:0 fatty acid. High yield of final products was achieved (80% for sulfatide and over 90% for glucosylceramide and GM1 ganglioside). The greatest advantage of the procedure was purity and particularly high isoform purity (97%) of products compared to reactions utilizing soluble nonimmobilized enzyme. Prepared labeled lipids were subsequently used as internal standards in the MS/MS quantitative analysis. In summary, the immobilized SCDase on MMB cellulose has the following advantages: reusability, long-term stability, high rate of conversion, low production of by-products (isoform purity) and effectiveness for

preparation of low amounts of sphingolipids. This system has an universal application for the preparation of SFL specifically labeled in the fatty acid moiety and is useful for studies in various fields of sphingolipid biochemistry.

B. Analysis of sphingolipids in human urine and its use for the differencial diagnosis of lysosomal storage disorders

B.1 Pitfalls of urinary sphingolipids quantification

Evaluation of commonly used reference parameters for the expression of lipid concentrations excluded urinary creatinine as a reference factor for biased results at its low values. Instead of that, we recommended urinary volume or sphingomyelin as more realiable normalizers.

B.2 Quantity of sphingolipids in urine

Quantitative analysis of excreted urinary SFL was demonstrated as important first step in laboratory diagnosis of suspected Sap-B or prosaposin deficiencies.

Massive increase in urinary sulfatides is also typical for MLD while increase in Gb3Cer for Fabry disease. Their diagnoses are then confirmed by enzyme assays and genotyping. However, in cases with defective prosaposin protein routine enzymology fails and the MS/MS proof of multiple SFL excreted in patient´s urine is the basis for the differential laboratory diagnosis and final confirmation by DNA analysis.

B.3 Changes in a pattern of sphingolipid urinary isoforms: new markers for diagnosis of MLD, Fabry disease and prosaposin deficiency

Tandem mass spectrometry examination of sphingolipid molecular species in urine revealed a shift in the isoform pattern to species with longer chain fatty acids (C22:0, C24:0 and C24:1) that can potentially be used for diagnosis of prosaposin and Sap-B deficiences, MLD and Fabry disease. For screening of MLD and prosaposin deficiency,

a new method utilizing selective capture of sulfatides to DEAE membrane has been developed and successfully tested on 50 controls and 21 patients. Long term stability of sulfatides bound to the membrane allows transportation of dry samples and solves the problem of complicated transportation of liquid samples of urine.

C. Analysis of sphingolipids in human tissues and cells - a contribution to general knowledge of pathology of lysosomal storage disorders (C.1-C.3)

Tandem mass spectrometry of SFL in cells and tissue biopsy or autopsy samples was found effective for diagnosis of unsolved cases of LSD. For example, analysis of SFL in the autoptic kidney samples, skin fibroblasts and some other tissues confirmed the diagnosis of Fabry disease and prosaposin deficiency, later verified by DNA analysis. Analysis of Fabry myocardium showed - in addition to the massive accumulation of Gb3Cer, small increase in toxic lyso-derivative which may contribute to the manifestations of disease. These derivatives are supposed to have important regulatory and signaling functions but their role in the lysosomal pathology has not yet been fully elucidated

In the placenta, GM1 ganglioside was for the first time reported in this tissue. MS identified Gb3Cer and GM3 ganglioside as most abundant SFL. The presence of Gb3Cer, GM1 and GM3 gangliosides and cholesterol along with caveolin 1 in the placental blood villous capillaries suggests the existence of caveola-associated microdomains (rafts) at the apical pole of endothelial cells in the placental capillary network. This represents a unique finding pointing to specific features of endothelial apical pole of placental vilous capillaries. The physiological significance of this finding is open for further investigation.

D. *In vitro* and *in situ* enzymology of lysosomal storage disorders by tandem mass spectrometry

D.1 Determination of lysosomal enzyme activities in cell homogenates

Determination of lysosomal β-glucocerebrosidase activity using natural substrate (glucosylceramide with C12:0 fatty acid) confirmed zero activity in fibroblast homogenates from patient with the most serious form of Gaucher type II disease ("collodion baby" phenotype).

D.2 Tandem mass spectrometry monitoring of degradation pathways in living cells

Results from experiments utilizing mass- and radiolabeled substrates for loadings in fibroblast cultures from patients with GM1 gangliosidosis were compared. Both approaches, either using [^{3}H]GM1 ganglioside (radiolabeled) or its C18:0-D_3 analogue (mass labeled), clearly showed hindered degradation of critical GSL.

The use of MS/MS in dynamic metabolic experiments with mass labeled lipid substrates in living cells increases quantification accuracy and throughput why eliminating working risk and restrictions of radioisotope methods.

In conclusion, MS/MS is a robust and sensitive analytical procedure efficient in determining the composition of endogenous sphingolipid classes in various biological materials and is effective in monitoring their metabolic fate. Its ability to establish metabolomic profiles of SFL under normal and pathological conditions in cells and tissues can contribute to a better understanding of the biological significance of sphingolipid molecules.

References

Aerts J. M., Groener J. E., Kuiper S., et al., 2008, *Elevated globotriaosylsphingosine is a hallmark of Fabry disease.* Proc Natl Acad Sci U S A. **105**(8): p. 2812-2817.

Asfaw B., Schindler D., Ledvinova J., et al., 1998, *Degradation of blood group A glycolipid A-6-2 by normal and mutant human skin fibroblasts.* J Lipid Res. **39**(9): p. 1768-1780.

Asfaw B., Ledvinova J., Dobrovolny R., et al., 2002, *Defects in degradation of blood group A and B glycosphingolipids in Schindler and Fabry diseases.* J Lipid Res. **43**(7): p. 1096-1104.

Berna L., Asfaw B., Conzelmann E., et al., 1999, *Determination of urinary sulfatides and other lipids by combination of reversed-phase and thin-layer chromatographies.* Anal Biochem. **269**(2): p. 304-311.

Bilkova Z., Slovakova M., Horak D., et al., 2002, *Enzymes immobilized on magnetic carriers: efficient and selective system for protein modification.* J Chromatogr B Analyt Technol Biomed Life Sci. **770**(1-2): p. 177-181.

Bilkova Z., Castagna A., Zanusso G., et al., 2005, *Immunoaffinity reactors for prion protein qualitative analysis.* Proteomics. **5**(3): p. 639-647.

Bilkova Z., Slovakova M., Minc N., et al., 2006, *Functionalized magnetic micro- and nanoparticles: optimization and application to micro-chip tryptic digestion.* Electrophoresis. **27**(9): p. 1811-1824.

Boscaro F., Pieraccini G., la Marca G., et al., 2002, *Rapid quantitation of globotriaosylceramide in human plasma and urine: a potential application for monitoring enzyme replacement therapy in Anderson-Fabry disease.* Rapid Commun Mass Spectrom. **16**(16): p. 1507-1514.

Bradova V., Smid F., Ulrich-Bott B., et al., 1993, *Prosaposin deficiency: further characterization of the sphingolipid activator protein-deficient sibs. Multiple glycolipid elevations (including lactosylceramidosis), partial enzyme deficiencies and ultrastructure of the skin in this generalized sphingolipid storage disease.* Hum Genet. **92**(2): p. 143-152.

Carter H. E., Glick F. J., Norris W. P., et al., 1947, *Biochemistry of the Sphingolipides .3. Structure of Sphingosine.* J Biol Chem. **170**(1): p. 285-294.

Cech N. B. and Enke C. G., 2001, *Practical implications of some recent studies in electrospray ionization fundamentals.* Mass Spectrom Rev. **20**(6): p. 362-387.

Cole R. B., 2010, *Electrospray and MALDI Mass Spectrometry, Fundamentals, Instrumetation, Practicalities, and Biological Applications.* 2nd ed: John Wiley & Sons, ISBN-13: 978-0471741077

Cox T. M. and Cachon-Gonzalez M. B., 2012, *The cellular pathology of lysosomal diseases.* J Pathol. **226**(2): p. 241-254.

Cyberlipid September 2013 http://www.cyberlipid.org/phlip/aidethudi.htm

D'Angelo G., Polishchuk E., Di Tullio G., et al., 2007, *Glycosphingolipid synthesis requires FAPP2 transfer of glucosylceramide.* Nature. **449**(7158): p. 62-67.

D'Angelo G., Rega L. R., and De Matteis M. A., 2012, *Connecting vesicular transport with lipid synthesis: FAPP2.* Biochim Biophys Acta. **1821**(8): p. 1089-1095.

de Hoffman E. and Stroobant V., 2002, *Mass Spectrometry, Principles and Applications.*2nd ed: John Wiley & Sons, ISBN-13: 978-0471485667

Dekker N., van Dussen L., Hollak C. E., et al., 2011, *Elevated plasma glucosylsphingosine in Gaucher disease: relation to phenotype, storage cell markers, and therapeutic response.* Blood. **118**(16): p. 118-127.

Desnick R. J., Sweeley C. C., and Krivit W., 1970, *A method for the quantitative determination of neutral glycosphingolipids in urine sediment.* J Lipid Res. **11**(1): p. 31-37.
Desnick R. J., Ioannou Y. A., and Eng C. M., 2001, *α-Galactosidase A Deficiency: Fabry Disease*, in *The Metabolic and Molecular Bases of Inherited Disease*, Scriver, et al., Editors., McGraw-Hill: New York. p. 3733-3774.
Domon B. and Costello C. E., 1988, *Structure elucidation of glycosphingolipids and gangliosides using high-performance tandem mass spectrometry.* Biochemistry. **27**(5): p. 1534-1543.
Douglas D. J., 2009, *Linear quadrupoles in mass spectrometry.* Mass Spectrom Rev. **28**(6): p. 937-960.
Dulcks T. and Juraschek R., 1999, *Electrospray as an ionisation method for mass spectrometry.* J Aerosol Sci. **30**(7): p. 927-943.
Fauler G., Rechberger G. N., Devrnja D., et al., 2005, *Rapid determination of urinary globotriaosylceramide isoform profiles by electrospray ionization mass spectrometry using stearoyl-d35-globotriaosylceramide as internal standard.* Rapid Commun Mass Spectrom. **19**(11): p. 1499-1506.
Finn L. S., Zhang M., Chen S. H., et al., 2000, *Severe type II Gaucher disease with ichthyosis, arthrogryposis and neuronal apoptosis: molecular and pathological analyses.* Am J Med Genet. **91**(3): p. 222-226.
Forni S., Fu X., Schiffmann R., et al., 2009, *Falsely elevated urinary Gb3 (globotriaosylceramide, CTH, GL3).* Mol Genet Metab. **97**(1): p. 91.
Futerman A. H., 2006, *Intracellular trafficking of sphingolipids: relationship to biosynthesis.* Biochim Biophys Acta. **1758**(12): p. 1885-1892.
Godfrey D. I. and Rossjohn J., 2011, *New ways to turn on NKT cells.* J Exp Med. **208**(6): p. 1121-1125.
Goni F. M. and Alonso A., 2006, *Biophysics of sphingolipids I. Membrane properties of sphingosine, ceramides and other simple sphingolipids.* Biochim Biophys Acta. **1758**(12): p. 1902-1921.
Grosch S., Schiffmann S., and Geisslinger G., 2012, *Chain length-specific properties of ceramides.* Prog Lipid Res. **51**(1): p. 50-62.
Gu M., Kerwin J. L., Watts J. D., et al., 1997, *Ceramide profiling of complex lipid mixtures by electrospray ionization mass spectrometry.* Anal Biochem. **244**(2): p. 347-356.
Hakomori S., 1981, *Glycosphingolipids in cellular interaction, differentiation, and oncogenesis.* Annu Rev Biochem. **50**: p. 733-764.
Hakomori S., 1998, *Cancer-associated glycosphingolipid antigens: their structure, organization, and function.* Acta Anat (Basel). **161**(1-4): p. 79-90.
Hakomori S. I., 2008, *Structure and function of glycosphingolipids and sphingolipids: recollections and future trends.* Biochim Biophys Acta. **1780**(3): p. 325-346.
Han X. and Gross R. W., 2003, *Global analyses of cellular lipidomes directly from crude extracts of biological samples by ESI mass spectrometry: a bridge to lipidomics.* J Lipid Res. **44**(6): p. 1071-1079.
Han X. and Gross R. W., 2005, *Shotgun lipidomics: electrospray ionization mass spectrometric analysis and quantitation of cellular lipidomes directly from crude extracts of biological samples.* Mass Spectrom Rev. **24**(3): p. 367-412.
Haynes C. A., Allegood J. C., Park H., et al., 2009, *Sphingolipidomics: methods for the comprehensive analysis of sphingolipids.* J Chromatogr B Analyt Technol Biomed Life Sci. **877**(26): p. 2696-2708.

Hermanson G. T., 1996, *Bioconjugate Techniques*. 1st ed: Academic Press, Inc., ISBN-13: 978-0123423368

Hsu F. F., Bohrer A., and Turk J., 1998, *Electrospray ionization tandem mass spectrometric analysis of sulfatide. Determination of fragmentation patterns and characterization of molecular species expressed in brain and in pancreatic islets.* Biochim Biophys Acta. **1392**(2-3): p. 202-216.

Hsu F. F. and Turk J., 2000, *Structural determination of sphingomyelin by tandem mass spectrometry with electrospray ionization.* J Am Soc Mass Spectrom. **11**(5): p. 437-449.

Hu Q., Noll R. J., Li H., et al., 2005, *The Orbitrap: a new mass spectrometer.* J Mass Spectrom. **40**(4): p. 430-443.

Huotari J. and Helenius A., 2011, *Endosome maturation.* EMBO J. **30**(17): p. 3481-3500.

Chatterjee S., Gupta P., Pyeritz R. E., et al., 1984, *Immunohistochemical localization of glycosphingolipid in urinary renal tubular cells in Fabry's disease.* Am J Clin Pathol. **82**(1): p. 24-28.

Chatterjee S., Castiglione E., Kwiterovich P. O., Jr., et al., 1986, *Evaluation of urinary cells in acid cholesteryl ester hydrolase deficiency.* Clin Genet. **29**(5): p. 360-368.

Chester M. A., 1998, *IUPAC-IUB Joint Commission on Biochemical Nomenclature (JCBN). Nomenclature of glycolipids--recommendations 1997.* Eur J Biochem. **257**(2): p. 293-298.

Ii T., Ohashi Y., and Nagai Y., 1995, *Structural elucidation of underivatized gangliosides by electrospray-ionization tandem mass spectrometry (ESIMS/MS).* Carbohydr Res. **273**(1): p. 27-40.

Ito M., Kurita T., and Kita K., 1995, *A novel enzyme that cleaves the N-acyl linkage of ceramides in various glycosphingolipids as well as sphingomyelin to produce their lyso forms.* J Biol Chem. **270**(41): p. 24370-24374.

Ito M., Kita K., Kurita T., et al., 2000, *Enzymatic N-deacylation of sphingolipids.* Methods Enzymol. **311**: p. 297-303.

Iwamori M. and Moser H. W., 1975, *Above-normal urinary excretion of urinary ceramides in Farber's disease, and characterization of their components by high-performance liquid chromatography.* Clin Chem. **21**(6): p. 725-729.

Jennings K. R., 2000, *The changing impact of the collision-induced decomposition of ions on mass spectrometry.* Int J Mass Spectrom. **200**(1-3): p. 479-493.

Jordan J. A. and DeLoia J. A., 1999, *Globoside expression within the human placenta.* Placenta. **20**(1): p. 103-108.

Kanter J. L., Narayana S., Ho P. P., et al., 2006, *Lipid microarrays identify key mediators of autoimmune brain inflammation.* Nat Med. **12**(1): p. 138-143.

Kasper D. C., Herman J., De Jesus V. R., et al., 2010, *The application of multiplexed, multi-dimensional ultra-high-performance liquid chromatography/tandem mass spectrometry to the high-throughput screening of lysosomal storage disorders in newborn dried bloodspots.* Rapid Commun Mass Spectrom. **24**(7): p. 986-994.

Kebarle P., 2000, *A brief overview of the present status of the mechanisms involved in electrospray mass spectrometry.* J Mass Spectrom. **35**(7): p. 804-817.

Kerwin J. L., Tuininga A. R., and Ericsson L. H., 1994, *Identification of molecular species of glycerophospholipids and sphingomyelin using electrospray mass spectrometry.* J Lipid Res. **35**(6): p. 1102-1114.

Kita K., Kurita T., and Ito M., 2001, *Characterization of the reversible nature of the reaction catalyzed by sphingolipid ceramide N-deacylase. A novel form of reverse hydrolysis reaction.* Eur J Biochem. **268**(3): p. 592-602.
Kitatani K., Idkowiak-Baldys J., and Hannun Y. A., 2008, *The sphingolipid salvage pathway in ceramide metabolism and signaling.* Cell Signal. **20**(6): p. 1010-1018.
Kolter T., Winau F., Schaible U. E., et al., 2005, *Lipid-binding proteins in membrane digestion, antigen presentation, and antimicrobial defense.* J Biol Chem. **280**(50): p. 41125-41128.
Kolter T. and Sandhoff K., 2010, *Lysosomal degradation of membrane lipids.* FEBS Lett. **584**(9): p. 1700-1712.
Kolter T., 2011, *A view on sphingolipids and disease.* Chem Phys Lipids. **164**(6): p. 590-606.
Korecka L., Jezova J., Bilkova Z., et al., 2005, *Magnetic enzyme reactors for isolation and study of heterogeneous glycoproteins.* J Magn Magn Mater. **293**(1): p. 349-357.
Korecka L., Jankovicova B., Krenkova J., et al., 2008, *Bioaffinity magnetic reactor for peptide digestion followed by analysis using bottom-up shotgun proteomics strategy.* J Sep Sci. **31**(3): p. 507-515.
Kuhn R. and Wiegandt H., 1963, *Die Konstitution Der Ganglio-N-Tetraose Und Des Gangliosids Gi.* Chemische Berichte-Recueil. **96**(3): p. 866-880.
Lahiri S. and Futerman A. H., 2007, *The metabolism and function of sphingolipids and glycosphingolipids.* Cell Mol Life Sci. **64**(17): p. 2270-2284.
Laviad E. L., Albee L., Pankova-Kholmyansky I., et al., 2008, *Characterization of ceramide synthase 2: tissue distribution, substrate specificity, and inhibition by sphingosine 1-phosphate.* J Biol Chem. **283**(9): p. 5677-5684.
Ledvinova J., Poupetova H., Hanackova A., et al., 1997, *Blood group B glycosphingolipids in alpha-galactosidase deficiency (Fabry disease): influence of secretor status.* Biochim Biophys Acta. **1345**(2): p. 180-187.
Leinekugel P., Michel S., Conzelmann E., et al., 1992, *Quantitative correlation between the residual activity of beta-hexosaminidase A and arylsulfatase A and the severity of the resulting lysosomal storage disease.* Hum Genet. **88**(5): p. 513-523.
Levine T. P., 2007, *A lipid transfer protein that transfers lipid.* J Cell Biol. **179**(1): p. 11-13.
Levy M. and Futerman A. H., 2010, *Mammalian ceramide synthases.* IUBMB Life. **62**(5): p. 347-356.
Li S. C., Kihara H., Serizawa S., et al., 1985, *Activator protein required for the enzymatic hydrolysis of cerebroside sulfate. Deficiency in urine of patients affected with cerebroside sulfatase activator deficiency and identity with activators for the enzymatic hydrolysis of GM1 ganglioside and globotriaosylceramide.* J Biol Chem. **260**(3): p. 1867-1871.
Li Y., Scott C. R., Chamoles N. A., et al., 2004, *Direct multiplex assay of lysosomal enzymes in dried blood spots for newborn screening.* Clin Chem. **50**(10): p. 1785-1796.
Lieser B., Liebisch G., Drobnik W., et al., 2003, *Quantification of sphingosine and sphinganine from crude lipid extracts by HPLC electrospray ionization tandem mass spectrometry.* J Lipid Res. **44**(11): p. 2209-2216.

Lyden T. W., Anderson C. L., and Robinson J. M., 2002, *The endothelium but not the syncytiotrophoblast of human placenta expresses caveolae.* Placenta. **23**(8-9): p. 640-652.
Maceyka M., Milstien S., and Spiegel S., 2009, *Sphingosine-1-phosphate: the Swiss army knife of sphingolipid signaling.* J Lipid Res. **50 Suppl**: p. S272-276.
Maceyka M., Harikumar K. B., Milstien S., et al., 2012, *Sphingosine-1-phosphate signaling and its role in disease.* Trends Cell Biol. **22**(1): p. 50-60.
Mano N., Oda Y., Yamada K., et al., 1997, *Simultaneous quantitative determination method for sphingolipid metabolites by liquid chromatography/ionspray ionization tandem mass spectrometry.* Anal Biochem. **244**(2): p. 291-300.
Martin O. C. and Pagano R. E., 1994, *Internalization and sorting of a fluorescent analogue of glucosylceramide to the Golgi apparatus of human skin fibroblasts: utilization of endocytic and nonendocytic transport mechanisms.* J Cell Biol. **125**(4): p. 769-781.
Masserini M. and Ravasi D., 2001, *Role of sphingolipids in the biogenesis of membrane domains.* Biochim Biophys Acta. **1532**(3): p. 149-161.
Mayor S. and Pagano R. E., 2007, *Pathways of clathrin-independent endocytosis.* Nat Rev Mol Cell Biol. **8**(8): p. 603-612.
McDonnell L. A. and Heeren R. M., 2007, *Imaging mass spectrometry.* Mass Spectrom Rev. **26**(4): p. 606-643.
McLuckey S. A. and Wells J. M., 2001, *Mass analysis at the advent of the 21st century.* Chem Rev. **101**(2): p. 571-606.
Mikami M., Takamatsu K., Tanaka J., et al., 1993, *Characteristic alteration in the concentration of IV 3NeuAc alpha-nLc4Cer in the villi of human placenta during the gestational period.* Placenta. **14**(4): p. 407-416.
Mills K., Johnson A., and Winchester B., 2002, *Synthesis of novel internal standards for the quantitative determination of plasma ceramide trihexoside in Fabry disease by tandem mass spectrometry.* FEBS Lett. **515**(1-3): p. 171-176.
Mills K., Eaton S., Ledger V., et al., 2005, *The synthesis of internal standards for the quantitative determination of sphingolipids by tandem mass spectrometry.* Rapid Commun Mass Spectrom. **19**(12): p. 1739-1748.
Mitsutake S., Kita K., Okino N., et al., 1997, *[14C]ceramide synthesis by sphingolipid ceramide N-deacylase: new assay for ceramidase activity detection.* Anal Biochem. **247**(1): p. 52-57.
Mitsutake S., Kita K., Nakagawa T., et al., 1998, *Enzymatic synthesis of 14C-glycosphingolipids by reverse hydrolysis reaction of sphingolipid ceramide N-deacylase: detection of endoglycoceramidase activity in a seaflower.* J Biochem. **123**(5): p. 859-863.
Murphy R. C., Fiedler J., and Hevko J., 2001, *Analysis of nonvolatile lipids by mass spectrometry.* Chem Rev. **101**(2): p. 479-526.
Neumann S. and van Meer G., 2008, *Sphingolipid management by an orchestra of lipid transfer proteins.* Biol Chem. **389**(11): p. 1349-1360.
Nguyen G. K. and Smith R., 2004, *Repair renal tubular cells: a potential false-positive diagnosis in urine cytology.* Diagn Cytopathol. **31**(5): p. 342-346.
Nichols B., 2003, *Caveosomes and endocytosis of lipid rafts.* J Cell Sci. **116**(Pt 23): p. 4707-4714.
Olling A., Breimer M. E., Peltomaa E., et al., 1998, *Electrospray ionization and collision-induced dissociation time-of-flight mass spectrometry of neutral glycosphingolipids.* Rapid Commun Mass Spectrom. **12**(10): p. 637-645.

Pang H., Le P. U., and Nabi I. R., 2004, *Ganglioside GM1 levels are a determinant of the extent of caveolae/raft-dependent endocytosis of cholera toxin to the Golgi apparatus.* J Cell Sci. **117**(Pt 8): p. 1421-1430.
Parton R. G., 1994, *Ultrastructural localization of gangliosides; GM1 is concentrated in caveolae.* J Histochem Cytochem. **42**(2): p. 155-166.
Paschke E., Fauler G., Winkler H., et al., 2011, *Urinary total globotriaosylceramide and isoforms to identify women with Fabry disease: a diagnostic test study.* Am J Kidney Dis. **57**(5): p. 673-681.
Perry R. H., Cooks R. G., and Noll R. J., 2008, *Orbitrap mass spectrometry: instrumentation, ion motion and applications.* Mass Spectrom Rev. **27**(6): p. 661-699.
Platt F. M. and Lachmann R. H., 2009, *Treating lysosomal storage disorders: current practice and future prospects.* Biochim Biophys Acta. **1793**(4): p. 737-745.
Porter M. T., Fluharty A. L., Trammell J., et al., 1971, *A correlation of intracellular cerebroside sulfatase activity in fibroblasts with latency in metachromatic leukodystrophy.* Biochem Biophys Res Commun. **44**(3): p. 660-666.
Postle A. D., 2008, *Phospholipid Profiling*, in *Metabolomics, Metabonomics and Metabolite Profiling*, Griffiths, Editor, Royal Society of Chemistry: Cambridge. p. 116-133.
Sakuraba H., Sawada M., Matsuzawa F., et al., 2006, *Molecular pathologies of and enzyme replacement therapies for lysosomal diseases.* CNS Neurol Disord Drug Targets. **5**(4): p. 401-413.
Sandhoff K., Kolter T., and Harzer K., 2001, *Sphingolipid Activator Proteins*, in *The Metabolic and Molecular Bases of Inherited Disease*, Scriver, et al., Editors., McGraw-Hill: New York. p. 3371-3388.
Sandhoff K. and Kolter T., 2003, *Biosynthesis and degradation of mammalian glycosphingolipids.* Philos Trans R Soc Lond B Biol Sci. **358**(1433): p. 847-861.
Scigelova M. and Makarov A., 2006, *Orbitrap mass analyzer--overview and applications in proteomics.* Proteomics. **6 Suppl 2**: p. 16-21.
Shaner R. L., Allegood J. C., Park H., et al., 2009, *Quantitative analysis of sphingolipids for lipidomics using triple quadrupole and quadrupole linear ion trap mass spectrometers.* J Lipid Res. **50**(8): p. 1692-1707.
Scherer M., Leuthauser-Jaschinski K., Ecker J., et al., 2010, *A rapid and quantitative LC-MS/MS method to profile sphingolipids.* J Lipid Res. **51**(7): p. 2001-2011.
Schnaar R. L., Suzuki A., and Stanley P., 2009, *Glycosphingolipids,* in *Essentials of Glycobiology*, Varki, et al., Editors., Cold Spring Harbor Laboratory Press: New York. p. 129-141.
Schueler U. H., Kolter T., Kaneski C. R., et al., 2003, *Toxicity of glucosylsphingosine (glucopsychosine) to cultured neuronal cells: a model system for assessing neuronal damage in Gaucher disease type 2 and 3.* Neurobiol Dis. **14**(3): p. 595-601.
Schulze H., Kolter T., and Sandhoff K., 2009, *Principles of lysosomal membrane degradation: Cellular topology and biochemistry of lysosomal lipid degradation.* Biochim Biophys Acta. **1793**(4): p. 674-683.
Schwarzmann G., Hoffmann-Bleihauer P., Schubert J., et al., 1983, *Incorporation of ganglioside analogues into fibroblast cell membranes. A spin-label study.* Biochemistry. **22**(21): p. 5041-5048.
Sleno L. and Volmer D. A., 2004, *Ion activation methods for tandem mass spectrometry.* J Mass Spectrom. **39**(10): p. 1091-1112.

Solder E., Rohr I., Kremser C., et al., 2009, *Imaging of placental transport mechanisms: a review.* Eur J Obstet Gynecol Reprod Biol. **144 Suppl 1**: p. S114-120.
Sonderfeld S., Conzelmann E., Schwarzmann G., et al., 1985, *Incorporation and metabolism of ganglioside GM2 in skin fibroblasts from normal and GM2 gangliosidosis subjects.* Eur J Biochem. **149**(2): p. 247-255.
Spacil Z., Elliott S., Reeber S. L., et al., 2011, *Comparative triplex tandem mass spectrometry assays of lysosomal enzyme activities in dried blood spots using fast liquid chromatography: application to newborn screening of Pompe, Fabry, and Hurler diseases.* Anal Chem. **83**(12): p. 4822-4828.
Stevenson C. E., Takabe K., Nagahashi M., et al., 2011, *Targeting sphingosine-1-phosphate in hematologic malignancies.* Anticancer Agents Med Chem. **11**(9): p. 794-798.
Strasberg P., Grey A., Warren I., et al., 1989, *Simultaneous fractionation of four placental neutral glycosphingolipids with a continuous gradient.* J Lipid Res. **30**(1): p. 121-127.
Suzuki K., 1998, *Twenty five years of the "psychosine hypothesis": a personal perspective of its history and present status.* Neurochem Res. **23**(3): p. 251-259.
Svennerholm L., 1963, *Chromatographic Separation of Human Brain Gangliosides.* J Neurochem. **10**: p. 613-623.
Takabe K., Paugh S. W., Milstien S., et al., 2008, *"Inside-out" signaling of sphingosine-1-phosphate: therapeutic targets.* Pharmacol Rev. **60**(2): p. 181-195.
Taki T., Matsuo K., Yamamoto K., et al., 1988, *Human placenta gangliosides.* Lipids. **23**(3): p. 192-198.
Takizawa T., Anderson C. L., and Robinson J. M., 2005, *A novel Fc gamma R-defined, IgG-containing organelle in placental endothelium.* J Immunol. **175**(4): p. 2331-2339.
Taylor P. J., 2005, *Matrix effects: the Achilles heel of quantitative high-performance liquid chromatography-electrospray-tandem mass spectrometry.* Clin Biochem. **38**(4): p. 328-334.
Tedde G., Pirino A., Esposito F., et al., 1990, *Mechanisms of regulation of the capillary bed in the human chorionic villi.* Arch Ital Anat Embriol. **95**(2): p. 105-112.
Turecek F., Scott C. R., and Gelb M. H., 2007, *Tandem mass spectrometry in the detection of inborn errors of metabolism for newborn screening.* Methods Mol Biol. **359**: p. 143-157.
Ulrich-Bott B. and Wiegandt H., 1984, *Micellar properties of glycosphingolipids in aqueous media.* J Lipid Res. **25**(11): p. 1233-1245.
van Meer G., 2011, *Dynamic transbilayer lipid asymmetry.* Cold Spring Harb Perspect Biol. **3**(5): p. 1-11
Vitner E. B., Platt F. M., and Futerman A. H., 2010, *Common and uncommon pathogenic cascades in lysosomal storage diseases.* J Biol Chem. **285**(27): p. 20423-20427.
von Figura K., Gieselmann V., and Jaeken J., 2001, *Metachromatic Leukodystrophy*, in *The Metabolic and Molecular Bases of Inherited Disease*, Scriver, et al., Editors., McGraw-Hill: New York. p. 3695-3724.
Warnock D. G., Valbuena C., West M., et al., 2010, *Renal Manifestation of Fabry Disease*, in *Fabry Disease*, Elstein, Altarescu, and Beck, Editors., Springer Science+Business Media B.V.: Dordrecht. p. 211-243.
Wennekes T., van den Berg R. J., Boot R. G., et al., 2009, *Glycosphingolipids--nature, function, and pharmacological modulation.* Angew Chem Int Ed Engl. **48**(47): p. 8848-8869.

Westerlund B. and Slotte J. P., 2009, *How the molecular features of glycosphingolipids affect domain formation in fluid membranes.* Biochim Biophys Acta. **1788**(1): p. 194-201.

Whitfield P. D., Sharp P. C., Johnson D. W., et al., 2001, *Characterization of urinary sulfatides in metachromatic leukodystrophy using electrospray ionization-tandem mass spectrometry.* Mol Genet Metab. **73**(1): p. 30-37.

Yamaguchi Y., Sasagasako N., Goto I., et al., 1994, *The Synthetic Pathway for Glucosylsphingosine in Cultured Fibroblasts.* J Biochem. **116**(3): p. 704-710.

Yamakawa T., Kiso N., Handa S., et al., 1962, *On the structure of brain cerebroside sulfuric ester and ceramide dihexoside of erythrocytes.* J Biochem. **52**: p. 226-227.

Yamakawa T., 1996, *A reflection on the early history of glycosphingolipids.* Glycoconj J. **13**(2): p. 123-126.

Zhou X., Turecek F., Scott C. R., et al., 2001, *Quantification of cellular acid sphingomyelinase and galactocerebroside beta-galactosidase activities by electrospray ionization mass spectrometry.* Clin Chem. **47**(5): p. 874-881.

LIST OF RESEARCH FELLOWSHIPS, GRANT PROJECTS, SCIENTIFIC AWARDS, TEACHING ACIVITIES, MEMBERSHIPS, CERTIFIED COURSES, PRESENTATIONS AND PUBLICATIONS

Research fellowship

Prof. Frank Turecek's research group, Department of Chemistry, University of Washington, Seattle, Washington, USA – status: visiting scientist – 17.9.-21.12.2007
- Application of mass spectrometry in enzymology of LSD

Grant projects

Principal investigator of the grant project of the Grant Agency of the Charles University in Prague the project No. 19509 - Tandem mass spectrometry of sphingolipids: isoform profile analysis and its aplication in diagnosis and studies of inherited disorders of sphingolipid metabolism (2009-2011) - final rating: exceptionally good

Coinvestigator of the grant project ot the Internal Grant Agency of the Ministry of Health the project No. NT/12239 - Niemann-Pick disease type C : clinical, molecular genetic, biochemical and morphological study. Development of new diagnostic and predictive algorithms (2011-2015), Principal investigator: MUDr. Martin Hřebíček, PhD

Coinvestigator of the grant project ot the Internal Grant Agency of the Ministry of Health the project No. NT/14015 - Progress in methods of laboratory diagnostics of inherited lysosomal neurodegenerative disorders (2013-2015), Principal investigator: RNDr. Jana Ledvinová, PhD

Scientific awards

3rd price from Scientia Foundation for best scientific works of students from the First Faculty of Medicine, Charles University in Prague; published in the year 2009

Teaching activities

from 2010 - participation in the teaching of the elective subject Glycolipids (Department of Biochemistry, Faculty of Science, Charles University in Prague, pregraduate students from the 4th and 5th years of studies, Master degree study program)

Memberships

from 2006 - participation in the member-group Mnr 100 of European Study Group of Inherited Disorders
from 2007 - the Czech Society for Biochemistry and Molecular Biology

from 2011 - the Czech Society for Mass Spectrometry

Certified courses

June 2008 - FEBS Workshop: Lipids as regulators of cell function, Island of Spetses, Greece (Spetses Membrane Summer Schools)

Presentations

Oral presentations
May 2007 - 22nd Working Days Inherited Metabolic Diseases, Průhonice, Praha - Tandem MS screening of urinary lipids: first step in laboratory diagnosis of saposin deficiences

June 2007 – Final conference of the PhD project GAČR 303/03/H065, KDDL, 1.LF UK, Praha : MS/MS of sphingolipids: efficient screening method for saposin deficiences

February 2008 – MassSpec-Forum Vienna-2008, Faculty of Chemistry, University of Vienna, Vienna, Austria: Lysosomal storage disorders: MS/MS screening method for sap-B and pSap deficiencies

April 2009 - European Consensus on Diagnostics in Fabry Disease, 1st Expert meeting: Diagnostic use and value of Gb3 and Lyso-Gb3 in Fabry disease, Bad Nauheim, Germany: MS/MS evaluation of Gb3Cer in M. Fabry and other LSDs and diagnostic value of this analysis

September 2010 - 11th School of Mass Spectrometry, Hotel Horizont, Pec pod Sněžkou: Tandemová hmotnostní spektrometrie sfingolipidů s aplikací pro metabolické studie a diagnostiku sfingolipidos

October 2011 - 1st Annual Conference of the Czech Society for Mass Spectrometry, Fakulta vojenského zdravotnictví Univerzity Obrany, Hradec Králové: Tandemová hmotnostní spektrometrie sfingolipidů s aplikací v diagnostice sfingolipidos: nové biomarkery v moči

May 2012, 27th Working Days Inherited Metabolic Diseases 2012, Košice, Slovak Republic: MS/MS Profiling of Sulfatide Isoforms in Urinary Spots on a DEAE Membrane for Diagnosis of Metachromatic Leukodystrophy and Another Sulfatidoses

June 2012 - 2nd Czech Lipidomics Conference and Workshop ICCTI a INER, Hotel Prestige, Znojmo, Česká republika: Changes in urinary isoform profile in metachromatic leukodystrophy: diagnostic application and pathological basis

July 2013 - 3rd European Lipidomics Meeting, Faculty of Chemical Technology, University of Pardubice, Pardubice, Czech Republic: Lipidomics in diagnosis and research of lysosomal storage disorders

Posters: 21 poster presentations
(23rd Working Days Inherited Metabolic Diseases, Senec Slovak Republic - awarded the best poster: *Immobilized sphingolipid ceramide N-deacylase: new way for semisynthesis of specific sphingolipids)*

Publications

Original Articles:
Kuchar L., Rotkova J., Asfaw B., et al., *Semisynthesis of C17:0 isoforms of sulphatide and glucosylceramide using immobilised sphingolipid ceramide N-deacylase for application in analytical mass spectrometry.* Rapid Commun Mass Spectrom, 2010. **24**(16): p. 2393-2399
(IF 2,509**)**

Kuchar L., Ledvinova J., Hrebicek M., et al., *Prosaposin deficiency and saposin B deficiency (activator-deficient metachromatic leukodystrophy): report on two patients detected by analysis of urinary sphingolipids and carrying novel PSAP gene mutations.* Am J Med Genet A, 2009. **149A**(4): p. 613-621
(IF 2,304**)**

Kuchar L., Asfaw B., Poupetova H., et al., *Direct tandem mass spectrometric profiling of sulfatides in dry urinary samples for screening of metachromatic leukodystrophy.* Clin Chim Acta, 2013. **425C**: p. 153-159
(IF 2,850**)**

Hulkova H., Ledvinova J., Kuchar L., et al., *Glycosphingolipid profile of the apical pole of human placental capillaries: the relevancy of the observed data to Fabry disease.* Glycobiology, 2012. **22**(5): p. 725-732
(IF 3,537**)**

Musalkova D., Lukas J., Majer F., et al., *Rapid isolation of lysosomal membranes from cultured cells.* Folia Biol (Praha), 2013. **59**(1): p. 41-46
(IF 1,219**)**

Chapter in the Book
Kuchar L., Asfaw B., and Ledvinova J., *Tandem Mass Spectrometry of Sphingolipids: Application in Metabolic Studies and Diagnosis of Inherited Disorders of Sphingolipid Metabolism*, in *Tandem Mass Spectrometry - Applications and Principles*, Prasain, Editor 2012, InTech: Rijeka. p. 739-768

Journal published conference abstracts:
Kuchar L., Hlavatá J., Asfaw B., et al., *Changed isoform profiles in sphingolipid storage disorders: a new pre-diagnostic tool.* Int J Clin Pharm Th, 2010. **48**(Suppl. 1):p. S76
An extended conference abstract to request of Editors (IF 1.200)

***Published consensus from the expert meetings**:*
Gal A., Hughes D. A., and Winchester B., *Toward a consensus in the laboratory diagnostics of Fabry disease - recommendations of a European expert group.* J Inherit Metab Dis, 2011. **34**(2): p. 509-14 (*L.K. is on the list of invited members of the expert team).*

Manuscripts in preparation
Renal lipid distribution in Fabry mouse by mass spectrometry and imunohistochemical imaging, *Ladislav Kuchar, Helena Faltyskova, Lukas Krasny, Robert Dobrovolny, Helena Hůlková, Jana Ledvinova, Michael Volny, Martin Strohalm, Robert J. Desnick and Vladimir Havlicek*

Pancreas – the underexplored organ in Fabry disease: revival
of blood group history in the second patient, blood group B secretor
J. Rybová, J. Ledvinová, H. Hůlková, L. Kuchař, B. Asfaw, M. Elleder, L.Skultety, V. Havlíček

SUPPLEMENTARY PUBLICATIONS

Publictions in Impacted Journals related to the topic of PhD thesis

A – Kuchar L., Rotkova J., Asfaw B., et al., *Semisynthesis of C17:0 isoforms of sulphatide and glucosylceramide using immobilised sphingolipid ceramide N-deacylase for application in analytical mass spectrometry.* Rapid Commun Mass Spectrom, 2010. **24**(16): p. 2393-2399

B – Kuchar L., Ledvinova J., Hrebicek M., et al., *Prosaposin deficiency and saposin B deficiency (activator-deficient metachromatic leukodystrophy): report on two patients detected by analysis of urinary sphingolipids and carrying novel PSAP gene mutations.* Am J Med Genet A, 2009. **149A**(4): p. 613-621

C – Kuchar L., Asfaw B., Poupetova H., et al., *Direct tandem mass spectrometric profiling of sulfatides in dry urinary samples for screening of metachromatic leukodystrophy.* Clin Chim Acta, 2013. **425C**: p. 153-159

D – Hulkova H., Ledvinova J., Kuchar L., et al., *Glycosphingolipid profile of the apical pole of human placental capillaries: the relevancy of the observed data to Fabry disease.* Glycobiology, 2012. **22**(5): p. 725-732

Non impacted publications related to topic of this PhD thesis

E – **Chapter in the Book**
Kuchar L., Asfaw B., and Ledvinova J., *Tandem Mass Spectrometry of Sphingolipids: Application in Metabolic Studies and Diagnosis of Inherited Disorders of Sphingolipid Metabolism*, in *Tandem Mass Spectrometry - Applications and Principles*, Prasain, Editor 2012, InTech: Rijeka. p. 739-768

F – **Journal published conference abstracts**
Kuchar L., Hlavatá J., Asfaw B., et al., *Changed isoform profiles in sphingolipid storage disorders: a new pre-diagnostic tool.* Int J Clin Pharm Th, 2010. **48**(Suppl. 1):p. S76
An extended conference abstract to request of Editors

Publictions in Impacted Journals not related to topic of this PhD thesis

G – Musalkova D., Lukas J., Majer F., et al., *Rapid isolation of lysosomal membranes from cultured cells.* Folia Biol (Praha), 2013. **59**(1): p. 41-46

Published consensus from the expert meetings

H – Gal A., Hughes D. A., and Winchester B., *Toward a consensus in the laboratory diagnostics of Fabry disease - recommendations of a European expert group.* J Inherit Metab Dis, 2011. **34**(2): p. 509-14 (*L.K. is on the list of invited members of the expert team).*

SUPPLEMENTARY PUBLICATIONS

Publications in impacted journals related to topic of this PhD thesis

Supplementary publication A

Kuchar L., Rotkova J., Asfaw B., et al., *Semisynthesis of C17:0 isoforms of sulphatide and glucosylceramide using immobilised sphingolipid ceramide N-deacylase for application in analytical mass spectrometry.* Rapid Commun Mass Spectrom, 2010. **24**(16): p. 2393-2399

RAPID COMMUNICATIONS IN MASS SPECTROMETRY
Rapid Commun. Mass Spectrom. 2010; **24**: 2393–2399
Published online in Wiley InterScience (www.interscience.wiley.com) DOI: 10.1002/rcm.4659

RCM

Semisynthesis of C17:0 isoforms of sulphatide and glucosylceramide using immobilised sphingolipid ceramide N-deacylase for application in analytical mass spectrometry

L. Kuchař[1], J. Rotková[2], B. Asfaw[1], J. Lenfeld[3], D. Horák[3], L. Korecká, Z. Bílková[2] and J. Ledvinová[1]***

[1]Institute of Inherited Metabolic Disorders, General Faculty Hospital and Charles University First Faculty of Medicine, Prague, Czech Republic
[2]University of Pardubice, Faculty of Chemical Technology, Department of Biological and Biochemical Sciences, Academy of Sciences of the Czech Republic, Prague, Czech Republic
[3]Institute of Macromolecular Chemistry, Academy of Sciences of the Czech Republic, Prague, Czech Republic

Received 21 April 2010; Revised 2 June 2010; Accepted 7 June 2010

Sphingolipid ceramide N-deacylase (SCDase, EC 3.5.1.69) is a hydrolytic enzyme isolated from *Pseudomonas* sp. TK 4. In addition to its primary deacylation function, this enzyme is able to reacylate lyso-sphingolipids under specific conditions. We immobilised this enzyme on magnetic macroporous cellulose and used it to semisynthesise C17:0 glucosylceramide and C17:0 sulphatide, which are required internal standards for quantification of the corresponding glycosphingolipids (GSL) by tandem mass spectrometry. A high rate of conversion was achieved for both lipids (80% for C17:0 sulphatide and 90% for C17:0 glucosylceramide). In contrast to synthesis with a soluble form of the enzyme, use of immobilised SCDase significantly reduced the contamination of the sphingolipid products with other isoforms, so further purification was not necessary. Our method can be effectively used for the simple preparation of specifically labelled sphingolipids of high isoform purity for application in mass spectrometry. Copyright © 2010 John Wiley & Sons, Ltd.

Sphingolipids (SFL) are complex molecules composed of a hydrophobic ceramide (N-acylsphingoid) and a hydrophilic portion, with either a saccharide or phosphorylcholine moiety. In glycosphingolipids (GSL), oligosaccharide chains of varying complexity are attached by their reducing end to the terminal hydroxyl group of the sphingoid.[1]

Recently, tandem mass spectrometry (MS/MS) has become very useful for analysis and quantification of sphingolipids in different biological materials. For this purpose, sphingolipid species that are not abundant in nature are required as internal standards (IST).

In recent years, an enzymatic reaction catalyzed by sphingolipid ceramide N-deacylase (SCDase, EC 3.5.1.69) was found to be effective for the preparation of specific sphingolipid molecules.[2–7] The enzyme is an acid hydrolase isolated from the culture medium of the bacteria *Pseudomonas* sp. TK4 by ammonium sulphate precipitation and high-performance liquid chromatography (HPLC) purification. Its substrate specificity is not identical to that of acid ceramidase (EC 3.5.1.23).[4]

*Correspondence to: J. Ledvinová, Ke Karlovu 2 (Building D), 128 00 Prague 2, Czech Republic.
E-mail: jledvin@cesnet.cz
**Correspondence to: Z. Bílková, Studentska 95, 532 10 Pardubice, Czech Republic. E-mail: Zuzana.Bilkova@upce.cz

The molecular mass of the SCDase protein is 52 kDa. SCDase has optimal activity at pH 5–6 (hydrolysis) and is stable between pH 4–9; it is potently inhibited by Hg^{2+}, Cu^{2+} and Zn^{2+}, maintains 80% of its initial activity after 30 min at 60°C and can be stored at −85°C for 2 months without any loss of activity. The addition of Triton X-100 at concentrations of 0.4–0.8% increases its hydrolytic activity by approximately 10-fold.[4]

SCDase catalyses the conversion of GSL into lyso-derivatives (N-deacylated GSL, lyso-GSL) under acidic conditions (pH 5, detergent concentrations up to 0.8%) by splitting the amide bond between the sphingoid and fatty acid in the ceramide. Under modified conditions (pH 7, detergent concentrations up to 0.1%) the enzyme catalyses the reverse reaction, i.e., reacylation. The effectiveness of the condensation is influenced by the type of lyso-GSL and fatty acid.[5]

This work was primarily prompted by the demand for convenient sphingolipid internal standards (ISTs) for MS/MS analysis, which is applicable to laboratory diagnostics of inherited lysosomal disorders of sphingolipid storage (especially prosaposin and saposin B deficiencies, metachromatic leukodystrophy, and Gaucher and Fabry diseases).[2,6–10]

SCDase is the most important and expensive component of the reaction mixture, so we looked for conditions that would enable us to reuse the enzyme, e.g., by utilising the principle of enzyme immobilisation on the surface of solid particles.

The use of carriers with magnetic properties overcomes problems associated with liquid gel slurries in high-throughput and standard laboratory applications.[11] Magnetic particles provide an universal system that is consistent, stable, easy to handle and exceptionally flexible compared to standard chromatographic resins. These particles serve as carriers of surface-immobilised enzymes and can be easily recovered in a magnetic field when the reaction is terminated.

Here we describe the immobilisation of SCDase on magnetic carriers using standard procedures, and its utilisation for the preparation of the specific sphingolipid isoforms C17:0 SGalCer and C17:0 GlcCer as ISTs for MS/MS.

EXPERIMENTAL

Abbreviations

Gangliotetraosylceramide – Gg4Cer, globotriaosylceramide – Gb3Cer, glucosylceramide – GlcCer, sulphatide - SGalCer. For deacylated derivatives, the prefix lyso- is used, i.e., lyso-globotriaosylceramide – lyso-Gb3Cer. Glycosphingolipids are abbreviated according to the IUPAC-IUB Commission on Biochemical Nomenclature.[12]

Materials

Sphingolipid ceramide N-deacylase (SCDase) was purchased from TAKARA Bio. Inc. (Otsu, Japan). Magnetic macroporous cellulose beads (op. L 1680; 125–250 μm) were kindly provided by Dr. J. Lenfeld from the Institute of Macromolecular Chemistry, Academy of Sciences of the Czech Republic, Prague, Czech Republic, and are available upon request by e-mail (lenfeld@imc.cas.cz). Macroporous PERLOZA® MT 100 cellulose beads provided by Iontosorb (Prague, Czech Republic) can be used as an equivalent alternative. The enzyme substrates Gg4Cer, lyso-Gb3Cer and stearic acid (C18:0) used for optimisation reactions and lyso-GlcCer were purchased from Matreya LLC (Pleasant Gap, PA, USA). Lyso-SGalCer was from Calbiochem-Novabiochem GmbH (Schwalbach, Germany), and margaric acid (C17:0) acid was obtained from Larodan Fine Chemicals AB (Malmö, Sweden). Sodium cyanoborohydride ($NaCNBH_3$) and bovine serum albumin (BSA) were from Sigma-Aldrich Co. (St. Louis, MO, USA). Sodium periodate was from Fluka (Seelze, Germany). HPTLC-Fertigplatten, Kieselgel 60 and orcinol were purchased from Merck Chemicals Ltd. (Darmstadt, Germany). All other chemicals were of p.a. grade quality. Organic solvents for tandem mass spectrometry were of mass spectrometry grade.

Substrates and products of the enzyme reaction were evaluated with a CAMAG II TLC scanner (Camag Scientific, Switzerland) equipped with CATS3 analytical software and an AB/MDS SCIEX API 3200 triple quadrupole tandem mass spectrometer (Foster City, CA, USA) equipped with Analyst 1.4.1 software.

Immobilisation of sphingolipid ceramide N-deacylase on magnetic macroporous bead cellulose (MMB cellulose)

SCDase was immobilised onto MMB cellulose using a standard enzyme immobilisation procedure.[13,14] Briefly: 100 μL of settled particles was washed five times with distilled water and then was activated with $NaIO_4$ by mixing with an equal volume (100 μL) of freshly prepared 0.2 M $NaIO_4$ before starting the binding reaction. The mixture was incubated for 1.5 h at room temperature while mixing on a rotator (Multi Bio RS-24, Biosan, Riga, Latvia). The activated particles were washed 10 times with 0.1 M phosphate buffer at pH 7 (PB), and then 250 mI.U. of SCDase (5 mI.U./μL) and 200 μL of PB were added. The mixture was incubated for 10 min at room temperature while mixing on a rotator. Next, 200 μL of $NaCNBH_3$ was added to stabilise the formed Schiff base, and the reaction was incubated overnight on a rotator at 4°C. The particles with immobilised enzyme were washed with PB, followed by 1 M NaCl in PB and finally with PB again. After that, the activation of immobilised SCDase was done by incubation with 100 nmol of Gg4Cer substrate in 300 μL of 50 mM acetate buffer containing 0.8% Triton X-100 at 37°C for 1 h. Then the products were washed three times with 50 mM phosphate buffer (pH 7) containing 0.1% Triton X-100 (storage buffer). Immobilised SCDase was stored in storage buffer at 4°C.

Examination of SCDase catalytic activity: hydrolysis and synthesis for estimation of optimum molar ratio of substrates

For examination of the *hydrolytic activity* of the immobilised SCDase, the substrate Gg4Cer was incubated with the bio-activated particles using the same standard procedure as described for the soluble enzyme.[3,4] Briefly, 20 nmol of Gg4Cer with 20 μL of settled MMB cellulose containing bound SCDase was incubated in 50 mM acetate buffer (pH 5) with 0.8% Triton X-100 for 30 min at 37°C with mixing on a rotator.

The *reverse synthetic reaction* was performed under standard conditions[5] using lyso-Gb3Cer as the substrate because a high rate of conversion has been reported for soluble enzyme.[6] To optimise the reaction, different molar ratios of the precursors, lyso-derivative and fatty acid were tested. Briefly, SCDase immobilised on MMB cellulose (100 μL of settled particles) was distributed into four tubes. Each 25 μL aliquot was mixed with a precise molar ratio of the substrates (20 nmol of the lyso-Gb3Cer mixed with C18:0 fatty acid in molar ratios of 1:1, 1:2, 1:3 and 1:4) in 200 μl of phosphate buffer (pH 7.0) containing 0.1% Triton X-100. The reaction was incubated for 20 h at 37°C while mixing on a rotator.[5]

Magnetic particles were separated with a magnetic separator (Dynal MPC-S, Dynal Biotech ASA, Oslo, Norway), and the supernatant containing the reaction product was evaporated under a stream of nitrogen and resuspended in 300 μL of chloroform/methanol (2:1, v/v; C:M). A 20 μL aliquot of chloroform:methanol solution, which corresponded to approximately 2 nmol of the reaction product, was evaporated under nitrogen. The reaction products were analyzed using HPTLC (chloroform/methanol/10% acetic acid, 5:4:1, v/v/v[6]) with orcinol detection and densitometry.

Semisynthesis of specific sphingolipid isoforms: C17:0 sulphatide and C17:0 glucosylceramide

For the semisyntheses, 50 nmol of lyso-SGalCer or lyso-GlcCer and 50 nmol of C17:0 fatty acid were incubated with immobilised SCDase (0.1 mI.U./20 μL of settled particles) in

DOI: 10.1002/rcm

300 μL phosphate buffer (pH 7.0) containing 0.1% Triton X-100. For comparison, the reaction with soluble SCDase for semisynthesis of C17:0 GlcCer was performed. The reaction mixture was incubated for 20 h at 37°C while mixing on a rotator. The magnetic particles were separated and the supernatant processed as described above. A 5 μL aliquot of C:M solution, which corresponded to approximately 0.5 nmol of the reaction product, was evaporated under a stream of nitrogen and analysed with electrospray ionisation tandem mass spectrometry (ESI-MS/MS) and HPTLC (to determine the overall purity of the lipid preparation).

The macroporous character of the cellulose beads requires exhaustive washing before each subsequent use; therefore, either twenty 1-min washes or overnight elution with storage buffer was required to produce clean particles.

Tandem mass spectrometry of C17:0 sulphatide and C17:0 glucosylceramide

Instrument settings

Samples of semisynthesised SFL were applied by direct injection with a syringe pump into the SCIEX API 3200 tandem mass spectrometer equipped with an ESI source. Analysis 1.4.1 software was used to operate the instrument and process the data. Sphingolipids were analysed by precursor ion scan in the negative ion mode for SGalCer and in the positive ion mode for GlcCer. Pauses between the ranges for mass scans were set to 5.007 ms with Q1 and Q3 operating in unit resolution mode. The settling time (ms) and intensity threshold (counts per second (cps)) were set to 0.

The curtain gas pressure was 10 psi in both ion modes. Nitrogen was used as the collision gas with the pressure set to 10 and 5 psi in negative and positive ion modes, respectively. The capillary spray voltage was 4.5 kV with different polarities depending on the ion mode. The temperature of the nebulising gas was 200°C. The ion source gas pressure was adjusted to 20 psi for source gas 1 in both modes and 45 psi in negative mode or 25 psi in positive ion mode for source gas 2. The interface heater was turned on for analysis of both lipids.

Ion optics settings for SGalCer measurements were −140 V for the declustering potential and −10.4 V for the entrance potential. The collision energy was set to −130 V with a collision cell exit potential of −2 V. GlcCer was measured with a declustering potential of 47 V. The entrance potential of the collision cell was 4.9 V and the collision energy was 48 V. The collision cell exit potential was set to 5.6 V.

Sample analysis

Approximately 0.5 nmol of the reaction products in 500 μL of the appropriate solvent (see below) was continuously injected by a syringe pump into the ESI-MS/MS system at a flow rate of 50 μL/min. GlcCer was resuspended in methanol with 10 mM NH_4COOH to create $[M+H]^+$ ions in the positive ion mode, whereas SGalCer was re-suspended in methanol to create $[M–H]^-$ ions in the negative ion mode. The precursor ion scan was performed for a fragment of *m/z* 264.4 (the sphingosine base fragment) for GlcCer and a fragment of *m/z* 97 (the sulphate group) for the SGalCer.

RESULTS

Examination of the hydrolytic activity of the immobilised SCDase

The rate of hydrolysis of Gg4Cer by SCDase-activated MMB cellulose was 62% after 20 h as compared to 48% with the soluble enzyme under the same reaction conditions. This result confirmed the superiority of the immobilised enzyme over the soluble enzyme in a standard hydrolysis reaction.

SCDase reacylation activity: optimisation of the fatty acid to lyso-sphingolipid ratio

A series of reactions was carried out to identify the best ratio of substrates for enzymatic semisynthesis of bioactivated MMB cellulose. Various molar ratios of lyso-Gb3Cer and stearic acid (1:1, 1:2, 1:3 and 1:4) were tested for the synthesis of C18:0 Gb3Cer. The reaction products were analysed using HPTLC and evaluated by densitometry. A 1:1 ratio of fatty acid to lyso-sphingolipid was found to produce the best results (Table 1).

Preparation of C17:0 GlcCer by soluble SCDase: purity of the product

To compare both methods of synthesis, C17:0 GlcCer was prepared in bulk solution containing a soluble form of SCDase. Mass spectra revealed a considerable amount of contaminants in the final product; the contaminants were identified as GlcCer isoforms with C16:0 and C18:0 fatty acids (see Fig. 1(A)). The total yield of GlcCer synthesis was 99% (data not shown), but only 36% of the lyso-GlcCer was converted into the desired C17:0 isoform. The remaining 63% of the product consisted of contaminating isoforms.

MS analysis of a lipid extract of commercial SCDase (2:1 chloroform/methanol, v/v) confirmed the presence of C16:0 and C18:0 fatty acids, indicating that the crude enzyme preparation was the main source of the fatty acid contaminants (data not shown).

Table 1. The effects of different molar ratios of substrates on the formation of the C18:0 Gb_3Cer product. Reactions were catalysed by the SCDase-activated MMB cellulose

Ratio lyso-Gb_3Cer/stearic acid	1:1	1:2	1:3	1:4
*lyso-Gb_3Cer**	143	216	219	310
*C18:0 Gb_3Cer**	1401	1478	1403	1307
synthesis (%)	**91**	**87**	**86**	**81**

*Evaluated by densitometry in arbitrary units.

Reaction conditions: 20 nmol lyso-Gb_3Cer, different molar amounts of stearic acid and 0.48 mI.U./100 μL of bioactivated MMB cellulose in 200 μL of 50 mM phosphate buffer (pH 7) containing 0.1% Triton X-100 were incubated for 20 h at 37°C.

TLC analysis: the solvent system was chloroform/methanol/10% acetic acid (5:4:1); Detection: orcinol.

Substrates: lyso-Gb_3Cer and stearic acid. Product: C18:0 Gb_3Cer.

DOI: 10.1002/rcm

RCM

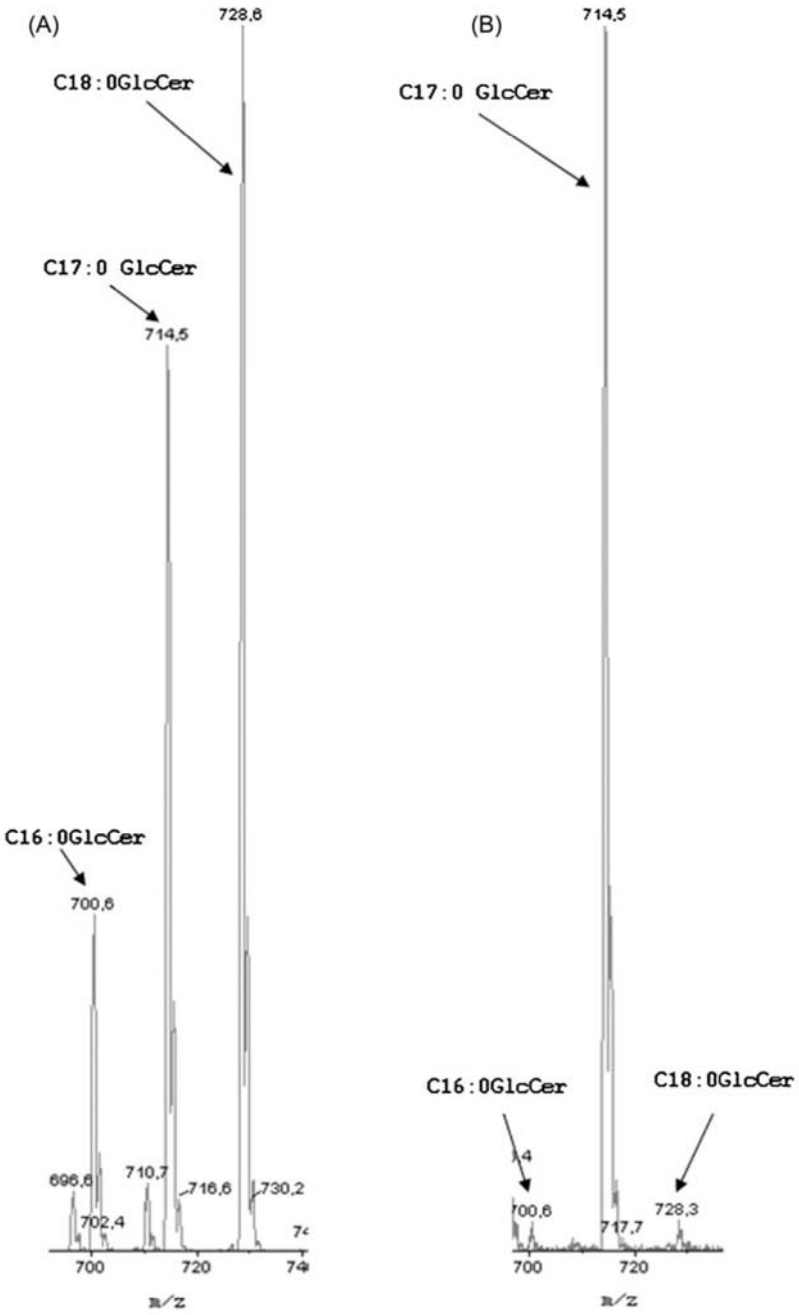

Figure 1. ESI-MS/MS analysis of C18:0 and C16:0 isoform contaminants and comparison of the soluble and immobilised SCDase reaction products. Semisynthesis of C17:0 GlcCer using (A) soluble SCDase and (B) SCDase-activated MMB cellulose. Reaction conditions: 50 nmol lyso-glucosylceramide and 50 nmol C17:0 fatty acid either with (A) 0.5 mI.U. of soluble SCDase or with (B) 0.1 mI.U./20 μl of bioactivated MMB cellulose in 300 μL of phosphate buffer at pH 7 with 0.1% Triton X-100 were incubated for 20 h at 37°C. ESI-MS/MS: the sample was directly injected by a syringe pump at a flow rate of 10 μL/min. C17:0 glucosylceramide was dissolved in methanol with 10 mM NH_4COOH and scanned for precursor ions at *m/z* 264 (specific fragment of C18:1 sphingoid base) in positive ion mode for 1 min.

DOI: 10.1002/rcm

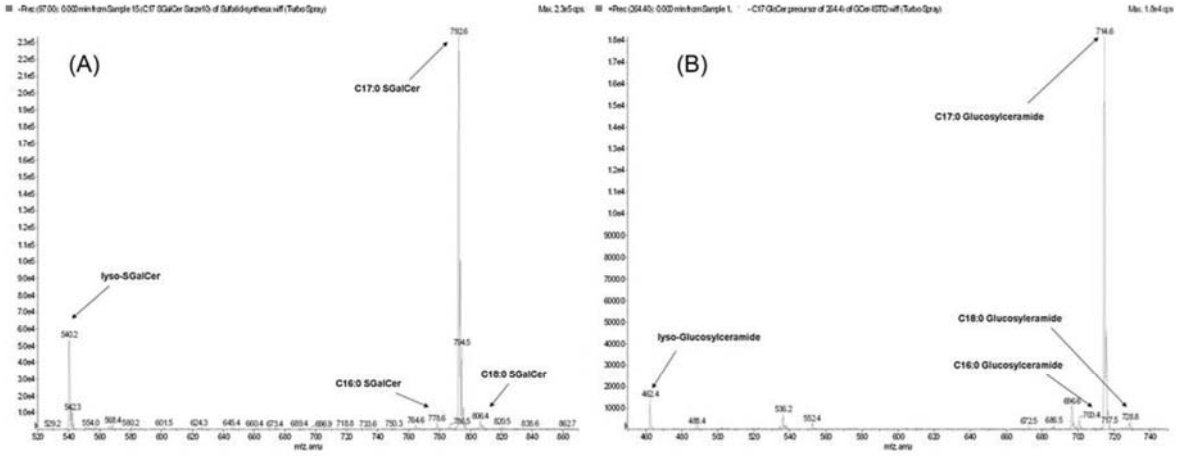

Figure 2. ESI-MS/MS analysis of C17:0 sulphatide (A) and C17:0 glucosylceramide (B) prepared with the SCDase-activated MMB cellulose. Reaction conditions: 50 nmol lyso-SGalCer or lyso-GlcCer, 50 nmol C17:0 fatty acid and 0.1 mI.U./20 μL of bioactivated MMB cellulose were incubated in 300 μL of phosphate buffer at pH 7 with 0.1% Triton X-100 for 20 h at 37°C. ESI-MS/MS: the sample was directly injected by a syringe pump at a flow rate of 10 μL/min. C17:0 SGalCer was dissolved in methanol and scanned for precursor ions at *m/z* 97 (sulphate group) in negative ion mode for 1 min. C17:0 GlcCer was dissolved in methanol with 10 mM NH_4COOH and scanned for precursor ions at *m/z* 264 (sphingoid fragment) in positive ion mode for 1 min.

Preparation of C17:0 sulphatide and C17:0 GlcCer using SCDase-activated macroporous bead cellulose

C17:0 SGalCer and C17:0 GlcCer ISTs were prepared from the respective lyso-derivatives using the immobilised SCDase.

Each reaction was repeated three times. Mass spectra (Figs. 1(A), 1(B) and Figs. 2(A), 2(B)) clearly demonstrated that the enzymatic semisynthesis effectively produced specific sphingolipids with much higher isoform purities (minimum production of molecular species other than the desired isoform) in comparison to catalysis by the soluble enzyme. With the immobilised enzyme, 80% of lyso-SGalCer and 90% of lyso-GlcCer were acylated and converted into C17:0 SGalCer and GlcCer, respectively. Only trace amounts of contaminating isoforms (about 3% in both lipid preparations) were detected when using carefully washed SCDase-activated MMB cellulose. In Figs. 3(A)–3(C), the results from three subsequently performed semisyntheses of SGalCer using newly prepared unwashed SCDase-activated MMB cellulose are presented. During these steps, almost all of the contaminating C16:0 and C18:0 isoforms were removed (Figs. 3(A)–3(C)). Different commercial batches of SCDase may contain different amounts of fatty acids, but the 'pre-run procedure' with lyso-SFL is recommended before every synthesis of specific glycosphingolipids on new SCDase-activated MMB cellulose.

Products were also analyzed by HPTLC to examine contamination by other compounds, especially sphingolipids. The purities of the synthesised ISTs were satisfactory (data not shown).

SCDase immobilised on MMB cellulose maintained its activity without any loss after 15 uses. Long-term stability was also achieved, since the enzyme retained the same activity after 1.5 years in storage buffer at 4°C.

DISCUSSION

Immobilisation of SCDase: preparation of SCDase-activated magnetic macroporous bead cellulose

A carrier with superparamagnetic properties was chosen for the simple and gentle separation of products from the reaction mixture. MMB cellulose was selected for its hydrophilic properties and high specific surface area, which provides maximum binding activity. The character of the particles and the chosen method of immobilisation resulted in a system with many advantages.

The standard procedure used for enzyme immobilisation was based on the creation of a Schiff base between the primary amino group of the enzyme and the aldehyde group of the activated MMB cellulose. The advantage of this method is that the reactive aldehyde groups are formed on the solid phase, while the enzyme molecule is not affected by the oxidation. The resulting Schiff base is mildly reduced with cyanoborohydride to form a stable bond.[15]

The prepared SCDase-activated MMB cellulose had a higher rate of substrate conversion for both the deacylation and reacylation reactions than the soluble enzyme using standard conditions.[5] The optimal substrate ratio for synthesis was 1:1.

This result and the ability to use the immobilised enzyme multiple times make it a promising tool for the preparation of specific sphingolipid species, especially if only a moderate amount of product is needed.

Advantages and disadvantages of SCDase-activated magnetic macroporous bead cellulose compared to the soluble enzyme

Although it has been successfully applied to sphingolipid semisynthesis,[2,5–7,16,17] the use of soluble SCDase results in the presence of contaminating fatty acids in the reaction mixture (resulting in low isoform purity of the product),

DOI: 10.1002/rcm

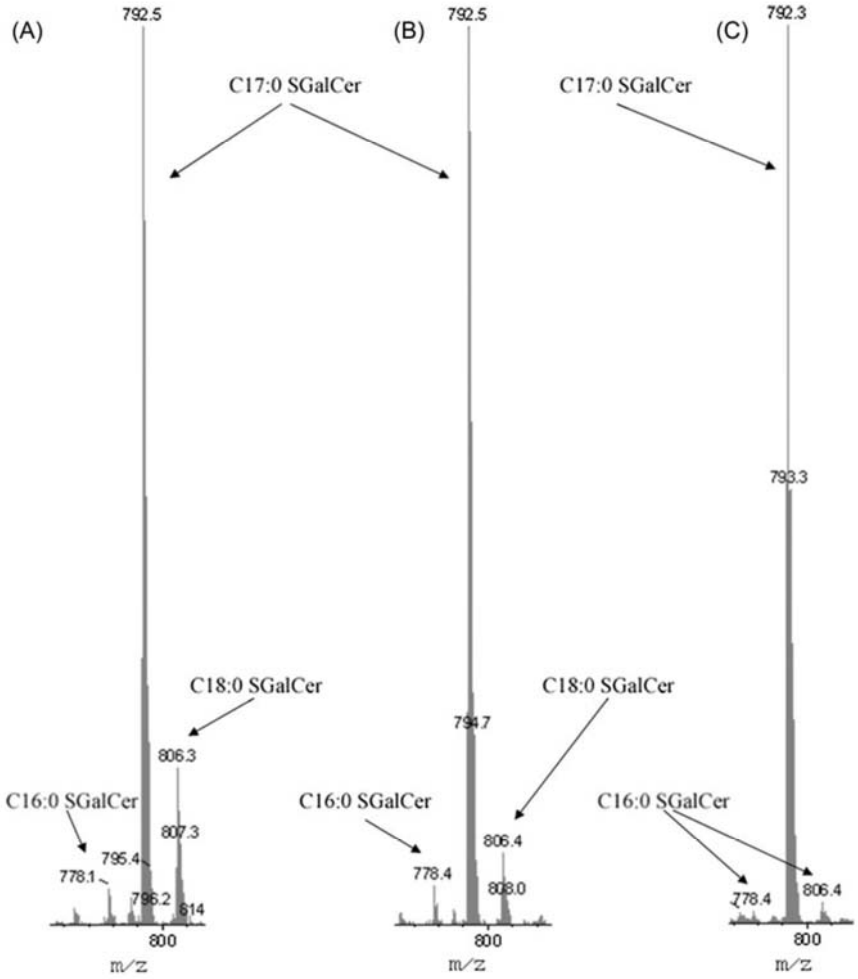

Figure 3. ESI-MS/MS analysis of C18:0 and C16:0 isoform contaminants in the course of preparation of new SCDase-activated MMB cellulose. Lyso-sulphatide was used as the optimisation compound. First (A), second (B) and third (C) semisyntheses of C17:0 SGalCer on new SCDase-activated MMB cellulose. Reaction conditions: 50 nmol lyso-SGalCer, 50 nmol C17:0 fatty acid and 0.1 mI.U./20 μL of bioactivated macroporous cellulose beads were incubated in 300 μL of phosphate buffer at pH 7 containing 0.1% Triton X-100 for 20 h at 37°C. ESI-MS/MS: sample was directly injected by syringe pump at a flow rate of 10 μL/min. C17:0 SGalCer was dissolved in methanol and scanned for precursor ions of *m/z* 97 (sulphate group) in negative ion mode for 1 min.

which may hinder some studies. In some of our experiments with the soluble enzyme, the amounts of co-synthesised C16:0, and particularly of C18:0 isoforms, were even greater than those of the target glycolipid, C17:0 GlcCer (Fig. 1(A)), especially when small amounts (up to 100 μg) of sphingolipids were synthesised. Because commercial SCDase is prepared by ammonium sulphate precipitation of culture media from the bacterium *Pseudomonas* sp. TK4 and C16:0 and C18:0 are generally abundant fatty acids, the presence of these compounds in the enzyme preparation is not surprising. However, there is only one paper that mentions the presence of some impurities in newly synthesised glycolipids, and the contaminating compounds were not characterised.[2] It is difficult to remove fatty acid contaminants from the soluble enzyme preparation without unfavourably affecting its activity. Immobilisation of the enzyme onto the surface of the carrier allows the majority of lipid and non-lipid contaminants to be washed away without affecting enzyme function.

The situation is more complicated for the reverse reaction than for hydrolysis if only one specific isoform is synthesised. Soluble SCDase gave a relatively low yield for the final product (e.g., 36% for C17:0 GlcCer) and a large amount of isoform by-products (see Fig. 1(A)), which are hardly removable. In contrast, the yields of the reacylation reaction of lyso-derivatives in terms of the C17:0 isoforms were

DOI: 10.1002/rcm

80% for SGalCer and 90% for GlcCer using the SCDase-activated MMB cellulose.

Fauler *et al.*[2] moved the reaction equilibrium of the soluble enzyme towards the desired molecular species of Gb3Cer under reaction conditions of high substrate saturation. Nevertheless, only 25% of lyso-Gb3Cer was converted into the pure Gb3Cer isoform under these conditions, with high consumption of the enzyme and precursor substrates.

The main advantages of the SCDase-activated carrier were its stability and availability for immediate use. SCDase-activated MMB cellulose with particles sizes of 125–250 μm did not show any decrease in activity after 15 reuses and was still active after 1.5 years of storage in storage buffer at 4°C.

A limitation of the MMB cellulose is that it generally exists in a narrow range of mechanical stability; however, this can be easily overcome by using dilute suspensions, handling gently and avoiding high-pressure applications (e.g., centrifugation). In addition, thorough washing is required for the removal of residual lipids (and fatty acids) before the next reaction. This is an imperative but routine step in all procedures with reusable carriers (e.g., HPLC and affinity chromatography).

For some studies, separation of the product from the remaining lipid precursors and other, mostly non-lipid contaminants might be required (this is not necessary for MS/MS). This requirement is easily accomplished by simple chromatographic procedures.[6]

Another way to prepare sphingolipid isoforms is chemical synthesis utilising acid chlorides and lyso-sphingolipids;[18] however, the acid chlorides are highly reactive compounds that can react not only with the amino group of the sphingosine moiety, but also with the hydroxyl groups of the saccharide.[19] These products would have the same mass as the required sphingolipids and would be indistinguishable by mass spectrometry. Only NMR spectra can show the position of the fatty acid in the compound. Other procedures for organic synthesis have also been applied for the preparation of sphingolipid species,[20] but time expenditure and relatively low yields were always the main disadvantages.

In summary, SCDase immobilised on a magnetic carrier was used for the first time for preparation of the specific molecular species C17:0 SGalCer and C17:0 GlcCer, that are useful standards for MS/MS quantification. The SCDase-activated MMB cellulose has the following advantages: reusability, long-term stability, high rate of conversion, low production of by-products and effectiveness for preparation of low amounts of sphingolipids. The isoform purities of the synthesised sphingolipid species were about 97%. This immobilised system can be universally used for the preparation of sphingolipids that are specifically labelled in the fatty acid moiety and could be further applied in different fields of sphingolipid biochemistry.

Acknowledgements

This work was supported by the grant projects GAUK 19509 from the Grant Agency of Charles University and MSM 0021620806 and MSM 0021627502 from the Ministry of Education and Youth of the Czech Republic.

REFERENCES

1. Stults CL, Sweeley CC, Macher BA. *Methods Enzymol.* 1989; **179**: 167.
2. Fauler G, Rechberger GN, Devrnja D, Erwa W, Plecko B, Kotanko P, Breunig F, Paschke E. *Rapid Commun. Mass Spectrom.* 2005; **19**: 1499.
3. Ito M, Kita K, Kurita T, Sueyoshi N, Izu H. *Methods Enzymol.* 2000; **311**: 297.
4. Ito M, Kurita T, Kita K. *J. Biol. Chem.* 1995; **270**: 24370.
5. Kita K, Kurita T, Ito M. *Eur. J. Biochem.* 2001; **268**: 592.
6. Mills K, Johnson A, Winchester B. *FEBS Lett.* 2002; **515**: 171.
7. Mills K, Morris P, Lee P, Vellodi A, Waldek S, Young E, Winchester B. *J. Inherit. Metab. Dis.* 2005; **28**: 35.
8. Fuller M, Sharp PC, Rozaklis T, Whitfield PD, Blacklock D, Hopwood JJ, Meikle PJ. *Clin. Chem.* 2005; **51**: 688.
9. Kuchar L, Ledvinova J, Hrebicek M, Myskova H, Dvorakova L, Berna L, Chrastina P, Asfaw B, Elleder M, Petermoller M, Mayrhofer H, Staudt M, Krageloh-Mann I, Paton BC, Harzer K. *Am. J. Med. Genet. A* 2009; **149A**: 613.
10. Whitfield PD, Sharp PC, Johnson DW, Nelson P, Meikle PJ. *Mol. Genet. Metab.* 2001; **73**: 30.
11. Bilkova Z, Slovakova M, Horak D, Lenfeld J, Churacek J. *J. Chromatogr. B Analyt. Technol. Biomed. Life Sci.* 2002; **770**: 177.
12. Chester MA. *Eur. J. Biochem.* 1998; **257**: 293.
13. Bilkova Z, Castagna A, Zanusso G, Farinazzo A, Monaco S, Damoc E, Przybylski M, Benes M, Lenfeld J, Viovy JL, Righetti PG. *Proteomics* 2005; **5**: 639.
14. Korecka L, Jezova J, Bilkova Z, Benes M, Horak D, Hradcova O, Slovakova M, Viovy JL. *J. Magn. Magn. Mater.* 2005; **293**: 349.
15. Hermanson GT. *Bioconjugate Techniques* (1st edn). Academic Press, Inc.: New York, 1996.
16. Mitsutake S, Kita K, Nakagawa T, Ito M. *J. Biochem. (Tokyo)* 1998; **123**: 859.
17. Mitsutake S, Kita K, Okino N, Ito M. *Anal. Biochem.* 1997; **247**: 52.
18. Mills K, Eaton S, Ledger V, Young E, Winchester B. *Rapid Commun. Mass Spectrom.* 2005; **19**: 1739.
19. Thevenet S, Wernicke A, Belniak S, Descotes G, Bouchu A, Queneau Y. *Carbohydr. Res.* 1999; **318**: 52.
20. Zhou X, Turecek F, Scott CR, Gelb MH. *Clin. Chem.* 2001; **47**: 874.

SUPPLEMENTARY PUBLICATIONS

Publications in impacted journals related to topic of this PhD thesis

Supplementary publication B

Kuchar L., Ledvinova J., Hrebicek M., et al., *Prosaposin deficiency and saposin B deficiency (activator-deficient metachromatic leukodystrophy): report on two patients detected by analysis of urinary sphingolipids and carrying novel PSAP gene mutations.* Am J Med Genet A, 2009. **149A**(4): p. 613-621

RESEARCH ARTICLE

AMERICAN JOURNAL OF medical genetics PART A

Prosaposin Deficiency and Saposin B Deficiency (Activator-Deficient Metachromatic Leukodystrophy): Report on Two Patients Detected by Analysis of Urinary Sphingolipids and Carrying Novel PSAP Gene Mutations

Ladislav Kuchař,[1] Jana Ledvinová,[1]* Martin Hřebíček,[1] Helena Myšková,[1] Lenka Dvořáková,[1] Linda Berná,[1] Petr Chrastina,[1] Befekadu Asfaw,[1] Milan Elleder,[1] Margret Petermöller,[2] Heidi Mayrhofer,[3] Martin Staudt,[3] Ingeborg Krägeloh-Mann,[3] Barbara C. Paton,[4] and Klaus Harzer[3]**

[1]Charles University in Prague, 1st Medical Faculty, Institute of Inherited Metabolic Disorders of 1st Faculty of Medicine and General Teaching Hospital, Prague, Czech Republic

[2]Department of Pediatrics, HSK-Klinik, Wiesbaden, Germany

[3]Department of Pediatrics and Child Development, Universitäts-Kinderklinik, Tübingen, Germany

[4]Formerly from Department of Genetic Medicine, Women's and Children's Hospital, Adelaide, Australia

Received 27 March 2008; Accepted 13 December 2008

Prosaposin deficiency (pSap-d) and saposin B deficiency (SapB-d) are both lipid storage disorders caused by mutations in the *PSAP* gene that codes for the 65–70 kDa prosaposin protein, which is the precursor for four sphingolipid activator proteins, saposins A–D. We report on two new patients with *PSAP* gene defects; one, with pSap-d, who had a severe neurovisceral dystrophy and died as a neonate, and the other with SapB-d, who presented with a metachromatic leukodystrophy-like disorder but had normal arylsulfatase activity. Screening for urinary sphingolipids was crucial to the diagnosis of both patients, with electrospray ionization tandem mass spectrometry also providing quantification. The pSap-d patient is the first case with this condition where urinary sphingolipids have been investigated. Multiple sphingolipids were elevated, with globotriaosylceramide showing the greatest increase. Both patients had novel mutations in the *PSAP* gene. The pSap-d patient was homozygous for a splice-acceptor site mutation two bases upstream of

How to Cite this Article:
Kuchař L, Ledvinová J, Hřebíček M, Myšková H, Dvořáková L, Berná L, Chrastina P, Asfaw B, Elleder M, Petermöller M, Mayrhofer H, Staudt M, Krägeloh-Mann I, Paton BC, Harzer K. 2009. Prosaposin deficiency and saposin B deficiency (activator-deficient metachromatic leukodystrophy): Report on two patients detected by analysis of urinary sphingolipids and carrying novel PSAP gene mutations.
Am J Med Genet Part A 149A:613–621.

Additional supporting information may be found in the online version of this article.

Abbreviations: ASA, arylsulfatase A (EC 3.1.6.8); ESI-MS/MS, electrospray ionization tandem mass spectrometry; Gb3Cer, globotriaosylceramide; GlcCer, glucosylceramide; HPTLC, high performance thin layer chromatography; IST, internal standards; LacCer, lactosylceramide; MLD, metachromatic leukodystrophy; MS/MS, tandem mass spectrometry; OFC, occipital–frontal circumference; pSap, prosaposin; pSap-d, prosaposin deficiency; Sap(s), saposin(s) including SapA, SapB, SapC, SapD; SapA-d, SapB-d, SapC-d, SapD-d, deficiency of the respective Sap; TLC, thin layer chromatography.

Grant sponsor: Ministry of Education and Youth; Grant number: MSM 0021620806; Grant sponsor: Ministry of Health of the Czech Republic; Grant number: MZOVFN2005; Grant sponsor: Grant Agency of the Czech Republic; Grant number: 303/03H065.

*Correspondence to:
Dr. Jana Ledvinová, Institute of Inherited Metabolic Disorders, Charles University in Prague, First Faculty of Medicine, Ke Karlovu 2, 128 08 Prague, Czech Republic. E-mail: jledvin@cesnet.cz
**Correspondence to:
Dr. Klaus Harzer, Department of Pediatrics and Child Development, Universitäts-Kinderklinik, Hoppe-Seyler-Str. 1, Tübingen D 72076, Germany. E-mail: harzer-rottenburg@t-online.de

Published online 6 March 2009 in Wiley InterScience (www.interscience.wiley.com)
DOI 10.1002/ajmg.a.32712

exon 10. This mutation led to a premature stop codon and yielded low levels of transcript. The SapB-d patient was a compound heterozygote with a splice-acceptor site variant exclusively affecting the SapB domain on one allele, and a 2 bp deletion leading to a null, that is, pSap-d mutation, on the other allele. Phenotypically, pSap-d is a relatively uniform disease of the neonate, whereas SapB-d is heterogeneous with a spectrum similar to that in metachromatic leukodystrophy. The possible existence of genotypes and phenotypes intermediate between those of pSap-d and the single saposin deficiencies is speculated.

Key words: sphingolipid activator proteins; prosaposin; urinary lipids; mass spectrometry; *PSAP* gene; saposin deficiency; metachromatic leukodystrophy

INTRODUCTION

Prosaposin (pSap) is a non-enzymic 65–70 kDa glycoprotein encoded by the *PSAP* gene [Sandhoff et al., 2001]. Amongst its roles, pSap is the precursor for four saposins (Saps) A–D, which are formed by proteolysis. The Saps, also known as sphingolipid activator proteins, are indispensable cofactors for the intralysosomal degradation of a number of sphingolipids and seem to interact directly with the specific lipid hydrolases and/or facilitate presentation of the lipid substrates to these enzymes [Sandhoff et al., 2001; Spiegel et al., 2005]. Defects in the *PSAP* gene can cause a deficiency of either the entire pSap protein (prosaposin deficiency, pSap-d) or an individual Sap: SapA-d, SapB-d, SapC-d, or SapD-d, with, to date, SapD-d only being reported in an animal model [Matsuda et al., 2004]. In humans, pSap-d is a unique neonatal condition with an acute generalized neurovisceral dystrophy associated with the storage of multiple sphingolipids, whereas each isolated Sap deficiency is generally similar to a particular sphingolipid hydrolase-deficiency, namely, SapA-d to Krabbe leukodystrophy [Spiegel et al., 2005], SapB-d to metachromatic leukodystrophy (MLD), and SapC-d to Gaucher disease [Sandhoff et al., 2001]. The pathologies and biochemical phenotypes observed in pSap-d and the single Sap-deficient diseases have provided indirect insight into the specific roles and normal functions, including certain neurotrophic effects, of p-Sap and/or the individual Saps.

We report on two additional patients, one with pSap-d and the other with SapB-d. Both patients were detected by urinary glycosphingolipid analysis and they also have novel *PSAP* mutation(s). Tandem mass spectrometry (MS/MS) of the urinary lipids proved to be an efficient screening method. The distinctive pattern found in urine from the present pSap-d patient, with elevations in multiple sphingolipids, including ceramide, constitutes the first urine sphingolipid analysis for this condition.

PATIENTS AND METHODS

Patient 1

Patient 1 was born at term (weight, 3.2 kg [P50]; length, 50 cm [P50]; occipital–frontal circumference [OFC], 32 cm [1.5 cm below P10]) after an uneventful pregnancy to parents who were first cousins. The mother had noticed frequent and rhythmic movements of the child in late pregnancy. Directly after birth he had precipitate movements and clonic fits that were resistant to anticonvulsive drugs. Sucking and swallowing were insufficient and tube feeding was started. After 3 weeks he had increased serum C-reactive protein and needed additional oxygen. A chest X-ray revealed pulmonary infiltrations. At the age of 4 weeks, he presented with muscle hypotonia, myoclonus and periods of twitching of the right arm and hand that were unresponsive to drugs. The liver and spleen were enlarged, which was confirmed by sonography, with the liver and spleen vertical diameters increased to 7 and 7.5 cm, respectively. Laboratory tests showed increased liver enzymes. Testing of white blood cell lysosomal enzymes revealed a very low galactosylceramide β-galactosidase (EC 3.2.1.46) activity. On ECG, there were signs of mitral insufficiency. In the eye fundi, the optic disks were atrophic, the right more so than the left, and the maculae were not demarcated. Sonography of the slightly microcephalic skull showed small ventricles and periventricular punctate echogenicities. On cerebral magnetic resonance imaging (MRI) a thin corpus callosum and bilateral absence of the gyrus cinguli were found; the periventricular white matter regions showed striking multiple symmetrical signal changes [similar to those reported in Elleder et al., 2005] suggestive of gray matter heterotopias (Fig. 1), although there was no complete iso-intensity with gray matter. An electroencephalogram (EEG) revealed general changes with invariant alpha-activity, multi-focal sharp waves, but no ictual patterns which were also absent when the child had clonic jerk sequences of the limbs and head. At the age of 5 weeks, cerebrospinal fluid analysis revealed an increased total protein (349 mg/dl; normal for age, 53 22 [SD] mg/dl). In the smears of a bone marrow aspirate a few storage macrophage-like cells were seen. Electron microscopy of a skin biopsy revealed generalized lysosomal storage (Fig. 2). The child deteriorated and parenteral nourishment was necessary. Repeated pulmonary infections led to death at the age of 55 days (weight, 3.85 kg [0.35 kg below P10]; length, not recorded; OFC, 35.5 cm [2 cm below P10]). In a urinary sample collected at day 44 a number of glycosphingolipids were elevated on lipid thin layer

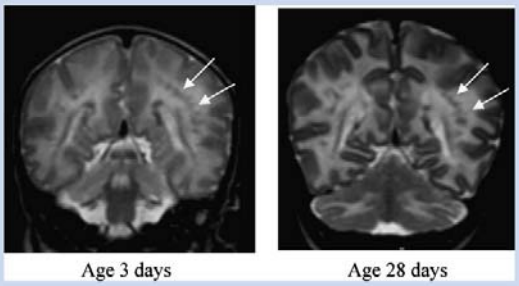

FIG. 1. Cranial MRI scans (T2 weighted) for patient 1 (pSap-d). Note the absence of gyri cinguli and the corpus callosum, which is thinned. The arrows point to dark lesions arranged in a chain-like manner that are suggestive of gray matter heterotopias.

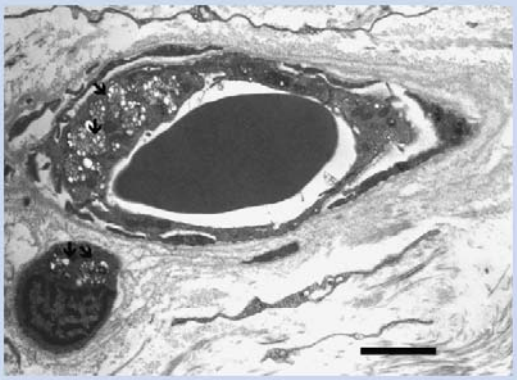

FIG. 2. Skin biopsy from patient 1 (pSap-d). Arrows mark clusters of heterogeneous lysosomal storage material containing bright (electron-lucent) vesicles in an endothelial cell (capillary vessel, upper half) and a perivascular cell (bottom left hand corner). Bar at bottom, 3 μm.

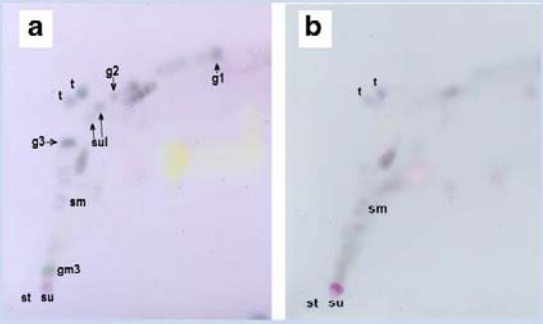

FIG. 3. Urinary lipids in (a) patient 1 (pSap-d; 44-day-old), and (b) a normal control infant (11-month-old, with similarly low urinary creatinine as in patient 1) analysed by two-dimensional TLC (direction of first solvent (chloroform/methanol/water 14:6:1, by volume) was upward, and of the second solvent (chloroform/methanol/conc. acetic acid/water 40:8:1:1) from left to right). Lipids from each 3 ml urine sample were separated on silica-gel HPTLC plates and stained with anisaldehyde/sulfuric acid. Symbols (alphabetic): *g1*, glucosylceramide; *g2*, dihexosylceramides; *g3*, globotriaosylceramide; *gm3*, G_{M3} ganglioside (preliminary identification); *sm*, sphingomyelin; *st*, start of sulfatide test; *su*, start of urinary lipid extract; *sul*, patient sulfatide (double spot); *t*, sulfatide test (double spot, different fatty acid type as compared to *sul*) calibrated to an amount equivalent to 10-fold of the mean normal sulfatide amount in 3 ml urine from 1- to 10-year-old children (n = 5). Note the intense spots for *g1*, *g3*, and *gm3* in (a). [Color figure can be viewed in the online issue, which is available at www.interscience.wiley.com.]

chromatography (TLC) (Fig. 3). The complex sphingolipidosis suggested a diagnosis of **pSap-d**.

Patient 2

Patient 2 was born abroad 2 weeks before term after an uneventful pregnancy. When he was 7 months old and had started crawling, the parents noticed that the movements of his right arm and leg were poor. When he was admitted at the age of 9 months, he had signs of a mild, right-sided, arm-accentuated spastic hemiparesis. Skull sonography revealed a left-temporal, large porencephalic cyst, and distension of the left-ventricle, suggesting a preceding infarction of the medial cerebral artery. An MRI scan confirmed the medial artery infarction, which probably occurred at or around the time of birth, and frontal sickle-shaped fluid pools were evident, suggesting retarded myelination. At the age of 12 months (weight, 10.5 kg [P50]; length, 80 cm [P75]; OFC, 47.5 cm [P50]), his spastic hemiparesis, with slight flexion of joints, did not prevent him from rolling over, although there was some hypotonia of the trunk muscles. At the age of 18 months his hemiparetic problems, with hand-fisting and accentuated patellar reflex on the right side, were moderate. He was able to reach a standing position. At the age of 23 months he had lost his previous ability to walk a few steps and was unable to stand freely or to crawl as actively as before. His limb muscles had distinctly reduced power. At 25 months of age he had muscle hypotonia, very weak peripheral reflexes and no Babinski sign. Laboratory values revealed an increased cerebrospinal fluid protein of 98 mg/dl (normal for age, 45 15 mg/dl), but lactate was normal. At 28 months he was able to sit, stand, and play a little, but only with assistance. He often had periods of unmotivated crying. At 43 months he had his first generalized epileptic seizure, had lost his active speech and interest in toys, and had lower limb spasticity with a back-curved right knee. His hands were fisted and almost no longer used. His feet were held in the extensor position and he had a distinct spastic tetraparesis. A skull MRI scan revealed extensive white matter lesions with preserved U-fibers. Conduction velocity of the ulnar nerve was reduced to 12.7 m/sec (normal for age, >38 m/sec). Laboratory values showed normal activities of white blood cell lysosomal enzymes, including arylsulfatase A (ASA; EC 3.1.6.8) and galactosylceramide β-galactosidase (EC 3.2.1.46). Repeated infections, EBV positivity, and feeding problems were noted. At the age of 4 years, a preliminary diagnosis of MLD was made because of the finding of highly elevated urinary sulfatide. In view of the normal white blood cell ASA activity, **SapB-d** was suggested. Five months later the severely retarded, tetraspastic child had almost no eye contact with the examiner or fixation with the eyes. At the age of 5 years there was an additional tonic epileptic fit and the valproate dose was increased to 24 mg/kg body weight. At the age of 6 years (weight, 16.2 kg [P3]; length, 110 cm [P3]; OFC, 53 cm [P75]) generalized muscle hypertonicity, pes equinovarus, and eye pupils that were unreactive to light were noted.

Urine Samples

Urine samples (24 hr collection) from patient 1 and 2 were kept frozen at −20°C. Frozen samples from Fabry patients, MLD patients, healthy children up to 12 years and adult controls were available.

Enzyme Assays, Fibroblast Loading Tests, and Lipid Thin Layer Chromatography

The indicated methods were used for the determination of enzyme activities with radioactive substrates [Elleder et al., 2005], loading fibroblasts with radioactive glucosylceramide [Harzer et al., 1989], globotriaosylceramide [Schlote et al., 1991], sulfatide and sphingomyelin [Elleder et al., 2005], the TLC analysis of fibroblasts [Elleder et al., 2005], extraction of urine (please refer to supporting information S1 which may be found in the online version of this article), and TLC of urinary lipids [Schlote et al., 1991].

Tandem Mass Spectrometry (MS/MS) Analysis of Urinary Sphingolipids

Preparation of lipid extracts for MS/MS analysis. Sonicated urine samples (150 µl) were extracted by mixing with 700 µl of a mixture of two volumes chloroform (no. 650471 Sigma–Aldrich Co., St. Louis, MO; grade CHROMASOLV® for HPLC 99.9%) to one volume methanol (no. 34966 Sigma–Aldrich; grade CHROMASOLV® for LC–MS Riedel-de Haën), containing a mixture of six internal standards (IST; for the sources, see later): 40 ng [C17:0]sulfatide, 35 ng [C17:0]GlcCer, 25 ng [C17:0]Gb3Cer, 50 ng [C17:0]ceramide, 50 ng [C16:0-D_3]LacCer, and 50 ng [C17:0]sphingomyelin. The samples were vortexed for a few seconds at 5 min intervals three times. Then 150 µl Milli-Q® water was added and the mixing procedure repeated. After 30 min at room temperature the samples were centrifuged (14,500*g*, 5 min). Each separated lower phase was filtered (PTFE syringe pump filter) and re-washed by mixing with 500 µl Milli-Q® water [Han and Gross, 2005], the mixture centrifuged and separated as above. The final lower phases were evaporated under nitrogen. The dry residues were recovered with 500 µl chloroform–methanol 2:1 (v/v), and divided into 300 µl (positive ion mode) and 200 µl (negative ion mode) aliquots. The aliquots were evaporated under nitrogen. Before analysis the positive ion mode aliquot was dissolved in 300 µl 10 mM ammonium formate (no. 55674 Sigma–Aldrich; grade puriss. p.a. for LC–MS Fluka) in methanol [Liebisch et al., 1999; Fuller et al., 2005] and the negative mode aliquot in 200 µl methanol [Whitfield et al., 2001]. Lipids from cultured fibroblasts were extracted as described [Asfaw et al., 1998] with chloroform/methanol 2:1 (v/v) containing IST in the above-mentioned concentrations.

Electrospray ionization (ESI)-MS/MS analysis. The MS/MS equipment comprised an AB/MDS SCIEX API 3200 triple-quadrupole mass spectrometer (AB/MDS Sciex, Concord, Canada) with an ionspray source and an Agilent 1100 Autosampler (Agilent Technologies, Inc., Santa Clara, CA). Electrospray conditions and mass spectrometer ion optics were optimized for sphingolipid measurements using standard samples with lipid 10 µg/ml (for detailed conditions, see supporting information Table I which may be found in the online version of this article). Direct flow injection analysis, with methanol as the mobile phase, was done at a flow rate of 50 µl/min. Using the multiple reaction monitoring mode, the sphingolipids from a given sample were analyzed in series: For each sphingolipid, a 20 µl lipid extract aliquot corresponding to 6 µl urine, or to 0.2 µg fibroblast protein, was injected into the methanol mobile phase. Analysis was optimized for each sphingolipid, resulting in a sufficiently symmetrical peak shape with at least 12 measuring points per peak (e.g., see peaks in supporting information Fig. 1 which may be found in the online version of this article). This method allowed quantification of all major isoforms of each sphingolipid, distinguished by their fatty acid moiety (C16:0 to C26:0 fatty acids, non-substituted types and hydroxy-derivatives; details tabulated in supporting information Table II which may be found in the online version of this article). The negative ion mode was used for the analysis of sulfatide and the positive ion mode for neutral glycosphingolipids, ceramide, and sphingomyelin.

Quantification of sulfatide, Gb3Cer, dihexosylceramides (including LacCer and digalactosylceramide), monohexosylceramides (mainly GlcCer), ceramide, and sphingomyelin was done by single point calibration with a standard lipid concentration of 600 ng/ml (external calibration standard) corrected by the signal ratio toward IST. The concentrations of standard lipids and individual IST (see above) in the external calibration point were within the previously determined linear range of 50 ng–7 µg lipid per ml. The concentrations of IST in the external calibration point and in the patient samples were the same [De Hoffmann and Stroobant, 2002]. Reproducibility of all measurements was 93% or higher. The Student's *t*-test was used to determine statistical significance. The following porcine lipid standards were used: Sulfatide (no. 131305P) and sphingomyelin (no. 860062P) were from Avanti Polar Lipids, Inc., Alabaster, AL and Gb3Cer (no. 1067) and ceramide (no. 1056) from Matreya LLC, Pleasant Gap, PA. LacCer (bovine, no. G3166) and GlcCer (from human Gaucher spleen, no. G9884) were from Sigma–Aldrich. The MS/MS method cannot differentiate between the glucose (e.g., in GlcCer) and galactose (e.g., in digalactosylceramide) moieties because of the same mass. Therefore, GlcCer and galactosylceramide, as well as LacCer and digalactosylceramide, were quantified as monohexosylceramides and dihexosylceramides, respectively. Chemical identity and purity of sphingolipids used as calibration standards and as IST were proved by high performance TLC (HPTLC) and mass spectrometry (e.g., see supporting information Fig. 2 which may be found in the online version of this article). Purity of all sphingolipid standards was >97%.

Lipid internal standards. [C17:0]Gb3Cer (no. 2923.90), C16:0-D_3-LacCer (no. 1534), and [C17:0]sphingomyelin (no. 1890), were from Matreya, and [C17:0]ceramide (no. 860517P) from Avanti. Internal standards which were not commercially available, [C17:0]sulfatide and [C17:0]GlcCer, were prepared from lyso-sulfatide (no. 573755, Calbiochem-Novabiochem GmbH, Schwalbach, Germany) and lyso-GlcCer (no. 1306, Matreya) by linking the lyso-compounds with C17:0 fatty acid (no. 10-1700-13, Larodan, Malmø, Sweden) using enzymatic semisynthesis with sphingolipid ceramide *N*-deacylase from *Pseudomonas* sp. TK4 (no. TAK 4462, Takara Shuzo, Shiga, Japan) as described [Mills et al., 2002]. The homogeneity of commercial and synthesized standards was confirmed by HPTLC and their identity by ESI-MS/MS.

Molecular Analysis

Genomic DNA and total mRNA were isolated from the patients' cultured fibroblasts and from the parents' peripheral leukocytes by

standard techniques. The *PSAP* gene was analyzed for mutations as described previously [Hůlková et al., 2001; Elleder et al., 2005]. Briefly, all coding exons and intron–exon boundaries were amplified from genomic DNA and sequenced directly from gel-purified PCR products using automated fluorescent sequencers. The mRNA was reverse-transcribed using Superscript II (Gibco®) and oligo-dT. RT-PCR products were sequenced as described above. Sequences were numbered sequentially from the A of the first ATG codon, which was designated 1 (reference genomic sequence: GenBank [http://www.ncbi.nlm.nih.gov/], NC_000010.9; reference mRNA sequence: GenBank, NM_002778.1; protein sequence: UniProtKB/Swiss-Prot [http://www.expasy.org/sprot/], P07602 [SAP_HUMAN]).

RESULTS

Electron Microscopic Findings in Skin Biopsy

Confirming earlier results by A. Bornemann (Tübingen, personal communication), there was generalized dermal lysosomal storage expressed in the eccrine glands, capillary endothelium (Fig. 2), perivascular macrophages, Schwann cells, adipocytes, and some fibroblasts of patient 1. The storage lysosomes were around 1 μm in diameter and were filled with pleiomorphic, predominantly multivesicular structures; individual vesicles were around 170 nm in diameter.

Biochemical Findings in Cultured Skin Fibroblasts

Fibroblast homogenates from patient 1 had a partially reduced activity of glucosylceramide β-glucosidase (EC 3.2.1.45), a more markedly reduced activity of galactosylceramide β-galactosidase, but a normal sphingomyelinase (EC 3.1.4.12) activity (for quantitative data, see supporting information S6 which may be found in the online version of this article). The activity of galactosylceramide β-galactosidase was normal in fibroblast homogenates from patient 2 (glucosylceramide β-glucosidase and sphingomyelinase not tested).

Thin layer chromatographic analysis of lipids extracted from fibroblasts (corresponding to about 0.5 mg protein) of patient 1 revealed intensely stained spots for ceramide, GlcCer, and LacCer similar to [Elleder et al., 2005]; other glycosphingolipids were not studied. The corresponding spots on chromatograms from control cells were about 3- to 10-fold less intense. Ceramide was additionally quantified by MS/MS and an amount of 16.2 μg/mg fibroblast protein found for patient 1 (normal range [n = 4], 3.6–6.2 μg/mg). A three to fourfold increase in dihexosylceramide and Gb3Cer concentrations in fibroblasts was also confirmed by MS/MS. Of these lipid elevations, only one was found to occur also in fibroblasts of patient 2: There was a fourfold increase in Gb3Cer.

Metabolic experiments with radioactive sphingolipid substrates (tritium-labeled on their ceramide moieties) loaded onto living fibroblast cultures from patient 1 and patient 2 gave similar results to those described for an earlier pSap-d [Elleder et al., 2005] and an earlier SapB-d [Schlote et al., 1991] patient, respectively. In fibroblasts from patient 1 there was an impaired turnover of [^{3}H]ceramide (derived from loaded [^{3}H]glucosylceramide or [^{3}H]sphingomyelin). For cells from both patient 1 and patient 2, there was a reduced turnover of loaded [^{3}H]globotriaosylceramide and [^{3}H]sulfatide (supporting information S7 may be found in the online version of this article).

Urinary Lipid Findings by Thin Layer Chromatography

Based on comparison with the staining intensity of lipids on the chromatogram from a control urine sample, the chromatogram for patient 1 (pSap-d) showed markedly increased levels of Gb3Cer, GlcCer, and G_{M3} ganglioside (preliminary identification), and sulfatides and dihexosylceramides were also elevated (Fig. 3). Sulfatides were also clearly elevated in the urine extract from patient 2 (SapB-d), and there was a slight increase in Gb3Cer.

Urinary Lipid Findings by MS/MS

Table I summarizes the quantitative urinary sphingolipid findings in patients 1 (pSap-d) and 2 (SapB-d), as compared to findings in Fabry disease, MLD, and normal controls. The data were standardized relative to the concentration of sphingomyelin as a reference cellular sphingolipid. Lipid marked with footnotes c and e indicate that there was a statistically significant elevation when compared to the appropriate control group (infantile/late infantile controls for pSap-d, SapB-d, and MLD; adult controls for Fabry disease).

In patient 1, the abundance of Gb3Cer was elevated ($P < 0.001$) to a similar extent to that found in Fabry disease patients (Table I). However, patient 1 also showed additional elevations in sulfatide ($P < 0.001$) and the LacCer/digalactosylceramide ($P < 0.001$), monohexosylceramide (including GlcCer; $P < 0.001$), and ceramide ($P < 0.001$) fractions.

In patient 2, the elevated concentration of sulfatide ($P < 0.001$) was of a similar magnitude to that found in MLD (Table I). The distinct increase in the concentration of Gb3Cer ($P < 0.001$) was also remarkable.

The high elevations of the two urinary marker glycolipids, Gb3Cer, and sulfatide, had different proportions in patients 1 and 2: Gb3Cer and sulfatide concentrations accounted for 60% and 20% of excreted glycosphingolipids in patient 1, respectively, while they accounted for 21% and 59% in patient 2.

In Figure 4, the percent distribution of concentrations of the main urinary sphingolipids is shown. This format, which allowed for a simple standardization of urinary lipid values in the absence of reference parameters, confirmed most of the findings summarized in Table I. The combined percentages for sulfatide, Gb3Cer, dihexosylceramides, glucosylceramide, and ceramide was higher in the diseases studied than for controls, with pSap-d having the highest percentage, consistent with the unique urinary multiple sphingolipid elevations in this condition.

PSAP Gene Analysis

Patient 1 (pSap-d). Patient 1 was found to be homozygous for a point mutation, c.1006-2A > G, in the *PSAP* gene. The mutation is located two bases upstream of the exon 10 acceptor splice site and alters the consensus splice site sequence. Analysis of the patient's cDNA sequence identified a splicing error with activation of a cryptic splice site in intron 9 leading to both an insertion of 70 bases

TABLE I. Urinary Sphingolipids in Patient 1 (pSap-d), Patient 2 (SapB-d), and in Pathologic and Normal Controls (ESI-MS/MS Determination)

	Lipid values[a] expressed as µg/100 µg sphingomyelin				
	Sulfatide	Globotriaosylceramide	Lactosyl- and digalactosylceramide	Monohexosylceramide (mainly glucosylceramide)	Ceramide
Patient 1 (pSap-d) 44-day-old	67[c]	208[c]	45[c]	26[c]	17[c]
Patient 2 (SapB-d) 50-month-old	145[c]	51[c]	35[c]	14[c]	6.3
Metachromatic leukodystrophy 1- to 5-year-old (n = 6)	120[c] 38[d]	8.8 3.3	14 5.3	6.2 1.7	3.8 1.1
Fabry disease males 24- to 54-year-old (n = 10)	6.8 2.5[d]	201[c] 102	35[e] 19	3.5 1.4	4.8 1.7
Infantile/late-infantile controls 0.5- to 12-year-old (n = 16)	14 5.2[d]	15 8.2	10.2 3.0	4.4 1.0	4.3 1.8
Adult controls males and females[b] 17- to 60-year-old (n = 12)	9.7 2.5[d]	21 14	16 6.1	4.4 1.4	5.8 2.8

[a]Mean of three determinations for patients 1 and 2. For the analytical reproducibility, see Patients and Methods Section.
[b]Fabry carrier status was excluded in control females molecularly.
[c]Statistical significance $P < 0.001$.
[d]Standard deviation.
[e]Statistical significance $P < 0.01$.

from the intronic sequence into the mRNA (r.1006-70_1006-lins) and a premature stop codon. Each of the parents was found to be a carrier for the mutation. While it was possible to amplify the mutant mRNA by RT-PCR in the patient, the same analysis in the parents showed that, in comparison to the wild-type transcript, only trace amounts of the mutant transcript were present.

Patient 2 (SapB-d). Patient 2 was found to be heterozygous for two mutations. The first mutation, c.577-2A > G, is a splicing mutation located in the acceptor splice site of intron 5. The second mutation is a 2bp deletion, c.828-829delGA, located in exon 8. The latter mutation leads to a frameshift and a premature stop codon. No transcript corresponding to the c.828-829delGA sequence was detected by RT-PCR in the patient. As this mutation leads to a premature stop codon, the most likely explanation for the absence of transcript is nonsense-mediated decay. Two transcripts from the other allele, which carries the c.577-2A > G, were found. Analysis of these indicated that the acceptor splice site in intron 5 was rendered non-functional by the mutation, with either of two different downstream acceptor sites being used instead. In the first transcript a cryptic splice site in exon 6 was used, since the mRNA contained a

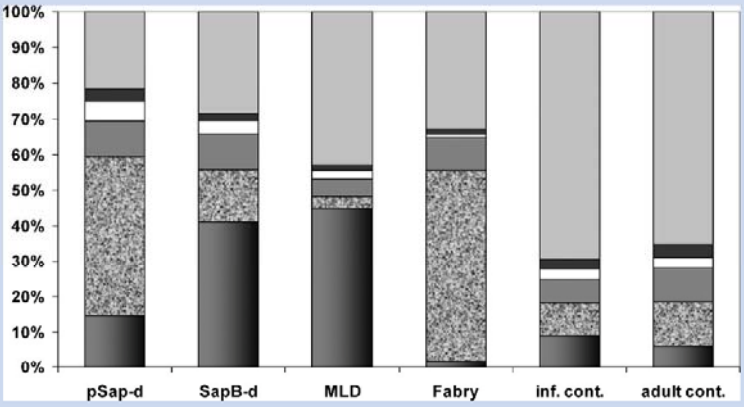

FIG. 4. Percent distribution of main urinary sphingolipids. Order of column sections from bottom to top: sulfatide (right edge dark), globotriaosylceramide (sand-like), dihexosylceramides (gray), glucosylceramide (light), ceramide (black), sphingomyelin (light gray). Total analysed lipids were about 2–8 mg/L urine. Columns: *pSap-d*, patient 1; *SapB-d*, patient 2; *MLD*, metachromatic leukodystrophy group (mean, Table I); *Fabry*, Fabry disease group (mean, Table I); *inf. cont.*, infantile/late-infantile controls (mean, Table I); *adult cont.*, adult controls (mean, Table I).

deletion of 21 bp from exon 6 (15 of them encoding SapB; r.577-_597del). In the second transcript the whole of exon 6 was deleted (r.577_720del) and the exon 7 acceptor splice site was used. These in-frame deletions affected only the SapB domain, while the sequence encoding the remaining Saps was intact and in frame. Analysis of the parental genomic DNA showed that the mother was a carrier of c.577-2A > G sequence variant while the father was heterozygous for c.828-829delGA.

DISCUSSION

Disorders caused by defects in the *PSAP* gene [Sandhoff et al., 2001] form a poorly known sub-group of lysosomal lipid storage diseases that are clinically and metabolically highly variable. Reports on the few known cases of pSap-d [Harzer et al., 1989; Bradová et al., 1993; Hůlková et al., 2001; Millat et al., 2003; Elleder et al., 2005] have indicated that this disorder should be considered in the differential diagnosis of neonates with unexplained neurologic signs, in particular, if these are combined with visceral involvement. The central nervous system changes in pSap-d may be caused not only by early lipid storage, but also by primary deficits in the organization of cerebral architecture, since pSap and/or some of its products are known to have essential neurotrophic functions. The present pSap-d patient was clinically and biochemically very similar to the earlier reported pSap-d patients [Harzer et al., 1989; Bradová et al., 1993; Hůlková et al., 2001; Millat et al., 2003; Elleder et al., 2005].

The diagnosis in the present SapB-d patient was complicated by the early finding of a massive infarction of the left arteria cerebri media, presumably coincidental to the leukodystrophy. However, the finding of high urinary sulfatide eventually led to a molecular diagnosis of SapB-d. This patient was similar to earlier reported patients [e.g., Schlote et al., 1991; Henseler et al., 1996]. Descriptions of other patients [Hahn et al., 1982; Rafi et al., 1992] suggest a highly variable clinical phenotype in SapB-d, similar to that in ASA–deficient MLD.

Urine is an accessible and non-invasive sample that can also be considered to be an "indirect kidney biopsy" for lipid and other analyses, due to the presence of portions of kidney cells [Desnick et al., 1970]. Solid materials from desquamated renal tubule epithelial and glomerular cells seem to provide the main source of urinary sphingolipids and other lipids, although some contribution from blood cells and plasma cannot be excluded, for example, in patients with kidney disease.

For patient and control urine samples, the proportion of each of the main sphingolipids relative to the total concentration of these sphingolipids can be calculated without standardization to a reference parameter (Fig. 4). In normal controls sphingomyelin accounted for more than 60% of these sphingolipids, but in the patients, the proportion of sphingomyelin was considerably less due to the preponderance of other sphingolipids. The relative proportions of individual urinary sphingolipids were, in general, diagnostically informative. However, the quantitative lipid signals from the mass spectrometric sphingolipid analysis of urine extracts should be standardized to a reference parameter (supporting information S8 may be found in the online version of this article). We used the ratio of signals for the different sphingolipids, including ceramide, to the urinary sphingomyelin concentration (Table I), in analogy to a described approach [Berná et al., 1999].

In this study we have demonstrated for the first time the use of urinary sphingolipid analysis when diagnosing the rare pSap-d condition. We have also confirmed the usefulness of this procedure when screening for SapB-d and other sphingolipidoses (Table I). In particular, urinary lipid analysis by ESI-MS/MS for the present pSap-d neonate verified the complex urinary lipid changes in this condition and allowed quantification of individual sphingolipid classes. There was a large increase in the concentration of Gb3Cer (within the range seen in adult Fabry disease) along with increases in sulfatide, dihexosylceramides (LacCer and digalactosylceramide), GlcCer, and ceramide. On the other hand, ESI-MS/MS analysis in the new patient with SapB-d showed a urinary concentration of sulfatide similar to that in MLD, and an elevated concentration of Gb3Cer, though lower than in adult Fabry disease males (see also supporting information S9 which may be found in the online version of this article). The urinary concentration of LacCer/digalactosylceramide was also increased in the SapB-d patient (Table I). Digalactosylceramide is a substrate that, like Gb3Cer, is thought to depend on intact SapB for its degradation by α-galactosidase A (EC 3.2.1.22) [Bradová et al., 1993] and, therefore, would be expected to be increased in SapB-d. Other authors [Li et al., 1985] have also reported elevated levels of this dihexosylceramide (in addition to LacCer, Gb3Cer, and sulfatide) in urine from SapB-d patients.

The c.1006-2A > G splice-site mutation in patient 1 (pSap-d) results in a premature stop codon with, when compared to the wild-type transcript, only traces of the mutant transcript detected by RT-PCR, indicating that it was probably largely removed through nonsense-mediated decay. Consistent with this view, another premature stop codon mutation located downstream of the SapB domain, as in the present patient, also results in an apparently mRNA-negative (pSap-d) allele [Diaz-Font et al., 2005]. Although we could not completely exclude the possibility that the residual mutant transcript gave rise to small amounts of functional SapA and SapB in our patient in vivo, the patient's clinical and biochemical phenotype was as severe as in previously described patients, supporting the view that functional SapA and SapB were absent.

The two mutations carried by patient 2 (SapB-d) affect the fate of the prosaposin transcript in very different ways. A 2 bp deletion (c.828-829delGA) in exon 8 on one allele results in complete absence of the transcript, most likely due to nonsense-mediated decay, so no pSap or Saps would be generated from this allele. On the other allele, the c.577-2A > G splicing mutation leads to the formation of two alternative transcripts, both of which carry an in-frame deletion of a portion of the SapB domain. This mutation exclusively affects the SapB domain and should not result in the deficiency of other Saps. In keeping with this finding, the biochemical and also clinical phenotype in this patient were consistent with an isolated absence of SapB.

To date, four different genotypes (all homozygous), including the one for the present patient, have been reported for pSap-d [Schnabel et al., 1992; Hůlková et al., 2001; Millat et al., 2003]. All have led to a complete loss of functional pSap and Saps and a rather uniform phenotype. In contrast, for the SapB-d condition not only late infantile but also later manifesting, even adult, phenotypes

[Hahn et al., 1982; Rafi et al., 1992] have been described. SapC-d is similar to SapB-d in this respect, with patients presenting with a range of phenotypes including neuronopathic and non-neuronopathic forms [Tylki-Szymańska et al., 2007]. In deficiencies of single Saps the second allele can be a null (pSap-d) allele, with the three active Saps derived from only one allele (refer to [Diaz-Font et al., 2005; Tylki-Szymańska et al., 2007] for examples of SapC-d and the patients described in [Holtschmidt et al., 1991; Deconinck et al., 2008] and the present patient for examples of SapB-d).

However, other mutant *PSAP* genotypes may occur which affect the function of more than one Sap domain but less than the whole pSap. In a two-saposin-deficient (Saps C and D inactive) mouse model, the resulting phenotype [Sun et al., 2007] included some but not all features of pSap-d mice [Fujita et al., 1996]. One 28-month-old patient [Wenger et al., 1989] was described to have SapB-d, but was not studied molecularly. Of note, his clinical and pathologic findings indicated a generalized neurovisceral dystrophy comparable to that in pSap-d, in addition to symptoms suggestive of MLD. The study of additional mutant *PSAP* genotypes and phenotypes should contribute to the better understanding of the functions of the pSap/Saps system.

ACKNOWLEDGMENTS

Dr. P. Bauer, Department of Medical Genetics of the University of Tübingen, is thanked for providing samples from the parents of the pSap-d patient. Dr. B. Kustermann-Kuhn and Mrs. J. Backes, Universitäts-Kinderklinik Tübingen, are thanked for their assistance with thin layer chromatographic lipid urinalysis. Professor F. Turecek, Department of Chemistry, University of Washington, Seattle, U.S.A., is thanked for valuable discussions on MS/MS methodology. This work was supported by the research projects MSM 0021620806 from the Ministry of Education and Youth and MZOVFN2005 from the Ministry of Health of the Czech Republic, and by the Grant Agency of the Czech Republic (No 303/03H065).

REFERENCES

Asfaw B, Schindler D, Ledvinová J, Černý B, Šmíd F, Conzelmann E. 1998. Degradation of blood group A glycolipid A-6-2 by normal and mutant human skin fibroblasts. J Lipid Res 39:1768–1780.

Berná L, Asfaw B, Conzelmann E, Černý B, Ledvinová J. 1999. Determination of urinary sulfatides and other lipids by combination of reversed-phase and thin-layer chromatographies. Anal Biochem 26:304–311.

Bradová V, Šmíd F, Ulrich-Bott B, Roggendorf W, Paton BC, Harzer K. 1993. Prosaposin deficiency: Further characterization of the sphingolipid activator protein-deficient sibs. Hum Genet 92:143–152.

De Hoffmann E, Stroobant V. 2002. External standard method. Sources of error. Internal standard method. In: De Hoffmann E, Stroobant V, editors. Mass spectrometry: Principles and applications, 2nd edition. Chichester, New York: John Wiley & Sons. pp 199–203.

Deconinck N, Messaaoui A, Ziereisen F, Kadhim H, Sznajer Y, Pelc K, Nassogne MC, Vanier M-T, Dan B. 2008. Metachromatic leukodystrophy without arylsulfatase A deficiency: A new case of saposin-B deficiency. Eur J Paediatr Neurol 12:46–50 [epub July 2007].

Desnick RJ, Sweeley CC, Krivit W. 1970. A method for the quantitative determination of neutral glycosphingolipids in urine sediment. J Lipid Res 11:31–37.

Diaz-Font A, Cormand B, Santamaria R, Vilageliu L, Grinberg D, Chabás A. 2005. A mutation within the saposin D domain in a Gaucher disease patient with normal glucocerebosidase activity. Hum Genet 117: 275–277.

Elleder M, Jeřábková M, Befekadu A, Hřebíček M, Berná L, Ledvinová J, Hůlková H, Rosewich H, Schymik N, Paton BC, Harzer K. 2005. Prosaposin deficiency—A rarely diagnosed, rapidly progressing, neonatal neurovisceral lipid storage disease. Report of a further patient. Neuropediatrics 36:171–180.

Fujita N, Suzuki K, Vanier M-T, Popko B, Maeda N, Klein A, Henseler M, Sandhoff K, Nakayasu H, Suzuki K. 1996. Targeted disruption of the mouse sphingolipid activator protein gene: A complex phenotype, including severe leukodystrophy and wide-spread storage of multiple sphingolipids. Hum Mol Genet 5:711–725.

Fuller M, Sharp PC, Rozaklis T, Whitfield PD, Blacklock D, Hopwood JJ, Meikle PJ. 2005. Urinary lipid profiling for the identification of Fabry hemizygotes and heterozygotes. Clin Chem 51:688–694.

Hahn AF, Gordon BA, Feleki V, Hinton GG, Gilbert JJ. 1982. A variant form of metachromatic leukodystrophy without arylsulfatase deficiency. Ann Neurol 12:33–36.

Han X, Gross RW. 2005. Shotgun lipidomics: Electrospray ionization mass spectrometric analysis and quantitation of cellular lipidomes directly from crude extracts of biological samples. Mass Spectrom Rev 24:367–412.

Harzer K, Paton BC, Poulos A, Kustermann-Kuhn B, Roggendorf W, Grisar T, Popp M. 1989. Sphingolipid activator protein deficiency in a 16-week-old atypical Gaucher disease patient and his fetal sibling: Biochemical signs of combined sphingolipidoses. Eur J Pediatr 149:31–39.

Henseler M, Klein A, Reber M, Vanier M-T, Landrieu P, Sandhoff K. 1996. Analysis of splice-site mutation in the sap-precursor gene of a patient with metachromatic leukodystrophy. Am J Hum Genet 58:65–74.

Holtschmidt H, Sandhoff K, Kwon HY, Harzer K, Nakano T, Suzuki K. 1991. Sulfatide activator protein. Alternative splicing that generates three mRNAs and a newly found mutation responsible for a clinical disease. J Biol Chem 266:7556–7560.

Hůlková H, Červenková M, Ledvinová J, Tocháčková M, Hřebíček M, Poupetová H, Befekadu A, Berná L, Paton BC, Harzer K, Böör A, Šmíd F, Elleder M. 2001. A novel mutation in the coding region of the prosaposin gene leads to complete deficiency of prosaposin and saposins, and is associated with a complex sphingolipidosis dominated by lactosylceramide accumulation. Hum Mol Genet 10:927–940.

Li S-C, Kihara H, Serizawa S, Li Y-T, Fluharty AL, Mayes JS, Shapiro LJ. 1985. Activator protein required for the enzymatic hydrolysis of cerebroside sulfate. Deficiency in urine of patients affected with cerebroside sulfatase activator deficiency and identity with activators for the enzymatic hydrolysis of G_{M1} ganglioside and globotriaosylceramide. J Biol Chem 260:1867–1871.

Liebisch G, Drobnik W, Reil M, Trumbach B, Arnecke R, Olgemoller B, Roscher R, Schmitz G. 1999. Quantitative measurement of different ceramide species from crude cellular extracts by electrospray ionization tandem mass spectrometry (ESI-MS/MS). J Lipid Res 40:1539–1546.

Matsuda J, Kido M, Tadano-Aritomi K, Ishizuka I, Tominaga K, Toida K, Takeda E, Suzuki K, Kuoda Y. 2004. Mutation in saposin D domain of sphingolipid activator protein gene causes urinary system defects and cerebellar Purkinje cell degeneration with accumulation of hydroxy fatty acid-containing ceramide in the mouse. Hum Mol Genet 13:2709–2723.

Millat G, Verot L, Rodriguez-Lafrasse C, DiMarco JN, Rimet Y, Poujol A, Girard N, Monges G, Livet MO, Vanier M-T. 2003. Fourth reported

family with prosaposin deficiency. In: Elleder M, Ledvinová J, Hřebíček M, Poupetová H, Kožich V, editors. Book of abstracts 14th ESGLD workshop (September 18th–21st, 2003). Podebrady/Prague: Guarant Ltd. p 81.

Mills K, Johnson A, Winchester B. 2002. Synthesis of novel internal standards for the quantitative determination of plasma ceramide trihexoside in Fabry disease by tandem mass spectrometry. FEBS Lett 515:171–176.

Rafi MA, Amini S, Zhang X-L, Wenger DA. 1992. Correction of sulfatide metabolism after transfer of prosaposin cDNA to cultured cells from a patient with SAP-1 deficiency. Am J Hum Genet 50:1252–1258.

Sandhoff K, Kolter T, Harzer K. 2001. Sphingolipid activator proteins. In: Scriver CR, Beaudet AL, Sly WS, Valle D, editors. The Metabolic and molecular bases of inherited diseases, 8th edition. New York: McGraw-Hill. pp 3371–3388.

Schlote W, Harzer K, Christomanou H, Paton BC, Kustermann-Kuhn B, Schmid B, Seeger J, Beudt U, Schuster I, Langenbeck U. 1991. Sphingolipid activator protein 1 deficiency in metachromatic leucodystrophy with normal arylsulphatase A activity. A clinical, morphological, biochemical, and immunological study. Eur J Pediatr 150:584–591.

Schnabel D, Schröder M, Fürst W, Klein A, Hurwitz R, Zenk T, Weber J, Harzer K, Paton BC, Poulos A, Suzuki K, Sandhoff K. 1992. Simultaneous deficiency of sphingolipid activator proteins 1 and 2 is caused by a mutation in the initiation codon of their common gene. J Biol Chem 267:3312–3315.

Spiegel R, Bach G, Sury V, Mengistu G, Meidan B, Shalev S, Shneor Y, Mandel H, Zeigler M. 2005. A mutation in the saposin A coding region of the prosaposin gene in an infant presenting as Krabbe disease: First report of saposin A deficiency in humans. Mol Genet Metab 84:160–166.

Sun Y, Witte DP, Zamzow M, Ran H, Quinn B, Matsuda J, Grabowski GA. 2007. Combined saposin C and D deficiencies in mice lead to a neuronopathic phenotype, glucosylceramide and α–hydroxy ceramide accumulation, and altered prosaposin trafficking. Hum Mol Genet 16:957–971.

Tylki-Szymańska A, Czartoryska B, Vanier M-T, Poorthuis BJMH, Groener JAE, Ługowska A, Millat G, Vaccaro AM, Jurkiewicz E. 2007. Non-neuronopathic Gaucher disease due to saposin C deficiency. Clin Genet 72:538–542. [epub October 2007].

Wenger DA, DeGala G, Williams C, Taylor HA, Stevenson RE, Pruitt JR, Miller J, Garen PD, Balentine JD. 1989. Clinical, pathological, and biochemical studies on an infantile case of sulfatide/GM1 activator protein deficiency. Am J Med Genet 33:255–265.

Whitfield PD, Sharp PC, Johnson DW, Nelson P, Meikle PJ. 2001. Characterization of urinary sulfatides in metachromatic leukodystrophy using electrospray ionization-tandem mass spectrometry. Mol Genet Metab 73:30–37.

Supplementary Materials to the Paper entitled

Prosaposin Deficiency and Saposin B Deficiency (Activator-Deficient Metachromatic Leukodystrophy); Report on Two Patients Detected by Analysis of Urinary Sphingolipids and Carrying Novel PSAP Gene Mutations.

(American Journal of Medical Genetics, vol. ….)

Supplementary material S1:

For thin layer chromatography, urinary lipids were extracted as follows: First, 3 ml urine was acidified with 10 µl concentrated hydrochloric acid and left at 6° C for 10 h. The sample was then mixed with 9 ml methanol and 8 ml chloroform and phase-partitioned with 5 ml water. The clear portion of the upper phase was removed and the lower phase partitioned twice more in the same way. The final lower phase was dried and the residue re-extracted with 1 ml chloroform/methanol 2:1 (v/v). The extract was concentrated 20-fold and then applied as a spot to the lower left corner of a silica gel HPTLC plate (no. 1.05631, Merck, Darmstadt, Germany) for two-dimensional separation.

Supplementary material S2 (= supplementary Table 1):

Supplementary Table 1 - Conditions of ion source and quadrupole section of mass analyzer

	Ceramide	Monohexosyl-ceramides	Lactosyl- & digalactosyl-ceramide	Globo-triaosyl-ceramide	Sphingo-myelin	Sulfatide
Courtain gas (psi)	10	10	10	10	10	10
Voltage (kV)	4.5	4.5	4.5	4.5	4.5	-4.5
Temperature (°C)	200	200	200	200	200	200
Source gas 1 (psi)	20	20	20	20	20	20
Source gas 2 (psi)	55	55	55	45	55	45
Declustering potential (V)	60	47	65	78	76	-150
Entrance potential (V)	5	4.9	6	7.9	5.6	-9
Collision energy (V)	42	48	64	74	37	-130
Collision gas (psi)	5	5	5	3	5	3
Collision cell exit potential (V)	5.7	5.6	5.6	5.4	4.1	-1

Nitrogen was used as the collision gas

Supplementary material S3 (= supplementary Fig. 1):

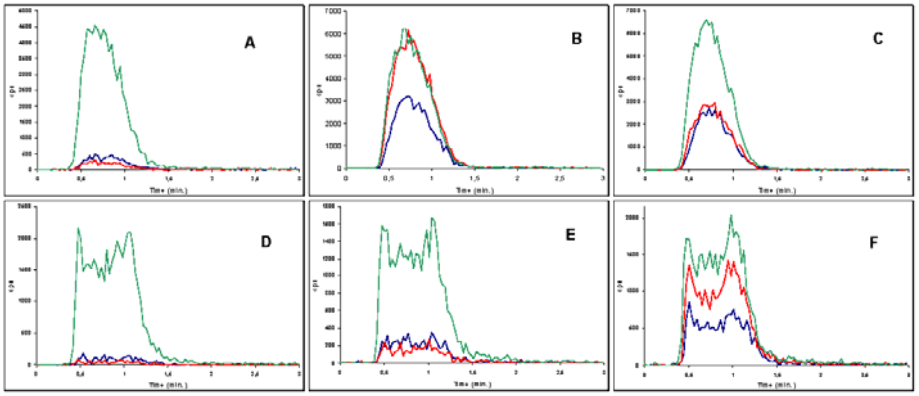

Supplementary Fig. 1: Examples of extracted ion current of MS/MS measurements of selected isoforms of sphingolipids (sulfatides and monohexosylceramides [MHC]) in urine. Abscissa = time of measurement in minutes, ordinate = signal intensity in counts per second (cps). A – sulfatide, infantile control; B – sulfatide, patient 2 (SapB-d); C – sulfatide, patient 1 (pSap-d); D – MHC, infantile control; E – MHC, patient 2 (SapB-d); F – MHC, patient 1 (pSap-d). Different colors represent specific lipid isoform as follows: blue for C16:0 isoforms (sufatide and MHC), red for C24:0 (sulfatide) or C24:1 (MHC) isoforms. Green is for ISTs ([C17:0]sulfatide or [C17:0]MHC). Differences in concentration of lipids are evident when comparing signals of urinary isoforms to signals of internal standards in controls and in patients. Please note that in the infantile control samples (A and D) the signals were also sufficiently high to be measured.

Supplementary material S4 (=supplementary Table 2):

Supplementary Table 2 – Transition ion pairs for MRM measurement and quantitation of sphingolipids

Ceramide			
Isoform by fatty acid	**Parent ion**	**Daughter ion**	**Scan time**
C14:0	**510.7**	**264.4**	**100 ms**
C16.0	**538.8**	**264.4**	**100 ms**
C18:0	**566.8**	**264.4**	**100 ms**
C18:0-OH	**582.8**	**264.4**	**100 ms**
C20:0	**594.9**	**264.4**	**100 ms**
C22:0	**622.8**	**264.4**	**100 ms**
C22:1-OH	**636.9**	**264.4**	**100 ms**
C24:0	**650.8**	**264.4**	**100 ms**
C24:1	**648.8**	**264.4**	**100 ms**
C24:2	**646.8**	**264.4**	**100 ms**
C26:0	**678.8**	**264.4**	**100 ms**
C26:1	**676.8**	**264.4**	**100 ms**
C26:2	**674.8**	**264.4**	**100 ms**
C24:0-OH	**666.7**	**264.4**	**100 ms**
C24:1-OH	**664.7**	**264.4**	**100 ms**
C24:2-OH	**662.7**	**264.4**	**100 ms**
C26:0-OH	**694.7**	**264.4**	**100 ms**
C26:1-OH	**692.7**	**264.4**	**100 ms**
C22:0-OH	**638.8**	**264.4**	**100 ms**
C17:0 (internal standard)	**552.6**	**264.4**	**100 ms**
Monohexosylceramides			

Isoform by fatty acid	Parent ion	Daughter ion	Scan time
C16:0	700.8	264.4	100 ms
C18:0	728.8	264.4	100 ms
C20:0	756.9	264.4	100 ms
C22:0	784.9	264.4	100 ms
C22:1	782.9	264.4	100 ms
C22:1-OH	798.9	264.4	100 ms
C24:0	812.9	264.4	100 ms
C24:1	810.9	264.4	100 ms
C24:2	808.9	264.4	100 ms
C24:0-OH	828.9	264.4	100 ms
C24:1-OH	826.9	264.4	100 ms
C24:2-OH	824.8	264.4	100 ms
C26:0	840.9	264.4	100 ms
C26:1	838.9	264.4	100 ms
C26:2	836.7	264.4	100 ms
C26:0-OH	856.9	264.4	100 ms
C17:0 (internal standard)	714.5	264.4	100 ms
Lactosyl- and digalactosylceramide			
Isoform by fatty acid	**Parent ion**	**Daughter ion**	**Scan time**
C16:0	862.7	264.4	100 ms
C18:0	890.7	264.4	100 ms
C20:0	918.7	264.4	100 ms
C22:0	946.8	264.4	100 ms
C22:1	944.8	264.4	100 ms
C22:1-OH	960.8	264.4	100 ms
C24:0	974.9	264.4	100 ms

C24:1	**972.9**	**264.4**	**100 ms**
C24:2	**970.9**	**264.4**	**100 ms**
C24:0-OH	**990.9**	**264.4**	**100 ms**
C24:1-OH	**988.9**	**264.4**	**100 ms**
C22:0-OH	**962.6**	**264.4**	**100 ms**
C16:0-D_3 (internal standard)	**865.7**	**264.4**	**100 ms**
Globotriaosylceramide			
Isoform by fatty acid	**Parent ion**	**Daughter ion**	**Scan time**
C16:0	**1024.6**	**264.4**	**100 ms**
C18:0	**1052.7**	**264.4**	**100 ms**
C18:1	**1068.7**	**264.4**	**100 ms**
C20:0	**1080.8**	**264.4**	**100 ms**
C22:0	**1108.7**	**264.4**	**100 ms**
C22:1	**1106.8**	**264.4**	**100 ms**
C22:0-OH	**1124.8**	**264.4**	**100 ms**
C22:1-OH	**1122.7**	**264.4**	**100 ms**
C24:0	**1136.8**	**264.4**	**100 ms**
C24:1	**1134.8**	**264.4**	**100 ms**
C24:2	**1132.6**	**264.4**	**100 ms**
C24:0-OH	**1152.8**	**264.4**	**100 ms**
C24:1-OH	**1150.8**	**264.4**	**100 ms**
C24:2-OH	**1148.8**	**264.4**	**100 ms**
C26:0	**1164.8**	**264.4**	**100 ms**
C26:1	**1162.9**	**264.4**	**100 ms**
C26:2	**1160.8**	**264.4**	**100 ms**
C26:0-OH	**1180.9**	**264.4**	**100 ms**
C26:1-OH	**1178.6**	**264.4**	**100 ms**
C26:2-OH	**1176.7**	**264.4**	**100 ms**

C17:0 (internal standard)	1038.7	264.4	100 ms
Sphingomyelin			
Isoform by fatty acid	Parent ion	Daughter ion	Scan time
C16:0	703.7	184.2	100 ms
C16:1	701.7	184.2	100 ms
C18:0	731.7	184.2	100 ms
C18:1	729.7	184.2	100 ms
C20:0	759.8	184.2	100 ms
C20:1-OH	773.8	184.2	100 ms
C22:0	787.8	184.2	100 ms
C22:1	785.8	184.2	100 ms
C24:0	815.8	184.2	100 ms
C24:1	813.8	184.2	100 ms
C24:2	811.8	184.2	100 ms
C22:0-OH	803.8	184.2	100 ms
C22:1-OH	801.8	184.2	100 ms
C24:0-OH	831.8	184.2	100 ms
C24:1-OH	829.8	184.2	100 ms
C24:2-OH	827.8	184.2	100 ms
C22:2-OH	799.9	184.2	100 ms
C17:0 (internal standard)	717.7	184.2	100 ms
Sulfatide			
Isoform by fatty acid	Parent ion	Daughter ion	Scan time
C16:0	778.6	97.0	100 ms
C18:0	806.7	97.0	100 ms
C18:0-OH	822.7	97.0	100 ms
C20:0	834.7	97.0	100 ms

C20:0-OH	**850.7**	**97.0**	**100 ms**
C22:0	**862.8**	**97.0**	**100 ms**
C22:1-OH	**876.7**	**97.0**	**100 ms**
C22:0-OH	**878.7**	**97.0**	**100 ms**
C24:1	**888.8**	**97.0**	**100 ms**
C24:0	**890.7**	**97.0**	**100 ms**
C23:0-OH	**892.8**	**97.0**	**100 ms**
C24:1-OH	**904.8**	**97.0**	**100 ms**
C24:0-OH	**906.8**	**97.0**	**100 ms**
C26:1	**916.8**	**97.0**	**100 ms**
C26:0	**918.9**	**97.0**	**100 ms**
C26:1-OH	**932.8**	**97.0**	**100 ms**
C26:0-OH	**934.9**	**97.0**	**100 ms**
C17:0 (internal standard)	**792.7**	**97.0**	**100 ms**

Supplementary material S5 (= supplementary Fig. 2):

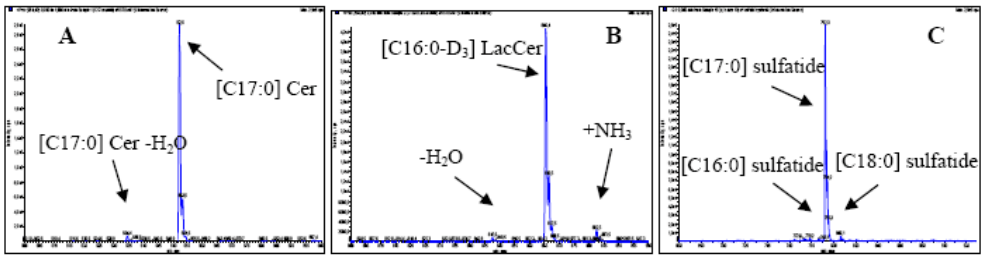

Supplementary Fig. 2: Chemical identity and isoform purity of selected sphingolipid standards: [C17:0]ceramide (A), [C16:0-D_3]lactosylceramide (B) and [C17:0]sulfatide (C). Abscissa = m/z (mass to charge ratio), Ordinate = signal intensity in cps. Precursor ion scans of the lipids used as internal standards were undertaken to prove their chemical identity. Precursor scan for ion with m/z 264.4 in positive ion mode was performed for ceramide and lactosylceramide (LacCer) and for ion with m/z 97 in negative ion mode for sulfatide. The ceramide and LacCer standard each revealed only a single major peak corresponding to the lipid isoform, with some minor peaks resulting from loss of water and, in the case of LacCer, formation of ammonia adducts, which can be explained as an effect of ammonium formate in methanol, also evident. Only traces of byproducts (up to 3%) were detected in [C17:0]sulfatide and consisted of [C16:0] and [C18:0] sulfatide isoforms probably generated during the enzymatic semisynthesis with fatty acids bound to the commercial enzyme preparation.

Supplementary material S6:

The following enzyme activities were found in fibroblast homogenates from patient 1: Glucosylceramide β–glucosidase (EC 3.2.1.45; 'low substrate assay' [Elleder et al., 2005; for reference, see main paper]); mean of duplicates: 1.65 units (where 1 unit = 1 nmol radioactive substrate cleaved per h per 10^6 cells; normal range [n=5], 2.2 – 4.9 units) and galactosylceramide β–galactosidase (EC 3.2.1.46; mean of duplicates: 0.41; normal range, 1.3

– 3.8 units), but a normal sphingomyelinase (EC 3.1.4.12; mean of duplicates: 22.0; normal range, 7.7 – 27.8 units) activity.

Supplementary material S7:

Metabolic experiments with radioactive sphingolipid substrates (tritium-labelled on their ceramide moieties) loaded onto living fibroblast cultures from patient 1 and patient 2 gave similar results to those described for an earlier pSap-d [Elleder et al., 2005; for references, see main paper] and an earlier SapB-d [Schlote et al., 1991] patient, respectively. Loading fibroblasts with [^{3}H]glucosylceramide resulted in a higher retention of radioactivity within ceramide in cells from patient 1 (31 % of incorporated radioactivity) than in control cells (4 to 8 %), demonstrating a block at ceramide degradation. This block was also evident when cells from patient 1 were loaded with [^{3}H]sphingomyelin (70 % of radioactivity recovered in ceramide compared to 10 to 14 % in controls). For cells from both patient 1 and patient 2, there was a reduced turnover of loaded [^{3}H]globotriaosylceramide (3- to 5-fold lower radioactivity in LacCer and other metabolites) and of independently loaded [^{3}H]sulfatide (about 3-fold lower radioactivity in galactosylceramide and other metabolites) in comparison to controls, a finding similar to that seen with metachromatic leukodystrophy cells.

Supplementary material S8:

The widely used urinary creatinine concentration proved unsuitable as a reference parameter in our experience, possibly due to the physiological considerations mentioned above. In particular, when the urinary creatinine concentration was lower than 1 mmol per litre, the ratios of quantitative MS/MS lipid signals to creatinine levels often appeared to be falsely high. Others have used the ratio of signal to urinary phospholipids, e.g., urinary phosphatidyl choline concentration [Whitfield et al., 2001; for reference, see main paper], whereas we used a ratio of specific lipid signal/urinary sphingomyelin concentration.

Supplementary material S9:

The lipid abnormalities in urine could be qualitatively explained by the specific absences of Saps [Sandhoff et al., 2001; for references, see main paper] in pSap-d (patient 1) and SapB-d (patient 2). But it was unclear, why the ratio of Gb3Cer to sulfatide concentration was about 3 in pSap-d versus about 0.3 in SapB-d (for individual Gb3Cer and sulfatide values, see Table I in main paper). Given that SapB is required for the breakdown of both of these glycolipids [Sandhoff et al., 2001] and it is absent in pSap-d as well as SapB-d, additional factors seem to have contributed to this difference. One factor might have been the discordant ages at the time of study (pSap-d, 44-day-old; SapB-d, 50-month-old). However, in pSap-d the absence of SapA, C and D, in addition to that of SapB, may also have indirectly contributed to the high elevation of urinary Gb3Cer. Moreover, a role for the absence of SapD in pSap-d might be deduced from the findings in a SapD-d mouse model [Matsuda et al., 2004], where the striking degeneration of renal tubule cells might be viewed as a factor relevant to sphingolipid levels.

In addition, there were increased urinary concentrations of LacCer/digalactosalceramide, monohexosylceramide and ceramide in the SapB-d patient (Table I of main paper). These non-sulfatide lipid elevations might be explained as secondary effects of the high sulfatide abundance in renal cells. Moreover, LacCer sulfate (a minor component of sulphated glycolipids compared to the predominating galactosylceramide sulfate [= sulfatide, as discussed above]) was also found to be elevated in patient 1 and patient 2 (results not shown).

SUPPLEMENTARY PUBLICATIONS

Publications in impacted journals related to topic of this PhD thesis

Supplementary publication C

Kuchar L., Asfaw B., Poupetova H., et al., *Direct tandem mass spectrometric profiling of sulfatides in dry urinary samples for screening of metachromatic leukodystrophy.* Clin Chim Acta, 2013. **425C**: p. 153-159

Clinica Chimica Acta 425 (2013) 153–159

Contents lists available at ScienceDirect

Clinica Chimica Acta

journal homepage: www.elsevier.com/locate/clinchim

Direct tandem mass spectrometric profiling of sulfatides in dry urinary samples for screening of metachromatic leukodystrophy

Ladislav Kuchař [a], Befekadu Asfaw [a], Helena Poupětová [a], Jitka Honzíková [a], František Tureček [b,*], Jana Ledvinová [a,**]

[a] Institute of Inherited Metabolic Diseases, First Faculty of Medicine and General Teaching Hospital, Charles University, 128 08 Prague, Czech Republic
[b] Department of Chemistry, University of Washington, Seattle, WA 98195-1700, USA

ARTICLE INFO

Article history:
Received 19 February 2013
Received in revised form 28 June 2013
Accepted 28 June 2013
Available online 6 July 2013

Keywords:
Urinary sulfatide
Isoforms
Screening for metachromatic leukodystrophy
Tandem mass spectrometry
DEAE-cellulose membrane
Dry urinary samples

ABSTRACT

Background: Prediagnostic steps in suspected metachromatic leukodystrophy (MLD) rely on clinical chemical methods other than enzyme assays. We report a new diagnostic method which evaluates changes in the spectrum of molecular types of sulfatides (3-O-sulfogalactosyl ceramides) in MLD urine.
Methods: The procedure allows isolation of urinary sulfatides by solid-phase extraction on DEAE-cellulose membranes, transportation of a dry membrane followed by elution and tandem mass spectrometry (MS/MS) analysis in the clinical laboratory. Major sulfatide isoforms are normalized to the least variable component of the spectrum, which is the indigenous C18:0 isoform. This procedure does not require the use of specific internal standards and minimizes errors caused by sample preparation and measurement.
Results: Urinary sulfatides were analyzed in a set of 21 samples from patients affected by sulfatidosis. The combined abundance of the five most elevated isoforms, C22:0, C22:0-OH, C24:0, C24:1-OH, and C24:0-OH sulfatides, was found to give the greatest distinction between MLD-affected patients and a control group.
Conclusions: The method avoids transportation of liquid urine samples and generates stable membrane-bound sulfatide samples that can be stored at ambient temperature. MS/MS sulfatide profiling targeted on the most MLD-representative isoforms is simple with robust results and is suitable for screening.

1. Introduction

Metachromatic leukodystrophy (MLD) is a rare autosomal recessive disorder caused by a deficiency of lysosomal arylsulfatase A (ASA). ASA desulfates 3-O-sulfogalactosyl ceramide (sulfatide, galactosylceramide I^3-sulfate) (Fig. 1) and is assisted by the nonenzymatic activator protein saposin B [1,2]. ASA deficiency, or lack of its activator protein causing saposin B and prosaposin deficiencies (Psap-d), results in accumulation of sulfatides in lysosomes and demyelination of the central and peripheral nervous system. The disease has several variants that differ in the clinical onset and severity. The late infantile form of MLD is most common and severe and results in death of the affected children in the first decade of life. The juvenile and adult forms have a milder course that manifests itself by gait disturbances, mental regression, and emotional disturbances [2].

Biochemical detection of MLD presents specific challenges. Since there is currently no approved therapy for MLD [3–7], detection of the late infantile form by newborn screening has not been considered, and a suitable method is not available so far. Enzyme assays in cell homogenates have been developed for ASA that use 4-nitrocatechol sulfate for UV/VIS or methylumbelliferyl sulfate for fluorescence detection of products [8–11]. However, the practical use of enzyme assays is hampered by the occurrence of two pseudodeficiency alleles of the ASA gene locus (EC 3.1.6.8) which are carried by a substantial group of the general population, estimated at 10 − 15% in Europe [2]. These benign pseudodeficiencies are caused by either a point mutation that removes the protein glycosylation site [12], or a mutation of a polyadenylation site [13], resulting in low ASA activity in *in vitro* assays, but not causing disease [14–17]. Other methods of diagnosis are based on clinical symptoms and changes caused by demyelination and deposition of sulfatides in metachromatic granules [18,19].

All MLD forms manifest themselves by an elevated concentration of sulfatides in urine. Previous bioanalytical methods of sulfatide detection were based on thin layer chromatography separation of native glycosphingolipids with densitometric evaluation [20], or utilized chemical derivatization combined with gas [21] or liquid [22] chromatography, or applied matrix-assisted laser desorption ionization mass spectrometry after sulfatide conversion into its lyso-form [23]. Recently, Meikle's group reported detection and quantitation

Abbreviations: CV, coefficient of variation; DEAE, Diethylaminoethyl; MLD, metachromatic leukodystrophy; Psap-d, prosaposin deficiency; ASA, arylsulfatase A; PTFE, polytetrafluoroethylene; SRM, selected reaction monitoring; MS/MS, tandem mass spectrometry; S/N, signal to noise ratio; IPN, isoform profile number (ratio of the sum of the major five isoforms and the C18:0 sulfatide); DUS, dry urinary sample.

* Corresponding author. Tel.: +1 206 685 2041; fax: +1 206 685 8665.
** Corresponding author. Tel.: +420 224967033; fax: +420 224967119.
E-mail addresses: turecek@chem.washington.edu (F. Tureček), jledvin@cesnet.cz (J. Ledvinová).

0009-8981/$ – see front matter © 2013 Elsevier B.V. All rights reserved.
http://dx.doi.org/10.1016/j.cca.2013.06.027

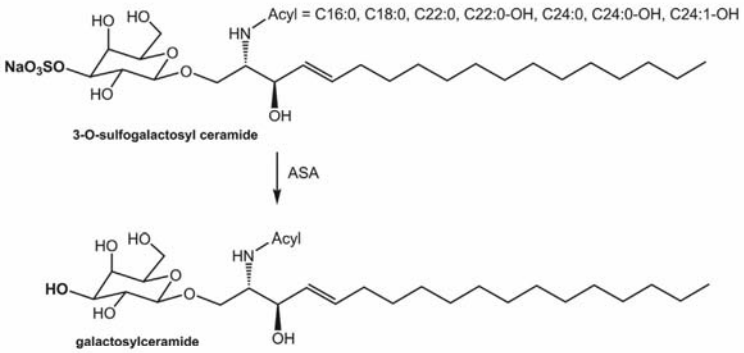

Fig. 1. The chemistry of sulfatide degradation catalyzed by arylsulphatase A.

of urine sulfatides by electrospray ionization mass spectrometry in the negative ion mode [24,25]. Norris et al. [26] have developed an assay for sulfatide detection in brain tissue that was based on positive ion electrospray tandem mass spectrometry of sulfatide–lithium ion adducts. Kuchař et al. [27] used tandem mass spectrometry in the negative ion mode to prove massive excretion of urinary sulfatides in patients with function defect of ASA protein activator saposin B (prosaposin and saposin B deficiencies) and also in MLD cases. A common feature of these procedures is that they use liquid–liquid extraction from urine to chloroform–methanol.

Tandem mass spectrometry provides specific data that allow examination of detailed patterns of molecular species and monitoring of changes in their relative abundance that can be related to the nature of the disease. Detailed MS/MS determination of variations in lipid composition has strongly influenced the clinical view in some diseases, and understanding such variations in relation to the disease may help identify new categories of biomarkers [28].

We now report a new laboratory procedure that uses ion-exchange membranes for an efficient and solvent-free sulfatide extraction from urine and produces dry samples that are readily transported and stored. Electrospray MS/MS is used for targeted lipidomic analysis of selected sulfatide isoforms for screening of MLD.

2. Materials and methods

2.1. Materials

Archived and anonymous urine samples (first morning or randomly taken specimens) were obtained from patients previously diagnosed with MLD (20 patients) or prosaposin deficiency (one patient), and controls (50 individuals). The study was approved by the Ethics Committee of the General University Hospital in Prague. MLD samples were obtained from patients afflicted with the late infantile form (7 patients, ages 2–5), juvenile form (4 patients, ages 7–17), and adult form (9 patients, ages 23–38). The prosaposin deficiency sample was from a 44-day old male infant. Samples (10 ml) were stored in plastic tubes at −20 °C. DEAE membranes were purchased from Sartorius Stedim Biotech GmbH (Goettingen, Germany, Sartobind D membrane A4 cat No. 94IEXD42-001). Chloroform (Sigma-Aldrich Co., St. Louis, MO; grade CHROMASOLV for HPLC 99.9%), methanol (Sigma-Aldrich; grade CHROMASOLV for LC–MS Riedel-de Haën or Fluka), *n*-hexane (Sigma-Aldrich; grade CHROMASOLV for LC–MS Fluka), 2-propanol (Sigma-Aldrich; grade CHROMASOLV for LC–MS Fluka) and ammonium acetate (Sigma-Aldrich, Fluka Analytical, puriss p.a. for mass spectroscopy ≥99.0%) were used as received. SUPELCOSIL ™ LC-Si HPLC Column 7.5 cm × 3 mm, 3 μm, was purchased from Supelco (Cat No 58980C30, Supelco, Bellefonte, PA, USA). Security Guard Kit (Phenomenex, KJO-4282) and Silica Cartridges (10 pcs, Phenomenex, AJO-4348) were supplied by Phenomenex Inc. (Torrance, CA, USA). C12:0 sulfatide was purchased from Avanti Polar Lipids Inc (Alabaster, AL, USA). C17:0 sulfatide was prepared as described previously [29]

2.2. Preparation of dry DEAE membrane with bound urinary sulfatides

DEAE membrane (Sartobind D, A4 29.7 × 21 cm) was cut into 1 × 1 cm squares. The squares were immersed for 15 min in the sufficient volume of urine (about 10 ml is recommended) which was previously thoroughly mixed for 1 min to disperse the sediment throughout the sample volume. The soaked DEAE membrane was placed on a laboratory stand and allowed to dry at laboratory temperature for about 5 h. No blotting material was used to speed up drying. The dried DEAE membranes (DUS) were stored at −20 °C prior to further processing.

2.3. Extraction of sulfatides from DEAE membrane

Sulfatides were extracted by ion-exchange using 0.2 M ammonium acetate in methanol. A membrane square was placed in a 1.5 ml Eppendorf tube with 1.4 ml 0.2 M ammonium acetate in methanol. This was followed by 30 min vortexing at 1400 rpm at room temperature. After intensive vortex mixing, the methanol solution was transferred to another Eppendorf tube and the solvent volume was reduced to <50 μl by evaporating under a stream of nitrogen at 40 °C for up to 20 min. Then 300 μl of MilliQ water was added followed by 700 μl of chloroform:methanol (2:1, v/v) and the mixture was vortexed at 1400 rpm for 30 min. The organic and water phases were separated by centrifugation at 14 000 × *g* for 5 min. A 340 μl portion of the organic phase was transferred to a glass vial and dried under stream of nitrogen. The residue was dissolved in 500 μl of methanol prior to tandem mass spectrometry analysis.

2.4. Tandem mass spectrometry

Mass spectra were measured on an ABI/MDS SCIEX API 3200 tandem mass spectrometer equipped with an ESI source and coupled to an Agilent HPLC 1100 series. Samples (20 μl of methanol solution) were introduced by flow injection at a mobile phase flow rate of 50 μl/min and electrosprayed in the negative ion mode to form $[M–H]^-$ ions. Generated ions were analyzed by SRM of precursor ions (Supplementary data Table S1) and the common HSO_4^- (*m/z* 97) fragment ion. Detailed instrument settings are described in the Supplementary data section.

2.5. Evaluation of sulfatide isoform profile: calculation of isoform profile number

The measured SRM peak heights of major MLD-related isoforms (C22:0, C22:0-OH, C24:0, C24:1-OH, and C24:0-OH see Fig. 2) were recorded and normalized to that of the indigenous C18:0 isoform to obtain the isoform profile number (IPN). Thus, the IPN value represents the ratio of the summed signals of five major elevated isoforms to the signal of the least variable C18:0 isoform.

The peak heights are proportional to the sulfatide concentrations through the corresponding response factors depending on the ionization efficiency, ion transfer, dissociation efficiency of $[M-H]^-$ ions, and fragment branching ratios. The data thus also reflect the relative abundance of each isoform in urine and are used for profiling samples from affected patients and controls.

2.6. Determination of analytical precision of the DEAE membrane method, linearity, and limits of quantification

Coefficients of variation (CV) of IPN were calculated to determine the precision of inter- and intra- assay measurements. For intra-assay analysis, one control and one MLD urine sample were used for preparation of DEAE membrane-bound sulfatides. Sulfatides were extracted from the dry membrane as described above and the extracts were repeatedly analyzed by MS. The intra CV was calculated from 10 measurements.

For inter-assay analysis, series of 10 samples of DEAE-bound sulfatides were prepared from one control and one MLD urine sample. The Inter CV was determined after analysis of 10 control and 10 MLD sulfatide extracts.

To determine the concentration dependence of the analytical precision, we used a standard sample of bovine brain sulfatides dissolved in methanol and applied on DEAE membranes. IPN was evaluated in DEAE membrane eluates over a broad range of concentrations (8 concentration points) varying from 10 to 5000 ng/membrane.

Limits of quantification for individual sulfatide isoforms in DUS were determined by a previously published method [27] using a C12:0 sulfatide internal standard.

To determine the linearity of the method, we used a standard sample of bovine brain sulfatides dissolved in methanol and applied to DEAE membranes. Signals of evaluated isoforms were measured over a broad range of concentrations from 10 to 20000 ng of sulfatides per membrane.

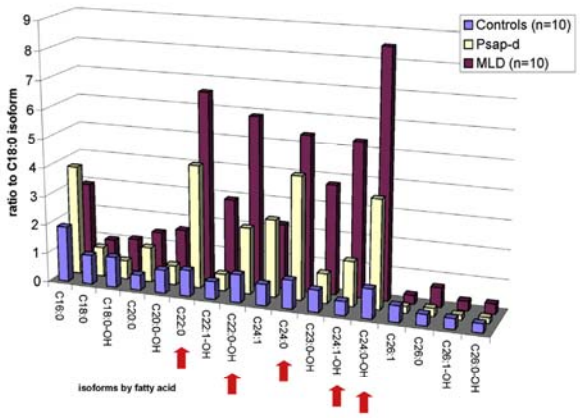

Fig. 2. Comparison of urinary isoform profiles from MLD and prosaposin deficiency (Psap-d) patients and controls. Arrows indicate components undergoing major changes.

2.7. Evaluation of matrix effects

Matrix effects of the co-eluted urine components from the DEAE membrane on the sulfatide signal were assessed in two ways, *e.g.*, using a post-extraction technique and a post-column infusion method. The latter provides the ability to design and modify methods to eliminate adverse effects of the matrix [30]. Briefly, an infusion pump is used that delivers a constant flow of the analyte or standard into the LC eluent before the ESI source and allows one to evaluate the influence of matrix on the analyte signal during the LC run [30].

The post-extraction addition method is based on a comparison of the different signal responses of the analyte with added matrix and dissolved only in a pure solvent.

Ion suppression (matrix) effects were examined by the post-extraction addition technique in six urine samples representing six independent sources of the same matrix (3 controls, 3 MLD) within a large range of creatinine concentrations (2.3–17.0 mmol/l) using published protocols [30–32]. DEAE membrane eluates were processed as described above, and the organic and water phases were separated. 340 μl of the organic (lower) phase was mixed with 10 μl of the C17:0 isoform (40 ng) solution, and the suppression of C17:0 sulfatide ion signal intensity was monitored for each urine sample.

We used post-column infusion analysis [30] with the C12:0 sulfatide standard to test whether matrix effects can be eliminated or reduced by HPLC (silica column) or LC separation (Security Guard Kit with silica cartridges; see details in the Supplementary data).

A sample was prepared by mixing the above described six urine samples and used as a source of matrix components. Post-column infusion of C12:0 sulfatide standard (40 ng in 500 μl of 2-propanol: H_2O, 90:10; v/v) at flow rate of 10 μl/min was used for matrix effect evaluation.

2.8. Stability of sulfatides on DEAE membrane

Sulfatides from six urine samples (3 controls and 3 MLD) were bound to the DEAE membrane as described and stored at laboratory temperature and at −20 °C prior to further processing. Samples were processed at different time intervals in the course of 100 days and individual IPNs were calculated.

2.9. Kidney sulfatide analysis

For tissue lipid analysis, lipid extracts of a formaline-fixed control kidney and a kidney from the patient with prosaposin deficiency were prepared by successive extraction of tissue homogenates with chloroform:methanol:water mixtures as described [33,34]. Aliquots corresponding to 1 mg of the wet weight of extracted tissue were analyzed by tandem mass spectrometry according to the previously published method [27].

3. Results

3.1. Analytical precision of a DEAE membrane method, linearity and limits of quantification

The average CV within the range from 10 to 5000 ng sulfatides/sample was 7%.

The analytical precision of the method gave an intra CV = 11% from repetitive analysis ($n = 10$) of one control sample. The MLD sample gave an intra CV = 4% ($n = 10$).

The inter CV was calculated from analyses of 10 DEAE membrane eluates. The Inter CV was 13% and 11% for the MLD and control samples, respectively.

Limits of quantification were determined for each evaluated isoform in urinary samples where the signal-to-noise ratio was at least 10:1.

Under these conditions, the limits of quantification were 4 pmol of one specific urinary sulfatide isoform per cm^2 of DEAE membrane.

Signal responses of individual isoforms were linear in a broad range of concentrations from 5 to 1500 pmol applied to the DEAE membrane, which is consistent with the concentration range for the determination of sulfatides in control and MLD urines.

3.2. Matrix effects

Because the urine samples contain the sulfatides in the presence of a large excess of low molecular mass compounds (matrix), the determination of matrix effects on the extraction and mass spectrometric analysis was essential [30]. DUS extracts showed matrix effects resulting in C17:0 sulfatide ion signal suppression by 76–84% due to the presence of extracted co-ionized urine components. However, the ion signal intensity of analyzed sulfatide isoforms was sufficient for reliable analysis. The ESI ion intensities of other sulfatides, for which we did not have synthetic standards, are presumably suppressed to a similar extent.

Nevertheless, we have tried to suppress the matrix effect using two alternative methods, one using HPLC coupled to ESI-MS/MS and the other using Security Guard Kit with two Silica cartridges (LC), which could be a fast and simple alternative to the HPLC method (for details see the Supplementary data).

HPLC fully removed matrix effects (Supplementary data Fig. 1A), which was confirmed by post-extraction addition and also by the post-column infusion method. LC utilizing a Security Guard Kit with two Silica cartridges reduced the signal intensity suppression from 75% to 17% (Supplementary data Fig. 1B) which was also confirmed by the methods mentioned above. Despite these benefits, the direct FIA-MS/MS was both faster and easier to manage while providing a rapid and reliable examination of suspected cases, which we verified in 20 MLD patients and 50 controls.

3.3. Stability of sulfatides on DEAE membrane

The stability of urinary sulfatides that were bound on DEAE membrane and stored from 1 to 100 days at laboratory temperature and at −20 °C was studied for six different urine samples with high and/or low levels of sulfatides (3 control and 3 MLD urines). The evaluation of the IPN measurements is summarized in Table 1. The IPN values were relatively stable in the course of 100 days of storage and provided a clear distinction between values for patients and controls.

Table 1
Stability of sulfatides bound to DEAE membrane under different storage conditions evaluated by IPN.

		Day						
		1	3	6	100	Avg	SD	CV%
C1	LT	7.69	6.73	8.06	6.07	7.14	0.91	12.71
	FR	7.30	8.28	8.03	6.40	7.50	0.84	11.24
C2	LT	9.51	10.05	8.44	7.78	8.95	1.03	11.46
	FR	8.50	8.34	9.55	8.80	8.80	0.54	6.12
C3	LT	8.62	9.86	10.26	6.79	8.88	1.56	17.57
	FR	11.04	8.62	9.98	8.55	9.55	1.19	12.50
MLD1	LT	48.86	51.69	40.40	43.16	46.03	5.16	11.22
	FR	36.42	37.19	48.27	35.53	39.35	5.98	15.20
MLD2	LT	32.33	20.63	25.30	20.50	24.69	5.56	22.53
	FR	31.22	28.20	30.62	34.63	31.17	2.65	8.51
MLD3	LT	27.07	29.83	20.99	27.70	26.40	3.79	14.37
	FR	21.76	24.20	24.32	24.99	23.82	1.42	5.95

IPN values are average of two measurements.
C – control; MLD – metachromatic leukodystrophy; LT – laboratory temperature; FR – storage in a freezer at −20 °C; values of IPN are in arbitrary units.

3.4. Evaluation of MLD-related isoforms in the total spectrum of urinary sulfatides

Five sulfatide isoforms C22:0, C22:0-OH, C24:0, C24:1-OH, and C24:0-OH which were most distinctly elevated in sulfatidoses (major isoforms; Fig. 2), were selected as being representative for analysis. In sulfatidoses, these major isoforms collectively accounted for 64% of total sulfatides.

The least variable parameter of the total profile was the C18:0 isoform which was therefore used for normalization of the five major elevated isoforms. To evaluate its variability, the percentage of C18:0 isoform of total sulfatides was calculated for 26 individual control and 10 MLD samples. The percentage of the C18:0 isoform in the total sulfatide spectrum was 7.0 ± 2.0% for controls ($n = 26$, creatinine levels 2.3–12.2 mmol/l) and 2.0 ± 1.0% for MLD patients ($n = 10$, creatinine 3.3–17 mmol/l) and prosaposin deficient patient (creatinine 0.4 mmol/l).

3.5. Isoform profile number (IPN) – a new MLD biomarker

The ratio of the combined signals of the *major isoforms* relative to the intrinsic C18:0 sulfatide reference (IPN) provides a clear-cut diagnostic parameter as shown in Fig. 3 for the set of 50 control samples, 20 MLD-affected patients (all three clinical variants), one MLD heterozygote and one prosaposin deficient patient.

3.6. Comparison of kidney and urinary sulfatide isoform profiles

The comparison of kidney and urinary sulfatide molecular types under normal conditions and in case of prosaposin deficiency is shown in Fig. 4. The data indicate that the urinary and kidney profiles from the control samples are distinctly different (Fig. 4A). The urinary profile from the prosaposin deficient patient differs from those of the controls (see Fig. 2) and follows the profile in the kidney (Fig. 4B).

Both the patient's and control kidney patterns show a similar composition of the major isoforms regardless of the absolute values for total sulfatides (85 μg/g tissue wet weight for control *versus* 3000 μg/g for the prosaposin deficient kidney).

4. Discussion

We have shown that a simple profiling of specifically increased sulfatide isoforms reliably identified all MLD and prosaposin deficient patients, indicating no false negatives, and distinguished all controls, indicating no false positives (Fig. 3). The implementation of DEAE membranes facilitates sample transportation, handling of large sample sets,

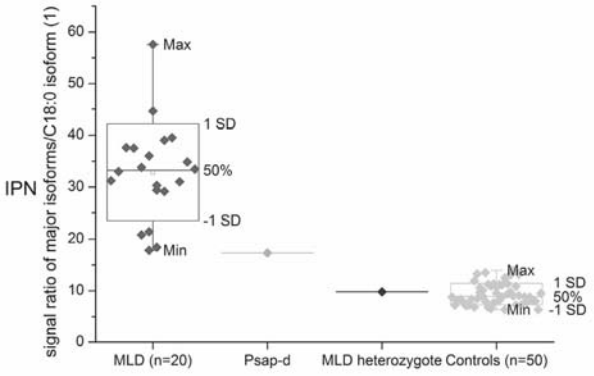

Fig. 3. Ratio of composed SRM intensities of major urinary isoforms to the SRM intensity of the intrinsic C18:0 reference (IPN) for MLD and prosaposin deficiency (Psap-d) patients, a heterozygote, and controls.

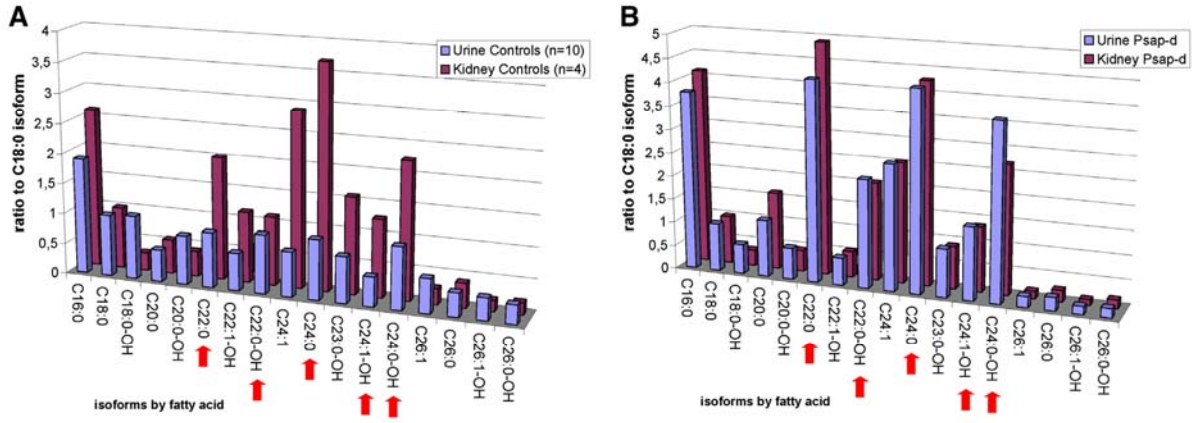

Fig. 4. Comparison of sulfatide isoform urinary and kidney profiles in controls (panel A) and a prosaposin deficiency (Psap-d) patient (panel B). The similarity of urinary and kidney profiles in Psap-d is obvious. Arrows indicate major changes in the isoform profiles.

and enables the partial purification of urinary sulfatides and thus higher sensitivity of the measurements. These are the key characteristics of the procedure that could be introduced as a screening method for MLD because enzyme-based dry-blood-spot analysis is still missing [35].

Selection of five MLD-related isoforms minimizes individual differences in collected samples in comparison with the previously reported analysis of Gb3Cer profile in urine of Fabry patients based on only one most elevated C24:0 isoform [36].

In an effort to simplify the analytical procedure and lower the cost, we sought the least variable component of the sulfatide spectrum to normalize the signal of major elevated isoforms. We found the sulfatide C18:0 isoform, which was the most stable parameter percent wise, and used it as an indigenous reference for calculating the isoform profile number IPN as a disease marker.

The low variability of the C18:0 isoform in the profile is possibly due to its constant production in biosynthetic pathways where the corresponding synthases preferentially synthesize the isoforms with long acyl chains C20-C24, thus keeping the amount of C18:0 isoform less variable [37,38].

Utilizing the C18:0 isoform as a normalizing parameter avoids isotope or mass-labeled external standards that are commonly used in other methods [24,25,27]. In addition, the C18:0 reference isoform is naturally present in the analyzed material along with the measured isoforms and thus compensates for errors caused by sample processing, *e.g.*, affinity binding, elution and extraction, and also for matrix effects [39].

The use of the C18:0 reference isoform also helps to resolve the long-standing problem of suitable evaluation of urinary lipids that results from inappropriate normalizing parameters (*e.g.* creatinine) [40,41]. Concentration of urine does not affect the measurement and evaluation using IPN values. Both types, the first morning specimens or samples taken randomly during the day may be used, but always perfectly mixed before any further handling.

The described method was thoroughly characterized by determining the analytical parameters and DUS storage stability. CV of IPN values did not depend on the total sulfatide level across a broad range of sample loadings which is essential for the method reliability. Intra- and inter-assay CV were always below 13%. This indicates that the IPN values are not affected by selective binding of some sulfatide isoforms to the DEAE membrane.

It should be noted that it is essential to achieve adequate signal-to-noise ratios (S/N) of the measured data to evaluate the correct IPN. The recommended minimum for the "quantitative" data is S/N ≥ 10 [31]. Our DEAE membrane method utilizing FIA-ESI-MS/MS revealed S/N ratios about 25 for control samples and 47 for MLD. This demonstrates that direct FIA-ESI-MS/MS provides reliable results. LC separation is not necessary to increase the S/N ratio, but represents an alternative method. Examples of measured data are shown in Supplementary data Fig. 2.

The stability of sulfatides on DEAE membrane under different storage conditions was found sufficient, as the IPN value provided clear differentiation between the control group and MLD patients at any time point up to 100 days of storage (Table 1). Samples are usually delivered to the analytical laboratory within one week after collection but even longer storage period does not have any negative impact on the outcome of the laboratory analysis and diagnosis.

Another advantage of the method is its ability to diagnose saposin B deficiency caused by mutations of prosaposin encoding gene. This rare disease is easily detectable by determination of sulfatide IPN in urine, although the *in vitro* enzyme assays fail.

Despite the differences among individual patients, the concentrations of the most abundant isoforms correlated with the total sulfatide values in all examined samples (Supplementary data Fig. 3). We assume that the method may also have the potential to distinguish common ASA pseudodeficiencies (ASA PD) which show low *in vitro* ASA activities but do not result in morbidity in ASA PD individuals who do not present significantly elevated urinary sulfatide levels [2,25]. This issue will be further investigated in dependence on the availability of PD ASA material.

The cause for the elevated urinary C22:0, C:22:0-OH, C24:0, C24:1-OH, and C24:0-OH sulfatide isoforms has not been exactly determined so far. It is presumed that the exfoliated renal tubule epithelium cells affected by lysosomal storage are the primary source of excreted sphingolipids in some LSD [2,42–44]. In the absence of renal damage, the renal epithelium cells appear in the urinary sediment in only very small quantities [45,46].

We compared the sulfatide profiles in urine and in extracts of kidney homogenates from normal individuals and from the prosaposin deficient patient [41].

The pattern of sulfatide isoforms was similar in the healthy kidney and in the kidney affected by lysosomal storage (Fig. 4 A,B; dark/purple highlighted bars).

In contrast, an altered urinary sulfatide profile (Fig. 4, light/blue bars) was found that exactly corresponded to the sulfatide kidney profile of the prosaposin deficient patient. This can be taken as an indirect evidence for changes in the composition of cellular types in the urinary sediment – desquamated urothelial cells in controls [45] and lipid-laden renal tubule cells [43] in patients with LSD.

The spectrum of the sulfatide isoforms in the kidney to a large extent corresponds to the expression of ceramide synthases (CerS, acyl-CoA: sphinganine N-acyltransferase, E. C. 2.3.1.24) that catalyze acylation of sphinganine in the endoplasmic reticulum [47]. The CerS2 form, which

is mainly expressed in kidney cells, is specific for acylation of sphingoid base with C22 through C24 fatty acids [38,47] which are major molecular forms of kidney sulfatides and are elevated in urine of patients with MLD and prosaposin deficiency. Expression of CerS in urothel has not been investigated so far.

5 . Conclusion

DEAE-bound urinary sulfatide profiling by tandem mass spectrometry offers a robust method for laboratory diagnosis of patients affected with MLD and prosaposin deficiency. The method relies on the increase of specific molecular types of sulfatides in urine. The selection of only five major elevated isoforms and the C18:0 isoform as an indigenous normalizing parameter both simplifies the analysis and lowers the cost, as it does not require specifically labeled lipid standards and analysis of additional standardizing parameter such as creatinine, sfingomyelin *etc.* Incorporating the DEAE membrane to selectively capture the sulfatides from urine allows the preparation of dry samples with high stability of bound sulfatides which is easy for transportation and further analysis.

Acknowledgments

This work was supported by Grant IGA MZ NT14015-3/2013 from the Grant Agency of the Ministry of Health, project PRVOUK-P24/LF1/3 from the Ministry of Education of the Czech Republic, Grant No 19509 from the Grant Agency of the Charles University in Prague, Grant SVV 266 504 from the Charles University in Prague, Czech Republic, grant project RVO-VFN64165 and Grant R01 DK067859, NIH, National Institutes of Diabetes, Kidney and Digestive Diseases (F. Turecek).

We thank Professor Klaus Harzer, Department of Pediatrics and Child Development, Universitäts-Kinderklinik, Tübingen, Germany, for providing the urine sample from patient with prosaposin deficiency.

The advisory role of Helena Hulkova, MD, PhD, in renal and urothelial cell pathology is gratefully acknowledged.

Appendix A. Supplementary data

Supplementary data to this article can be found online at http://dx.doi.org/10.1016/j.cca.2013.06.027.

References

[1] Sandhoff K, Kolter T, Harzer K. Sphingolipid activator proteins. In: Scriver CR, Beaudet AL, Sly WS, Valle D, editors. The metabolic and molecular bases of inherited disease. New York: McGraw-Hill; 2001. p. 3371–88.
[2] von Figura K, Gieselmann V, Jaeken J. Metachromatic leukodystrophy. In: Scriver CR, Beaudet AL, Sly WS, Valle D, editors. The metabolic and molecular bases of inherited disease. New York: McGraw-Hill; 2001. p. 3695–724.
[3] Batzios SP, Zafeiriou DI. Developing treatment options for metachromatic leukodystrophy. Mol Genet Metab 2012;105:56–63.
[4] Biffi A, Lucchini G, Rovelli A, Sessa M. Metachromatic leukodystrophy: an overview of current and prospective treatments. Bone Marrow Transplant 2008;42(Suppl. 2):S2–6.
[5] Matzner U, Lullmann-Rauch R, Stroobants S, et al. Enzyme replacement improves ataxic gait and central nervous system histopathology in a mouse model of metachromatic leukodystrophy. Mol Ther 2009;17:600–6.
[6] Sevin C, Aubourg P, Cartier N. Enzyme, cell and gene-based therapies for metachromatic leukodystrophy. J Inherit Metab Dis 2007;30:175–83.
[7] Stroobants S, Gerlach D, Matthes F, et al. Intracerebroventricular enzyme infusion corrects central nervous system pathology and dysfunction in a mouse model of metachromatic leukodystrophy. Hum Mol Genet 2011;20:2760–9.
[8] Baum H, Dodgson KS, Spencer B. The assay of arylsulphatases A and B in human urine. Clin Chim Acta 1959;4:453–5.
[9] Christomanou H, Sandhoff K. A sensitive fluorescence assay for the simultaneous and separate determination of arylsulphatases A and B. Clin Chim Acta 1977;79:527–31.
[10] Lee-Vaupel M, Conzelmann E. A simple chromogenic assay for arylsulfatase A. Clin Chim Acta 1987;164:171–80.
[11] Suzuki K. Enzymatic diagnosis of sphingolipidoses. Methods Enzymol 1987;138:727–62.
[12] Hohenschutz C, Eich P, Friedl W, Waheed A, Conzelmann E, Propping P. Pseudodeficiency of arylsulfatase A: a common genetic polymorphism with possible disease implications. Hum Genet 1989;82:45–8.
[13] Gieselmann V, Polten A, Kreysing J, von Figura K. Arylsulfatase A pseudodeficiency: loss of a polyadenylylation signal and N-glycosylation site. Proc Natl Acad Sci U S A 1989;86:9436–40.
[14] Dubois G, Harzer K, Baumann N. Very low arylsulfatase A and cerebroside sulfatase activities in leukocytes of healthy members of metachromatic leukodystrophy family. Am J Hum Genet 1977;29:191–4.
[15] Herz B, Bach G. Arylsulfatase A in pseudodeficiency. Hum Genet 1984;66:147–50.
[16] Chang PL, Davidson RG. Pseudo arylsulfatase-A deficiency in healthy individuals: genetic and biochemical relationship to metachromatic leukodystrophy. Proc Natl Acad Sci U S A 1983;80:7323–7.
[17] Kihara H, Ho CK, Fluharty AL, Tsay KK, Hartlage PL. Prenatal diagnosis of metachromatic leukodystrophy in a family with pseudo arylsulfatase A deficiency by the cerebroside sulfate loading test. Pediatr Res 1980;14:224–7.
[18] Dayan AD. Dichroism of cresyl violet-stained cerebroside sulfate ("sulfatide"). J Histochem Cytochem 1967;15:421–2.
[19] Suzuki K, Chen G. Metachromatic leucodystrophy: isolation and chemical analysis of metachromatic granules. Science 1966;151:1231–3.
[20] Philippart M, Sarlieve L, Meurant C, Mechler L. Human urinary sulfatides in patients with sulfatidosis (metachromatic leukodystrophy). J Lipid Res 1971;12:434–41.
[21] Berna L, Asfaw B, Conzelmann E, Cerny B, Ledvinova J. Determination of urinary sulfatides and other lipids by combination of reversed-phase and thin-layer chromatographies. Anal Biochem 1999;269:304–11.
[22] Natowicz MR, Prence EM, Chaturvedi P, Newburg DS. Urine sulfatides and the diagnosis of metachromatic leukodystrophy. Clin Chem 1996;42:232–8.
[23] Sugiyama E, Hara A, Uemura K. A quantitative analysis of serum sulfatide by matrix-assisted laser desorption ionization time-of-flight mass spectrometry with delayed ion extraction. Anal Biochem 1999;274:90–7.
[24] Tan MA, Fuller M, Zabidi-Hussin ZA, Hopwood JJ, Meikle PJ. Biochemical profiling to predict disease severity in metachromatic leukodystrophy. Mol Genet Metab 2010;99:142–8.
[25] Whitfield PD, Sharp PC, Johnson DW, Nelson P, Meikle PJ. Characterization of urinary sulfatides in metachromatic leukodystrophy using electrospray ionization-tandem mass spectrometry. Mol Genet Metab 2001;73:30–7.
[26] Norris AJ, Whitelegge JP, Yaghoubian A, et al. A novel mass spectrometric assay for the cerebroside sulfate activator protein (saposin B) and arylsulfatase A. J Lipid Res 2005;46:2254–64.
[27] Kuchar L, Ledvinova J, Hrebicek M, et al. Prosaposin deficiency and saposin B deficiency (activator-deficient metachromatic leukodystrophy): report on two patients detected by analysis of urinary sphingolipids and carrying novel PSAP gene mutations. Am J Med Genet A 2009;149A:613–21.
[28] Postle AD. Phospholipid profiling. In: Griffiths WJ, editor. Metabolomics, metabonomics and metabolite profiling. Cambridge: Royal Society of Chemistry; 2008. p. 116–33.
[29] Kuchar L, Rotkova J, Asfaw B, et al. Semisynthesis of C17:0 isoforms of sulphatide and glucosylceramide using immobilised sphingolipid ceramide N-deacylase for application in analytical mass spectrometry. Rapid Commun Mass Spectrom 2010;24:2393–9.
[30] Taylor PJ. Matrix effects: the Achilles heel of quantitative high-performance liquid chromatography-electrospray-tandem mass spectrometry. Clin Biochem 2005;38:328–34.
[31] Micova K, Friedecky D, Faber E, Polynkova A, Adam T. Flow injection analysis vs. ultra high performance liquid chromatography coupled with tandem mass spectrometry for determination of imatinib in human plasma. Clin Chim Acta 2010;411:1957–62.
[32] Rockville MD. FDA guidance for industry: bioanalytical method validation: US Department of Health and Human Services. Food and Drug Administration. Center for Drug Evaluation and Research; 2001 .
[33] Hulkova H, Cervenkova M, Ledvinova J, et al. A novel mutation in the coding region of the prosaposin gene leads to a complete deficiency of prosaposin and saposins, and is associated with a complex sphingolipidosis dominated by lactosylceramide accumulation. Hum Mol Genet 2001;10:927–40.
[34] Natomi H, Sugano K, Iwamori M, Takaku F, Nagai Y. Region-specific distribution of glycosphingolipids in the rabbit gastrointestinal tract: preferential enrichment of sulfoglycolipids in the mucosal regions exposed to acid. Biochim Biophys Acta 1988;961:213–22.
[35] Turecek F, Scott CR, Gelb MH. Tandem mass spectrometry in the detection of inborn errors of metabolism for newborn screening. Methods Mol Biol 2007;359:143–57.
[36] Paschke E, Fauler G, Winkler H, et al. Urinary total globotriaosylceramide and isoforms to identify women with Fabry disease: a diagnostic test study. Am J Kidney Dis 2011;57:673–81.
[37] Ben-David O, Pewzner-Jung Y, Brenner O, et al. Encephalopathy caused by ablation of very long acyl chain ceramide synthesis may be largely due to reduced galactosylceramide levels. J Biol Chem 2011;286:30022–33.
[38] Laviad EL, Albee L, Pankova-Kholmyansky I, et al. Characterization of ceramide synthase 2: tissue distribution, substrate specificity, and inhibition by sphingosine 1-phosphate. J Biol Chem 2008;283:5677–84.
[39] De Livera AM, Dias DA, De Souza D, et al. Normalizing and integrating metabolomics data. Anal Chem 2012;84:10768–76.
[40] Forni S, Fu X, Schiffmann R, Sweetman L. Falsely elevated urinary Gb3 (globotriaosylceramide, CTH, GL3). Mol Genet Metab 2009;97:91.
[41] Kuchar L, Asfaw B, Ledvinova J. Tandem mass spectrometry of sphingolipids: application in metabolic studies and diagnosis of inherited disorders of sphingolipid

metabolism. In: Prasain JK, editor. Tandem mass spectrometry — applications and principles. Rijeka: InTech; 2012. p. 739–68.
[42] Chatterjee S, Gupta P, Pyeritz RE, Kwiterovich Jr PO. Immunohistochemical localization of glycosphingolipid in urinary renal tubular cells in Fabry's disease. Am J Clin Pathol 1984;82:24–8.
[43] Warnock DG, Valbuena C, West M, Oliveira JP. Renal manifestation of Fabry disease. In: Elstein D, Altarescu G, Beck M, editors. Fabry Disease. Dordrecht: Springer Science + Business Media B.V.; 2010. p. 211–43.
[44] Iwamori M, Moser HW. Above-normal urinary excretion of urinary ceramides in Farber's disease, and characterization of their components by high-performance liquid chromatography. Clin Chem 1975;21:725–9.
[45] Chatterjee S, Castiglione E, Kwiterovich Jr PO, Hoeg JM, Brewer HB. Evaluation of urinary cells in acid cholesteryl ester hydrolase deficiency. Clin Genet 1986;29:360–8.
[46] Nguyen GK, Smith R. Repair renal tubular cells: a potential false-positive diagnosis in urine cytology. Diagn Cytopathol 2004;31:342–6.
[47] Levy M, Futerman AH. Mammalian ceramide synthases. IUBMB Life 2010;62:347–56.

Supplementary Data:

Direct Tandem Mass Spectrometric Profiling of Sulfatides in Dry Urinary Samples for Screening of Metachromatic Leukodystrophy

Ladislav Kuchař, Befekadu Asfaw, Helena Poupětová, Jitka Honzíková, [+]František Tureček [*] and Jana Ledvinová[*]

Institute of Inherited Metabolic Diseases, First Faculty of Medicine and General Teaching Hospital, Charles University, 128 08 Prague, Czech Republic

[+]Department of Chemistry, University of Washington, Seattle, WA 98195-1700, USA

[*] Corresponding author: Jana Ledvinová, Institute of Inherited Metabolic Diseases, First Faculty of Medicine and General Teaching Hospital, Charles University, 128 08 Prague, Czech Republic; Tel.: +420 224967034, Fax.: +420 224967119

e-mail address: jledvin@cesnet.cz

František Tureček, Department of Chemistry, University of Washington, Seattle, WA 98195-1700, USA

Phone +1 206-685-2041, Fax +1 206-685-8665,

e-mail: turecek@chem.washington.edu

Abbreviations:

CV - coefficient of variation; cps - counts per second; S/N - signal to noise ratio

Table S1. Ion *m/z* Values for Selected Ion Monitoring

Sulfatide	Precursor $(M - H)^-$ Ion *m/z*	Formula	data aqusition times in ms all isoforms	major + C18:0 isoforms
C16:0	778.5	$C_{40}H_{76}NO_{11}S$	100	
C17:0 (IS)	792.5	$C_{41}H_{78}NO_{11}S$	100	
C18:0	806.6	$C_{42}H_{80}NO_{11}S$	100	500
C18:0-OH	822.6	$C_{42}H_{80}NO_{12}S$	100	
C20:0	834.6	$C_{44}H_{84}NO_{11}S$	100	
C20:0-OH	850.6	$C_{44}H_{84}NO_{12}S$	100	
C22:0	**862.6**	**$C_{46}H_{88}NO_{11}S$**	**100**	**500**
C22:1-OH	876.6	$C_{46}H_{86}NO_{12}S$	100	
C22:0-OH	**878.7**	**$C_{46}H_{88}NO_{12}S$**	**100**	**500**
C24:1	888.7	$C_{48}H_{90}NO_{11}S$	100	
C24:0	**890.7**	**$C_{48}H_{92}NO_{11}S$**	**100**	**500**
C23:0-OH	892.7	$C_{47}H_{90}NO_{12}S$	100	
C24:1-OH	**904.7**	**$C_{48}H_{90}NO_{12}S$**	**100**	**500**
C24:0-OH	**906.7**	**$C_{48}H_{92}NO_{12}S$**	**100**	**500**
C26:1	916.7	$C_{50}H_{94}NO_{11}S$	100	
C26:0	918.7	$C_{50}H_{96}NO_{11}S$	100	
C26:1-OH	932.7	$C_{50}H_{94}NO_{12}S$	100	
C26:0-OH	934.7	$C_{50}H_{96}NO_{12}S$	100	

Footnote: The most abundant urinary isoforms from MLD patients are shown with bold characters.

Method of tandem mass spectrometry analysis

Instrument Settings

Mass spectra were measured on an ABI/MDS SCIEX API 3200 tandem mass spectrometer equipped with an ESI source and coupled to an Agilent HPLC 1100 series. Samples (20 µL of methanol solution) were introduced by flow injection at a flow rate of 50 µL/min. The Analyst 1.5 software was used to operate the instruments and process the data. Sulfatides were analyzed by selected reaction monitoring (SRM) in the negative ion mode. Delays between mass transitions were set to 5 ms with Q1 and Q3 operating at unit mass resolution. The curtain gas pressure was 10 psi. Nitrogen was used as the collision gas with pressure set

at 7 psi. The capillary spray voltage was -4.5 kV. The temperature of the nebulizing gas was 200°C. The ion source gas pressure was adjusted to 10 psi for source gas 1 and 35 psi for source gas 2. The interface heater was turned on during the analysis. The ion optics settings for sulfatide measurements were -152 V for the declustering potential and -9 V for the entrance potential. The collision energy was set to -130V with a collision cell exit potential of -8.5V.

Sample Analysis

Sulfatide-containing lipid samples prepared as described above were injected by an autosampler into the methanol mobile phase with a flow rate of 50 µL/min. The sample was resuspended in methanol and electrosprayed in the negative ion mode to form $[M–H]^-$ ions. SRM of sulfatides used precursor ions shown in supplementary Table S1 and monitored the common HSO_4^- (*m/z* 97) fragment ion. The data acquisition time for each transition pair was 100 ms when all 18 isoforms were measured (supplementary Table S1). The data acquisition time was extended to 500 ms when only five major isoforms and C18:0 sulfatide (indigenous internal standard) were measured.

HPLC and LC ESI-MS/MS methods to suppress matrix effects

Normal-phase HPLC was performed on LC-Si HPLC Column 7.5 cm x 3mm, 3 µm. LC was performed using Security Guard Kit with two silica cartridges (cartridge size of 4.0 x 3.0 mm). Gradient elution was done in a binary system of mobile phase A consisting of n-hexane:2-propanol (60:40) and mobile phase B consisting of 2-propanol:H_2O (90:10). The gradient elution program for HPLC separation was as follows: 100% of mobile phase A for 8 min, linear gradient exchange to 100% B over 3 min and finally 100% of phase B for 29 min. The LC program with Security Guard Kit was as follows: 100% of mobile phase A for 1 min,

linear exchange of gradient to 100% B over 0.5 min and finally 100% of phase B for 2.5 min. Both methods were performed at a constant flow rate of 150 µl/min. ESI-MS/MS conditions were as described above (Supplement - Instrument Settings).

Matrix effect suppression with HPLC and LC

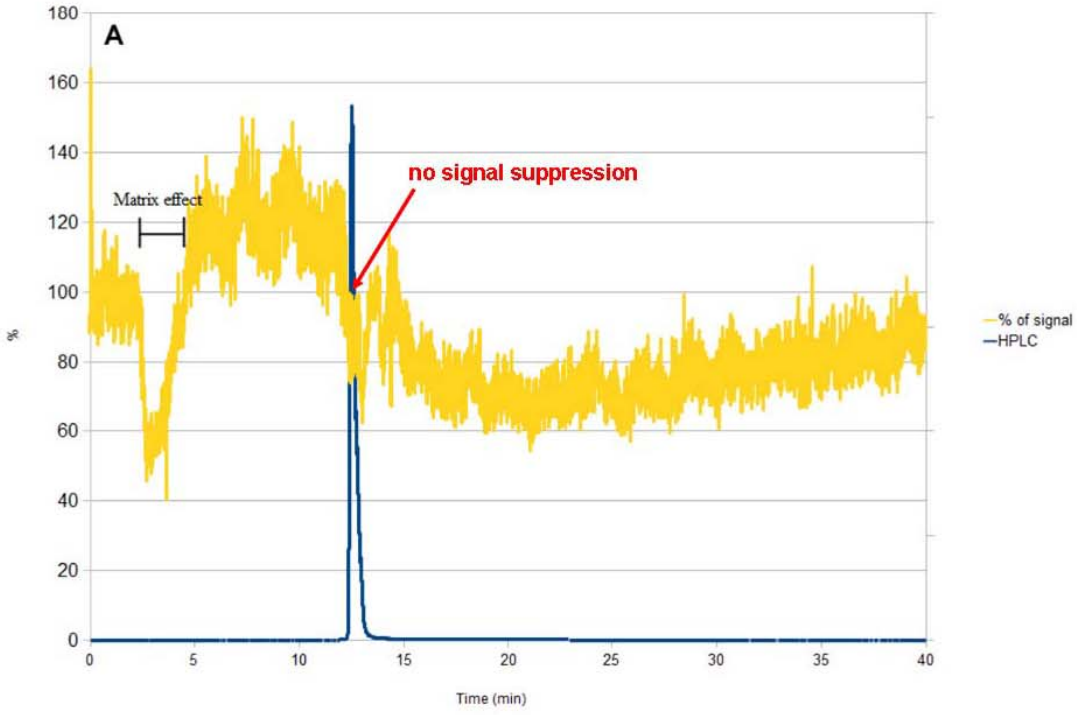

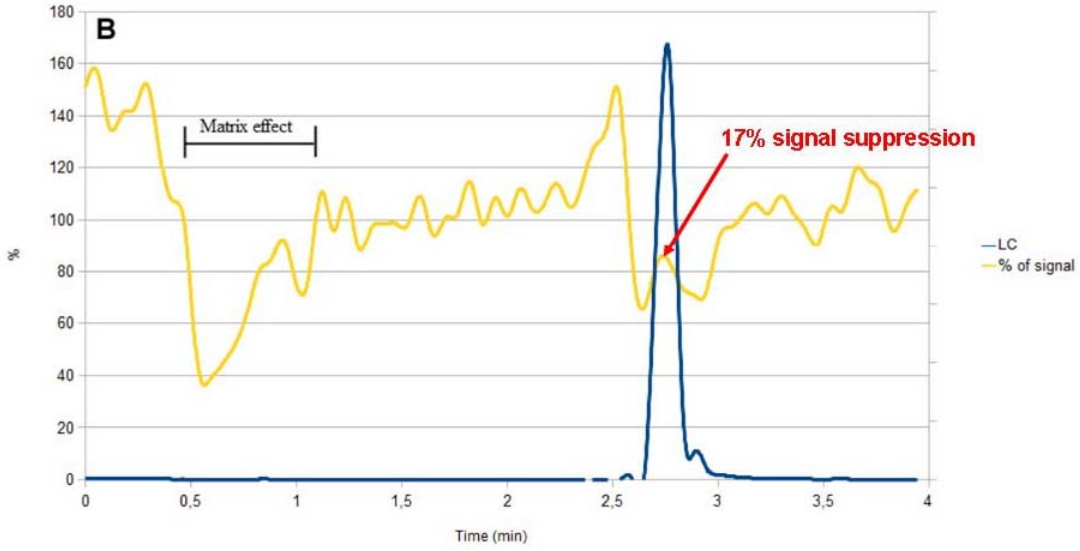

Supplementary Fig. 1. Elution profile of C12:0 sulfatide signal suppression caused by matrix effects (yellow line) in the course of HPLC (A) and LC (B) separations in post-column infusion. The yellow line represents the relative variation of the signal of C12: 0 sulfatide normalized to 100% in the absence of matrix. The bar above the yellow line shows the region of major matrix effects. The blue line represents the chromatographic trace of C12:0 sulfatide in the course of HPLC and LC separation.

Examples of measured data

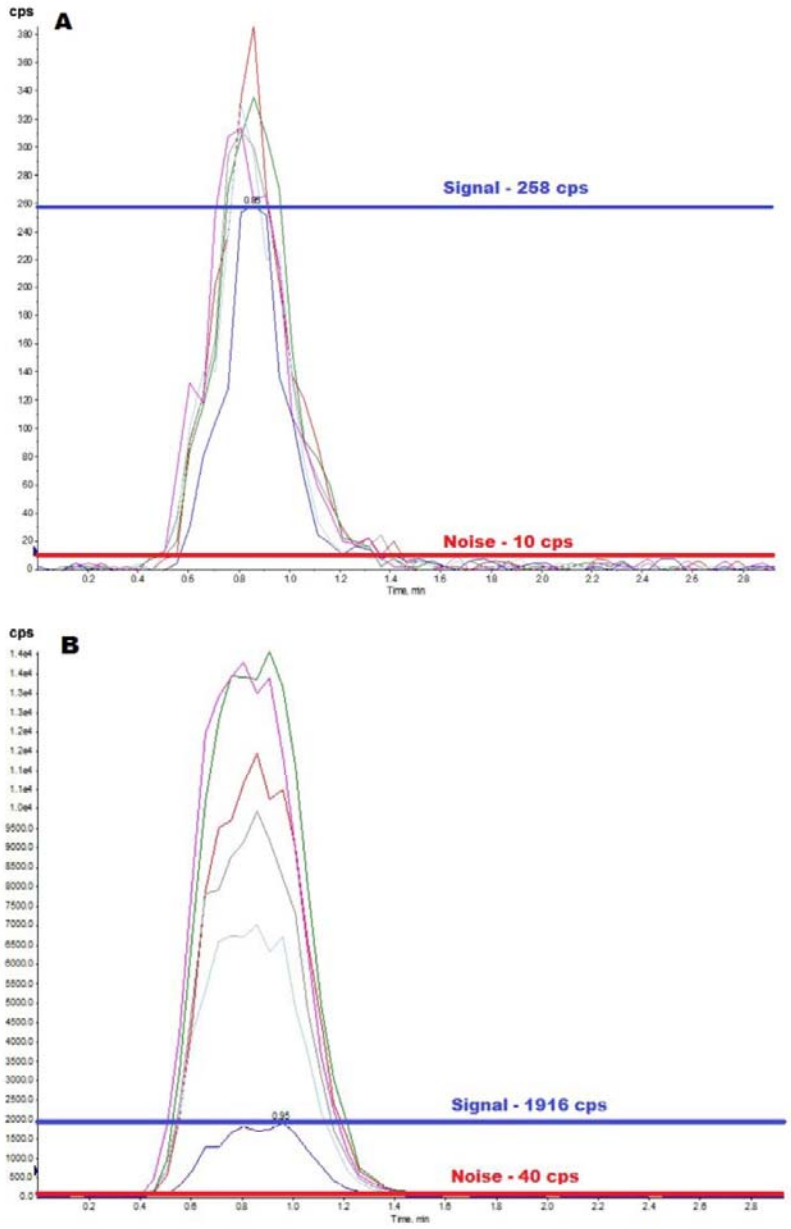

Supplementary Fig. 2. Extracted ion current of selected sulfatide isoforms in control (A) and MLD (B) urine samples. The horizontal lines indicate the typical noise and minimum signal levels. Panel A: The red line represents the noise level which was 10 cps (amu) in control samples. The S/N ratio for each isoform was above 25. Panel B: In the MLD sample, the noise level was 40 cps (red line) and the S/N ratio was above 45 for each measured isoform. An S/N ratio of 10 was taken as a base limit for quantification. The dynamic range of signal intensity was 10-380 cps in control urine and 40-14000 cps in MLD urine. Note the different ordinate scales in graphs (A) and (B).

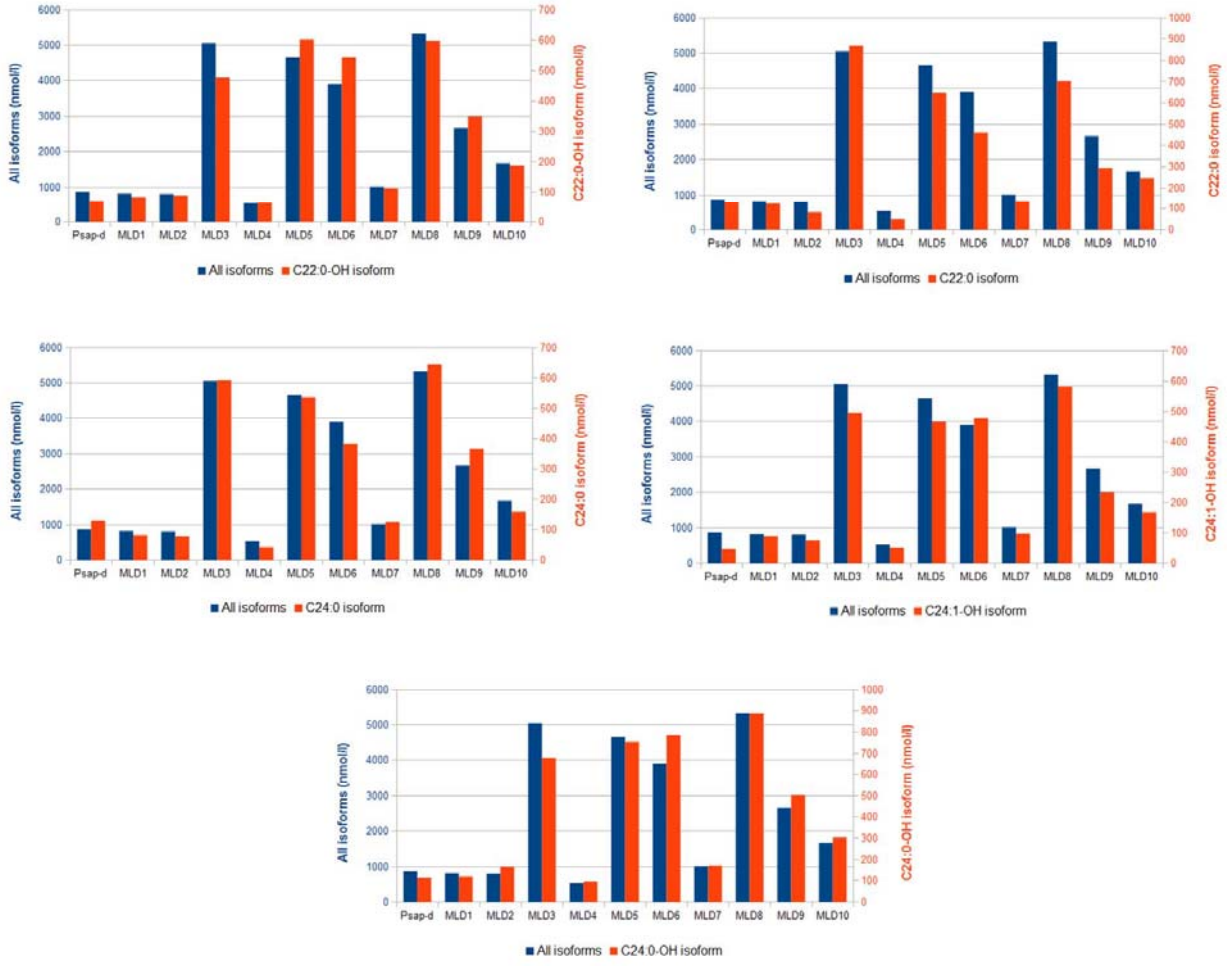

Supplementary Fig. 3. Comparison of molar concentrations of total sulfatides (blue columns) and major individual isoforms (red columns) from sulfatidosis affected patients. (A) C22:0 (B) C22:0-OH (C) C24:0 (D) C24:1-OH (E) C24:0-OH. The left y-axes represent the range of total sulphatides concentration; the right y-axes show concentrations of individual isoforms. Molar concentrations of major individual isoforms were calculated from their percentage abundance in total urinary sulfatides.

SUPPLEMENTARY PUBLICATIONS

Publications in impacted journals related to topic of this PhD thesis

Supplementary publication D

Hulkova H., Ledvinova J., Kuchar L., et al., *Glycosphingolipid profile of the apical pole of human placental capillaries: the relevancy of the observed data to Fabry disease.* Glycobiology, 2012. **22**(5): p. 725-732

Glycobiology vol. 22 no. 5 pp. 725–732, 2012
doi:10.1093/glycob/cws050
Advance Access publication on February 7, 2012

Glycosphingolipid profile of the apical pole of human placental capillaries: The relevancy of the observed data to Fabry disease

Helena Hůlková[2], Jana Ledvinová[1,2], Ladislav Kuchař[2], František Šmíd[3], Jitka Honzíková[2], and Milan Elleder[2]

[2]Institute of Inherited Metabolic Disorders, First Faculty of Medicine and General University Hospital, Charles University in Prague, Ke Karlovu 2, 120 00 Praha 2 and [3]Institute of Clinical Biochemistry and Laboratory Diagnostics, First Faculty of Medicine and General University Hospital, U Nemocnice 2, 120 00 Praha 2, Czech Republic

Received on June 24, 2011; revised on January 26, 2012; accepted on January 31, 2012

A series of six full-term placentas and umbilical cords were examined using the *in situ* detection of globotriaosylceramide (Gb3Cer), GM1 ganglioside (GM1), GM3 ganglioside (GM3), cholesterol and caveolin 1. Immunohistochemical study showed uniform distinct staining of the apical membrane of villous capillary endothelial cells for Gb3Cer, GM1, GM3 and cholesterol. There was also a strong signal for caveolin 1. The immunophenotype suggests the presence of caveola-associated raft microdomains. The immunophenotype was almost completely shared with the extravillous intravascular trophoblast in the basal plate. It was absent in the endothelial cells of umbilical vessels and in the capillaries of somatic structures (heart, lung, skeletal muscle and skin) in neonates as well as in adults, including capillaries of the proliferative endometrium. Results of *in situ* analyses were confirmed by lipid chromatographic analysis of tissue homogenates and by tandem mass spectrometry. Lysosomal Gb3Cer turnover was followed in three placentas including umbilical cords from Fabry disease (α-galactosidase A deficiency). Lysosomal storage was restricted to vascular smooth muscle cells and to endothelial cells of umbilical vessels. Placental villous capillary endothelial cells displaying a strong non-lysosomal staining for Gb3Cer were free of lysosomal storage.

Keywords: Fabry disease / gangliosides / glycosphingolipids / placental capillaries

Introduction

Our interest in the study of the glycosphingolipid (GSL) profile of placental endothelial cells was induced by our engagement in studies of globotriaosylceramide (Gb3Cer) lysosomal storage in Fabry disease [α-galactosidase A (α-Gal A) deficiency], where it represents the main lysosomally stored lipid, followed by digalactosylceramide and in specific instances also blood group B glycolipids (Elleder 2010; Hrebicek and Ledvinova 2010). Recently, we used immunohistochemical *in situ* detection of Gb3Cer in a sample of placenta in a case of Fabry disease and were surprised by strong staining of the villous capillaries free of lysosomal storage. As we are not aware of any detailed study of Gb3Cer in normal placentas as all the so far reports of placental pathology in Fabry disease have been focused on Gb3Cer lysosomal storage demonstrated with electron microscopy (Popli et al. 1990; Vedder et al. 2006; Bouwman et al. 2010). This prompted a comprehensive study of the capillary GSL profile in normal placentas. We used *in situ* analysis of Gb3Cer, GM1 ganglioside (GM1) and GM3 ganglioside (GM3), paralleled by *extra situ* biochemical analysis and tandem mass spectrometry (MS/MS). The lipid *in situ* profile of placental villous capillaries was compared with that of endothelial cells of the uteroplacental vessels, umbilical vessels and with that of the somatic capillaries.

Results

In situ *analysis*

Gb3Cer *in situ* detection in the fetal (villous) part of placentas gave a uniform, relatively strong, linear or finely granular signal in the apical membrane of the fetal villous capillary endothelium. Lipid was also detectable, to variable extents, in fibroblasts and Hoffbauer cells. Both villous cyto- and syncytiotrophoblast were always negative (Figure 1A). In the basal plate (maternal portion), the extravillous stromal trophoblast strongly positive for large spectrum cytokeratin (CK LS) showed variable staining for Gb3Cer, ranging from negative to strongly positive. The cells lining the lumina of the uteroplacental vessels, expressing cytokeratin, also stained positive, at the apical pole membrane (Figure 1C and D). Gb3Cer immunostaining was resistant to acetone pre-extraction and completely eliminated by total lipid extraction. Endothelium

[1]To whom correspondence should be addressed: Tel: +420-224967033; Fax: +420-224967119; e-mail: jledvin@cesnet.cz

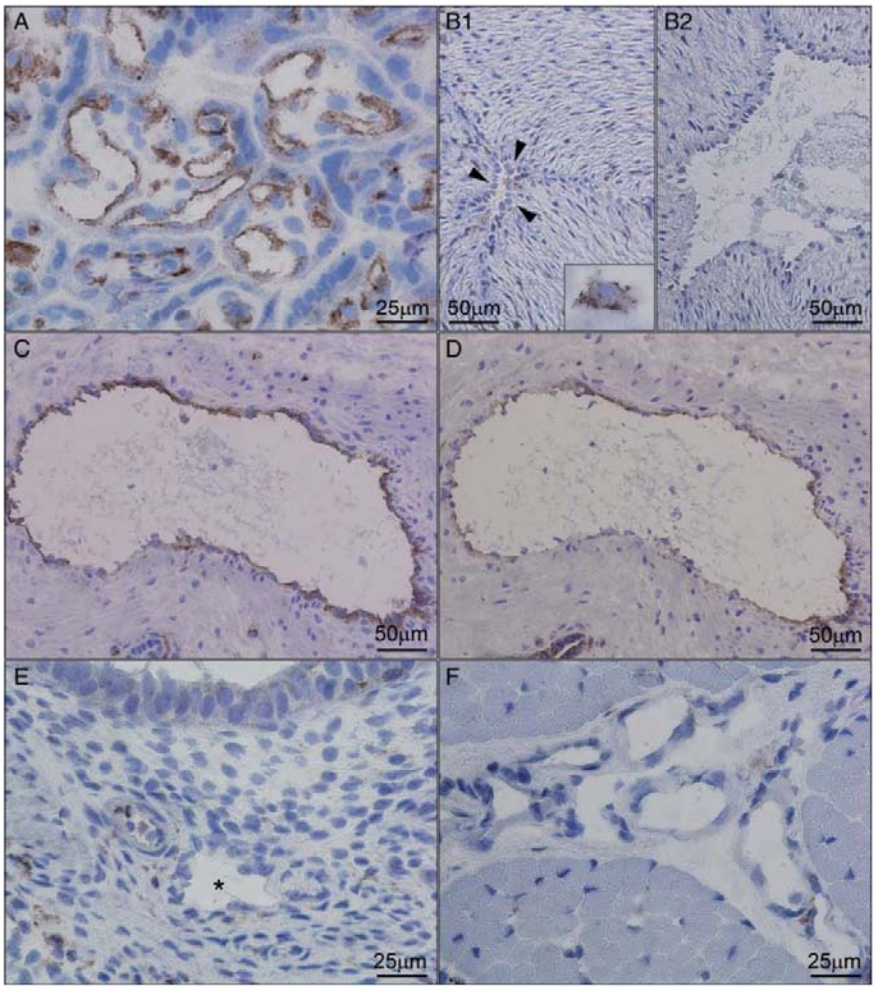

Fig. 1. Immunohistochemistry of Gb3Cer. (**A**) Placental villi. Signal for Gb3Cer was localized in the apical membrane of the villous capillary endothelium. (**B**) The absence of the signal in the endothelium of both arterial (B1) and venous (B2) umbillical vessels. Gb3Cer-negative endothelial cells lining a narrow lumen of the umbilical artery in B1 are marked with arrowheads. Insert in B1 demonstrates the positive Gb3Cer staining of a mast cell in the umbilicus in the Wharton's jelly as an internal control. (**C**) Strong signal for Gb3Cer in cells lining a lumen of the uteroplacental vessel in the basal plate. (**D**) The section parallel to (C). These cells displayed also clear positivity for cytokeratin, suggesting their origin from endovascular trophoblast invasion. (**E**) Gb3Cer was not detectable in endometrial capillaries in the proliferative phase (the capillary lumen is marked with an asterisk). (**F**) Gb3Cer-negative capillaries in the skeletal muscle from an infant.

from non-pregnant endometrium (proliferative state) did not display Gb3Cer expression (Figure 1E).

Gb3Cer was not detectable in any of the vessel wall elements (smooth muscle cells and endothelial cells) of umbilical cord vein or of the umbilical cord arteries (Figure 1B1 and B2). The only cell type that was positive was mast cells in the Wharton's jelly. Gb3Cer was also negative in capillaries in somatic tissues (blood capillaries in the skin, skeletal muscle, heart and lung) of three infants succumbing to diseases unrelated to lysosomal storage (Figure 1F). This fits with our studies in adults (M.E., personal observation).

Correlation with other lipids. GM1 was detected with both techniques (with anti-GM1 monoclonal antibody and with Cholera toxin B-subunit) in the apical membrane of the villous capillary endothelium, correlating with the presence of Gb3Cer (Figure 2A1 and A2). Villous trophoblast did not display any significant regular signal. However, the extravillous trophoblast in the basal plate expressed intensive GM1 staining. Especially cells lining the lumina of uteroplacental vessels displayed staining comparable with that for Gb3Cer. Staining of umbilical vessels was negative with the exception of a weak signal in fibroblasts and in mast cells. Somatic capillaries expressed variable staining intensity. The staining was abolished by total lipid pre-extraction.

Signal for GM3 paralleled that for GM1 in the apical membrane of placental villous capillaries (Figure 2B) and was also abolished by total lipid extraction. It was absent in the

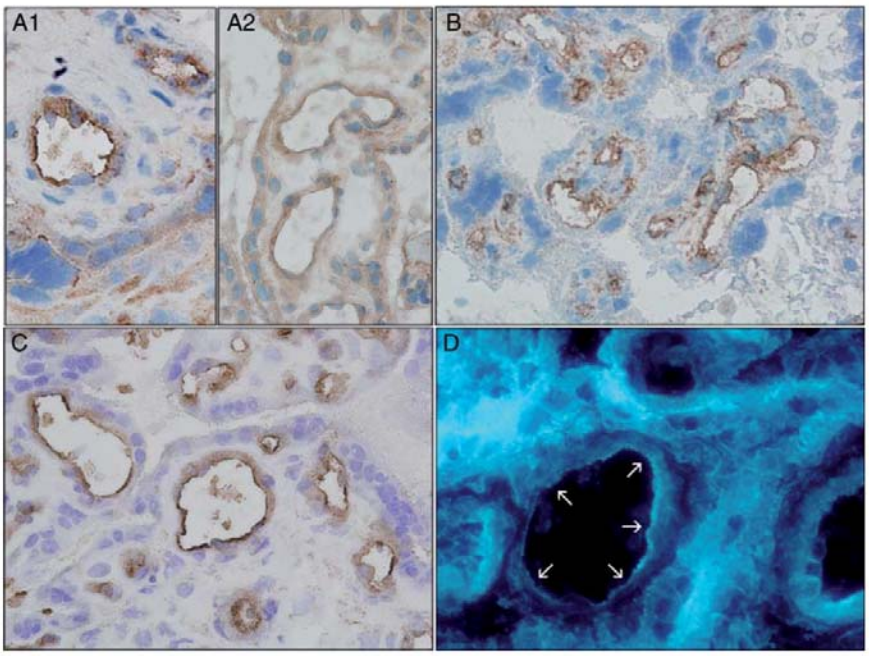

Fig. 2. Immunohistochemical profile of the capillary endothelium in placental villi. (**A**) Strong signal for GM1 with both specific antibody (A1) and with CTX (A2). (**B**) Endothelium of villous placental capillaries expressed also GM3; staining with an anti-GM3 monoclonal antibody. (**C**) The presence of caveolin 1 in the villous capillary endothelium demonstrated by immunohistochemistry using a monoclonal antibody. (**D**) Cholesterol detection in chorionic villi using Filipin. Besides general signal in all villous structures, there is a dense linear signal at the apical pole of endothelial cells lining a capillary lumen (marked with arrows).

endothelium in all other sites examined (umbilical vessels and somatic capillaries).

Filipin detection of cholesterol showed a strong signal in all villous structures. The trophoblast layer displayed a strong signal. Capillaries in all sites examined displayed a linear (almost continuous) or a dense microgranular signal at the apical pole (Figure 2D).

Correlation with caveolin 1. Caveolin 1 was best detected in cryostat sections of unfixed tissue. The signal was strong in the apical pole of the villous capillary endothelium (Figure 2C). Similar signal was seen in the capillary endothelium in all sites studied. Endothelium of the umbilical vessels was negative, and only smooth muscle cells were reactive.

The expression of usual endothelial protein markers (CD31 and CD34 antigens and factor VIII-related antigen) in the villous capillary endothelium was quite unspecific. Signals for both CD31 and CD34 antigens were strong. Signal for the factor VIII-related antigen was weak and irregular.

Electron microscopy of the normal villous capillary endothelium showed a linear apical pole with occasional groups of caveolae; Weibel-Palade granules were rare.

Biochemical lipid analysis

High-performance thin-layer chromatography (HPTLC) and MS/MS analysis demonstrated the presence of Gb3Cer and other frequently occurring neutral GSLs (ceramide mono- and dihexosides, globoside) in homogenates of placental tissue. Acidic GSLs were represented by GM3 in particular, but week resorcinol positive bands of more complex sialylated GSL were also detected.

Thin-layer chromatography (TLC) mobility of these bands suggested different oligosaccharide series than gangliosseries when compared with brain gangliosides (Figure 3). When TLC overlay with cholera toxin B subunit (CTX) was used for TLC detection, trace amount of GM1 has been proved (Figure 4). The GM1-CTX positivity was just at the detection limit corresponding approximately to <0.25 pmol GM1.

Results from MS/MS lipid analysis are summarized in Table I. Values were standardized to sphingomyelin, the major ubiquitous sphingolipid of the cell. GM3 represents the most abundant acidic sphingolipid and Gb3Cer the most abundant neutral component of the GSL pattern. Monosialylated tetrahexosylceramide fraction includes IV^3NeuAc-nLc_4Cer (SPG, sialylparagloboside) as a major component and traces of GM1 (≤0.12% of the total fraction). These compounds are not discriminated by MS/MS because of the same mass and ion products. Bands of more complex gangliosides of suspected neolacto-series (nLc_4Cer) were also detected in agreement with previous report (Taki et al. 1988) but their further characterization was not intention of this project.

Evaluation of lysosomal Gb3Cer storage in Fabry disease

The mosaic discrete storage pattern was demonstrable by both immunohistochemistry and electron microscopy in vascular smooth muscle cells and in endothelial cells of the umbilical cord vessels (Figure 5A) in all three female umbilical samples. Extensive examination did not disclose lysosomal Gb3Cer storage in the endothelial cells of villous capillaries, which in the two female siblings expressed the physiological non-lysosomal Gb3Cer localization in their apical pole (Figure 5B). In the full-term placenta stored for a prolonged time in formalin, the physiological staining for Gb3Cer in villous capillaries was minimal.

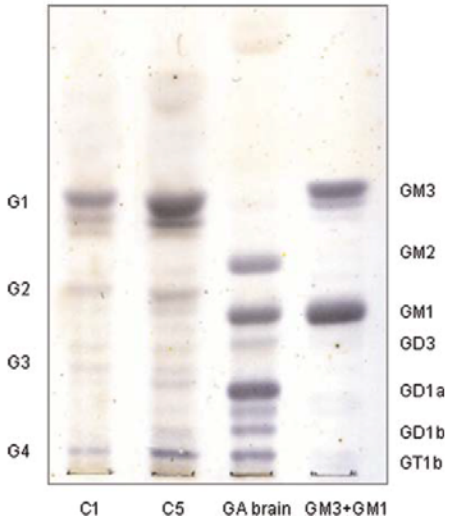

Fig. 3. HPTLC profile of human placenta gangliosides. C1 and C5, two different placenta specimens; GA brain, brain gangliosides (frontal lobe GM2 gangliosidosis/Tay-Sachs disease); GM3 + GM1, standards GM3 and GM1. Placental gangliosides were applied in aliquots corresponding to 3 mg of tissue protein (equivalents of 45 nmol of tissue sphingomyelin for C1 and 65 nmol of tissue sphingomyelin for C5). Solvent system chloroform/methanol/0,5% $CaCl_2$ (55:45:10; v/v/v) was used for development. The spots were visualized with a resorcinol–HCL reagent. G1, G2, G3, G4, major placental gangliosides identified by Taki et al. (1988) as GM3, IV^3NeuAc-nLc$_4$Cer (SPG), VI^3NeuAc-nLc$_6$Cer (i-type ganglioside), VI^3NeuAc-,IV^6[II^3-NeuAc-LcNAc]-nLc$_6$ Cer (I-type ganglioside), respectively. For brain gangliosides, Svennerholm nomenclature is used (Chester 1998).

Discussion

Gb3Cer expression in the placental blood capillaries represents a unique finding which points to specific features of their endothelial apical pole. The so far studies on Gb3Cer in endothelial cells point to its receptor function for ligands represented by bacterial cytotoxins of the verotoxin family (Muthing et al. 2009; Betz et al. 2011). Many aspects of Gb3Cer biology have been reviewed recently (Lingwood et al. 2010). However, the bulk of studies describing Gb3Cer expression and integration into membrane microdomains were carried out in cultured endothelial cells or in established cell lines (Keusch et al. 1996; Jacewicz et al. 1999; Muthing et al. 1999; Schweppe et al. 2008). Therefore, this *ex vivo* approach makes the comparison with our *in situ* results hardly possible. Results of *in situ* Gb3Cer detection are extremely rare and point to the absence of immunodetectable Gb3Cer in the human skin (Kanekura et al. 2005), in capillaries of human dorsal root ganglia (Ren et al. 1999) or to a variable

Table I. GSLs in human placenta (in pmol/nmol sphingomyelin)

	Gb4Cer	Gb3Cer	CDH	CMH	SPG + GM1	GM3
C1	12.8	27.1	27.8	22.7	7.0	51.9
C2	11.5	32.1	15.2	16.7	5.4	37.6
C3	19.1	20.4	15.1	20.2	4.3	50.1
C4	15.9	35.1	12.5	23.2	4.5	51.6
C5	13.5	35.3	16.0	19.2	N.Q.	N.Q.

Coefficient of variation of the method was <7%. C1-5, different normal human placentas; N.Q., not quantified. The MS/MS does not differentiate between the glucosyl (e.g. in glucosylceramide) and galactosyl (e.g. in galactosylceramide) moieties because of the same mass. Therefore, glucosylceramide and galactosylceramide, lactosylceramide and digalactosylceramide, and SPG and GM1 are quantified as monohexosylceramides (CMH), dihexosylceramides (CDH), and SPG + GM1 fraction, respectively. Samples were measured in duplicates.

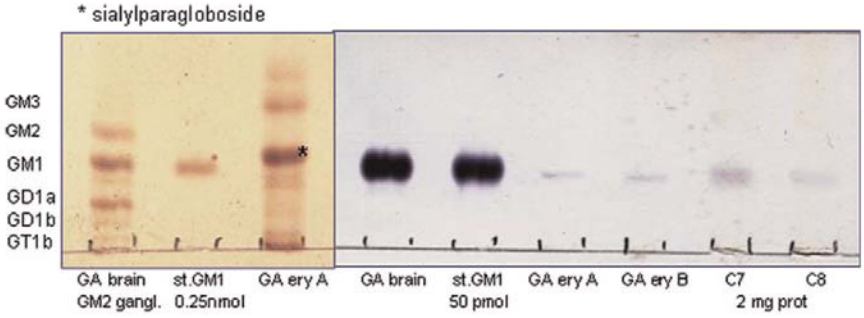

Fig. 4. GM1 in human placenta detected by CTX overlay. GA brain, brain gangliosides (frontal lobe GM2 gangliosidosis/Tay-Sachs disease); st.GM1, standard GM1 ganglioside; GA ery A and B, erythrocyte membrane gangliosides; C7 and C8, ganglioside fractions of two different placenta specimens (2 mg of tissue protein aliquots equivalent to 40 nmol of tissue sphingomyelin). Gangliosides were separated on HPTLC aluminum sheets (silica gel 60) developed with the chloroform/methanol/water (65:35:8, v/v/v). Left part of the chromatogram was detected with orcinol, right part with CTX.

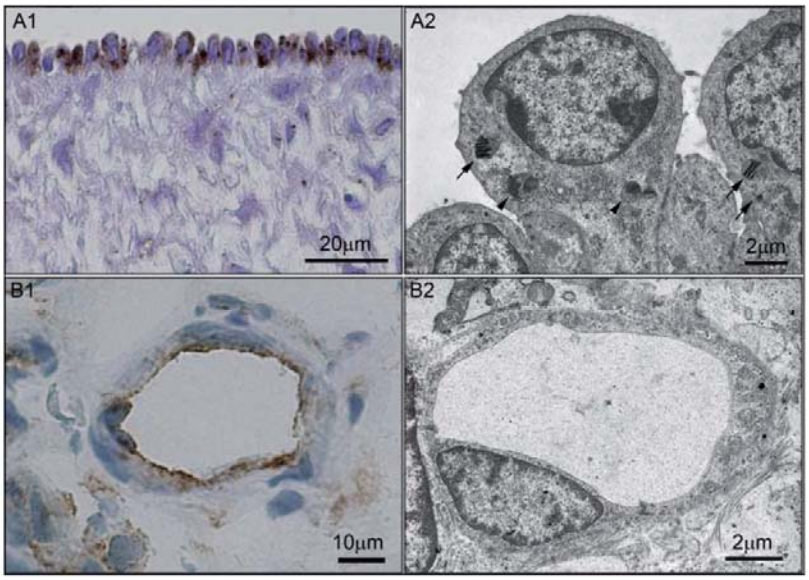

Fig. 5. Comparison with Fabry disease. (**A**) Umbilical vein of a Fabry female fetus. (A1) Mosaic discrete storage of Gb3Cer in the endothelial cells lining a lumen of the umbilical vein demonstrated by immunohistochemistry. (A2) Electron microscopy correlation with A1. Discrete storage lysosomes containing either liquid crystals of polar lipids (marked with arrows) or lipopigment deposits (marked with arrowheads). Compared with negative staining for Gb3Cer in control umbilical vessels in Figure 2B1 and B2. (**B**) Villous placental capillaries of a Fabry female fetus. (B1) Linear Gb3Cer staining at the apical pole of a villous capillary comparable with that seen in controls (Figure 1A). (B2) Ultrastructural correlation with B1. The absence of lysosomal storage in a placental villous capillary.

expression of the lipid in human glomeruli improved by pre-extraction with acetone. Unfortunately, the presence of Gb3Cer in renal interstitial capillaries was not mentioned, only positivity in renal tubules (Chark et al. 2004).

Our *in situ* results using the immunoperoxidase technique clearly reflect the situation in vivo. They indicate that the villous capillaries differ by the high Gb3Cer signal not only from endothelial cells of the umbilical vessels but from endothelial cells of the somatic capillaries as well. Positivity for GM1 and cholesterol and their combination with caveolin 1 (see also Lyden et al. 2002) suggest the presence of caveola-associated microdomains (Parton 1994; Pang et al. 2004) at the apical pole of endothelial cells in the placental capillary network, unique with regard to their high levels of Gb3Cer. The physiological significance of this finding is open for further studies, which may discover whether it is related to the clathrin-independent endocytosis (Nichols 2003; Mayor and Pagano 2007), to specific transport processes known to exist at this level (Takizawa et al. 2005; Solder et al. 2009) or to the regulation of the humoral control of the placental microcirculation (Tedde et al. 1990).

With regard to the maternal part of the placenta, the cells lining uteroplacental vessels displayed Gb3Cer and other GSL expression comparable with that in villous capillaries.

However, their immunophenotype (expression of cytokeratin) fits with the general view of their origin from trophoblast invading the basal plate (Frank and Kaufmann 2006). If this generally held view is correct, it means that trophoblast, which invade vessels and eventually line them, must undergo some type of transformation, since it is Gb3Cer free in the villous part. It remains to be established if the glycolipid expression was induced by the hormonal conditions of pregnancy. It would thus be interesting to follow the expression of Gb3Cer and other GSL in endometrial capillaries (and in capillary endothelium generally) during the physiological hormonal cycle and even during pregnancy. Our samples from the non-pregnant proliferative endometrium indicated that Gb3Cer is absent during this phase of the monthly cycle.

Lipid biochemical analysis of placental homogenates confirmed the presence of lipids detected by immunohistochemistry, i.e. Gb3Cer, GM1 and GM3. In previous studies, the occurrence of the main neutral and sialylated groups of GSL in human placenta has been reported (Taki et al. 1988; Strasberg et al. 1989; Mikami et al. 1993; Jordan and DeLoia 1999). In the first step of our study, we analyzed the GSL pattern in human placenta by HPTLC and confirmed the presence of the main fractions—globotetraosylceramide (Gb4Cer), Gb3Cer, dihexosylceramides, monohexosylceramides, GM3 and lower amounts of more complex sialylated GSL, classified as belonging to oligosaccharide nLc_4Cer only (Taki et al. 1988; Mikami et al. 1993). In the next stage, lipids were quantified by MS/MS and GM3 and Gb3Cer were found as the most abundant constituents in the spectrum of placental GSL. Monosialylated tetrasaccharide lipid fraction corresponded by structure and ion fragmentation to both $IV^3NeuAc\text{-}nLc_4Cer$ (SPG) and $II^3NeuAc\text{-}Gg_4Cer$ (GM1) that cannot be differentiated by MS/MS. However, using the specific binding of GM1 by CTX, we clearly demonstrated the presence of the minor amount of

GM1 in placental homogenates besides major sialylated GSLs —GM3 and GSLs of nLc_4Cer. Although gangliosides bearing ganglio-series backbone were not reported in placental tissue so far, the presence of detectable amount of GM1, a characteristic component of cellular membranes and their lipid domains (rafts) is not surprising.

Distribution of lysosomal storage in Fabry disease was confined to smooth muscle cells in the umbilical wall and to endothelial cells of the umbilical vessels. This corresponded to the previous reports (Vedder et al. 2006; Bouwman et al. 2010). We find interesting comparison of the tendency to lysosomal Gb3Cer storage in umbilical endothelial cells in contrast to placental villous capillaries, both exposed to α-Gal A deficiency for the same period of time. The umbilical endothelial cells expressed lysosomal storage despite the absence of detectable Gb3Cer in normal conditions, probably indicating a presence of early turnover of Gb3Cer in both smooth muscle cells and endothelial cells demasked by α-Gal A deficiency. This contrasts with endothelial cells of the placental villous capillaries, which were free of lysosomal storage but expressed Gb3Cer in detectable amount physiologically. We suggest that this may be caused by the linkage of Gb3Cer to clathrin-independent endocytosis in placental villous capillaries, a process which is reputed to realize transport from cell membrane to various cell compartments including transcytosis, passing the lysosomal system (Nichols 2003; Pang et al. 2004; Norkin and Kuksin 2005; Lajoie and Nabi 2010).

Conclusions

Gb3Cer expression in the placental blood villous capillaries represents a unique finding which points to specific features of their endothelial apical pole. By this, the villous capillaries differ not only from endothelial cells of the umbilical vessels but from endothelial cells of the somatic capillaries as well. The physiological significance of this finding is open for further investigation. Our studies were, for all practical purposes, limited to full-term matured placentas. Therefore, further studies should focus on earlier gestational phases.

Our observations raise one more question; is it possible that Gb3Cer, at the apical pole of placental villous capillaries (and even in cells lining uteroplacental vessels), might be degraded by enzyme replacement therapy during treatment of pregnant Fabry patients (Bouwman et al. 2010)? Transport of the enzyme, from maternal to fetal blood, would fit with the current knowledge of transplacental transport of macromolecules (Takizawa et al. 2005; Solder et al. 2009).

Materials and methods

The study was approved by the Ethics Committee of the General Teaching Hospital and the First Faculty of Medicine, Charles University, Prague (Nr. 207/10 S-IV).

In situ *analysis*

Samples from six placentas and umbilical cords from physiological, full-term, deliveries were (i) frozen in liquid nitrogen and used for both immunohistochemistry and biochemistry and (ii) fixed in 4% buffered paraformaldehyde for histology and electron microscopy. Both fetal (villous) and maternal (basal plate) portions of the placentas were used.

GSLs were also studied immunohistochemically in endothelial cells of somatic structures (heart, lung, skeletal muscle, skin) in three neonates succumbing to a disease lysosome unrelated.

Parallel to controls, three placental samples including umbilical cords from Fabry disease (fixed in formalin) were also analyzed. Two were from a premature delivery of two female siblings (34 weeks) and one was from a full-term placenta (female). Mother of two female siblings was partially symptomatic carrier for Fabry disease not treated by enzyme. Heterozygote status of both siblings was confirmed by DNA analysis. Another analyzed placenta with an umbilical cord was from a full-term delivery of a female child (heterozygosity confirmed by DNA analysis; healthy mother, father a hemizygote for Fabry disease). The samples were (i) processed for electron microscopy and (ii) soaked in ascending concentrations (maximum 40%) of buffered solutions of saccharose and incubated overnight at 4°C. Blocks were then cut with a cryostat and the sections processed for Gb3Cer detection using the same method as for the unfixed control samples.

GSL detection

Gb3Cer was detected using mouse monoclonal antibody (clone BGR23, lot A20118; Seikagaku Corporation, Tokyo, Japan). For the detection of GM1, two different approaches were used: (i) with the CTX described in a recent study (Smid et al. 2010) and (ii) with monoclonal antibody (clone GMB16, lot A70114, Seikagaku Corporation). GM3 was detected with mouse monoclonal antibody (clone GMR6, lot AX0116; Seikagaku Corporation). Cryostat sections were used with and without pretreatment with cold anhydrous acetone (15 min, 4°C) for removal of possible apolar lipid admixture and for glycolipid fixation. The sections were then briefly post-fixed with 4% buffered paraformaldehyde (5 min at 4°C). Endogenous peroxidase was blocked using a standard procedure involving an aqueous solution of sodium azide (0.1%) and hydrogen peroxide (1% in phosphate-buffered saline). Care was taken to avoid use of organic solvents during the pre-incubation steps, since methanol, if used for endogenous peroxidase inhibition, would remove a significant amount of GSL. The incubation with primary antibodies (dilution 1:50–100) ranged from 1 to 4 h at 37° (GM3 overnight at 4°C). Each of the immunostaining was performed also after complete lipid extraction, consisting of the following steps: 50% ethanol for 10 min, chloroform:methanol:water (C:M:W, 4:8:3; v/v/v) for 30 min and chloroform:methanol (C:M, 2:1; v/v) for 30 min; all at room temperature. Details of the immunostaining of Gb3Cer have been published (Keslova-Veselikova et al. 2008).

Protein immunophenotype of endothelial cells was evaluated using monoclonal antibodies against CD31, CD34 and factor VIII-related antigens (DAKO, Glostrup, Denmark), caveolin 1 (LifeSpan Biosciences, Seattle) and cytokeratins (CK LS; Immunotech, Marseile, France). Detection was carried out in paraffin sections, with the exception of caveolin

1, which was detected in both cryostat and paraffin sections. The bound primary antibodies were detected using the appropriate DAKO Envision® kits with 3,3′-diaminobenzidine tetrachloride chromogen (DAKO).

Cholesterol was detected with freshly prepared Filipin solution (Sigma-Aldrich, St Louis) and using the protocol published (Kruth et al. 1986) with slight modification.

Electron microscopy of the capillary apical pole. Fixed samples of controls were used for ultrastructure analysis. Samples were dehydrated in ascending ethanol solutions and embedded in an Epon-Araldite mixture. Ultrathin sections were double stained with uranyl acetate and lead nitrate and examined in JEM 1200 EX electron microscope.

The presence of lysosomal storage in Fabry disease was analyzed using both Gb3Cer immunodetection and electron microscopy.

Biochemical analysis

Preparation and analysis of lipid extracts. Samples of five full-term placentas were used for lipid analysis. Samples of the villous parts of placentas were weighted and homogenized in water, and aliquots were taken for protein determination (Hartree 1972). Homogenized tissues were extracted successively with mixtures of chloroform:methanol:water (C:M:W, 20:10:1; 10:20:1; 10:10:1; v/v/v) and the preparation of GSLs was carried out as described previously (Natomi et al. 1988). Purified sphingolipids were re-dissolved by C:M (1:1; v/v) to original volume corresponding to the given concentration of protein (in μg/μL) of lipid extract.

Aliquots were separated on HPTLC Silica 60 plates (Merck, Germany) using C:M:W (65:35:8; v/v/v) or C:M:0.5% $CaCl_2$ (55:45:10; v/v/v) systems. Spots were visualized with orcinol or resorcinol–HCl reagents. Two-step TLC overlay (HPTLC aluminum sheets silica gel 60; Merck) was used for the detection of GM1 with CTX (Biotin labeled; Sigma-Aldrich; Smid et al. 2010).

Quantification of sphingolipids by MS/MS. Aliquots of total lipid extracts corresponding to 72 μg of protein for neutral sphingolipids and 144 μg of protein for acidic sphingolipids were transferred to glass vial. Preparation of sample and MS/MS analysis were carried out by previously described procedure using mixture of internal standards (ISTs) and lipid calibrants for external calibration point evaluation (Kuchar et al. 2009). Briefly, both tissue extracts containing IST and external calibration point mixtures were evaporated under the stream of nitrogen. Finally, samples were reconstituted in methanol with 5 mM ammonium formate. Measurement and quantification were performed on AB/MDS SCIEX API 3200 triple-quadruple mass spectrometer by Multiple Reaction Monitoring (MRM) in a positive ion mode using the fragment of m/z 264.4 for neutral GSL (the sphingosine-base fragment) and of m/z 184.2 for sphingomyelin (phosphocholine fragment).

GM1 and GM3 were measured by MRM in a negative ion mode using the specific fragment of m/z 291 corresponding to sialic acid. C17:0 GM1 (C17:0 GM1 ITS) was used as IST for both gangliosides using similar strategy described for the quantification of neutral GSLs (Mills et al. 2005). C17:0 GM1 ITS was semi-synthesized using immobilized Sphingolipid ceramide N-deacylase from Pseudomonas species (TAKARA Bio. Inc., Otsu, Japan; Kuchar et al. 2010). GM1 and GM3 external point calibrants were from Matreya (Pleasant Gap). Linearity of the method was tested prior to analysis (Kuchar et al. 2009). Signal ratios of GM1 and GM3 to C17:0 GM1 IST were linear in the range of concentrations of placental GM3.

Gb4Cer was quantified similarly using C17:0 Gb3Cer IST (Matreya).

Funding

The study was supported by a research project of the Ministry of Education Youth and Sports, Czech Republic (MSM 0021620806) and by the grant IGA MZ NS/10342-3/2009 from the Ministry of Health, Czech Republic.

Acknowledgements

The excellent technical assistance of Mrs. Lenka Kryšpinova is greatly acknowledged.

Conflict of interest

None declared.

Abbreviations

α-Gal A, α-galactosidase A; CK LS, large spectrum cytokeratin; CTX, Cholera toxin B-subunit; Gb3Cer, globotriaosylceramide; Gb4Cer, globotetraosylceramide; GM1, GM1 ganglioside; GM3, GM3 ganglioside; GSL, glycosphingolipid; HPTLC, high-performance thin-layer chromatography; IST, internal standards; MS/MS, tandem mass spectrometry; nLc_4Cer, neolacto-series; SPG, sialylparagloboside; TLC, thin-layer chromatography.

Glycosphingolipids are abbreviated according to recommendations of the IUPAC-IUB Commission on Biochemical Nomenclature (Chester 1998).

References

Betz J, Bielaszewska M, Thies A, Humpf HU, Dreisewerd K, Karch H, Kim KS, Friedrich AW, Muthing J. 2011. Shiga toxin glycosphingolipid receptors in microvascular and macrovascular endothelial cells: Differential association with membrane lipid raft microdomains. *J Lipid Res*. 52:618–634.

Bouwman MG, Hollak CE, van den Bergh Weerman MA, Wijburg FA, Linthorst GE. 2010. Analysis of placental tissue in Fabry disease with and without enzyme replacement therapy. *Placenta*. 31:344–346.

Chark D, Nutikka A, Trusevych N, Kuzmina J, Lingwood C. 2004. Differential carbohydrate epitope recognition of globotriaosyl ceramide by verotoxins and a monoclonal antibody. *Eur J Biochem*. 271:405–417.

Chester MA. 1998. IUPAC-IUB Joint Commission on Biochemical Nomenclature (JCBN). Nomenclature of glycolipids–recommendations 1997. *Eur J Biochem*. 257:293–298.

Elleder M. 2010. Subcellular, cellular and organ pathology of Fabry disease. In: Elstein D, Altarescu G, Beck M, editors. *Fabry Disease*. New York: Springer. p. 39–80.

Frank HG, Kaufmann P. 2006. Nonvillous parts and trophoblast invasion. In: Bernischke K, Kaufmann P, Baergen R, editors. *Pathology of the Human Placenta*. New York: Springer. p. 191–312.

Hartree EF. 1972. Determination of protein: A modification of the Lowry method that gives a linear photometric response. *Anal Biochem*. 48:422–427.

Hrebicek M, Ledvinova J. 2010. Biochemistry of Fabry disease. In: Elstein D, Altarescu G, Beck M, editors. *Fabry Disease*. New York: Springer. p. 81–104.

Jacewicz MS, Acheson DW, Binion DG, West GA, Lincicome LL, Fiocchi C, Keusch GT. 1999. Responses of human intestinal microvascular endothelial cells to Shiga toxins 1 and 2 and pathogenesis of hemorrhagic colitis. *Infect Immun*. 67:1439–1444.

Jordan JA, DeLoia JA. 1999. Globoside expression within the human placenta. *Placenta*. 20:103–108.

Kanekura T, Fukushige T, Kanda A, Tsuyama S, Murata F, Sakuraba H, Kanzaki T. 2005. Immunoelectron-microscopic detection of globotriaosylceramide accumulated in the skin of patients with Fabry disease. *Br J Dermatol*. 153:544–548.

Keslova-Veselikova J, Hulkova H, Dobrovolny R, Asfaw B, Poupetova H, Berna L, Sikora J, Golan L, Ledvinova J, Elleder M. 2008. Replacement of alpha-galactosidase A in Fabry disease: Effect on fibroblast cultures compared with biopsied tissues of treated patients. *Virchows Arch*. 452:651–665.

Keusch GT, Acheson DW, Aaldering L, Erban J, Jacewicz MS. 1996. Comparison of the effects of Shiga-like toxin 1 on cytokine- and butyrate-treated human umbilical and saphenous vein endothelial cells. *J Infect Dis*. 173:1164–1170.

Kruth HS, Comly ME, Butler JD, Vanier MT, Fink JK, Wenger DA, Patel S, Pentchev PG. 1986. Type C Niemann-Pick disease. Abnormal metabolism of low density lipoprotein in homozygous and heterozygous fibroblasts. *J Biol Chem*. 261:16769–16774.

Kuchar L, Ledvinova J, Hrebicek M, Myskova H, Dvorakova L, Berna L, Chrastina P, Asfaw B, Elleder M, Petermoller M, et al. 2009. Prosaposin deficiency and saposin B deficiency (activator-deficient metachromatic leukodystrophy): Report on two patients detected by analysis of urinary sphingolipids and carrying novel PSAP gene mutations. *Am J Med Genet A*. 149A:613–621.

Kuchar L, Rotkova J, Asfaw B, Lenfeld J, Horak D, Korecka L, Bilkova Z, Ledvinova J. 2010. Semisynthesis of C17:0 isoforms of sulphatide and glucosylceramide using immobilised sphingolipid ceramide N-deacylase for application in analytical mass spectrometry. *Rapid Commun Mass Spectrom*. 24:2393–2399.

Lajoie P, Nabi IR. 2010. Lipid rafts, caveolae, and their endocytosis. *Int Rev Cell Mol Biol*. 282:135–163.

Lingwood CA, Binnington B, Manis A, Branch DR. 2010. Globotriaosyl ceramide receptor function - where membrane structure and pathology intersect. *FEBS Lett*. 584:1879–1886.

Lyden TW, Anderson CL, Robinson JM. 2002. The endothelium but not the syncytiotrophoblast of human placenta expresses caveolae. *Placenta*. 23:640–652.

Mayor S, Pagano RE. 2007. Pathways of clathrin-independent endocytosis. *Nat Rev Mol Cell Biol*. 8:603–612.

Mikami M, Takamatsu K, Tanaka J, Sasaki H, Sakayori M, Iwamori M, Nozawa S. 1993. Characteristic alteration in the concentration of IV 3NeuAc alpha-nLc4Cer in the villi of human placenta during the gestational period. *Placenta*. 14:407–416.

Mills K, Morris P, Lee P, Vellodi A, Waldek S, Young E, Winchester B. 2005. Measurement of urinary CDH and CTH by tandem mass spectrometry in patients hemizygous and heterozygous for Fabry disease. *J Inherit Metab Dis*. 28:35–48.

Muthing J, Duvar S, Heitmann D, Hanisch FG, Neumann U, Lochnit G, Geyer R, Peter-Katalinic J. 1999. Isolation and structural characterization of glycosphingolipids of in vitro propagated human umbilical vein endothelial cells. *Glycobiology*. 9:459–468.

Muthing J, Schweppe CH, Karch H, Friedrich AW. 2009. Shiga toxins, glycosphingolipid diversity, and endothelial cell injury. *Thromb Haemost*. 101:252–264.

Natomi H, Sugano K, Iwamori M, Takaku F, Nagai Y. 1988. Region-specific distribution of glycosphingolipids in the rabbit gastrointestinal tract: Preferential enrichment of sulfoglycolipids in the mucosal regions exposed to acid. *Biochim Biophys Acta*. 961:213–222.

Nichols B. 2003. Caveosomes and endocytosis of lipid rafts. *J Cell Sci*. 116:4707–4714.

Norkin LC, Kuksin D. 2005. The caveolae-mediated sv40 entry pathway bypasses the golgi complex en route to the endoplasmic reticulum. *Virol J*. 2:38.

Pang H, Le PU, Nabi IR. 2004. Ganglioside GM1 levels are a determinant of the extent of caveolae/raft-dependent endocytosis of cholera toxin to the Golgi apparatus. *J Cell Sci*. 117:1421–1430.

Parton RG. 1994. Ultrastructural localization of gangliosides; GM1 is concentrated in caveolae. *J Histochem Cytochem*. 42:155–166.

Popli S, Leehey DJ, Molnar ZV, Nawab ZM, Ing TS. 1990. Demonstration of Fabry's disease deposits in placenta. *Am J Obstet Gynecol*. 162:464–465.

Ren J, Utsunomiya I, Taguchi K, Ariga T, Tai T, Ihara Y, Miyatake T. 1999. Localization of verotoxin receptors in nervous system. *Brain Res*. 825:183–188.

Schweppe CH, Bielaszewska M, Pohlentz G, Friedrich AW, Buntemeyer H, Schmidt MA, Kim KS, Peter-Katalinic J, Karch H, Muthing J. 2008. Glycosphingolipids in vascular endothelial cells: Relationship of heterogeneity in Gb3Cer/CD77 receptor expression with differential Shiga toxin 1 cytotoxicity. *Glycoconj J*. 25:291–304.

Smid F, Ledvinova J, Petr T, Smidova J, Vitek L. 2010. Methods based on binding affinity of the B-subunit of cholera toxin to gangliosides in biochemistry and histology. In: Melbourne EL, editors. *Cholera: Symptoms, Diagnosis and Treatment*. Hauppauge, New York: Nova Science Publishers, Inc. p. 1–17.

Solder E, Rohr I, Kremser C, Hutzler P, Debbage PL. 2009. Imaging of placental transport mechanisms: A review. *Eur J Obstet Gynecol Reprod Biol*. 144(Suppl. 1):S114–S120.

Strasberg P, Grey A, Warren I, Skomorowski MA. 1989. Simultaneous fractionation of four placental neutral glycosphingolipids with a continuous gradient. *J Lipid Res*. 30:121–127.

Taki T, Matsuo K, Yamamoto K, Matsubara T, Hayashi A, Abe T, Matsumoto M. 1988. Human placenta gangliosides. *Lipids*. 23:192–198.

Takizawa T, Anderson CL, Robinson JM. 2005. A novel Fc gamma R-defined, IgG-containing organelle in placental endothelium. *J Immunol*. 175:2331–2339.

Tedde G, Pirino A, Esposito F, Fenu G. 1990. Mechanisms of regulation of the capillary bed in the human chorionic villi. *Arch Ital Anat Embriol*. 95:105–112.

Vedder AC, Strijland A, vd Bergh Weerman MA, Florquin S, Aerts JM, Hollak CE. 2006. Manifestations of Fabry disease in placental tissue. *J Inherit Metab Dis*. 29:106–111.

SUPPLEMENTARY PUBLICATIONS

Non impacted publications related to topic of this PhD thesis

Supplementary publication E – Chapter in the Book

Kuchar L., Asfaw B., and Ledvinova J., *Tandem Mass Spectrometry of Sphingolipids: Application in Metabolic Studies and Diagnosis of Inherited Disorders of Sphingolipid Metabolism*, in *Tandem Mass Spectrometry - Applications and Principles*, Prasain, Editor 2012, InTech: Rijeka. p. 739-768

TANDEM MASS SPECTROMETRY

APPLICATIONS AND PRINCIPLES

Edited by **Jeevan K. Prasain**

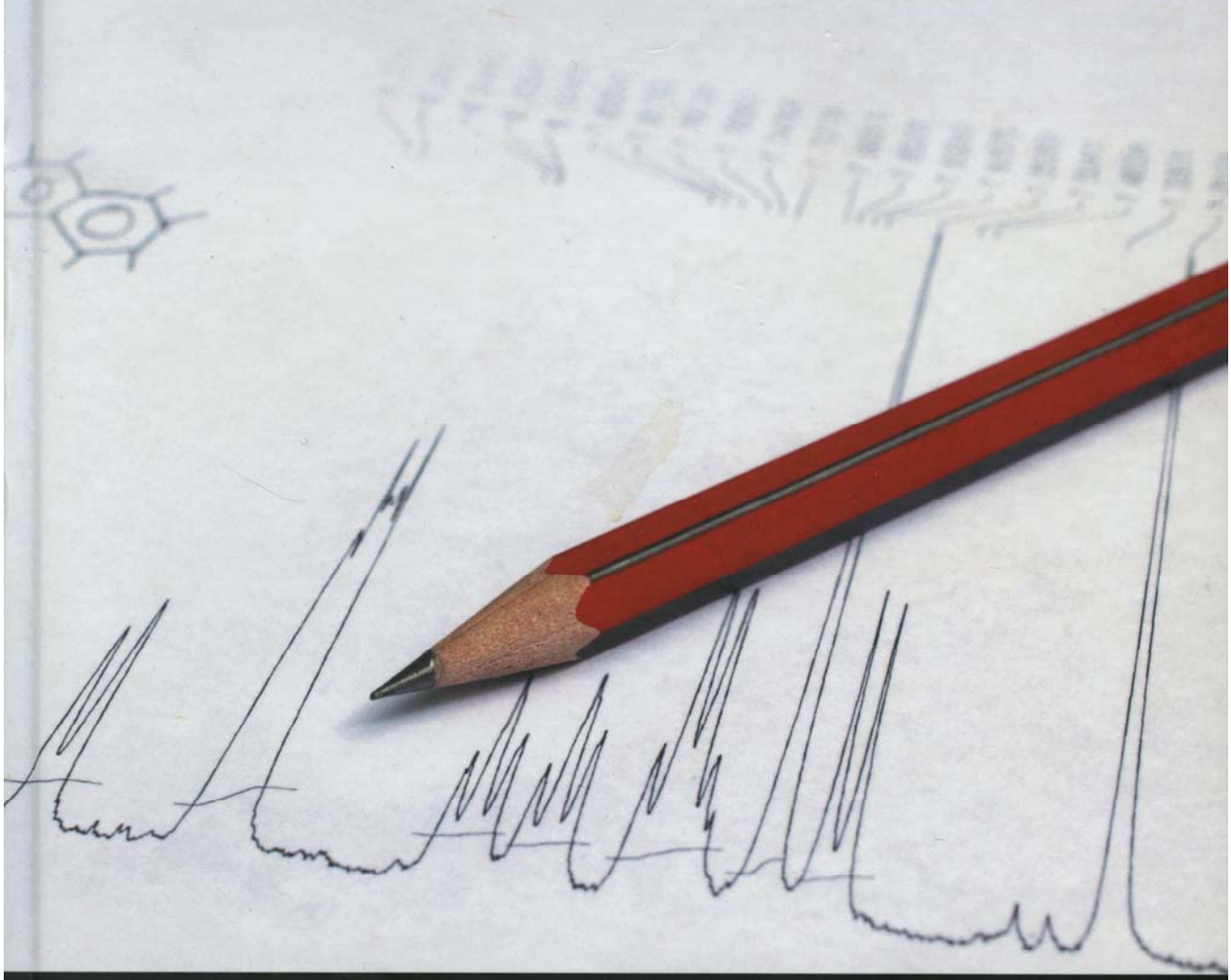

INTECH

TANDEM MASS SPECTROMETRY – APPLICATIONS AND PRINCIPLES

Edited by **Jeevan K. Prasain**

INTECHWEB.ORG

Tandem Mass Spectrometry – Applications and Principles
Edited by Jeevan K. Prasain

Published by InTech
Janeza Trdine 9, 51000 Rijeka, Croatia

Publishing Process Manager Martina Durovic
Technical Editor Teodora Smiljanic
Cover Designer InTech Design Team

First published February, 2012
Printed in Croatia

A free online edition of this book is available at www.intechopen.com
Additional hard copies can be obtained from orders@intechweb.org

Tandem Mass Spectrometry – Applications and Principles,
Edited by Jeevan K. Prasain
p. cm.
ISBN 978-953-51-0141-3

30

Tandem Mass Spectrometry of Sphingolipids: Application in Metabolic Studies and Diagnosis of Inherited Disorders of Sphingolipid Metabolism

Ladislav Kuchař, Befekadu Asfaw and Jana Ledvinová
Institute of Inherited Metabolic Disorders, First Faculty of Medicine, Charles University in Prague and General University Hospital in Prague
Czech Republic

1. Introduction

Sphingolipids are an amazingly diverse category of lipids found in all eukaryotes and in some prokaryotes and viruses. They are primarily a component of plasma membranes and of intracellular organelle membranes, including those of the nucleus, mitochondria, endosomes, and lysosomes (Hirabayashi, et al., 2006; Kaushik, et al., 2006; R. Ledeen & Wu, 2011; R. W. Ledeen & Wu, 2008; Prinetti, et al., 2009; van Meer, et al., 2008). Sphingolipids are also an important constituent of plasma lipoprotein classes (Schweppe, et al., 2010; Wiesner, et al., 2009) and of the multilamellar water barrier of the skin (Holleran, et al., 2006). In addition, they are excreted in urine, mostly in the cellular debris of urinary sediment. Urinary sediment analysis, or "indirect biopsy," of kidney cellular elements (Desnick, et al., 1970) can provide information that helps to diagnose certain lysosomal storage diseases (Kitagawa, et al., 2005; Kuchar, et al., 2009; Whitfield, et al., 2001).

Sphingolipids are a heterogenous group. Amide bonds link long-chain fatty acids to aminoalcohols from the sphingoid group, of which sphing-4-enin ({2S,3R,4R}-2-aminooctadec-4-ene-1,3-diol, historically called sphingosine) and its saturated derivative (sphinganine) are the most abundant. Longer or shorter sphingoids, which may be saturated or hydroxylated, also occur in lesser quantities.

The name sphingosine was chosen by German clinician and chemist J. L. W. Tchudichum in 1884 to reflect the enigmatic, "Sphinx-like" properties of the sphingolipid compounds first isolated from the brain. Fatty acid variations include mostly C16-C24 acyl chains, which are often saturated but can also exhibit a degree of unsaturation or hydroxylation (e.g., C24:1, C24:1-OH fatty acids). The general name for N-acylated sphingoids is ceramide. Sphingomyelin and glycosphingolipids have a headgroup in the phosphodiester or glycosyl linkage to the hydroxyl on the carbon-1. The latter compounds are classified as either *neutral glycosphingolipids* with uncharged sugars (glucose, galactose, N-acetylglucosamine, N-acetylglalactosamine and fucose) or *acidic glycosphingolipids* with ionized functional groups (sulfates) or charged sugar moieties (N-acetylneuraminic acid or "sialic" acid).

Two examples of sphingolipid structures are shown in Fig. 1.

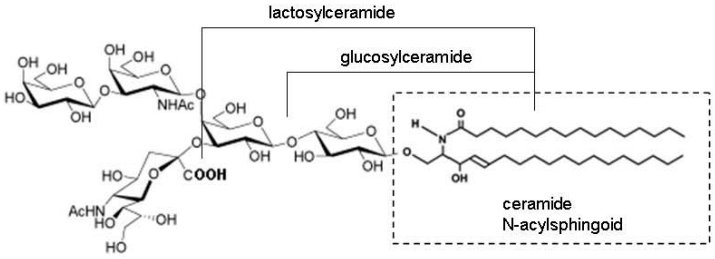

GM1 ganglioside (Galβ1-3GalNAcβ1-4(NeuAcα2-3)Galβ1-4Glcβ-Cer)

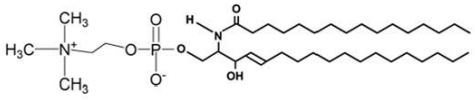

Sphingomyelin (N-acyl-sphing-4-enine-1-phosphocholine)

Fig. 1. GM1 ganglioside - a representative acidic sphingolipid; sphingomyelin - a representative phosphosphingolipid.

The simplest glycosphingolipids are the monohexosylceramides glucosylceramide (GlcCer, Glcβ1-1´Cer) and galactosylceramide (galactocerebroside, GalCer, Galβ1-1´Cer). The latter is less abundant but is specific to neural tissue, where it is also present in a sulfated form (sulfatide). Galactosylceramide also gives rise to small Gala-series of glycosphingolipids (Tab. 1). Glucosylceramide is a key compound in sphingolipid metabolic pathways; more complex glycosphingolipids are derived from the stepwise elongation of the oligosaccharide chain in the Golgi compartment. The addition of β-linked galactose yields lactosylceramide (LacCer, Galβ1-4GlcβCer), whose oligosaccharide chain is the precursor to the different core structures of more complex glycosphingolipids (Tab. 1). These structures are specific to certain tissues: e.g., neolacto-series predominate in leukocytes, lacto-series in secretory organs, globo-series in erythrocytes and ganglio-series in nervous tissue (Schnaar, et al., 2009). This diversity is related to the functional differences between the individual glycosphingolipids.

The catabolism of sphingolipids occurs in acidic cell compartments, i.e. late endosomes and lysosomes. Degraded lipids are embedded in inner membranes rich in negatively charged lipids such as bis(monoacylglycero)phosphate (BMP) (Kolter & Sandhoff, 2010). Sequential degradation steps proceed from the non-reducing end of the oligosaccharide chain catalyzed by soluble lysosomal hydrolases. For lipids with oligosaccharide chains shorter than four sugars, the assistance of small sphingolipid activator proteins (the saposins A, B, C, or D or the GM2 activator protein) is required (Sandhoff, et al., 2001). The sphingoids and fatty acids produced can be degraded in the cytoplasm and processed through the salvage pathway, where they become the building blocks of new membranes (Kitatani, et al., 2008). They can also be used in the regulation systems that control cell function (Kolter & Sandhoff, 2010).

Inherited defects in gene-coding enzymes or proteins involved in sphingolipid degradation result in the accumulation of non-degraded substrates in the lysosomes. "Traffic jams" in the endolysosomal system caused by the accumulation of lipids co-precipitated with other

hydrophobic substances severely impair cell function and lead to lysosomal storage diseases (sphingolipidoses) (Desnick, et al., 2001; Liscum, 2000; Sandhoff, et al., 2001; Schulze & Sandhoff, 2011; von Figura, et al., 2001). Studies of these defects, however, may unveil the complicated mechanisms of cell function and regulation. Recent information learned about the role of NPC1 and NPC2 proteins in the intracellular transport of cholesterol can serve as an example (Infante, et al., 2008; Kwon, et al., 2009; Storch & Xu, 2009; Xu, et al., 2008).
Hitherto, more than 400 structurally distinct sphingolipid variants in mammals have been listed in SphinGOMAP® (http://www.sphingomap.org and http://www.glycoforum.gr.jp) (Aug 2011). A detailed sphingolipid nomenclature is available at http://www.chem.qmul.ac.uk/iupac/lipid/lip1n2.html (Aug 2011) and http://www.chem.qmul.ac.uk/iupac/lipid/lip3n4.html (Aug 2011).

Root names of series	Core structures	Abbreviations
Lacto-	Gal(β1→3)GlcNAc(β1→3)Gal(β1→4)Glc(β1→1')Cer	Lc
Neolacto-	Gal(β1→4)GlcNAc(β1→3)Gal(β1→4)Glc(β1→1')Cer	nLc
Globo-	GalNAc(β1→3)Gal(α1→4)Gal(β1→4)Glc(β1→1')Cer	Gb
Isoglobo-	GalNAc(β1→3)Gal(α1→3)Gal(β1→4)Glc(β1→1')Cer	iGb
Ganglio-	Gal(β1→3)GalNAc(β1→4)Gal(β1→4)Glc(β1→1')Cer	Gg
Gala-	Gal(α1→4)Gal(β1→1')Cer	Ga

Note: key structures characteristic for each series are underlined

Table 1. The major root structures of vertebrate glycosphingolipids.

Physiological sphingolipid function at the cellular level is highly complex. Sphingolipids participate in many cellular events, including cell-cell recognition, the modulation of membrane protein functions, adhesions, intra- and extra-cellular signaling and many still undiscovered processes (Kitatani, et al., 2008). Their rigid, highly saturated character and ability to undergo hydrogen bonding and dipolar interactions predetermines them to cluster into semiordered structures called lipid microdomains – rafts, together with cholesterol and specific set of proteins (Goldschmidt-Arzi, et al., 2011; Helms & Zurzolo, 2004; Holthuis, et al., 2003). They function as important mediators of membrane transport and signaling.
In recent years, investigation of the metabolism and biological functions of sphingolipid biomolecules has increased (Wennekes, et al., 2009). As a result, more accurate methods of analyzing sphingolipids have been developed. A leading method of analysis, tandem mass spectrometry (tandem MS or MS/MS), provides high selectivity and sensitivity of measurement. Indisputable advantage of this technique is a possibility to identify various molecular species of different sphingolipid classes in crude biological samples.
We will focus on the contribution of tandem mass spectrometry to the study of sphingolipids and the usefulness of the technique in diagnosing inherited disorders of sphingolipid degradation. The topics discussed will include the following:

- Tandem mass spectrometry used to analyze sphingolipids in tissues, cells and urine (both the general approach used and its applications in the diagnosis of sphingolipidoses)
- The investigation of the sphingolipid degradation pathway in living cells using stable isotopes or atypical fatty acid labeling
- Sphingolipid isoform profiling, which is a useful tool for diagnosing disorders associated with Gb3Cer and sulfatide storage.

2. Electrospray ionization tandem mass spectrometry of sphingolipids

The equipment used was an AB/MDS SCIEX API 3200 triple quadrupole mass spectrometer. Multiple reaction monitoring was used in positive (neutral glycosphingolipids) and negative (acidic glycosphingolipids) ion mode. Superior sensitivity and selectivity were exhibited when the technique was used in conjunction with normal phase HPLC separation.

2.1 Electrospray ionization

Electrospray ionization abbreviated as ESI is one of the soft ionization methods used in mass spectrometry (Cole, 2010; de Hoffman & Stroobant, 2002). A strong electric field is applied to the analyte solution as it passes through a metal capillary at atmospheric pressure. This field is created using a high voltage (a voltage of up to 6kV) between the capillary tip and the counterelectrode. Droplets of analyte are formed under these conditions on the capillary tip, with ions generated and sorted on the surface. Cations are formed in positive ion mode and anions in negative ion mode. The generation of ions results from the electrochemical processes that occur on the capillary tip and the strong electric field used.

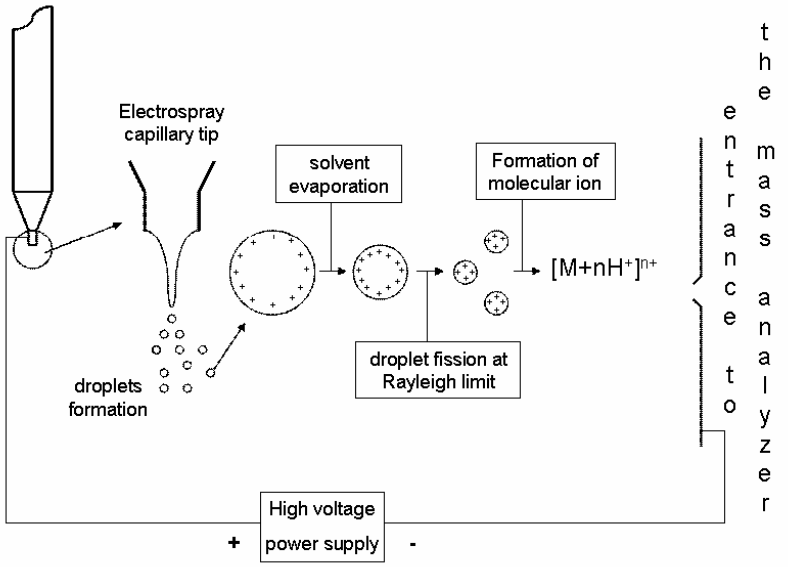

Fig. 2. Scheme of electrospray ionization process.

Droplets flow in the direction of the electric field and shrink in size as the solvent evaporates. When the accumulated surface charge of a droplet exceeds the surface tension force, the droplet breaks into smaller droplets via Rayleigh fission. This process is repeated until the ions on the surface of the droplet are able to overcome the forces holding them, at which point molecular ions are formed (Fig. 2) (Cole, 2010; de Hoffman & Stroobant, 2002; Dulcks & Juraschek, 1999).

The distribution of compounds on the droplet surface results from their relative concentration and solubility. Less soluble compounds tend to be on the surface rather than in the bulk of the solution, which affects their ionization efficiency. The surface of each droplet is limited; thus, the concentration is more important than the total amount of the compound injected in the source (Cole, 2010; de Hoffman & Stroobant, 2002).
Matrix effects occur when additional compound ions are generated on the surface. These compounds can completely mask the analyte (Fig. 3). The salt concentration has a similar effect on ionization; the maximum tolerable concentration of salts is approximately 10^{-3}M (Cole, 2010; de Hoffman & Stroobant, 2002).
The matrix effect can negatively influence electrospray ionization. It is important to choose a sample preparation technique that removes interfering compounds. The use of HPLC or capillary electrophoresis separation prior to electrospray ionization can minimize the matrix effect (Cole, 2010; Micova, et al., 2010); indeed, we saw a 10-fold increase in signal intensity when HPLC was used (data not shown). Established methods of evaluating matrix effects are described in the literature (Taylor, 2005).

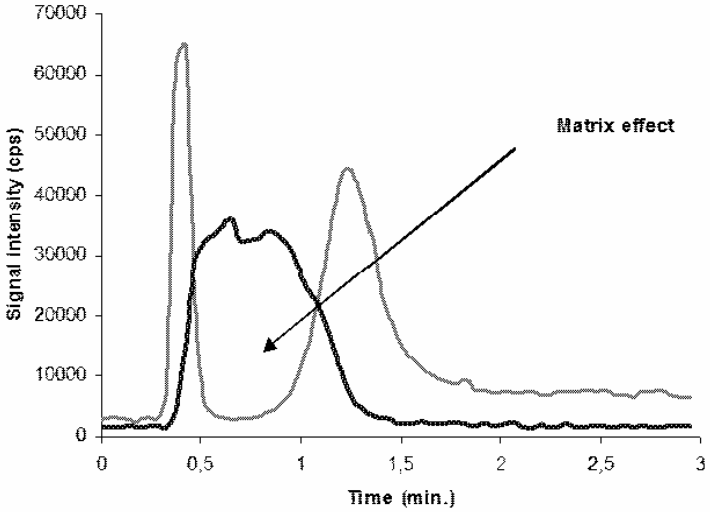

Fig. 3. Matrix effect interference in electrospray ionization conducted on a urinary sample. Total ion current (TIC) of ceramide, ceramide dihexoside and sphingomyelin. Red line: urinary sample after Folch extraction without purification. Visible signal decrease was caused by matrix effect. Blue line: sample after the purification process, which removed the matrix effects.

2.2 Quadrupole mass spectrometer

The quadrupole is a device that uses the stability of ion trajectories in oscillating electric fields to separate ions according to their m/z ratio (de Hoffman & Stroobant, 2002).
The device consists of four parallel circular or hyperbolic metal rods to which radiofrequency voltage (RF) and direct current (DC) are applied. The total electric field is composed of quadrupolar alternative fields superposed on a constant field resulting from

the application of potential on the rods. The result is a mass filter used to separate ions according to their m/z ratio (de Hoffman & Stroobant, 2002; Douglas, 2009).
The mathematical description of the total electric field is based on Mathieu equations (de Hoffman & Stroobant, 2002; Douglas, 2009). The equations can be used to generate a stability diagram for ions in the field. Direct current voltage (U) and radiofrequency voltage amplitude (V) are the only variables in the equations used to define ion position in these diagrams. The other parameters are constants, including the mass and the charge. Thus, changes in U and V determine a given ion's position in the diagram. Only ions in the stable region are able to pass the quadrupole mass filter through the stable trajectories. By continually changing U and V, the quadrupole mass spectrometer is able to scan for ions with different m/z ratios (Fig. 4).

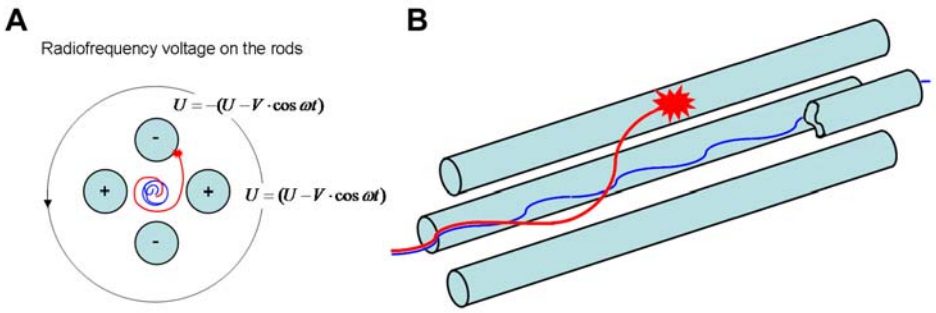

Fig. 4. A quadrupolar mass filter and the trajectories of two ions. Red line: an ion in an unstable region of the stability diagram on an unstable trajectory. Blue line: an ion in a stable region of the stability diagram passing the quadrupole on a stable trajectory. A) Section of the quadrupole illustrating radiofrequency voltage; B) Upper side view of the ion trajectories in the quadrupole.

Practically speaking, quadrupole mass spectrometers are hampered by mass resolution and mass range limitations. The useful level of resolution is one mass unit, and the highest detectable m/z is 4000 (de Hoffman & Stroobant, 2002; McLuckey & Wells, 2001).

2.3 Triple quadrupole tandem mass spectrometry

Triple quadrupole tandem mass spectrometry uses three quadrupoles in a series. The first and third quadrupoles function as mass analyzers, whereas the middle quadrupole, with only the radio frequency voltage used, is employed as a collision cell that does not separate ions according to their m/z ratios. Instead, it works as an ion channel that systematically returns ions to the center of the rods (de Hoffman & Stroobant, 2002; McLuckey & Wells, 2001).
Collision induced dissociation is a process of changing the accelerated ion kinetic energy to internal energy using collisions in a collision cell filled with inert gas (N_2, Ar, or He). Analyte fragments are produced if the volume of accumulated internal energy is greater than the energy of the chemical bonds in the molecule (Cole, 2010; de Hoffman & Stroobant, 2002; McLuckey & Wells, 2001; Sleno & Volmer, 2004).

The static mode (in which only one selected m/z is measured) and the scanning mode (in which a range of m/z ratios is measured) are both used with the first and third quadrupole to attain four specific types of measurement (Cole, 2010; de Hoffman & Stroobant, 2002; McLuckey & Wells, 2001; Sleno & Volmer, 2004):

1. Product ion scans. To attain these measurements, the first quadrupole is used in the static mode, whereas the third quadrupole is used to scan products of collision induced dissociation.
2. Precursor ion scans. To attain these measurements, the first quadrupole is used in scanning mode to determine the mass range of precursor ions which are fragmented in the process of collision induced dissociation. The third quadrupole functions in static mode and is set on the m/z value of the selected fragment which is usually structure specific.
3. Neutral loss scans. The technique used for this purpose monitors the loss of neutral fragments. The first and third quadrupoles are used for scanning with a constant mass offset that represents the neutral fragment loss.
4. Single or multiple reaction monitoring. Here, the first and third quadrupoles work in the static mode and scan the m/z values of the analyte and its selected fragment. A pair of precursor-product ions of this type is called a transition pair. This technique is used extensively in quantitative analysis because it yields the greatest possible measurement sensitivity.

Tandem mass spectrometry exhibits higher selectivity and sensitivity (with a higher signal-to-noise ratio because noise is suppressed) than does simple mass spectrometry. This advantage also makes this technique useful when tandem mass spectrometry is coupled with HPLC separation (Haynes, et al., 2009; Sullards, et al., 2011).

2.4 Tandem mass spectrometry of sphingolipids: ionisation, fragmentation and specificity of sphingolipid analysis

2.4.1 Ionization

The ionization of sphingolipids by electrospray ionization varies for different classes of sphingolipids. This variation can be used in intrasource separation in lipid analyses (Han & Gross, 2005; Haynes, et al., 2009).

Neutral sphingolipids are usually protonated by ammonium formiate, ammonium acetate, formic or acetic acid. Ammonium salts exhibit the highest degree of ionization efficiency and are widely used (Mano, et al., 1997). Neutral salts of Li^+ or Na^+ are also used for ionization and generate ion-lipid adducts (Boscaro, et al., 2002; Olling, et al., 1998).

Acids are generally used for H^+ transfer in solution to basic groups on analyte or to creation of cluster of protonated solvents which later transfer H+ to analyte in the process of charge separation. On the other hand neutral amonium salts are usually added to the solution to facilitate the analysis of polar and neutral analytes by adduct formation and later protonation in the process of ionization through gas-phase reactions. Sodium and lithium aducts are also aded in form of neutral salts; the ionisation process has the character of specific charge separation (Cech & Enke, 2001; Kebarle, 2000).

We found that for positive ion mode measurements, 5 mM ammonium formiate is a more efficient additive for use in sphingolipid ionization than is ammonium acetate. However, when using HPLC combined with mass spectrometry, we prefer to use ammonium acetate and acetic acid because of their better solubility in methanol. The ions generated during the electrospray ionization process were $[M+H]^+$.

Acidic sphingolipids, such as sulfatides or gangliosides, have acidic groups that lose H^+ even in pure methanol. It is also possible to create chloride adducts (Han & Gross, 2005) using halogenated solvents that can also abstract protons (Cech & Enke, 2001).
For measurements in negative ion mode, we used pure methanol solvent to generate $[M-H]^-$ ions.

2.4.2 Fragmentation

Fragmentation studies of sphingolipids revealed characteristic fragments useful for tandem mass spectrometric analysis (Domon & Costello, 1988; Fuller, et al., 2005; Gu, et al., 1997; Hsu, et al., 1998; Hsu & Turk, 2000; Ii, et al., 1995; Kerwin, et al., 1994; Liebisch, et al., 1999; Mano, et al., 1997; Murphy, et al., 2001; Olling, et al., 1998; Whitfield, et al., 2001). The most common fragments used for sphingolipid analysis in positive ion mode are structurally derived from ceramide with C18:1 sphingosine. When the amide bond is broken, followed by the formation of ion derived from sphingoid structure minus one water molecule, the fragment with the m/z value of 282 is produced. If another molecule of water is lost, the fragment with the m/z value of 264 is generated (Fig. 5A) (Gu, et al., 1997; Liebisch, et al., 1999; Murphy, et al., 2001; Olling, et al., 1998). These product ions have different uses. The 264 m/z fragments are used to analyze sphingolipids, whereas the 282 m/z fragments are used to analyze N-deacylated sphingolipids (lysoderivatives) (Gu, et al., 1997; Lieser, et al., 2003; Olling, et al., 1998; Scherer, et al., 2010).
The ceramide fragments mentioned above are commonly used in tandem mass analysis, but other specific sphingolipid structures can also be used for this purpose. Sphingomyelin has characteristic phosphocholines that generate fragments with an m/z value of 184 (Fig. 5B) (Hsu & Turk, 2000; Kerwin, et al., 1994; Murphy, et al., 2001). Sialic acid is another example of a specific sphingolipid structure that is a component of gangliosides. Fragments of sialic acid have m/z values of 290 and 308 (Fig. 5C) (Domon & Costello, 1988; Ii, et al., 1995). A structure that is specific to sulfatides is the sulfate group, which exhibit an m/z value of 97. (Fig. 5D) (Hsu, et al., 1998; Whitfield, et al., 2001).

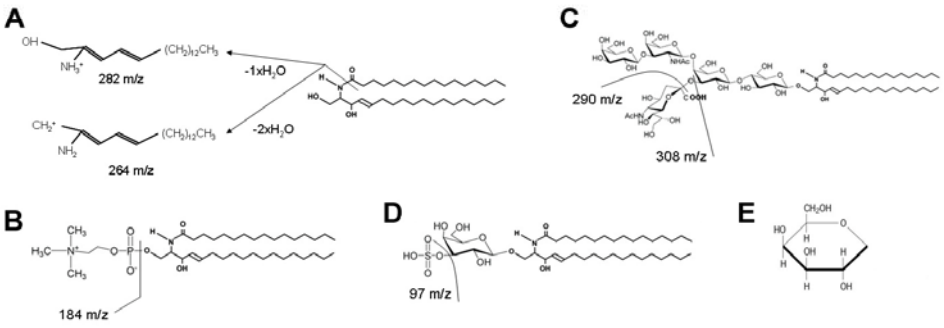

Fig. 5. Fragmentation of ceramide (A) and specific fragments of sphingomyelin (B), GM1 ganglioside (C) and sulphatides (D). Neutral fragment of hexose (galactose) is an example of fragmentation used in a neutral loss scan (E).

Another analytical approach involves scanning for the neutral loss of saccharides from oligosaccharide chains of glycosphingolipids (Fig. 5E and 6) (Boscaro, et al., 2002; Domon &

Costello, 1988; Olling, et al., 1998). In this approach, transition pairs consisting of analyzed glycosphingolipids and their products with shorter or missing oligosaccharides are measured (Fig. 6).

Neutral loss scanning is the technique of choice for glycosphingolipids containing dihydroceramide or sphinganine. Saturating the double bonds of sphing-4-enine reduces the production of sphingoid base fragments (Fig. 5A) in the positive mode, yielding a fragmentation (Fig. 6) efficiency of approximately 2-3%. In contrast, neutral loss scan fragmentation efficiency for the above-mentioned molecules is 10-15%. It is therefore crucial to select the best fragment to conduct a successful tandem mass analysis of sphingolipids.

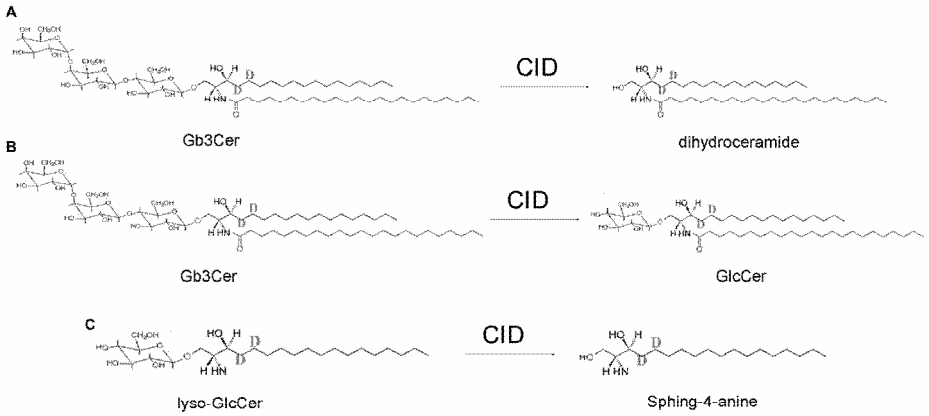

Fig. 6. Principle of neutral loss measurements of sphingolipids with deuterated dihydroceramide and sphing-4-anine in the ceramide region of the molecule. A) Complete loss of Gb3Cer oligosaccharide, B) Shortening of Gb3Cer oligosaccharide C) Neutral loss of saccharide part in lysoglycosphingolipids. CID – collision induced dissociation; Gb3Cer – globotriaosylceramide.

2.4.3 Specificity of mass spectrometry analysis of sphingolipids

Mass spectrometry analyzes molecules according to their m/z values. Different classes of sphingolipids are not represented by one specific molecule; rather, they are a heterogeneous group of molecules with different molecular masses. Their variability is mostly represented by a spectrum of fatty acids that form ceramide structures. Molecular species of individual sphingolipids are called isoforms, and their profiles are usually cell- and tissue-specific (Fig. 7). Therefore, it is important to determine the specific isoform profiles of sphingolipids in biological material before conducting a quantitative analysis.

2.5 Sample preparation for tandem mass spectrometric analysis

A common step in the processing of different biological samples (urine, plasma, cerebrospinal fluid, cells, bioptic or autoptic tissues, etc.) prior to tandem mass spectrometric analysis is the preparation of a lipid extract. Cells and tissues are homogenized, and aliquots of homogenate are usually taken for protein determination. Many extraction procedures have been introduced over the years, most of which have been

based on chloroform-methanol mixtures (Bligh & Dyer, 1959; Folch, et al., 1957) or less harmful solvents such as 2-propanol, ethylacetate, hexane or tetrahydrofuran (Heitmann, et al., 1996). The first approach remains the most popular and efficient. Widely used variations on the above-mentioned procedures and recommended methods of removing contaminants from total lipid extract were summarized by Schnaar R (Schnaar, 1994) and van Echten-Deckerd G (van Echten-Deckert, 2000).

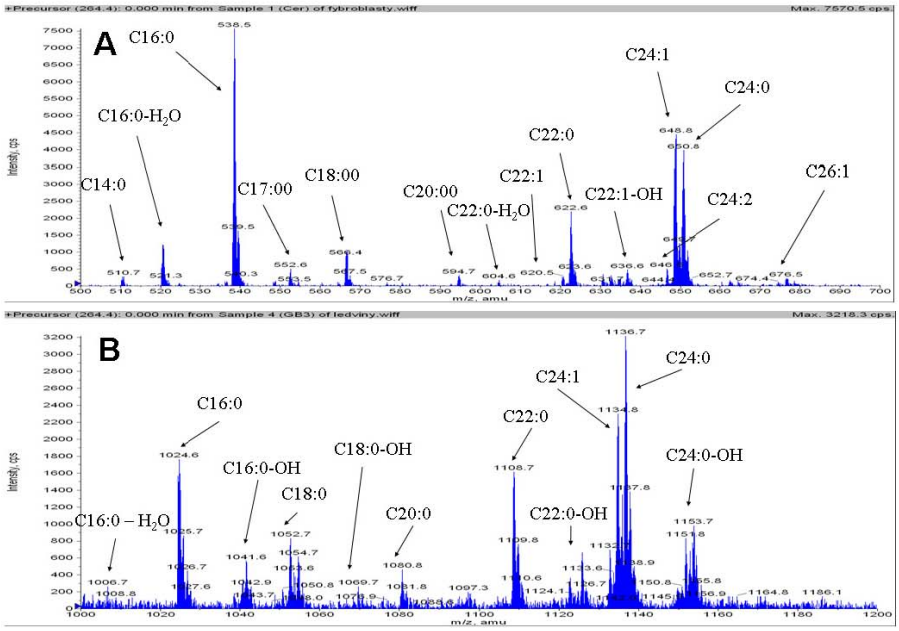

Fig. 7. Isoform profiles measured using precursor ion scans for different lipids and biological materials. Three-milligram protein aliquots of lipid extracts were dissolved in methanol with 5 mM ammonium formiate and measured using 1 min precursor ion scans for ceramide fragments with m/z values of 264 in positive ion mode. Isoforms with different fatty acid chain lengths are identified. A) ceramides in skin fibroblasts, B) Gb3Cer in the kidney.

2.5.1 Preparation of lipid extract from urine

Extracts were prepared as previously published (Kuchar, et al., 2009). First, 150 µl of sonicated urine was extracted with 700 µl of chloroform:methanol (2:1, v:v) containing internal standards in a polypropylene Eppendorf tube. Then, after 15 min of repeated vortexing at 5 min intervals, 150 µl of MilliQ water was added. The vortex mixing procedure was repeated for another 15 min. After a 20 min pause, the samples were centrifuged for 5 min at 14 000 *x* g. The lower organic layer was isolated using a Hamilton syringe and filtered using hydrophilic polytetrafluorethylene (PTFE) syringe filters. The samples were purified after the addition of 500 µl of MilliQ water and 15 min of vortexing. The organic and aqueous phases were separated by 5 min of centrifugation at 14 000 *x* g, and interfering salts and small organic molecules were removed with the upper water layer. The lower

organic layer containing the sphingolipids was collected, dried under a stream of nitrogen and stored in a freezer (-20°C).

2.5.2 Preparation of lipid extract from cultured fibroblasts

Fibroblast pellets were extracted by standard procedures using a chloroform:methanol:water mixtures as previously described (Asfaw, et al., 1998). The harvested cells from the 75 cm^2 cultivation flask were homogenized in 250 µl of MilliQ water by sonication. Next, 50 µl of homogenate was used for protein determination (Hartree, 1972). The remaining 200 µl of cell homogenate was mixed with 800 µl of chloroform:methanol (2:1, v/v) in a 15 ml glass tube. The mixture was rigorously vortexed twice for 1 min followed by a 15 min settling time at laboratory temperature. The organic and water layers were then separated during 10 min of centrifugation at 400 *x g*. The upper water and lower organic layers were collected, and the precipitated protein was left in the tube. The protein debris was washed with 500 µl of chloroform:methanol (2:1, v/v), and the organic layer without protein was added to the previously collected phases. The lipid extracts were dried under a stream of nitrogen and redissolved in 400 µl of chloroform:methanol (2:1, v/v). The extracts were then filtered using hydrophilic polytetrafluorethylene syringe pump filters. The filtrates were dried under a stream of nitrogen and stored in a freezer (-20°C) for processing.

2.5.3 Preparation of lipid extract from tissues

The basic procedures used in the tissue extraction process were generally the same as those used by Natomi H (Natomi, et al., 1988), though minor modifications were made. Tissue samples with a wet weight of up to 0.5 g were weighed and homogenized in water or methanol:water (10:1, v/v). Small portions of the homogenate were stored for protein quantification (Hartree, 1972), and the remaining portion was used to prepare the lipid extracts. Chloroform was added to the methanol:water homogenate to get a ratio of chloroform:methanol:water (20:10:1 v/v/v). After vortexing and sonication, the extracted samples were centrifuged and the supernatant collected. The sediment was reextracted with a more polar solvent mixture of chloroform, methanol, and water (10:20:1, v/v/v) and then with chloroform:methanol (1:1, v/v). The total volume of the extraction mixture corresponding to 20 volumes of the original tissue sample was added during every step in the extraction process. The supernatants were combined, filtered and dried under a stream of nitrogen. Dried samples were stored at freezer (-20°C) prior to processing and analysis.

2.5.4 Processing of extracted lipid samples prior to tandem mass analysis

Corresponding internal standards were added to the urinary samples during the extraction process (Kuchar, et al., 2009). The same volume of internal standards as was used for the urine samples was added to the appropriate aliquots of purified lipid extracts: 5 µg of cellular protein or 150 µg of tissue protein. Loading experiments with specifically labeled sphingolipid isoforms required 50 µg protein aliquots.

Finally, the samples were dried under a stream of nitrogen and dissolved in methanol with 5 mM ammonium formiate for measurement in the positive ion mode or in pure methanol for measurement in the negative ion mode.

2.6 Quantitative analysis of sphingolipids by tandem mass spectrometry

We used an AB/MDS SCIEX API 3200 triple quadrupole mass spectrometer equipped with an Agilent 1100 series LC system with an autosampler. The Analyst software version 1.5 was used to operate the hardware and process the measured data. Optimizations of electrospray ionization and tandem mass spectrometry conditions were conducted for each analyzed sphingolipid (Tab. 2). A standard lipid solution with a sphingolipid concentration of 5 μg/ml, was used in the optimization process. For positive ion measurement, 5 mM ammonium formiate in methanol was used to produce $[M+H]^+$ ions. To generate $[M-H]^-$ ions in negative ion mode, pure methanol was used.

We measured lipids using a flow injection analysis of 20 μl sample aliquots samples. We used pure methanol as the mobile phase with a flow rate of 50 μl/min. One lipid was analyzed during one injection to provide the best possible quantitative data. The scan time for a transition pair was usually 100 ms but in some cases was increased to 500 ms for higher sensitivity. The settling time was usually 0 ms. However, it was necessary to increase this parameter to 500-700 ms when the ion optics setting was changed to measure more than one class of sphingolipid in one injection. The resolution was generally set to unit (±1 m/z), but in some cases, we used a high resolution setting for the first quadrupole, as using such a setting can improve mass spectrometer sensitivity.

	CTH	CDH	CMH	lyso-CMH	Cer
Curtain Gas [psi]	10	10	10	10	10
Collision Gas (N_2) [psi]	3	5	5	5	5
Ion Spray Voltage [kV]	5,5	4,5	4,5	4,5	4,5
Temperature [°C]	200	200	200	200	200
Ion Source Gas 1 [psi]	15	20	20	20	20
Ion Source Gas 2 [psi]	20	55	55	55	55
Interface Heater	On	On	On	On	On
Declustering Potential [V]	82,5	65,0	47,0	53,0	60,0
Entrance Potential [V]	8,4	6,0	4,9	4,1	5,0
Collision Energy [V]	77,0	64,0	48,0	31,0	42,0
Collision Cell Exit Potential [V]	10,8	5,6	5,6	9,1	5,7

Table 2. Example of electrospray ionization and ion optics parameters used in tandem mass spectrometry to analyze selected sphingolipids (Sciex API 3200, product ion m/z 264, 5 mM ammonium formiate in methanol). CTH – ceramidetrihexoside; CDH – ceramidedihexoside, CMH and lyso-CMH – ceramidemonohexoside and its N-deacylated derivative.

Procedure of our quantitative analysis was described in a previous study (Kuchar, et al., 2009). Problems associated with the matrix effect were addressed using internal standards, whereas the calibration of the method was based on an external standard. Quantification was performed via single-point calibration using an external calibration point with a standard lipid concentration (an external calibration standard) corrected by the signal ratio toward internal standard (mostly C17:0 isoform which is not naturally

abundant) isoform (mostly with C17:0 fatty acid). All standard lipid concentrations were within the broad range of linear response. The internal standard concentration at the external calibration point and in the measured samples was the same. For the quantification procedure, molecular species of sphingolipids with fatty acids of chain lengths from C16 to C26 were selected.

2.7 Preparation of sphingolipids internal standards using enzymatic semi-synthesis

Not all internal standards are commercially available. Thus, we developed a method of enzymatic semi-synthesis using immobilized sphingolipid ceramide N-deacylase (*Pseudomonas sp*, TK4) on porous magnetic cellulose (Kuchar, et al., 2010). Magnetic macroporous bead cellulose was used as carrier for sphingolipid ceramide N-deacylase (SCDase) which was immobilized using a standard procedure (Bilkova, et al., 2005; Korecka, et al., 2005). A 100 µl aliquot of washed settled particles was activated with 0.2 M freshly prepared $NaIO_4$. The activated particles were then washed with 0.1 M phosphate buffer with a pH 7. Binding of 250 mI.U. of sphingolipid ceramide N-deacylase on activated magnetic macroporous bead cellulose was achieved by 10 min incubation in phosphate buffer with a pH 7. The formed Schiff base was stabilized via overnight incubation in a $NaCNBH_3$ solution. The final step consisted of washing particles in phosphate buffer with a pH 7. Immobilized sphingolipid ceramide N-deacylase was stored in phosphate buffer with a pH 7 with 0.1% Triton X-100 at 4°C.

Under specific conditions, this enzyme also catalyzes the reverse reaction (Kita, et al., 2001). Thus, lysoderivates can be reacylated with a specific fatty acid. Using this procedure, we prepared several internal standards with C17:0 fatty acids, e.g. sulfatides, glucosylceramides, and GM1 gangliosides. In this process, we incubated 50 nmol of lyso-glycosphingolipid, 50 nmol of C17:0 fatty acid and immobilized sphingolipid ceramide N-deacylase in 300 µl of pH 7 phosphate buffer with 0.1% Triton X-100 for 20 hrs at 37°C while mixing it on a rotator. The magnetic particles were separated, and the supernatant was transferred and dried under a stream of nitrogen. The quality of the prepared lipids was monitored by HPTLC and tandem mass spectrometry.

2.8 Standardization of quantitative data in urine

The results of sphingolipid quantification in cellular material are often related to protein concentration, a well-established standardization parameter (Liebisch, et al., 1999). Urinary sphingolipids mostly originate from desquamated renal tubular cells. The standardizing parameter commonly used for urinary metabolites is creatinine, but creatinine does not reflect the cellular origin of sphingolipids. Therefore, in urinary samples with a creatinine level lower than 1 mM, the concentration of excreted sphingolipids is artificially inflated (Fig. 8A), which may encourage the incorrect diagnosis of some patients with lysosomal storage diseases (e.g., Fabry disease, prosaposin and saposin B deficiencies, and sulfatidoses). Regarding Fabry disease, this issue has already been pointed out (Forni, et al., 2009). In our experience, such diagnostic errors are especially likely to occur with newborns or children up to six years of age, whose normal concentration of creatinine is generally low (≤ 4 mM). Surprisingly, urinary volume has been found to be much more convenient for use as a standardization parameter (Fig. 8B). It is also possible to use the ratio of the analyzed compound to sphingomyelin (Berna, et al., 1999; Kuchar, et al., 2009) or phosphatidylcholine

(Fuller, et al., 2005; Whitfield, et al., 2001), which are membrane-bound lipids that can be measured simultaneously in the same sample.

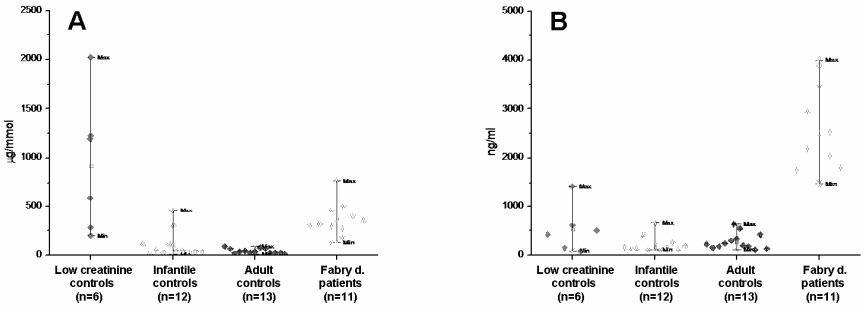

Fig. 8. Comparison of two methods of standardization of urinary Gb3Cer in three groups of samples: in controls with low creatinine (creatinine ≤1 mM), in controls with creatinine within a normal range (creatinine >1 mM-15 mM) and in Fabry patients. It is most critical to appropriately evaluate urine control samples with low creatinine concentrations, which are indistinguishable from samples from patients with Fabry disease (A). The use of urine volume as a standardization parameter makes it possible to differentiate more appropriately between controls and Fabry patients (B).

3. Sphingolipids in lysosomal storage disorders – mass spectrometric data useful for diagnosis and research

Flow injection analysis (FIA) combined with electrospray ionization tandem mass spectrometry makes it possible to determine the concentration of sphingolipids in various biological materials: e.g. urine, cultured fibroblasts and autoptic or bioptic tissue samples from different lysosomal storage disorders.
Examples of these analyses are presented in following paragraphs.

3.1 Sphingolipids in urine

Urine is a non-invasive diagnostic material that is of practical importance in diagnosing lysosomal disorders in which the storage of non-degraded substrate causes pathological processes in the kidneys. These disorders are characterized by the massive excretion of specific sphingolipids, e.g., Gb3Cer in Fabry disease (α-galactosidase A deficiency due to mutations of the *GLA* gene); multiple hydrophobic sphingolipids in complex sphingolipidoses, in which the defect is caused by mutations in the prosaposin gene (sphingolipids with a saccharide chain that is shorter than four monosaccharide units and ceramides are not degraded in prosaposin deficiency and Gb3Cer and sulfatides in saposin B deficiency due to defective activator proteins); sulfatides in metachromatic leukodystrophy (arylsulfatase A deficiency due to mutations of the *ARSA* gene) (Fuller, et al., 2005; Kuchar, et al., 2009; Whitfield, et al., 2001).
We developed a method of tandem mass spectrometry quantification of urinary sphingolipids that can be used in pre-diagnostic screening for the lysosomal disorders mentioned above (Kuchar, et al., 2009). Our data are presented in Table 3.

µg/l	sulfatide	CDH	Gb3Cer	CMH	Cer	SM
pSap-d 44-day-old	**756**	**507**	**2322**	**289**	**184**	1323
SapB-d 50-month-old	**2149**	**513**	**755**	**204**	101	1480
MLD late infantile (n= 6)	**3566 ±1855**	**397** ±220	261 ±188	**191** ±115	113 ±67	**3417 ±2448**
Fabry disease (male) (n=10)	88 ±17	**460 ±199**	**2615 ±915**	45 ±13	62 ±11	1602 ±1081
Controls infantile/juvenile (n=16)	155 ±48	113 ±37	152 ±68	52 ±23	45 ±12	1181 ±437

Table 3. Massive excretion of urinary sphingolipids in the case of saposin-B and prosaposin deficiencies and in patients with Fabry disease and metachromatic leukodystrophy. pSap-d - prosaposin deficiency, SapB-d - saposin B deficiency, MLD - metachromatic leukodystrophy; Cer - ceramide; CTH – ceramidetrihexoside; CDH – ceramidedihexoside, CMH – ceramidemonohexoside SM – sphingomyelin; Gb3Cer - globotriaosylceramide Values are in ng/µg of protein (mean±SD). Non-degraded sphingolipids related to particular lysosomal storage disorders are bolded.

Analyzing non-degraded metabolites can be very helpful in the pre-diagnosis of sphingolipid activator deficiencies in which routine enzymology fails to indicate deficient enzyme activity due to the detergents commonly used in the assays.
Urinary Gb3Cer has been suggested as biomarker for monitoring efficiency of enzyme replacement therapy of Fabry disease. Our tests in a group of Fabry male-patients showed however, that monitoring of this marker is not informative for all treated patients in general but for individual patients only (data not shown). Although excreted Gb3Cer is useful parameter for diagnosis, it is not reliable biomarker for clinical trials as also confirmed by another studies (Schiffmann, et al., 2010). Biological basis of urinary Gb3Cer and its isoforms is still subject of research.

3.2 Sphingolipids in cultured fibroblasts

Although cultured fibroblasts are not typical "storage cells," the concentration of non-degraded lipids increases significantly in some lysosomal storage disorders as documented in Table 4. Investigating sphingolipid profile can help in laboratory diagnosis of these rare diseases, especially among those suspected of having defective activators of lysosomal hydrolases.

3.3 Sphingolipids in tissues: Gb3Cer and lyso-Gb3Cer in Fabry myocardium and kidney

In some cases, a postmortem analysis of autoptic tissue has revealed metabolic defects. Here, we give two examples of tissue analysis that led to a final diagnosis confirmed by DNA analysis later on.

	Cer	CMH	CDH	Gb3Cer	SM
Prosaposin def.	**34,48**	**14,27**	**25,75**	**27,06**	45,70
saposin B def.	6,87	1,44	1,86	**21,36**	107,33
Fabry disease	3,76	1,89	2,10	**35,68**	42,62
Nieman-Pick A	4,15	1,67	5,63	0,51	**195,17**
Control 1	6,21	3,25	5,17	0,52	68,28
Control 2	1,18	2,67	1,37	5,17	21,04

Table 4. Increased concentration of sphingolipids in cultured skin fibroblasts in patients with sphingolipid activator deficiencies (saposin-B and prosaposin deficiencies) and in patients with defective enzyme proteins (in Fabry disease and metachromatic leukodystrophy). Values are in ng/μg of protein. Cer - ceramide; CDH – ceramidedihexoside, CMH – ceramidemonohexoside; SM – sphingomyelin; Gb3Cer - globotriaosylceramide. Non-degraded sphingolipids corresponding to particular lysosomal storage disorders are bolded.

The first example shows the accumulation of Gb3Cer in the kidneys of patients with Fabry disease and in cases of prosaposin deficiency (Tab. 5).

	Cer	CMH	CDH	Gb3Cer	sulfatide	SM
Fabry disease	0,5	1,0	3,7	**115,2**	0,5	24,0
Prosaposin def.	**39,1**	**23,9**	**49,8**	**57,6**	**39,6**	125,8
Control (n=3)	11,2	0,7	3,2	10,2	1,1	57,9

Table 5. Concentration of sphingolipids in the kidneys of Fabry male patient and in a case of prosaposin deficiency. Values are in ng/μg of protein, Control is represented by the mean value. Cer - ceramide; CDH – ceramidedihexoside, CMH – ceramidemonohexoside, SM – shingomyelin; Gb3Cer - globotriaosylceramide. Non-degraded sphingolipids related to particular lysosomal storage disorders are bolded.

Another example demonstrates the storage of Gb3Cer and lyso-Gb3Cer (globotriaosylsphingosine) in the myocardium of Fabry patient (Fig. 9). It is possible that the role of these derivates has been underrated (Dekker, et al., 2011). The role of lyso-Gb3Cer as a molecule that stimulates smooth muscle cell proliferation is now known. These findings indicate the possible role of lyso-Gb3Cer as a signal molecule (Aerts, et al., 2008).

4. The investigation of sphingolipid degradation pathways

4.1 Loading experiments on living cells using lipid substrates labeled with a stable isotope or containing atypical fatty acids

Loading experiments in cell cultures (also called feeding experiments) are frequently used to investigate the metabolic fate of exogenous compounds in living model systems. The main advantage of such experiments is that they assess the entire degradation system, including any nonenzymatic cofactors.

This method can be used to conduct a general analysis of metabolic pathways (Schwarzmann, et al., 1983; Sonderfeld, et al., 1985), intracellular transport or a distribution (Martin & Pagano, 1994) assessment of residual activity in enzyme-deficient cells

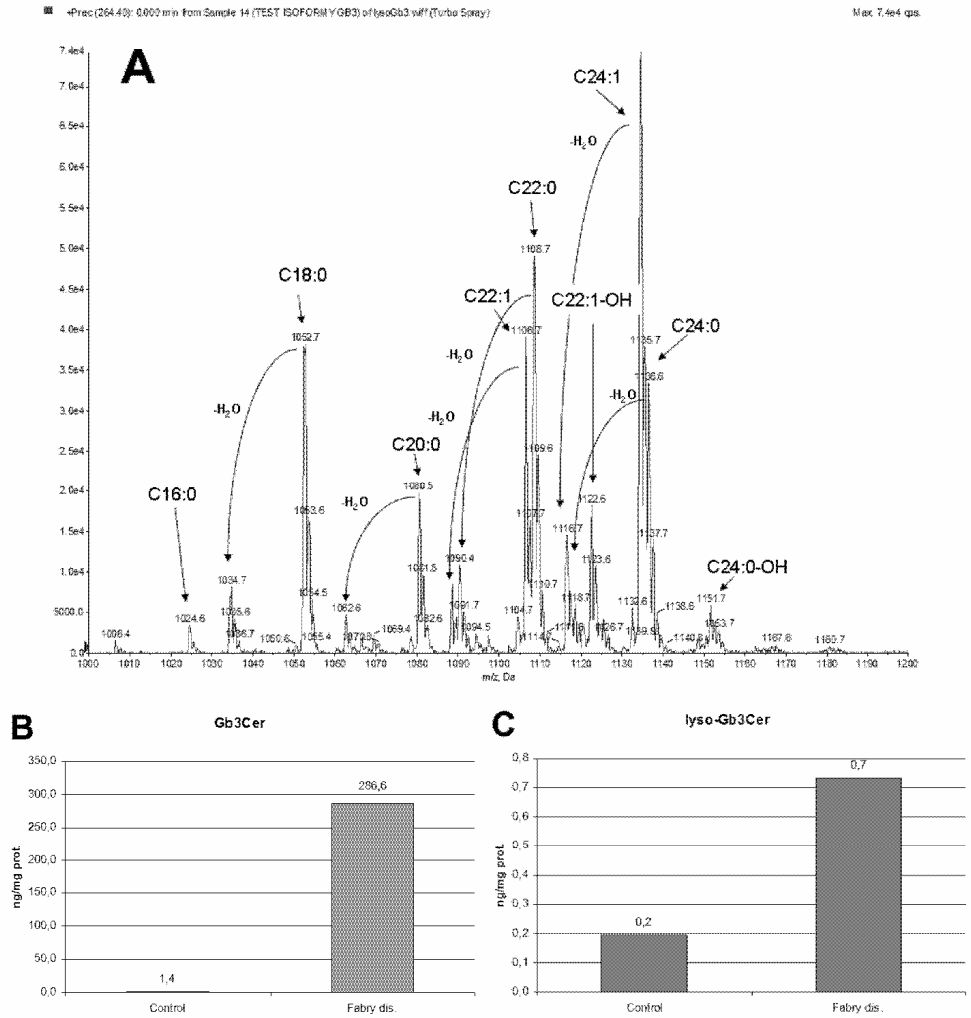

Fig. 9. Gb3Cer and lyso-Gb3Cer (globotriaosylsphingosine) in the myocardium of Fabry patient. A) Precursor ion spectrum of Gb3Cer molecular species in control myocardium. The spectrum was measured by a 1 min scan of a 3 mg protein aliquot of lipid extract dissolved in methanol with 5 mM ammonium formiate. The increased concentration of B) Gb3Cer and C) lyso-Gb3Cer is visible in the autoptic myocardium of Fabry patient in comparison to that of an age-matched control. Quantity was measured by flow injection analysis electrospray ionization tandem mass spectrometry using an multiple reaction monitoring scan. C17:0 Gb3Cer was used as the internal standard for lyso-Gb3Cer quantification similarly as described in (Mills, et al., 2005). Concentrations were measured by method with coefficient of variation - CV <7%.

(Leinekugel, et al., 1992; Porter, et al., 1971). The method can also be used to diagnose storage disorders.

This technique has been used to distinguish between metachromatic leukodystrophy and arylsulfatase A pseudodeficiency (Kihara, et al., 1980) and to identify deficiencies in nonenzymatic protein cofactors of lysosomal glycolipid catabolism (sphingolipid activator proteins) (Klein, et al., 1994; Schepers, et al., 1996; Schmid, et al., 1992; Sonderfeld, et al., 1985; Wrobe, et al., 2000), including prosaposin deficiency (Harzer, et al., 1989; Chatelut, et al., 1997).

In these experiments, the degradation products of labeled exogenous lipid substrates are determined using specific analytical methods. Traditionally, sphingolipids are labeled with radioisotopes, and their degradation products are separated chromatographically and traced using radioactivity assays. Recently, radiolabeled sphingolipids are often replaced by non-radioactive analogues with atypical molecular masses that can be analyzed by tandem mass analysis.

Sphingolipids can be labeled on different parts of the molecule using non-natural fatty acids, creating molecules with atypical m/z values. However, only a few labeled standards are commercially available. Sphingoids can also be deuterium labeled at the double bond to increase mass, but the fragmentation patterns will be altered (see Fragmentation, Fig. 6).

We compared the radioisotope and mass labeling methods in loading experiments involving fibroblast cultures from patients with inherited lysosomal storage diseases such as GM1 gangliosidosis. In this study, genetic variants of the *GLB1* (ß-galactosidase; ß-gal) gene were selected. Both approaches, the use of [^{3}H]GM1 ganglioside and the use of its C18:0-D_3 analogue, clearly showed that the impaired degradation of critical glycosphingolipids resulted from defects in β-gal function, as indicated in Fig. 10.

The experiments conducted with stable isotope-labeled substrates and tandem mass spectrometry facilitated a more accurate quantification analysis of the lipids, and the results were better correlated with the clinical and biochemical phenotypes of the samples. The procedure used to prepare the cellular lipids for tandem mass spectrometry analysis was simple and relatively rapid; unlike radioisotope assays, it did not require separation during the pre-analytical phase (Asfaw, et al., 2002; 1998). However, experiments with radiolabeled glycolipid substrates indicate the entire metabolic pattern (Fig 10A) and can thus make it possible to identify relevant metabolites to be further analyzed via tandem mass spectrometry.

Results similar to those obtained in analyzing the GM1 gangliosidosis were obtained by loading experiments using Gaucher fibroblasts and fibroblasts from patients with prosaposin deficiencies (data not shown).

4.2 Tandem mass determination of *in vitro* acid glycosidase activity

Enzymology, in combination with tandem mass spectrometry, is useful in lysosomal storage disorders screening and in evaluations of enzyme activity (Kasper, et al., 2010; Li, et al., 2004; Spacil, et al., 2011; Turecek, et al., 2007). One practical application of this technique is the analysis of lysosomal β-glucocerebrosidase activity using glucosylceramide with C12:0 fatty acid as the enzyme substrate. Tandem mass spectrometry evaluation techniques can be used with cells and tissue homogenates but also with dried blood spots as the screening material.

We followed Turecek´s method (Turecek, et al., 2007) in measuring lysosomal β-glucocerebrosidase activity in homogenates of cultured skin fibroblasts. The reaction

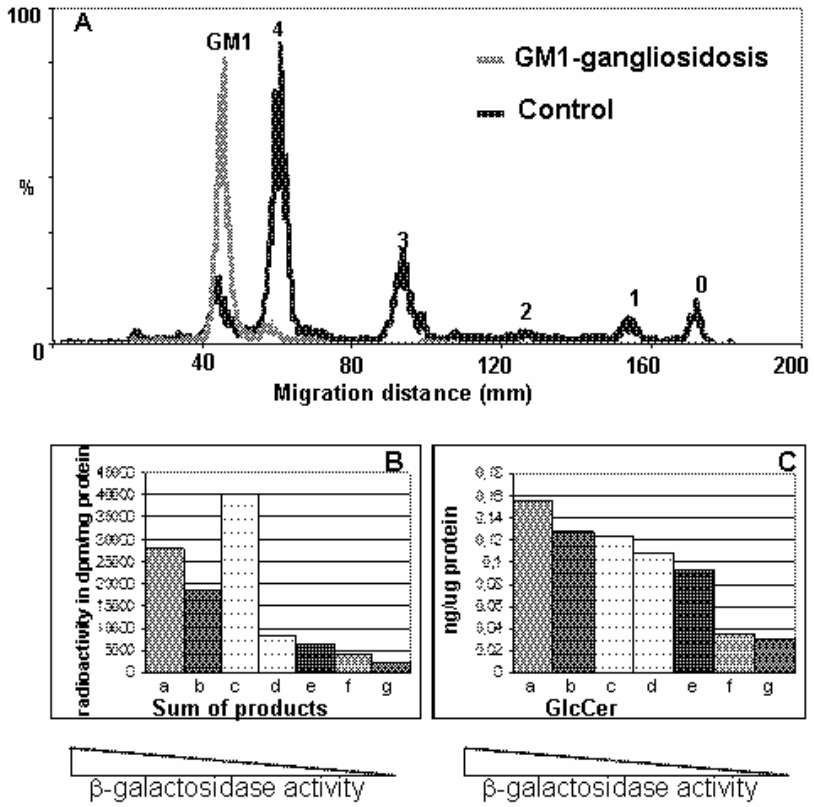

Fig. 10. In situ degradation of GM1 ganglioside by skin fibroblasts from control and β-galactosidase deficient patients. Tritium-labeled glycolipid GM1 ganglioside or a C18:0-D_3 analogue was added to the culture of skin fibroblasts in 25 cm^2 flasks. After 5 days, cells were harvested and lipids extracted. The radio-labeled lipid extracts were separated via TLC and analyzed using a linear scanner (Asfaw, et al., 1998), whereas the GM1 ganglioside with C18:0-D3 fatty acid and its degradation products were extracted and directly analyzed directly in tandem mass spectrometry (details in Materials and Methods). **A:** Degradation pattern of [^{3}H]GM1 ganglioside in control and β-galactosidase-deficient cells. The chromatographic positions of the products are indicated by the number of sugar residues on the glycolipid, which range from 0 (ceramide) to 4 (tetrahexosylceramide). **B:** Quantification of degradation products of [^{3}H]GM1 ganglioside (sum of all products on the TLC plate) in skin fibroblasts from the control and the different β-galactosidase-deficient genetic variants. The cell lines are arranged according to clinical phenotypes of GM1 gangliosidosis: a-control, b-adult GM1 gangliosidosis, c-Morquio B, d-adult GM1 gangliosidosis /Morquio B, e-juvenile GM1 gangliosidosis, f-infantile GM1 gangliosidosis, and g-infantile GM1 gangliosidosis. **C:** Quantification of GlcCer product formed from stable isotope-labeled GM1 ganglioside (C18:0-D_3) in the same cell lines as the radioactive analogue (B). Values are average of two samples.

mixture contained 0.5 µg of sample protein and 0.05% inactivated bovine serum albumin (BSA) to stabilize the enzyme. The mass spectrometry settings were optimized to prevent the artificial conversion of the substrate into the enzyme reaction product. An example of this analysis is presented in Figure 11.

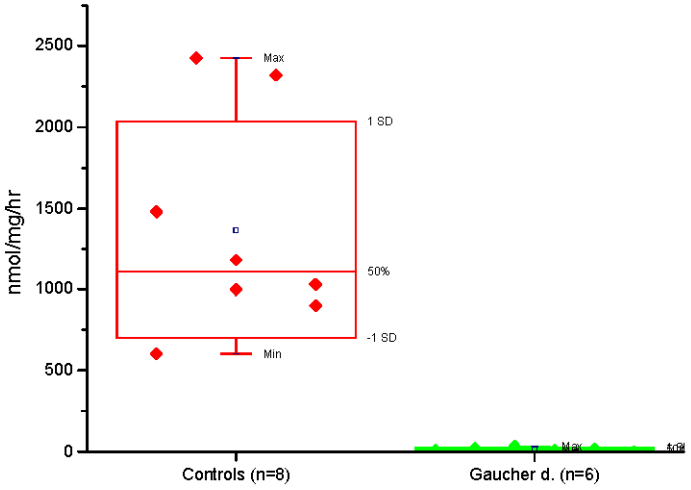

Fig. 11. Activity of lysosomal acid β-glucocerebrosidase in Gaucher and control fibroblasts as measured with natural substrate C12:0 glucosylceramide. The reaction product was analyzed by flow injection analysis electrospray ionization tandem mass spectrometry using a multiple reaction monitoring.

Nowadays, procedures are simplified by skipping laborious process of extraction of reaction mixture after incubation. Instead, HPLC is combined with mass spectrometry. The HPLC step purifies the sample, removing any potential interfering compounds (Kasper, et al., 2010; Spacil, et al., 2011).

5. Sphingolipid isoform profiling – a useful metabolomic approach to disorders involving Gb3Cer and sulfatide storage

Tandem mass spectrometry has advantages over HPLC and other analytical methods in helping to determine the individual molecular species (isoforms) of sphingolipids. Changes in isoform profiles may provide diagnostically important information and indicate specific pathological processes (Fauler, et al., 2005; Paschke, et al., 2011). For example, an analysis of urinary lipid extracts in a case of metachromatic leukodystrophy showed significant differences in sulfatide isoform profiles; such differences were also evident in cases of prosaposin and saposin B deficiency, two other sulfatide storage disorders. We also found changed patterns of globotriaosylceramide species in the urine of Fabry patients and patients with prosaposin gene defects. A shift in the isoform pattern to species with longer chain fatty acids was characteristic of both prosaposin and saposin B deficiencies.
The results presented in Table 6 were evaluated by determining the ratio of the various isoforms to the C18:0 isoform, which is invariable in the profile. The major advantages of

this procedure include simple sample preparation without internal standard and a simple data collection process; only a small number of transitions must be measured. The elevation of certain molecular species, particularly those with longer, hydroxylated chains (in the case of the sulfatides), is clearly demonstrated.

A

	Control	n=29	SapB-d	pSap-d	Fabry	n=11
Isoform	Min	Max			Min	Max
16:0	0,64	2,91	2,33	2,14	1,59	5,52
18:0	1,00	1,00	1,00	1,00	1,00	1,00
18:0-OH	0,42	2,23	0,32	0,09	0,03	0,15
20:0	0,46	2,09	1,98	1,69	1,33	2,96
22:0	**0,25**	**3,37**	**6,63**	**5,06**	**4,02**	**7,02**
22:1	0,43	3,71	0,66	0,42	0,34	0,87
22:0-OH	0,18	2,40	0,83	0,37	0,14	0,40
22:1-OH	0,17	5,44	1,10	0,27	0,39	0,56
24:0	**0,00**	**3,23**	**8,33**	**10,50**	**5,56**	**9,52**
24:1	**0,27**	**2,75**	**4,93**	**9,97**	**4,56**	**8,45**
24:2	0,27	4,88	0,65	0,53	0,36	0,88
24:0-OH	0,00	2,02	1,16	0,90	0,53	1,14
24:1-OH	0,47	2,67	0,46	0,33	0,17	0,39
24:2-OH	1,02	10,58	0,27	0,11	0,06	0,21
26:0	0,00	2,16	0,23	0,16	0,08	0,16
26:1	0,23	1,96	0,31	0,24	0,09	0,24
26:2	0,00	2,01	0,13	0,05	0,03	0,11
26:0-OH	0,14	2,36	0,22	0,04	0,02	0,13
26:1-OH	0,00	2,12	0,16	0,02	0,02	0,06
26:2-OH	0,58	8,34	0,10	0,04	0,02	0,10

B

	Control	n=29	SapB-d	pSap-d	MLD	n=15
Isoform	Min	Max			Min	Max
C16:0	0,86	3,92	2,86	3,79	1,92	4,57
C18:0	1,00	1,00	1,00	1,00	1,00	1,00
C18:0-OH	0,58	2,04	0,95	0,62	0,79	1,82
C20:0	0,19	0,80	1,64	1,19	0,67	2,06
C20:0-OH	0,31	1,94	1,30	0,67	1,00	3,20
C22:0	0,34	1,68	7,18	4,25	2,65	12,11
C22:1-OH	0,35	1,42	2,06	0,56	1,56	5,35
C22:0-OH	0,30	1,64	5,21	2,28	2,85	14,29
C24:1	0,48	1,98	2,59	2,65	1,02	5,21
C24:0	0,45	2,23	5,22	4,24	2,27	13,28
C23:0-OH	0,26	1,55	2,86	1,02	2,06	9,45
C24:1-OH	0,21	0,77	4,18	1,53	2,33	12,58
C24:0-OH	0,31	1,81	7,49	3,73	4,59	20,68
C26:1	0,32	1,84	0,23	0,23	0,18	0,59
C26:0	0,11	0,71	0,55	0,28	0,43	1,31
C26:1-OH	0,09	1,34	0,24	0,17	0,17	0,70
C26:0-OH	0,09	0,62	0,30	0,19	0,15	0,65

Table 6. Changed signal ratios of Gb3Cer isoforms (A) and sulfatide isoforms (B) (to the C18:0 species) in the urine of patients with lysosomal storage disorders. The C18:0 species were selected as the standard invariable parameter in the isoform pattern. Changes in the levels of specific isoforms in patients with lysosomal storage disorders are highlighted. SapB-d – saposin B deficiency; pSap-d – prosaposin deficiency; Fabry – Fabry disease; MLD - metachromatic leukodystrophy.

6. Conclusions

In this chapter, we have introduced a methods of complex sphingolipid analysis, covering sample preparation and final tandem mass spectrometry analysis for various biological materials. This approach has been used in various studies of lysosomal storage disorders and examples showing a range of applications are presented.

Findings in urine are very important in the pre-diagnosis of lysosomal storage disorders and especially in identifying defects in the protein activators of sphingolipid hydrolases. We have also drawn attention to the problems with evaluating urinary sphingolipids using creatinine and have thereby suggested a more reliable approach to standardize sphingolipid excretion.

The tandem mass analysis of sphingolipids in cells and tissues is useful in diagnosing unresolved cases (examples shown in this chapter). This method can also contribute

important information to lipidomic studies of the cellular function of these molecules and their bioactive derivatives.
The use of tandem mass spectrometry in loading experiments using labeled sphingolipids can increase quantification accuracy and throughput while eliminating working risk and restrictions by eliminating the need for radioactive analysis. Although tandem mass spectrometry cannot yet fully replace radioisotope methods, using this technique can improve the precision and specificity of the results of metabolic experiments.
The demand for useful screening methods for lysosomal storage disorders has led to the use of tandem mass spectrometry in enzymology. Analyses of enzyme activity using mass spectrometry performed on dried blood spots are highly sensitive and specific, and dried samples are easy to transport. Some methods use natural substrates, which is helpful in research studies of enzyme function and characteristics.
The aforementioned advantage of tandem mass spectrometry is the ability to analyze individual sphingolipid molecules (isoforms). Evaluation of isoform profiles can have diagnostic value in disorders involving storage of Gb3Cer or sulfatides. Metabolomic principles have a tremendous number of research applications, especially in the investigation of various cellular events.
In conclusion, tandem mass spectrometry is robust and sensitive analytical procedure that is still evolving. The method is efficient for determining the composition of endogenous sphingolipid classes in various biological materials and following their metabolic fate. Its ability to establish the metabolomic profiles of sphingolipids under normal and abnormal conditions contributes to a better understanding of the biological significance of sphingolipid molecules.

7. Acknowledgment

This work was supported by the grant project from the Ministry of Education of the Czech Republic MSM 0021620806, the grant No 19509 from the Grant Agency of the Charles University in Prague, the Grant SVV262502 from the Charles University in Prague, Czech Republic and by the grant project from the Ministry of Health of the Czech Republic MZOVFN2005

8. References

Aerts, J. M., Groener, J. E., Kuiper, S., Donker-Koopman, W. E., Strijland, A., Ottenhoff, R., van Roomen, C., Mirzaian, M., Wijburg, F. A., Linthorst, G. E., Vedder, A. C., Rombach, S. M., Cox-Brinkman, J., Somerharju, P., Boot, R. G., Hollak, C. E., Brady, R. O. & Poorthuis, B. J. (2008). Elevated globotriaosylsphingosine is a hallmark of Fabry disease. *Proc Natl Acad Sci U S A,* Vol. 105, No. 8, (Feb 26), pp. (2812-2817), 1091-6490 (Electronic)

Asfaw, B., Ledvinova, J., Dobrovolny, R., Bakker, H. D., Desnick, R. J., van Diggelen, O. P., de Jong, J. G., Kanzaki, T., Chabas, A., Maire, I., Conzelmann, E. & Schindler, D. (2002). Defects in degradation of blood group A and B glycosphingolipids in Schindler and Fabry diseases. *J Lipid Res,* Vol. 43, No. 7, (Jul), pp. (1096-1104), 0022-2275 (Print)

Asfaw, B., Schindler, D., Ledvinova, J., Cerny, B., Smid, F. & Conzelmann, E. (1998). Degradation of blood group A glycolipid A-6-2 by normal and mutant human skin fibroblasts. *J Lipid Res,* Vol. 39, No. 9, (Sep), pp. (1768-1780), 0022-2275 (Print)

Berna, L., Asfaw, B., Conzelmann, E., Cerny, B. & Ledvinova, J. (1999). Determination of urinary sulfatides and other lipids by combination of reversed-phase and thin-layer chromatographies. *Anal Biochem*, Vol. 269, No. 2, (May 1), pp. (304-311), 0003-2697 (Print)

Bilkova, Z., Castagna, A., Zanusso, G., Farinazzo, A., Monaco, S., Damoc, E., Przybylski, M., Benes, M., Lenfeld, J., Viovy, J. L. & Righetti, P. G. (2005). Immunoaffinity reactors for prion protein qualitative analysis. *Proteomics*, Vol. 5, No. 3, (Feb), pp. (639-647), 1615-9853 (Print)

Bligh, E. G. & Dyer, W. J. (1959). A rapid method of total lipid extraction and purification. *Can J Biochem Physiol*, Vol. 37, No. 8, (Aug), pp. (911-917),

Boscaro, F., Pieraccini, G., la Marca, G., Bartolucci, G., Luceri, C., Luceri, F. & Moneti, G. (2002). Rapid quantitation of globotriaosylceramide in human plasma and urine: a potential application for monitoring enzyme replacement therapy in Anderson-Fabry disease. *Rapid Commun Mass Spectrom*, Vol. 16, No. 16, pp. (1507-1514), 0951-4198 (Print)

Cech, N. B. & Enke, C. G. (2001). Practical implications of some recent studies in electrospray ionization fundamentals. *Mass Spectrom Rev*, Vol. 20, No. 6, (Nov-Dec), pp. (362-387), 0277-7037 (Print)

Cole, R. B. (Ed(s).). (2010) *Electrospray and MALDI Mass Spectrometry, Fundamentals, Instrumetation, Practicalities, and Biological Applications*, John Wiley & Sons, Inc., 978-0-471-74107-7, New Jersey

de Hoffman, E. & Stroobant, V. (2002) *Mass Spectrometry, Principles and Applications* (Second), John Wiley and Sons, Ltd, 0-471-48566-7, Chichester

Dekker, N., van Dussen, L., Hollak, C. E., Overkleeft, H., Scheij, S., Ghauharali, K., van Breemen, M. J., Ferraz, M. J., Groener, J. E., Maas, M., Wijburg, F. A., Speijer, D., Tylki-Szymanska, A., Mistry, P. K., Boot, R. G. & Aerts, J. M. (2011). Elevated plasma glucosylsphingosine in Gaucher disease: relation to phenotype, storage cell markers, and therapeutic response. *Blood*, Vol. No. (Aug 25), pp. 1528-0020 (Electronic)

Desnick, R. J., Ioannou, Y. A. & Eng, C. M. (2001). α-Galactosidase A Deficiency: Fabry Disease, In: *The Metabolic and Molecular Bases of Inherited Disease*, Scriver, C. R., Beaudet, A. L., Sly, W. S.&Valle, D., pp. (3733-3774), McGraw-Hill, 0-07-136321-1, New York

Desnick, R. J., Sweeley, C. C. & Krivit, W. (1970). A method for the quantitative determination of neutral glycosphingolipids in urine sediment. *J Lipid Res*, Vol. 11, No. 1, (Jan), pp. (31-37), 0022-2275 (Print)

Domon, B. & Costello, C. E. (1988). Structure elucidation of glycosphingolipids and gangliosides using high-performance tandem mass spectrometry. *Biochemistry*, Vol. 27, No. 5, (Mar 8), pp. (1534-1543), 0006-2960 (Print)

Douglas, D. J. (2009). Linear quadrupoles in mass spectrometry. *Mass Spectrom Rev*, Vol. 28, No. 6, (Nov-Dec), pp. (937-960), 1098-2787 (Electronic)

Dulcks, T. & Juraschek, R. (1999). Electrospray as an ionisation method for mass spectrometry. *Journal of Aerosol Science*, Vol. 30, No. 7, (AUG), pp. (927-943),

Fauler, G., Rechberger, G. N., Devrnja, D., Erwa, W., Plecko, B., Kotanko, P., Breunig, F. & Paschke, E. (2005). Rapid determination of urinary globotriaosylceramide isoform profiles by electrospray ionization mass spectrometry using stearoyl-d35-globotriaosylceramide as internal standard. *Rapid Commun Mass Spectrom*, Vol. 19, No. 11, pp. (1499-1506), 0951-4198 (Print)

Folch, J., Lees, M. & Sloane Stanley, G. H. (1957). A simple method for the isolation and purification of total lipides from animal tissues. *J Biol Chem*, Vol. 226, No. 1, (May), pp. (497-509), 0021-9258 (Print)

Forni, S., Fu, X., Schiffmann, R. & Sweetman, L. (2009). Falsely elevated urinary Gb3 (globotriaosylceramide, CTH, GL3). *Mol Genet Metab*, Vol. 97, No. 1, (May), pp. (91), 1096-7206 (Electronic)

Fuller, M., Sharp, P. C., Rozaklis, T., Whitfield, P. D., Blacklock, D., Hopwood, J. J. & Meikle, P. J. (2005). Urinary lipid profiling for the identification of fabry hemizygotes and heterozygotes. *Clin Chem*, Vol. 51, No. 4, (Apr), pp. (688-694), 0009-9147 (Print)

Goldschmidt-Arzi, M., Shimoni, E., Sabanay, H., Futerman, A. H. & Addadi, L. (2011). Intracellular localization of organized lipid domains of C16-ceramide/cholesterol. *J Struct Biol*, Vol. 175, No. 1, (Jul), pp. (21-30), 1095-8657 (Electronic)

Gu, M., Kerwin, J. L., Watts, J. D. & Aebersold, R. (1997). Ceramide profiling of complex lipid mixtures by electrospray ionization mass spectrometry. *Anal Biochem*, Vol. 244, No. 2, (Jan 15), pp. (347-356), 0003-2697 (Print)

Han, X. & Gross, R. W. (2005). Shotgun lipidomics: electrospray ionization mass spectrometric analysis and quantitation of cellular lipidomes directly from crude extracts of biological samples. *Mass Spectrom Rev*, Vol. 24, No. 3, (May-Jun), pp. (367-412), 0277-7037 (Print)

Hartree, E. F. (1972). Determination of protein: a modification of the Lowry method that gives a linear photometric response. *Anal Biochem*, Vol. 48, No. 2, (Aug), pp. (422-427), 0003-2697 (Print)

Harzer, K., Paton, B. C., Poulos, A., Kustermannkuhn, B., Roggendorf, W., Grisar, T. & Popp, M. (1989). Sphingolipid Activator Protein-Deficiency in a 16-Week-Old Atypical Gaucher Disease Patient and His Fetal Sibling - Biochemical Signs of Combined Sphingolipidoses. *Eur J Pediatr*, Vol. 149, No. 1, (Oct), pp. (31-39), 0340-6199

Haynes, C. A., Allegood, J. C., Park, H. & Sullards, M. C. (2009). Sphingolipidomics: methods for the comprehensive analysis of sphingolipids. *J Chromatogr B Analyt Technol Biomed Life Sci*, Vol. 877, No. 26, (Sep 15), pp. (2696-2708), 1873-376X (Electronic)

Heitmann, D., Lissel, M., Kempken, R. & Muthing, J. (1996). Replacement of chloroform throughout glycosphingolipid isolation. *Biomed Chromatogr*, Vol. 10, No. 5, (Sep-Oct), pp. (245-250), 0269-3879 (Print)

Helms, J. B. & Zurzolo, C. (2004). Lipids as targeting signals: lipid rafts and intracellular trafficking. *Traffic*, Vol. 5, No. 4, (Apr), pp. (247-254), 1398-9219 (Print)

Hirabayashi, Y., Igarashi, Y. & Merrill, A. H., Jr. (2006). Sphingolipids Synthesis, Transport and Cellular Signaling, In: *Sphingolipid Biology*, Hirabayashi, Y., Igarashi, Y.&Merrill, A. H., Jr., pp. (3-22), Springer-Verlag, 4-431-34198-6, Tokyo

Holleran, W. M., Takagi, Y. & Uchida, Y. (2006). Epidermal sphingolipids: metabolism, function, and roles in skin disorders. *FEBS Lett*, Vol. 580, No. 23, (Oct 9), pp. (5456-5466), 0014-5793 (Print)

Holthuis, J. C., van Meer, G. & Huitema, K. (2003). Lipid microdomains, lipid translocation and the organization of intracellular membrane transport (Review). *Mol Membr Biol*, Vol. 20, No. 3, (Jul-Sep), pp. (231-241), 0968-7688 (Print)

Hsu, F. F., Bohrer, A. & Turk, J. (1998). Electrospray ionization tandem mass spectrometric analysis of sulfatide. Determination of fragmentation patterns and characterization of molecular species expressed in brain and in pancreatic islets. *Biochim Biophys Acta*, Vol. 1392, No. 2-3, (Jun 15), pp. (202-216), 0006-3002 (Print)

Hsu, F. F. & Turk, J. (2000). Structural determination of sphingomyelin by tandem mass spectrometry with electrospray ionization. *J Am Soc Mass Spectrom*, Vol. 11, No. 5, (May), pp. (437-449), 1044-0305 (Print)

Chatelut, M., Harzer, K., Christomanou, H., Feunteun, J., Pieraggi, M. T., Paton, B. C., Kishimoto, Y., O'Brien, J. S., Basile, J. P., Thiers, J. C., Salvayre, R. & Levade, T. (1997). Model SV40-transformed fibroblast lines for metabolic studies of human prosaposin and acid ceramidase deficiencies. *Clin Chim Acta*, Vol. 262, No. 1-2, (Jun 27), pp. (61-76), 0009-8981 (Print)

Ii, T., Ohashi, Y. & Nagai, Y. (1995). Structural elucidation of underivatized gangliosides by electrospray-ionization tandem mass spectrometry (ESIMS/MS). *Carbohydr Res*, Vol. 273, No. 1, (Aug 22), pp. (27-40), 0008-6215 (Print)

Infante, R. E., Wang, M. L., Radhakrishnan, A., Kwon, H. J., Brown, M. S. & Goldstein, J. L. (2008). NPC2 facilitates bidirectional transfer of cholesterol between NPC1 and lipid bilayers, a step in cholesterol egress from lysosomes. *Proc Natl Acad Sci U S A*, Vol. 105, No. 40, (Oct 7), pp. (15287-15292), 1091-6490 (Electronic)

Kasper, D. C., Herman, J., De Jesus, V. R., Mechtler, T. P., Metz, T. F. & Shushan, B. (2010). The application of multiplexed, multi-dimensional ultra-high-performance liquid chromatography/tandem mass spectrometry to the high-throughput screening of lysosomal storage disorders in newborn dried bloodspots. *Rapid Commun Mass Spectrom*, Vol. 24, No. 7, (Apr 15), pp. (986-994), 1097-0231 (Electronic)

Kaushik, S., Massey, A. C. & Cuervo, A. M. (2006). Lysosome membrane lipid microdomains: novel regulators of chaperone-mediated autophagy. *EMBO J*, Vol. 25, No. 17, (Sep 6), pp. (3921-3933), 0261-4189 (Print)

Kebarle, P. (2000). A brief overview of the present status of the mechanisms involved in electrospray mass spectrometry. *J Mass Spectrom*, Vol. 35, No. 7, (Jul), pp. (804-817), 1076-5174 (Print)

Kerwin, J. L., Tuininga, A. R. & Ericsson, L. H. (1994). Identification of molecular species of glycerophospholipids and sphingomyelin using electrospray mass spectrometry. *J Lipid Res*, Vol. 35, No. 6, (Jun), pp. (1102-1114), 0022-2275 (Print)

Kihara, H., Ho, C. K., Fluharty, A. L., Tsay, K. K. & Hartlage, P. L. (1980). Prenatal diagnosis of metachromatic leukodystrophy in a family with pseudo arylsulfatase A deficiency by the cerebroside sulfate loading test. *Pediatr Res*, Vol. 14, No. 3, (Mar), pp. (224-227), 0031-3998 (Print)

Kita, K., Kurita, T. & Ito, M. (2001). Characterization of the reversible nature of the reaction catalyzed by sphingolipid ceramide N-deacylase. A novel form of reverse hydrolysis reaction. *Eur J Biochem*, Vol. 268, No. 3, (Feb), pp. (592-602), 0014-2956 (Print)

Kitagawa, T., Ishige, N., Suzuki, K., Owada, M., Ohashi, T., Kobayashi, M., Eto, Y., Tanaka, A., Mills, K., Winchester, B. & Keutzer, J. (2005). Non-invasive screening method for Fabry disease by measuring globotriaosylceramide in whole urine samples using tandem mass spectrometry. *Mol Genet Metab*, Vol. 85, No. 3, (Jul), pp. (196-202), 1096-7192 (Print)

Kitatani, K., Idkowiak-Baldys, J. & Hannun, Y. A. (2008). The sphingolipid salvage pathway in ceramide metabolism and signaling. *Cell Signal*, Vol. 20, No. 6, (Jun), pp. (1010-1018), 0898-6568 (Print)

Klein, A., Henseler, M., Klein, C., Suzuki, K., Harzer, K. & Sandhoff, K. (1994). Sphingolipid activator protein D (sap-D) stimulates the lysosomal degradation of ceramide in vivo. *Biochem Biophys Res Commun*, Vol. 200, No. 3, (May 16), pp. (1440-1448), 0006-291X (Print)

Kolter, T. & Sandhoff, K. (2010). Lysosomal degradation of membrane lipids. *FEBS Lett*, Vol. 584, No. 9, (May 3), pp. (1700-1712), 1873-3468 (Electronic)

Korecka, L., Jezova, J., Bilkova, Z., Benes, M., Horak, D., Hradcova, O., Slovakova, M. & Viovy, J. L. (2005). Magnetic enzyme reactors for isolation and study of heterogeneous glycoproteins. *Journal of Magnetism and Magnetic Materials*, Vol. 293, No. 1, (May 1), pp. (349-357), 0304-8853

Kuchar, L., Ledvinova, J., Hrebicek, M., Myskova, H., Dvorakova, L., Berna, L., Chrastina, P., Asfaw, B., Elleder, M., Petermoller, M., Mayrhofer, H., Staudt, M., Krageloh-Mann, I., Paton, B. C. & Harzer, K. (2009). Prosaposin deficiency and saposin B deficiency (activator-deficient metachromatic leukodystrophy): report on two patients detected by analysis of urinary sphingolipids and carrying novel PSAP gene mutations. *Am J Med Genet A*, Vol. 149A, No. 4, (Feb 15), pp. (613-621), 1552-4833 (Electronic)

Kuchar, L., Rotkova, J., Asfaw, B., Lenfeld, J., Horak, D., Korecka, L., Bilkova, Z. & Ledvinova, J. (2010). Semisynthesis of C17:0 isoforms of sulphatide and glucosylceramide using immobilised sphingolipid ceramide N-deacylase for application in analytical mass spectrometry. *Rapid Commun Mass Spectrom*, Vol. 24, No. 16, (Aug 30), pp. (2393-2399), 1097-0231 (Electronic)

Kwon, H. J., Abi-Mosleh, L., Wang, M. L., Deisenhofer, J., Goldstein, J. L., Brown, M. S. & Infante, R. E. (2009). Structure of N-terminal domain of NPC1 reveals distinct subdomains for binding and transfer of cholesterol. *Cell*, Vol. 137, No. 7, (Jun 26), pp. (1213-1224), 1097-4172 (Electronic)

Ledeen, R. & Wu, G. (2011). New findings on nuclear gangliosides: overview on metabolism and function. *J Neurochem*, Vol. 116, No. 5, (Mar), pp. (714-720), 1471-4159 (Electronic)

Ledeen, R. W. & Wu, G. (2008). Nuclear sphingolipids: metabolism and signaling. *J Lipid Res*, Vol. 49, No. 6, (Jun), pp. (1176-1186), 0022-2275 (Print)

Leinekugel, P., Michel, S., Conzelmann, E. & Sandhoff, K. (1992). Quantitative correlation between the residual activity of beta-hexosaminidase A and arylsulfatase A and the severity of the resulting lysosomal storage disease. *Hum Genet,* Vol. 88, No. 5, (Mar), pp. (513-523), 0340-6717 (Print)

Li, Y., Scott, C. R., Chamoles, N. A., Ghavami, A., Pinto, B. M., Turecek, F. & Gelb, M. H. (2004). Direct multiplex assay of lysosomal enzymes in dried blood spots for newborn screening. *Clin Chem,* Vol. 50, No. 10, (Oct), pp. (1785-1796), 0009-9147 (Print)

Liebisch, G., Drobnik, W., Reil, M., Trumbach, B., Arnecke, R., Olgemoller, B., Roscher, A. & Schmitz, G. (1999). Quantitative measurement of different ceramide species from crude cellular extracts by electrospray ionization tandem mass spectrometry (ESI-MS/MS). *J Lipid Res,* Vol. 40, No. 8, (Aug), pp. (1539-1546),

Lieser, B., Liebisch, G., Drobnik, W. & Schmitz, G. (2003). Quantification of sphingosine and sphinganine from crude lipid extracts by HPLC electrospray ionization tandem mass spectrometry. *J Lipid Res,* Vol. 44, No. 11, (Nov), pp. (2209-2216), 0022-2275 (Print)

Liscum, L. (2000). Niemann-Pick type C mutations cause lipid traffic jam. *Traffic,* Vol. 1, No. 3, (Mar), pp. (218-225), 1398-9219 (Print)

Mano, N., Oda, Y., Yamada, K., Asakawa, N. & Katayama, K. (1997). Simultaneous quantitative determination method for sphingolipid metabolites by liquid chromatography/ionspray ionization tandem mass spectrometry. *Anal Biochem,* Vol. 244, No. 2, (Jan 15), pp. (291-300), 0003-2697 (Print)

Martin, O. C. & Pagano, R. E. (1994). Internalization and sorting of a fluorescent analogue of glucosylceramide to the Golgi apparatus of human skin fibroblasts: utilization of endocytic and nonendocytic transport mechanisms. *J Cell Biol,* Vol. 125, No. 4, (May), pp. (769-781), 0021-9525 (Print)

McLuckey, S. A. & Wells, J. M. (2001). Mass analysis at the advent of the 21st century. *Chem Rev,* Vol. 101, No. 2, (Feb), pp. (571-606), 0009-2665 (Print)

Micova, K., Friedecky, D., Faber, E., Polynkova, A. & Adam, T. (2010). Flow injection analysis vs. ultra high performance liquid chromatography coupled with tandem mass spectrometry for determination of imatinib in human plasma. *Clin Chim Acta,* Vol. 411, No. 23-24, (Dec 14), pp. (1957-1962), 1873-3492 (Electronic)

Mills, K., Morris, P., Lee, P., Vellodi, A., Waldek, S., Young, E. & Winchester, B. (2005). Measurement of urinary CDH and CTH by tandem mass spectrometry in patients hemizygous and heterozygous for Fabry disease. *J Inherit Metab Dis,* Vol. 28, No. 1, pp. (35-48), 0141-8955 (Print)

Murphy, R. C., Fiedler, J. & Hevko, J. (2001). Analysis of nonvolatile lipids by mass spectrometry. *Chem Rev,* Vol. 101, No. 2, (Feb), pp. (479-526), 0009-2665 (Print)

Natomi, H., Sugano, K., Iwamori, M., Takaku, F. & Nagai, Y. (1988). Region-specific distribution of glycosphingolipids in the rabbit gastrointestinal tract: preferential enrichment of sulfoglycolipids in the mucosal regions exposed to acid. *Biochim Biophys Acta,* Vol. 961, No. 2, (Jul 22), pp. (213-222), 0006-3002 (Print)

Olling, A., Breimer, M. E., Peltomaa, E., Samuelsson, B. E. & Ghardashkhani, S. (1998). Electrospray ionization and collision-induced dissociation time-of-flight mass

spectrometry of neutral glycosphingolipids. *Rapid Commun Mass Spectrom*, Vol. 12, No. 10, pp. (637-645), 0951-4198 (Print)

Paschke, E., Fauler, G., Winkler, H., Schlagenhauf, A., Plecko, B., Erwa, W., Breunig, F., Urban, W., Vujkovac, B., Sunder-Plassmann, G. & Kotanko, P. (2011). Urinary total globotriaosylceramide and isoforms to identify women with Fabry disease: a diagnostic test study. *Am J Kidney Dis*, Vol. 57, No. 5, (May), pp. (673-681), 1523-6838 (Electronic)

Porter, M. T., Fluharty, A. L., Trammell, J. & Kihara, H. (1971). A correlation of intracellular cerebroside sulfatase activity in fibroblasts with latency in metachromatic leukodystrophy. *Biochem Biophys Res Commun*, Vol. 44, No. 3, (Aug 6), pp. (660-666), 0006-291X (Print)

Prinetti, A., Loberto, N., Chigorno, V. & Sonnino, S. (2009). Glycosphingolipid behaviour in complex membranes. *Biochim Biophys Acta*, Vol. 1788, No. 1, (Jan), pp. (184-193), 0006-3002 (Print)

Sandhoff, K., Kolter, T. & Harzer, K. (2001). Sphingolipid Activator Proteins, In: *The Metabolic and Molecular Bases of Inherited Disease*, Scriver, C. R., Beaudet, A. L., Sly, W. S.&Valle, D., pp. (3371-3388), McGraw-Hill, 0-07-136321-1, New York

Schepers, U., Glombitza, G., Lemm, T., Hoffmann, A., Chabas, A., Ozand, P. & Sandhoff, K. (1996). Molecular analysis of a GM2-activator deficiency in two patients with GM2-gangliosidosis AB variant. *Am J Hum Genet*, Vol. 59, No. 5, (Nov), pp. (1048-1056), 0002-9297 (Print)

Scherer, M., Leuthauser-Jaschinski, K., Ecker, J., Schmitz, G. & Liebisch, G. (2010). A rapid and quantitative LC-MS/MS method to profile sphingolipids. *J Lipid Res*, Vol. 51, No. 7, (Jul), pp. (2001-2011), 0022-2275 (Print)

Schiffmann, R., Waldek, S., Benigni, A. & Auray-Blais, C. (2010). Biomarkers of Fabry disease nephropathy. *Clin J Am Soc Nephrol*, Vol. 5, No. 2, (Feb), pp. (360-364), 1555-905X (Electronic)

Schmid, B., Paton, B. C., Sandhoff, K. & Harzer, K. (1992). Metabolism of GM1 ganglioside in cultured skin fibroblasts: anomalies in gangliosidoses, sialidoses, and sphingolipid activator protein (SAP, saposin) 1 and prosaposin deficient disorders. *Hum Genet*, Vol. 89, No. 5, (Jul), pp. (513-518), 0340-6717 (Print)

Schnaar, R. L. (1994). Isolation of glycosphingolipids. *Methods Enzymol*, Vol. 230, No. pp. (348-370), 0076-6879 (Print)

Schnaar, R. L., Suzuki, A. & Stanley, P. (2009). Glycosphingolipids, In: *Essentials of Glycobiology*, Varki, A., Cummings, R. D., Esko, J. D., Freeze, H. H., Stanley, P., Bertozzi, C. R., Hart, G. W.&Etzler, M. E., pp. Cold Spring Harbor Laboratory Press, 978-087969770-9, New York

Schulze, H. & Sandhoff, K. (2011). Lysosomal lipid storage diseases. *Cold Spring Harb Perspect Biol*, Vol. 3, No. 6, pp. 1943-0264 (Electronic)

Schwarzmann, G., Hoffmann-Bleihauer, P., Schubert, J., Sandhoff, K. & Marsh, D. (1983). Incorporation of ganglioside analogues into fibroblast cell membranes. A spin-label study. *Biochemistry*, Vol. 22, No. 21, (Oct 11), pp. (5041-5048), 0006-2960 (Print)

Schweppe, C. H., Hoffmann, P., Nofer, J. R., Pohlentz, G., Mormann, M., Karch, H., Friedrich, A. W. & Muthing, J. (2010). Neutral glycosphingolipids in human blood:

a precise mass spectrometry analysis with special reference to lipoprotein-associated Shiga toxin receptors. *J Lipid Res,* Vol. 51, No. 8, (Aug), pp. (2282-2294), 0022-2275 (Print)

Sleno, L. & Volmer, D. A. (2004). Ion activation methods for tandem mass spectrometry. *J Mass Spectrom,* Vol. 39, No. 10, (Oct), pp. (1091-1112), 1076-5174 (Print)

Sonderfeld, S., Conzelmann, E., Schwarzmann, G., Burg, J., Hinrichs, U. & Sandhoff, K. (1985). Incorporation and metabolism of ganglioside GM2 in skin fibroblasts from normal and GM2 gangliosidosis subjects. *Eur J Biochem,* Vol. 149, No. 2, (Jun 3), pp. (247-255), 0014-2956 (Print)

Spacil, Z., Elliott, S., Reeber, S. L., Gelb, M. H., Scott, C. R. & Turecek, F. (2011). Comparative triplex tandem mass spectrometry assays of lysosomal enzyme activities in dried blood spots using fast liquid chromatography: application to newborn screening of Pompe, Fabry, and Hurler diseases. *Anal Chem,* Vol. 83, No. 12, (Jun 15), pp. (4822-4828), 1520-6882 (Electronic)

Storch, J. & Xu, Z. (2009). Niemann-Pick C2 (NPC2) and intracellular cholesterol trafficking. *Biochim Biophys Acta,* Vol. 1791, No. 7, (Jul), pp. (671-678), 0006-3002 (Print)

Sullards, M. C., Liu, Y., Chen, Y. & Merrill, A. H., Jr. (2011). Analysis of mammalian sphingolipids by liquid chromatography tandem mass spectrometry (LC-MS/MS) and tissue imaging mass spectrometry (TIMS). *Biochim Biophys Acta,* Vol. No. (Jul 1), pp. 0006-3002 (Print)

Taylor, P. J. (2005). Matrix effects: the Achilles heel of quantitative high-performance liquid chromatography-electrospray-tandem mass spectrometry. *Clin Biochem,* Vol. 38, No. 4, (Apr), pp. (328-334), 0009-9120 (Print)

Turecek, F., Scott, C. R. & Gelb, M. H. (2007). Tandem mass spectrometry in the detection of inborn errors of metabolism for newborn screening. *Methods Mol Biol,* Vol. 359, No. pp. (143-157), 1064-3745 (Print)

van Echten-Deckert, G. (2000). Sphingolipid extraction and analysis by thin-layer chromatography. *Methods Enzymol,* Vol. 312, No. pp. (64-79), 0076-6879 (Print)

van Meer, G., Voelker, D. R. & Feigenson, G. W. (2008). Membrane lipids: where they are and how they behave. *Nat Rev Mol Cell Biol,* Vol. 9, No. 2, (Feb), pp. (112-124), 1471-0080 (Electronic)

von Figura, K., Gieselmann, V. & Jaeken, J. (2001). Metachromatic Leukodystrophy, In: *The Metabolic and Molecular Bases of Inherited Disease,* Scriver, C. R., Beaudet, A. L., Sly, W. S.&Valle, D., pp. (3695-3724), McGraw-Hill, 0-07-136321-1, New York

Wennekes, T., van den Berg, R. J., Boot, R. G., van der Marel, G. A., Overkleeft, H. S. & Aerts, J. M. (2009). Glycosphingolipids--nature, function, and pharmacological modulation. *Angew Chem Int Ed Engl,* Vol. 48, No. 47, pp. (8848-8869), 1521-3773 (Electronic)

Whitfield, P. D., Sharp, P. C., Johnson, D. W., Nelson, P. & Meikle, P. J. (2001). Characterization of urinary sulfatides in metachromatic leukodystrophy using electrospray ionization-tandem mass spectrometry. *Mol Genet Metab,* Vol. 73, No. 1, (May), pp. (30-37), 1096-7192 (Print)

Wiesner, P., Leidl, K., Boettcher, A., Schmitz, G. & Liebisch, G. (2009). Lipid profiling of FPLC-separated lipoprotein fractions by electrospray ionization tandem mass spectrometry. *J Lipid Res*, Vol. 50, No. 3, (Mar), pp. (574-585), 0022-2275 (Print)

Wrobe, D., Henseler, M., Huettler, S., Pascual Pascual, S. I., Chabas, A. & Sandhoff, K. (2000). A non-glycosylated and functionally deficient mutant (N215H) of the sphingolipid activator protein B (SAP-B) in a novel case of metachromatic leukodystrophy (MLD). *J Inherit Metab Dis*, Vol. 23, No. 1, (Feb), pp. (63-76), 0141-8955 (Print)

Xu, Z., Farver, W., Kodukula, S. & Storch, J. (2008). Regulation of sterol transport between membranes and NPC2. *Biochemistry*, Vol. 47, No. 42, (Oct 21), pp. (11134-11143), 1520-4995 (Electronic)

SUPPLEMENTARY PUBLICATIONS

Non impacted publications related to topic of this PhD thesis

Supplementary publication F – Journal published conference abstracts

Kuchar L., Hlavatá J., Asfaw B., et al., *Changed isoform profiles in sphingolipid storage disorders: a new pre-diagnostic tool.* Int J Clin Pharm Th, 2010. **48**(Suppl. 1):p. S76
An extended conference abstract to request of Editors

with Gaucher disease. Three of these patients may have been missed with the fluorimetric assay. Conclusion: In summary, the MS/MS assay is more sensitive than the fluorimetric test for measurement of lysosomal enzyme activity in dried blood spots. However, the relatively high cost of laboratory equipment and maintenance for the MS/MS technique as well as the more tedious work-up procedure may favor the fluorimetric method for suspected cases of Fabry disease.

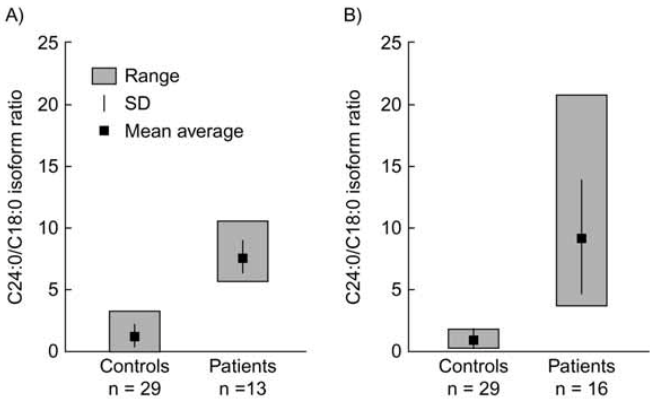

Figure 1 (Kuchar et al.). Ranges of the A: C24:0/C18:0 globotriaosylceramide (Gb_3) and B: C24:0-OH/C18:0 sulfatide isoform ratios in controls' and patients' urine samples.

Changed isoform profiles in sphingolipid storage disorders: a new pre-diagnostic tool

L. Kuchař, J. Hlavatá, B. Asfaw and J. Ledvinová

Institute of Inherited Metabolic Disorders, First Faculty of Medicine and University Hospital, Charles University, Prague, Czech Republic

Aim: To analyze tandem mass spectrometry (MS/MS) profiles of urinary sphingolipids in lysosomal storage diseases characterized by high levels of lipid excretion in the urine. We focused on the excretion patterns of molecular species of globotriaosylceramide (Gb_3) and sulfatides in samples from patients with Fabry disease, metachromatic leukodystrophy (MLD), and saposin B and prosaposin deficiencies. Methods: We used an AB/MDS SCIEX API 3200 tandem mass spectrometer for lipid quantification and profiling from urinary extracts. The positive ion mode was used for measurement of neutral sphingolipids and ceramide, and the negative ion mode for sulfatides. Spectra of molecular species (isoforms) with C16:0 to C26:0 fatty acids (saturated, unsaturated and also hydroxylated) in the ceramide moiety were scanned for each lipid. Results: All urinary samples from patients with the sphingolipidoses being studied showed an increased quantity of excreted Gb_3 and sulfatide regardless of the underlying degradation defect. There was also a clear shift in the isoform profiles towards molecular species with longer fatty acids (Figure 1). The ratio of C24 family species to C18:0 fatty acids was different in samples from patients compared with those from healthy volunteers. Conclusion: Based on the results of this study, we propose the Gb_3 C24 to C18:0 isoform ratio and the sulfatide C24:0-OH to C18:0 isoform ratio as new simple pre-diagnostic markers for rapid screening of patients suspected to have a lysosomal defect of Gb_3 or sulfatide degradation. The underlying metabolic explanation of this phenomenon is not yet clear and warrants further investigation. Acknowledgments: Supported by the grant project MSM 0021620806 Czech Republic and by the grant number 259039-19509/2009 from the Grant Agency of Charles University, Prague.

22q13 deletion syndrome (Phelan-McDermid syndrome): another disorder associated with low arylsulfatase A activity

O. Artigalás[1,2], G. Paskulin[3], M. Riegel[4] and I.V. Schwartz[1,2]

[1]Medical Genetics Service, Hospital de Clínicas de Porto Alegre, [2]Postgraduate Program in Genetics and Molecular Biology, Department of Genetics, Universidade Federal do Rio Grande do Sul, Rio Grande do Sul, Porto Alegre, [3]Clinical Genetics, Universidade Federal de Ciências da Saúde de Porto Alegre, Porto Alegre, Brazil, and [4]Institute of Medical Genetics, University of Zürich, Switzerland

Background: The etiologic heterogeneity of arylsulfatase A (ARSA) deficiency is widely known although the disorder is more frequently associated with metachromatic leukodystrophy (MLD) and pseudodeficiency of ARSA (PD-ARSA), it can also be secondary to multiple sulfatase deficiency and saposin B deficiency. Aim: To emphasize the need to expand the list of differential diagnosis of ARSA deficiency to include 22q13 deletion syndrome (Phelan-McDermid syndrome). Patient: We describe a Brazilian male patient sent for genetic evaluation owing to mental retardation, absence of speech, low activity of ARSA in leukocytes and a presumed diagnosis of MLD. During physical examination, no major abnormalities were found. Brain imaging revealed nothing unusual. Further metabolic tests confirmed low activity of ARSA in leukocytes and fibroblasts, but the pattern of sulfatide excretion in the urine was normal, which eliminates the possibility of MLD and suggests the diagnosis of ARSA pseudodeficiency. An allele associated with pseudodeficiency was present at the *ARSA* locus, and GTG-banded karyotype analysis showed the presence of a de novo apparently balanced reciprocal translocation [(46,XY,t(16;22)(p11.2;q13)]. However, fluorescent in situ hybridization and array competitive genomic hybridization showed a terminal deletion of the long arm of chromosome 22 including the *ARSA* gene allowing the diagnosis of 22q13-deletion syndrome to be made [46,XY, t(16;22)(p11.2;q13.32).arr 22q13.32.q13.33(48,138,838-49,52

SUPPLEMENTARY PUBLICATIONS

Publictions in Impacted Journals not related to topic of this PhD thesis

Supplementary publication G

Musalkova D., Lukas J., Majer F., et al., *Rapid isolation of lysosomal membranes from cultured cells.* Folia Biol (Praha), 2013. **59**(1): p. 41-46

Short Communication

Rapid Isolation of Lysosomal Membranes from Cultured Cells

(lysosomes / lysosomal membrane / methionine methyl ester / gradient centrifugation)

D. MUŠÁLKOVÁ, J. LUKÁŠ, F. MAJER, O. HŘEBÍČEK, E. SVOBODOVÁ, L. KUCHAŘ, J. HONZÍKOVÁ, H. HŮLKOVÁ, J. LEDVINOVÁ, M. HŘEBÍČEK

Institute of Inherited Metabolic Disorders, First Faculty of Medicine, Charles University in Prague and General University Hospital in Prague, Czech Republic

Abstract. We present a simple method for enrichment of lysosomal membranes from HEK293 and HeLa cell lines taking advantage of selective disruption of lysosomes by methionine methyl ester. Organelle concentrate from postnuclear supernatant was treated with 20 mmol/l methionine methyl ester for 45 min to lyse the lysosomes. Subsequently, lysosomal membranes were resolved on a step sucrose gradient. An enriched lysosomal membrane fraction was collected from the 20%/35% sucrose interface. The washed lysosomal membrane fraction was enriched 30 times relative to the homogenate and gave the yield of more than 8 %. These results are comparable to lysosomal membranes isolated by magnetic chromatography from cultured cells (Dietrich et al., 1998). The procedure effectively eliminated mitochondrial contamination and minimized contamination from other cell compartments. The enriched fractions retained the ability to acidify membrane vesicles through the activity of lysosomal vacuolar ATPase. The method avoids non-physiological overloading of cells with superparamagnetic particles and appears to be quite robust among the tested cell lines. We expect it may be of more general use, adaptable to other cell lines and tissues.

Received February 8, 2012. Accepted June 26, 2012.

This study was supported by the grant NS10342-3 from the Internal Grant Agency of the Ministry of Health of the Czech Republic and partially by SVV2012/2645.

Corresponding author: Martin Hřebíček, Institute of Inherited Metabolic Disorders, First Faculty of Medicine, Charles University in Prague and General University Hospital in Prague, Ke Karlovu 2, Prague 2, Czech Republic. Phone: (+420) 2 2496 7208; Fax: (+420) 2 2496 7119; e-mail: martin.hrebicek@lf1.cuni.cz

Abbreviations: EDTA – ethylenediamine tetraacetic acid, HRP – horseradish peroxidase, LAMP1 – lysosomal associated membrane protein 1, LM – lysosomal membranes, MME – methionine methyl ester, PBS – phosphate-buffered saline, SDH – succinate dehydrogenase, TEA – triethanolamine-EDTA-acetic acid.

Introduction

Lysosomal membranes (LM) are often isolated from biological material for proteomic studies (Schröder et al., 2007a,b; Callahan et al., 2009) or for the study of individual lysosomal membrane proteins (Meikle et al., 1995; Taute et al., 2002). Hypotonic lysis of lysosome-enriched fractions from isopycnic centrifugation on density gradients is a frequently used method for preparation of LM (Meikle et al., 1995). Lysosomes can be purified to high purity by well-established procedures from some animal tissues, for instance from rat liver, which was the principal source of lysosomes for most of the structural and biochemical studies of the organelle. Isolation from other tissues may require procedures tailored to achieve the required enrichment or yield (which are almost as a rule inversely related variables). The ability to isolate the organelles from readily available tissues is especially important in the study of human cells and general isolation procedures may need to be optimized for a specific tissue or for preservation of lysosomal functions (Graham, 2009) – hence the number of papers describing isolation of lysosomes from different tissues or cell lines. We have aimed to develop a simple method for isolation of human lysosomal membranes, which would allow us to perform biochemical studies on lysosomal ghosts – lysosomal membrane vesicles without lysosomal matrix proteins.

Lysosomes, mitochondria, and peroxisomes have similar and partially overlapping densities in sucrose and to a lesser extent in other gradient media, making their full separation based on density alone very difficult. The resolution of lysosomes, however, can be significantly improved by several techniques. Density perturbation of lysosomes in gradients can greatly enhance their separation from other organelles (Graham, 2009). Highly purified lysosomes were isolated from animal tissues by density shift of lysosomes after treatment of animals with Triton WR1339 (Leighton et al., 1968) or dextran (Arai et al., 1991). Mitochondria swell in the presence of calcium ions and become less dense, and addition of $CaCl_2$ in 1 millimolar final concentration to postnuclear supernatant improves their separation from lysosomes in Percoll gradients (Arai et al., 1991).

LM were also successfully isolated by magnetic chromatography after treatment of cultured skin fibroblasts with superparamagnetic magnetite/dextran nanoparticles; lysosomes containing endocytosed particles were retained on the magnetic column and LM were obtained after on-column hypotonic lysis of lysosomes (Diettrich et al., 1998).

Lysis of lysosomes and separation of lysosomal membranes by centrifugation is another technique suitable for enrichment of LM even from complex organelle fractions. Ohsumi et al. (1983) directly treated postnuclear supernatant from rat liver with a hypotonic buffer to lyse lysosomes and collected enriched LM by a four-step differential centrifugation procedure. Also, methyl esters of certain amino acids can be used for selective rupture of lysosomes (Goldman and Kaplan, 1973). They readily cross the lysosomal membrane and enter lysosomes, where they are converted to free amino acids, presumably by lysosomal hydrolases. Accumulation of free amino acids leads to lysosomal swelling and rupture across a wide concentration range. This property was used for disruption of the lysosomal function in tissues (Reeves et al., 1981) and for enrichment of LM from lysosomes (Symons and Jonas, 1987; Schröder et al., 2007a).

Here we present a simple method for isolation of LM from HEK293 and HeLa cell lines taking advantage of selective disruption of lysosomes by methionine methyl ester, which produces lysosomal membrane vesicles retaining the ability to acidify their content.

Material and Methods

HEK293 or HeLa cells from 12–22 confluent 75 cm^2 flasks were washed twice by PBS, collected by scraping, washed once in isotonic TEA buffer (10 mmol/l triethanolamine, 1 mmol/l EDTA Na_2, 10 mmol/l acetic acid, pH 7.2) with 250 mmol/l sucrose and homogenized in the total volume of 8 ml of the same buffer by 10 strokes of tight-fitting pestle B in the glass Dounce homogenizer (Kontes, Kimble Chase Kontes, Vineland, NJ). The homogenization and all further manipulations were performed at 4 °C unless specified otherwise. The homogenate was centrifuged for 10 min at 1,000 × *g* in a swing-out rotor in a tabletop centrifuge; the supernatant was collected and the pellet was re-homogenized by three strokes in the Dounce homogenizer in a total volume of 5 ml of TEA and centrifuged in the same conditions. Both portions of postnuclear supernatant were combined and centrifuged for 15 min at 11,000 × *g* to collect the organelle pellet. The organelle pellet was re-suspended in 8 ml of isotonic HEPES buffer (10 mmol/l HEPES, pH 7.2, 250 mmol/l sucrose, 1 mmol/l EDTA Na_2) and 20 mmol/l methionine methyl ester (MME, Sigma-Aldrich, St. Louis, MO) (Schröder et al., 2007a) and incubated for 45 min at room temperature with stirring. After that the suspension was placed on ice, protease inhibitors were added (Complete, Roche Diagnostic, Mannheim, Germany) to a 1× final concentration, and the suspension was centrifuged at 20,000 × *g* for 20 min. The pellet was resuspended in 8 ml of isotonic HEPES buffer.

The degree of lysosomal lysis was estimated from the amount of hexosaminidase activity released into the supernatant. Samples (200 µl) were taken at 15 min intervals, stored on ice after the addition of protease inhibitors (Complete, Roche), and centrifuged at 25,000 × *g* for 25 min. Supernatants were collected and hexosaminidase and glucocerebrosidase activity was measured as described below.

A linear sucrose gradient was prepared from 15 ml of 32.5 % (w/v) sucrose and 15 ml of 55.5% (w/v) sucrose using a gradient mixer. The gradient was overlaid with 8 ml of MME-treated organelle suspension. Alternatively, a step sucrose gradient was constructed in the following manner: 6 ml of 41% or 35% (w/v) sucrose in 10 mmol/l HEPES buffer was overlaid with 5 ml of 20% sucrose in the same buffer and, finally, by 5 ml of methionine methyl ester-treated organelle suspension. The gradients were centrifuged at 112,700 × g_{max} in SW 32 or SW 32.1 (Beckman-Coulter, München, Germany) overnight without braking and sixteen 1 ml fractions were collected from the top of the step gradient or the band at the 20/41% sucrose interface was collected by a cannula. The linear gradient was fractionated into nineteen 2 ml fractions from the top. The fractions with the highest glucocerebrosidase specific activity were diluted 10 or more times with 10 mmol/l Tris buffer pH 7.2, pelleted by ultracentrifugation at 250,000 × g_{max} for 2 h in 70 Ti rotor (Beckman-Coulter), and flash frozen in liquid nitrogen.

ATP-dependent acidification of lysosomal ghosts prepared by MME-dependent lysis of organelle suspension was determined by the acridine orange absorbance decrease assay as described previously (Dell' Antone, 1979; Moriyama et al., 1982). The reaction solution (1 ml) contained 20 mmol/l HEPES buffer, pH 7.2, 0.2 mol/l sucrose, 50 mmol/l kalium chloride, and 20 µmol/l acridine orange (Sigma-Aldrich). The absorbance of acridine orange was followed at 492 nm at room temperature using a Shimadzu UV-2550 photometer (Schimadzu, Duisburg, Germany) with slits set to 5 nm. Lysosomal membranes (10 µg of protein) were added and the absorbance at 492 nm was allowed to stabilize before the addition of ATP (sodium salt, Sigma-Aldrich) and $MgCl_2$, both to a final concentration of 2 mmol/l. Decrease of the absorbance at 492 nm was followed for more than 2 minutes, after which ammonium sulphate was added to a final concentration of 10 mmol/l and absorbance changes were followed for at least another minute.

The amount of lysosomal membrane protein LAMP1 in fractions during purification was determined by Western blotting. Ten µg of protein from each fraction were separated on a 7–15% gradient SDS-PAGE gel according to Laemmli (1970) and transferred onto PVDF Immobilon-P membrane (Millipore, Bedford, MA) by semi-dry blotting. The membrane was blocked with 3%

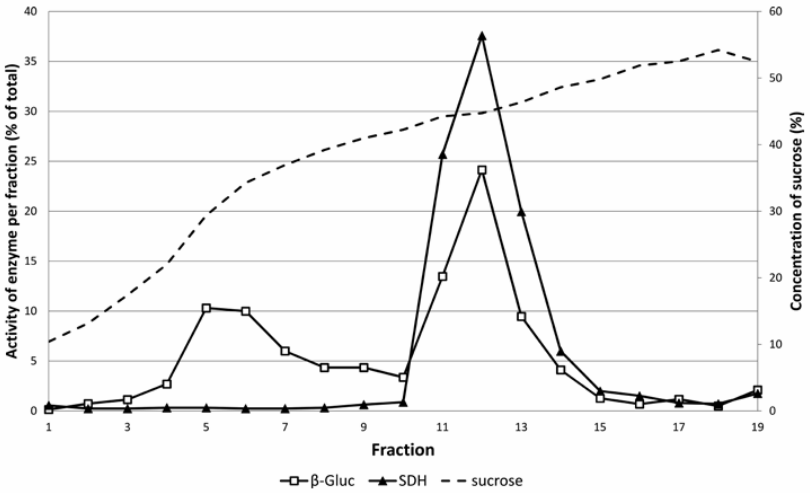

Fig. 1. Resolution of LM fraction from HeLa cells on the linear sucrose gradient
Organelle concentrate prepared from postnuclear supernatant was treated with 20 mmol/l MME for 45 min, overlaid onto linear 32.5%–55.5% sucrose gradient and centrifuged overnight at 112,700 × g_{max}. In fractions the activity of glucocerebrosidase (β-Gluc) and succinate dehydrogenase (SDH) was determined and expressed as percents of the total activity. Sucrose concentration is shown in percents (w/v).

BSA and 0.05% Tween 20-phosphate-buffered saline. The membrane was probed with anti-LAMP1 rabbit polyclonal antibody (1 : 5000, a kind gift of Dr. Carlsson, University of Umea, Sweden) at room temperature for 1 h, washed four times with PBS-Tween and then incubated with horseradish peroxidase (HRP)-conjugated goat anti-rabbit IgG (1 : 3000, Thermo Scientific, Rockford, IL) in PBS-Tween containing 1% BSA. After washing, the blot was developed with an enhanced chemiluminescence (ECL) detection kit (Thermo Scientific).

The activities of marker enzymes succinate dehydrogenase, acid and alkaline phosphatase, catalase, and NADPH – cytochrome *c* reductase were determined as described by Graham (1993). Glucocerebrosidase and total hexosaminidase activity was measured fluorimetrically (Wenger and Williams, 1991). Glucocerebrosidase, which does not have any transmembrane domains, is considered a peripheral lysosomal membrane protein and was used as a marker of lysosomal membrane (Schröder et al., 2007b). Sucrose concentrations in gradient fractions were determined by refractometry. Protein concentrations were measured using the Bradford method (Bradford, 1976).

Results and Discussion

We first attempted to obtain enriched LMs from MME-treated postnuclear supernatant by differential centrifugation according to Ohsumi et al. (1983). The fractions we obtained, however, contained multiple marker enzyme activities and specific activities of lysosomal markers did not suggest enrichment of LM (data not shown). We have therefore fractionated the MME-lysate on a linear 32.5%–55.5% sucrose gradient. There were two peaks of glucocerebrosidase activity – the first at about 30–41% and the second, which also contained significant mitochondrial contamination, at approximately 45% (Fig. 1). We have designed a step gradient (lysate/20% sucrose/41% sucrose) and collected a glucocerebrosidase-enriched membrane fraction from the 20%/41% sucrose interface. The fraction still contained some mitochondrial contamination, which was essentially eliminated by lowering sucrose concentration from 41% to 35% in the gradient – at the same time leading to a decreased yield of enriched LM (Fig. 2).

Lysosomal marker enzyme activity was enriched in the LM fraction recovered from the 20%/35% sucrose interface. We have also followed the amounts of prototypical lysosomal membrane protein LAMP1 (Schröder et al, 2010) in fractions by Western blotting, showing enrichment of the antigen during the purification process (Fig. 3). Glucocerebrosidase activity was enriched on average 15 times (7–22 times, 7 experiments in total); washing of the fraction in 10 mmol/l Tris further increased its specific activity approximately twice (Table 1). In a typical experiment, the postnuclear supernatant contained 89 % of the glucocerebrosidase activity, while organelle pellet retained 77 % activity. The highest of the 20%/35% interface fractions (fraction 11, enrichment relative to the homogenate 14×) contained 12 % of the homogenate glucocerebrosidase activity. The washed pellet from this fraction represented 8.8 % of the initial activity. Contaminating activities were generally low (less than 1 %) with the exception of catalase (2.6 %), suggesting mild contamination with peroxisomes (Table 1). While highly purified LM preparations contain plasma membrane marker proteins (Schröder et al., 2010), presumably originating from the plasma membrane portions entering the endosomal/lysosomal system via endocytosis, it should be noted that

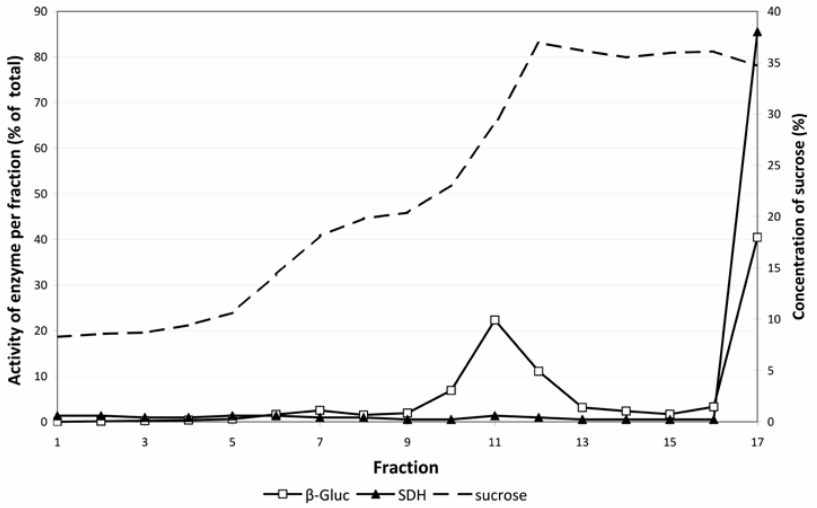

Fig. 2. Resolution of LM fraction from HeLa cells on the step sucrose gradient
MME-treated organelle concentrate was resolved on the step gradient created by overlaying 20% sucrose over 35% sucrose. The gradient was centrifuged overnight at 112,700 × g_{max}. In fractions the activity of glucocerebrosidase (β-Gluc) and succinate dehydrogenase (SDH) was determined and expressed as percents of the total activity. Concentration of sucrose is shown in percents (w/v).

some plasma membrane fragments may also focus on the 20%/35% (41%) sucrose interface (Scott et al., 1993) as LM, as was noted in some experiments. Spurious contamination of the LM fraction by plasma membrane arguably may occur as a result of the more vigorous homogenization.

We have determined activities of total hexosaminidase, a lysosomal matrix enzyme, in 25,000 × *g* supernatants of samples taken during MME treatment of the organelle concentrate as a measure of lysosomal lysis. The supernatant of the sample taken after 15 min contained 36.7 % of total hexosaminidase activity of the sample subjected to MME. The samples taken at 30, 45, and 60 min retained 39.0 %, 47.6 %, and 54.4 % of the initial hexosaminidase activity, respectively. At the same time the total hexosaminidase activity in the sample decreased by 13 % (9.81 nmol/ml/min at 0 min to 8.54 nmol/ml/min at 60 min). The increased concentration of MME (50 mmol/l) did not result in higher release of hexosaminidase into the supernatant. Glucocerebrosidase activity did not increase in the supernatant during the MME treatment. On the basis of these results, 45 min were chosen for MME treatment as a compromise between higher degree of lysosomal lysis and the risk of proteolysis.

We have not attempted to further enrich the core lysosomal membrane proteins by removing peripheral membrane proteins or loosely bound matrix proteins by high-salt washing, although these proteins may contaminate the enriched lysosomal fractions to a significant level. It is of interest that matrix proteins may associate, even temporarily, with the lysosomal membrane (Jadot et al, 1979) and some lysosomal proteins, including glucocerebrosidase, apparently exist in luminal and membrane-bound form (Imai, 1985).

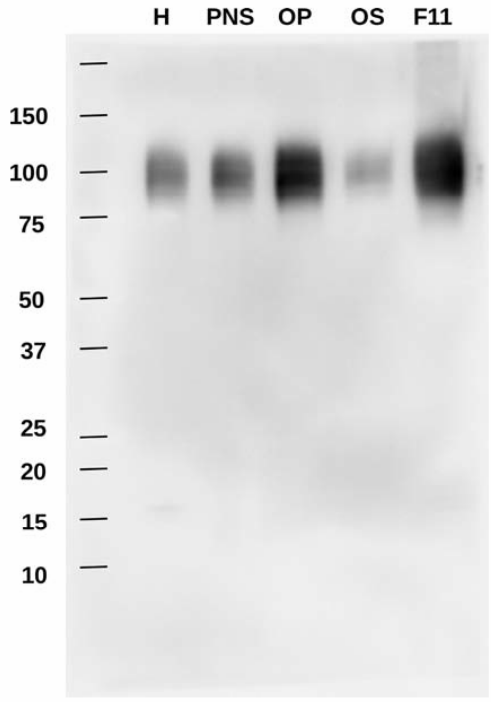

Fig. 3. Western blotting of subcellular fractions with anti-LAMP1 antibody
Ten µg of protein from each fraction were loaded to individual lanes. From the left: homogenate (H), post-nuclear supernatant (PNS), organelle pellet (OP), post-organellar supernatant (OS), and washed lysosomal membranes (F11). Positions of molecular weight markers in kilodaltons are shown on the left. Note the typical blurred appearance of the bands, which is assumed to be due to differential glycosylation.

Table 1. Purification of lysosomal membranes from HeLa cells. Typical values for protein concentration and glucocerebrosidase activity are shown.

Fraction	Protein		Glucocerebrosidase		
	Total (mg)	Yield (%)	Yield (%)	Specific activity (nmol/mg/min)	Purification factor
Homogenate	49.5	100.0	100.0	1.31	1.0
Nuclear pellet	8.1	16.4	8.4	0.67	-
Postnuclear supernatant	37.8	76.3	88.6	1.53	1.2
Organelle pellet	9.7	19.6	77.1	5.17	3.9
Postorganellar supernatant	21.3	43.1	11.2	0.34	-
LM Fraction (Fraction 11 from the sucrose gradient *#)	0.4	0.9	12.0	18.24	13.9
Washed LM fraction	0.1	0.3	8.8	38.5	29.6

* Organelle pellet was divided into two portions overlaid over two identical sucrose gradients. The values here are averaged from both gradients.
# Fraction 11 of the sucrose gradient had the highest specific glucocerebrosidase activity and was considered the LM fraction (see Fig. 2).

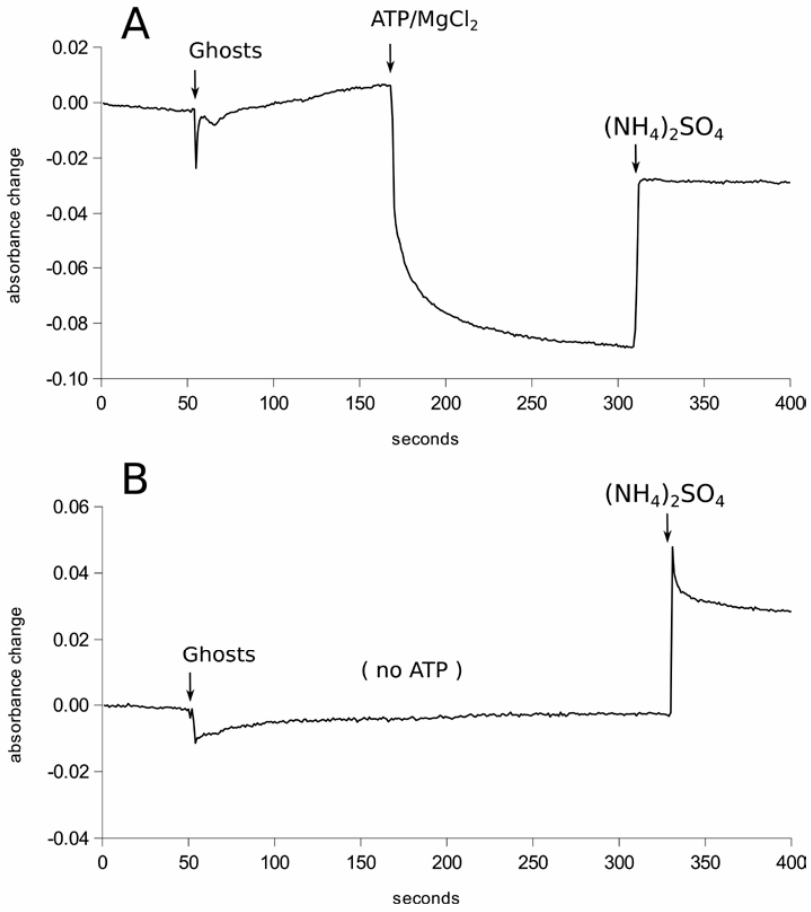

Fig. 4. Acidification of lysosomal ghosts after the addition of ATP
Acidification of washed lysosomal membrane vesicles was measured as the decrease of acridine orange absorbance at 492 nm. The reaction solution (1 ml) contained 20 mmol/l HEPES buffer, pH 7.2, 0.2 mol/l sucrose, 50 mmol/l kalium chloride, and 20 µmol/l acridine orange (Sigma-Aldrich). Lysosomal ghosts (10 µg of protein) were added (Ghosts) and the following reagents were added at the time points depicted by arrows: ATP and $MgCl_2$ (panel A), both to a final concentration of 2 mmol/l, and ammonium sulphate to a final concentration of 10 mmol/l. When ATP was omitted (panel B), the decrease of absorbance did not occur.

The washed lysosomal membranes were acidified after the addition of ATP (Fig. 4). The activity of the multiprotein complex of vacuolar ATPase, the proton pump residing in the lysosomal membrane which is responsible for the acidification of lysosomes, was apparently preserved in samples of enriched lysomal membrane fractions. Addition of ammonium sulphate (final concentration 10 mmol/l) resulted in alkalization of the membrane vesicles (Fig. 4).

We have sought to develop a simple method for the isolation of LM that would not require non-physiological overloading of the lysosomal/endosomal system with particles or detergents as the resulting cells are clearly abnormal. In our hands, the method of Ohsumi et al. (1983), originally optimized for rat liver tissue and based on hypotonic treatment of postnuclear supernatant followed by differential centrifugation, did not provide LM in sufficient yields and purity from HEK293 cells. Osmotic lysis of lysosomes with methyl esters of leucine or methionine, highly specific for the target organelle, was chosen for the release of LM, which were subsequently resolved on the step sucrose gradient. The enriched LM fraction could easily be collected from the 20%/35% interface. The procedure effectively eliminated mitochondrial contamination, minimized contamination from other cell compartments and appeared to be sufficiently robust. While it did not yield LM of very high purity, the enrichment was comparable to the magnetic chromatography technique developed by Diettrich et al. (1998). The method yielded similar results both for HEK293 and HeLa cell lines, suggesting that it may be adapted to other cell lines or possibly tissues.

References

Arai, K., Kanaseki, T., Ohkuma, S. (1991) Isolation of highly purified lysosomes from rat liver: identification of electron carrier components on lysosomal membranes. *J. Biochem.* **110**, 541-547.

Bradford, M. M. (1976) A rapid and sensitive method for the quantitation of microgram quantities of protein utilizing the principle of protein-dye binding. *Anal. Biochem.* **72**, 248-254.

Callahan, J. W., Bagshaw, R. D., Mahuran, D. J. (2009) The integral membrane of lysosomes: its proteins and their roles in disease. *J. Proteomics.* **72**, 23-33.

Dell' Antone, P. (1979) Evidence for an ATP-driven "proton pump" in rat liver lysosomes by basic dyes uptake. *Biochem. Biophys. Res. Commun.* **86**, 180-189.

Diettrich, O., Mills, K., Johnson, A. W., Hasilik, A., Winchester, B. G. (1998) Application of magnetic chromatography to the isolation of lysosomes from fibroblasts of patients with lysosomal storage disorders. *FEBS Lett.* **441**, 369-372.

Goldman, R., Kaplan, A. (1973) Rupture of rat liver lysosomes mediated by L-amino acid esters. *Biochim. Biophys. Acta* **318**, 205-216.

Graham, J. M. (1993) The identification of subcellular fractions from mammalian cells. In: *Biomembrane Protocols: I. Isolation and Analysis, Methods in Molecular Biology 19*, eds. Graham J. M., Higgins J. S., pp. 1-18, Humana Press, Totowa, NJ.

Graham, J. M. (2009) Subcellular fractionation and isolation of organelles. In: *Current Protocols in Cell Biology*, John Wiley & Sons Inc, Hoboken, NJ.

Imai, K. (1985) Characterization of β-glucosidase as a peripheral enzyme of lysosomal membranes from mouse liver and purification. *J. Biochem.* **98**, 1405-1416.

Jadot, M., Dubois, F., Wattiaux-De Coninck, S., Wattiaux, R. (1997) Supramolecular assemblies from lysosomal matrix proteins and complex lipids. *Eur. J. Biochem.* **249**, 862-869.

Laemmli, U. K. (1970) Cleavage of structural proteins during the assembly of the head of bacteriophage T4. *Nature* **227**, 680-685.

Leighton, F., Poole, B., Beaufay, H., Baudhuin, P., Coffey, J. W., Fowler, S., De Duve, C. (1968) The large-scale separation of peroxisomes, mitochondria, and lysosomes from the livers of rats injected with triton WR-1339. Improved isolation procedures, automated analysis, biochemical and morphological properties of fractions. *J. Cell. Biol.* **37**, 482-513.

Meikle, P. J., Whittle, A. M., Hopwood, J. J. (1995) Human acetyl-coenzyme A: α-glucosaminide N-acetyltransferase. Kinetic characterization and mechanistic interpretation. *Biochem. J.* **308 (Pt 1)**, 327-333.

Moriyama, Y., Takano, T., Ohkuma, S. (1982) Acridine orange as a fluorescent probe for lysosomal proton pump. *J. Biochem.* **92**, 1333-1336.

Ohsumi, Y., Ishikawa, T., Kato, K. (1983) A rapid and simplified method for the preparation of lysosomal membranes from rat liver. *J. Biochem.* **93**, 547-556.

Reeves, J. P., Decker, R. S., Crie, J. S., Wildenthal, K. (1981) Intracellular disruption of rat heart lysosomes by leucine methyl ester: effects on protein degradation. *Proc. Natl. Acad. Sci. USA* **78**, 4426-4429.

Schröder, B., Elsässer, H., Schmidt, B., Hasilik, A. (2007a) Characterisation of lipofuscin-like lysosomal inclusion bodies from human placenta. *FEBS Lett.* **581**, 102-108.

Schröder, B., Wrocklage, C., Pan, C., Jäger, R., Kösters, B., Schäfer, H., Elsässer, H., Mann, M., Hasilik, A. (2007b) Integral and associated lysosomal membrane proteins. *Traffic* **8**, 1676-1686.

Schröder, B. A., Wrocklage, C., Hasilik, A., Saftig, P. (2010) The proteome of lysosomes. *Proteomics* **10**, 4053-4076.

Scott, L., Schell, M. J., Hubbard, A. L. (1993) Isolation of plasma membrane sheets and plasma membraine domains from rat liver. In: *Biomembrane Protocols: I. Isolation and Analysis, Methods in Molecular Biology 19*, eds. Graham J. M., Higgins, J. S. pp. 59-69, Humana Press, Totowa, NJ.

Symons, L. J., Jonas, A. J. (1987) Isolation of highly purified rat liver lysosomal membranes using two Percoll gradients. *Anal. Biochem.* **164**, 382-390.

Taute, A., Wätzig, K., Simons, B., Lohaus, C., Meyer, H., Hasilik, A. (2002) Presence of detergent-resistant microdomains in lysosomal membranes. *Biochem. Biophys. Res. Commun.* **298**, 5-9.

Wenger, D. A., Williams, C. (1991) Screening for lysosomal disorders. In: *Techniques in Diagnostic Human Biochemical Genetics: a Laboratory Manual*, ed. Hommes F. A., pp. 587-617, Wiley-Liss, New York, NY.

SUPPLEMENTARY PUBLICATIONS

Published consensus from the expert meetings

Supplementary publication H

Gal A., Hughes D. A., and Winchester B., *Toward a consensus in the laboratory diagnostics of Fabry disease - recommendations of a European expert group.* J Inherit Metab Dis, 2011. **34**(2): p. 509-14 (*L.K. is on the list of invited members of the expert team).*

J Inherit Metab Dis (2011) 34:509–514
DOI 10.1007/s10545-010-9261-9

ORIGINAL ARTICLE

Toward a consensus in the laboratory diagnostics of Fabry disease - recommendations of a European expert group

Andreas Gal · Derralynn A. Hughes · Bryan Winchester

Received: 6 September 2010 / Revised: 28 November 2010 / Accepted: 2 December 2010 / Published online: 13 January 2011

Guidelines on diagnostics and therapy of Fabry disease have already been compiled in a number of European countries and are being prepared in others. A synthesis of these national guidelines seems to be a sensible option for preparing a prospective European consensus document in the not too distant future. While clinical diagnostics is extensively discussed in the various guidelines, at present there is no consensus on laboratory diagnostic tests for Fabry disease either at national level or at the level of the European Union. There is a widespread variation concerning the diagnostic value of the various methods, such as enzyme activity testing, gene analysis, biopsies, Gb3 measurement etc. and on what should be used and how they compare, if indeed they do. This results in lack of agreement regarding the clinical pathology of the condition.

While experts throughout Europe agree on many aspects of the laboratory diagnosis of Fabry disease (for a recent review see Winchester and Young 2010), there are some specific issues which need further discussion before a general recommendation can be made. In order to promote this process, three one-and-a-half day *ad hoc* meetings* of European experts** were organized in 2009 with the aim of defining a consensus on laboratory diagnostics of Fabry disease that should allow for laboratories performing this diagnostic service to work to the same standards. Invitations to attend the meetings were based on, in addition to geographic considerations, outstanding scientific accomplishments in the field and/or active involvement in the laboratory diagnostics of Fabry disease.

*'Diagnostic use and value of Gb3 and lysoGb3 in Fabry disease' (April 22-23, 2009, Bad Nauheim, Germany); 'Diagnostic use and value of measuring alpha-galactosidase A activity in Fabry disease' (July 16-17, 2009, Berlin, Germany); 'Diagnostic use and value of mutations of the GLA gene in Fabry disease' (November 3-4, 2009, Barcelona, Spain).
**J.M.F.G. Aerts (Amsterdam, The Netherlands), M. Beck (Mainz, Germany), O. Bodamer (Salzburg, Austria), A. Cooper (Manchester, United Kingdom), A. Gal (Hamburg, Germany), D. Germain (Paris, France), R. Giugliani (Zürich, Switzerland), D. Hughes (London, United Kingdom), L. Kuchar (Prague, Czech Republic), J. Ledvinova (Prague, Czech Republic), Z. Lukacs (Hamburg, Germany), C. Navarro (Vigo, Spain), E. Paschke (Graz, Austria), M. Piraud (Lyon, France), A. Rolfs (Rostock, Germany), C. Sa Miranda (Porto, Portugal), M. van Slegtenhorst (Rotterdam, The Netherlands), H. Treslova (Prague, Czech Republic), M.T. Vanier (Lyon, France), F.W. Verheijen (Rotterdam, The Netherlands), B. Winchester (London, United Kingdom).

Communicated by Douglas A. Brooks

Competing interest: None declared.

This recommendation was compiled by the authors on behalf of the 21 European Experts listed in the article.

A. Gal (✉)
Institut für Humangenetik, Universitätsklinikum
Hamburg-Eppendorf,
Martinistr. 52,
20246 Hamburg, Germany
e-mail: gal@uke.de

D. A. Hughes
Lysosomal Storage Disorders Unit,
Department of Academic Haematology, Royal Free Hospital
& University College Medical School,
Rowland Hill Street,
London NW3 2PF, UK
e-mail: d.hughes@medsch.ucl.ac.uk

B. Winchester
Biochemistry Research Group, UCL Institute of Child Health at
Great Ormond Street Hospital, University College London,
30 Guilford Street,
London WC1N 1EH, UK
e-mail: b.winchester@ich.ucl.ac.uk

Primary objectives of the initiative were (i) establishment of 'gold standards' and practical algorithms for diagnosis of Fabry disease, (ii) promotion of a concept of certification/accreditation for diagnostic and treatment centres of excellence, and (iii) provision of a platform for future treatment guidelines. In particular, three specific issues were selected by the organizers: the diagnostic utility of measurement of Gb3 and lysoGb3, evaluation of α-galactosidase A activity, and analysing mutations of the *GLA* gene in patients with Fabry disease. The most important goal of these workshops was to provide a platform for the experts to exchange ideas and experiences and share experimental data with each other, even if preliminary or yet unpublished, on the use, practical value, and significance of different laboratory approaches in the diagnostics of Fabry disease. All data were critically discussed by the panel and used to prepare this recommendation for the medical community. We hope that this document will serve as a starting point for further discussion that, in the end, should result in a consensus, provide essential guidance to physicians, and ensure a better differential and timely diagnosis of patients with Fabry disease.

Diagnostic use and value of measuring α-galactosidase A activity

In normal human tissues, there are two lysosomal glycosidases with α-galactosidase activity towards synthetic substrates. α-Galactosidase A (α-GAL; EC 3.2.1.22) which is deficient in Fabry disease, acts on terminal α-galactosyl residues in glycosphingolipids, whereas the so called α-galactosidase B is an α-*N*-acetylgalactosaminidase (α-NAGAL; EC 3.2.1.49) that acts on natural substrates with terminal α-*N*-acetylgalactosaminyl residues and is defective in Schindler disease. α-Galactosidase A does not catalyse the hydrolysis of the natural substrates of α-NAGAL whereas α-NAGAL may act on some natural substrates with terminal α-galactosyl residues (Clark and Garman 2009). As both enzymes act on synthetic α-galactoside substrates, α-*N*-acetylgalactosamine, a specific inhibitor of α-NAGAL is added to assays of α-galactosidase A activity for the diagnosis of Fabry disease. The genes (*GLA* and *NAGA*) encoding α-GAL and α-NAGAL are on chromosomes Xq22.1 and 22q13, respectively. Although the two genes show considerable homology, as they evolved from a common ancestral precursor (Clark and Garman 2009), α-galactosidase A and α-NAGAL have distinct physicochemical properties, and antibodies raised against one do not cross-react with the other.

α-Galactosidase A is a typical lysosomal hydrolase with optimal activity towards natural and synthetic substrates at pH 3.8–4.6. It is a glycoprotein and is transported to the lysosomes via the mannose-6-phosphate pathway. It is synthesized as a precursor of 50 kDa and is processed to a mature lysosomal form of 46 kDa by partial proteolysis and modification of its carbohydrates. The enzyme is a homodimer with an active site in each of the monomers. Hydrolysis of its natural substrates *in vivo* requires saposin B whereas that *in vitro* requires the addition of a detergent, usually sodium taurocholate. Patients with a genetic deficiency of saposin B also accumulate the substrates for α-galactosidase A, as in Fabry disease. The three-dimensional structure of recombinant human α-galactosidase A has been determined by X-ray crystallography at a resolution of 3.25 Å, and used to understand the effects of mutations on the structure and function of the enzyme (Garman and Garboczi 2004, Garman 2007).

After thorough clinical evaluation, determination of α-galactosidase A activity is the first step in the laboratory diagnosis of a patient suspected of having Fabry disease, unless there is a known familial *GLA* mutation, for which DNA analysis is straightforward (see later). The activity can be determined in various materials, such as plasma, leukocytes, fibroblasts, or dried blood spots (DBS); the assay is rapid, reliable, and cost-effective. Currently the assay of α-galactosidase A activity in leukocytes represents the diagnostic 'gold-standard'. A skin biopsy is rarely taken for initial diagnosis but studies on fibroblasts could be useful for molecular characterization of the enzyme deficiency. The most commonly used method of enzyme analysis is based upon cleavage of 4-methylumbelliferyl-α-D-galactoside, a synthetic fluorigenic substrate. Recently a substrate suitable to assay enzyme activity by electrospray ionization/tandem mass spectrometry (ESI/TMS) has also become available (Li et al. 2004, Zhang et al. 2010). The activity of α-galactosidase A should always be determined in the presence of α-*N*-acetylgalactosamine, which inhibits α-galactosidase B. In addition, another lysosomal enzyme, preferably β-galactosidase, should always be assayed to evaluate sample quality. As enzyme activity may diminish rapidly if the sample is inappropriately stored and/or transported, the diagnostic laboratory should be contacted in advance for information regarding appropriate sample storage and shipping conditions. About 2% of the population/Fabry patients carry the non-synonymous change c.937 G>T (p.Asp313Tyr). This variant has low α-galactosidase A activity in plasma compared to the wild-type and about 60% of the mean α-galactosidase A activity of the wild-type in cells. The p.Asp313Tyr variant is stable at lysosomal pH and is not disease-causing (pseudodeficiency).

Males with the classic Fabry disease phenotype can be reliably diagnosed by detecting complete deficiency or only negligible (<5% of mean normal) α-galactosidase A activity. Single male patients with attenuated phenotypes may show considerable residual enzyme activities (e.g.

Gaspar et al. 2010) that are still, however, well below the normal reference range. If initial enzyme activity analysis is performed on DBS of a male proband and shows pathologic values, a confirmatory assay, preferably on leukocytes, is recommended. For the index patient of any family with a biochemically proven α-galactosidase A deficiency, mutation analysis of the *GLA* gene should be offered. This test can confirm the diagnosis and may provide additional information for disease prognosis and therapy. It is essential when genetic counselling of family members is desired (see later).

Identification of heterozygous females is not reliably made by the measurements of α-galactosidase A activity because of the significant levels of activity that may be present in these samples due to random X-inactivation. Thus for females, a number of complementary diagnostic approaches is used currently, including measurement of urinary/plasma storage products, and histology/electron microscopy. However, only the identification of a disease-relevant heterozygous *GLA* mutation allows definite diagnosis of carrier status.

Neonatal screening for Fabry disease in males is technically feasible by measurement of α-galactosidase A activity in DBS using either the fluorigenic or mass spectrometric substrate and will detect cases both with complete deficiency and residual enzyme activity (Lin et al. 2009). High-throughput measurement of α-galactosidase A activity in leukocytes and DBS, for example by the technique of ESI/TMS, has been used to identify patients with Fabry disease in cohorts with advanced organ manifestations typical for Fabry disease (high-risk populations; for a recent review see Linthorst et al. 2010). It has been reported that β-glucuronidase activity is elevated in Fabry patients (Z. Lukacs, personal communication). Therefore the ratio of α-galactosidase A to β-glucuronidase activities may be helpful for increasing diagnostic discrimination, particularly for heterozygotes in these populations.

Diagnostic use and value of Gb3 and lysoGb3

Gb3 (Gb3Cer, globotriaosylceramide), also known as GL3 or CTH, is a substrate of α-galactosidase A and the main glycosphingolipid which accumulates when there is a deficiency of the enzyme. It may therefore be useful in diagnosis and assessment of disease burden. Deacylated Gb3, globotriaosylsphingosine (lysoGb3Cer or lysoGb3), is a minor metabolite recently identified in plasma of patients with Fabry disease. LysoGb3 might be more directly involved in the pathology and may also be useful in monitoring the disease (Aerts et al. 2008). Gb3 profiling (comparative analysis of various Gb3 isoforms) rather than measurement of the total urinary Gb3 concentrations, may represent a new diagnostic avenue in the future.

For biochemical analysis, Gb3 is easily accessible in various body fluids, including plasma and urine, and there are a number of validated assays including HPLC, TLC and LC/MS. In general, Gb3 should be measured in urine rather than in plasma, whereas lysoGb3 should be determined in plasma (Young et al. 2005, Togawa et al. 2010). Samples need to be sent fresh to the laboratory or should be frozen and subsequently transported frozen. It is recommended that both the biochemical analysis of lysoGb3 and Gb3 in plasma and urine, respectively, as well as the metabolite analysis are performed in specialized centers with appropriate experience. Gb3 inclusions can also be detected in cells of various tissues and organs, e.g. by biopsy of the conjunctiva, skin, kidney or heart, by electron microscopy and histochemistry including immunohistochemistry.

Plasma Gb3 levels do not correlate with disease manifestations: They are elevated in males with Fabry disease but are normal or only mildly elevated in females. Since Gb3 seems to be directly involved in the renal pathology of Fabry disease as a result of vascular compromise, podocyte toxicity, and focal tubular damage and sclerosis, quantification of urinary Gb3, that is derived primarily from tubular epithelial cells, is a possible diagnostic procedure for patients presenting with the classic Fabry disease phenotype (Sessa et al. 2003). A relationship between urinary Gb3 levels and Fabry disease severity as well as to therapeutic response has been demonstrated in a few studies (Whitfield et al. 2005, Banikazemi et al. 2007, Eng et al. 2001, Schiffmann et al. 2001). More recent studies suggest that there is no linear relationship between urinary Gb3 concentrations and end-organ effects of Fabry disease in male or in female patients. Furthermore it is currently unclear whether or not increased urinary Gb3 concentration can be taken as a specific marker for disease-related lysosomal storage. Whilst there is no doubt that Gb3 accumulates in patients with Fabry disease, from placental development onwards (Vedder et al. 2006), its role in the assessment or management of patients with this condition is contentious.

While single assessments of Gb3 add only very little to the diagnosis of patients with biochemically and/or clinically ascertained Fabry disease, serial measurements of total urinary Gb3 (plasma lysoGb3) in the same individual may be used to monitor the progression of the pathological process. In male patients, a response to ERT is indicated by a decline of urinary Gb3, whereas an increase after prolonged enzyme administration may point to the existence of interfering antibodies against infused α-galactosidase A (Schiffmann et al. 2006, Vedder et al. 2007, Hughes et al. 2008). Analysis of total urinary Gb3 from a 12-24 h urine sample may be a diagnostic adjunct in

females suspected of having Fabry disease when no male index patient is available for mutation analysis.

In symptomatic males with Fabry disease, plasma lysoGb3 is elevated probably from an early age, and is strikingly high in adult male patients, although no correlation has been found between plasma lysoGb3 and disease manifestations (Aerts et al. 2008). In females, plasma lysoGb3 levels increase steadily and show a weak correlation with disease manifestation. Provided that comprehensive analyses of plasma lysoGb3 data from large cohorts of patients with Fabry disease confirm the preliminary observations, lysoGb3 may prove to be a promising novel diagnostic tool (Rombach et al. 2010). Where gene alterations are found with unclear functional or pathological implications in females, the assessment of Gb3 metabolites/isoforms (urinary Gb3 and plasma lysoGb3) is recommended.

Diagnostic use and value of mutations of the *GLA* gene

The *GLA* gene, encoding α-galactosidase A, contains seven exons ranging from 92 to 291 base pairs (bp) in length. The coding region consists of 1,290 bp and encodes a polypeptide of 429 amino acids, with the first 31 residues representing a signal sequence. As of 30th of June 2009, a total of 599 *GLA* sequence changes, including 435 probable pathogenic point mutations (missense, nonsense, and splice site) and 150 disease-causing 'short length' rearrangements (mainly deletions and duplications affecting less than 65 nucleotides) as well as 14 DNA polymorphisms have been reported (for a recent review see Gal 2010). Large rearrangements involving one or more exons or the whole *GLA* gene seem to be infrequent (ca. 5%) in patients with Fabry disease. Most of the *GLA* mutations found in patients with Fabry disease are novel (unique, 'private'). The frequency of *de novo* mutations has been estimated to be 3-10%. There are a few reports of patients carrying two different, highly probable disease-causing *GLA* mutations on the same allele. In contrast, patients may carry one or more of the common *GLA* polymorphisms, including several non-synonymous changes, or rare non-pathogenic variants, in addition to their disease-causing mutation. To date, no experimentally validated data have been presented that any of these latter sequence variants, alone or in combination, are disease-causing.

As a practical approach one can define two classes of mutations to assess their pathogenic significance. Class 1 mutations are predicted to have high probability of causing disease because they create a premature stop codon (nonsense or frame-shift mutations) with the consequent loss of the protein, affect the evolutionarily conserved splice-site dinucleotides at the beginning or the end of one of the 6 *GLA* introns and interfere with the proper splicing of the *GLA* mRNA, or severely disrupt the coding sequence by a large rearrangement. Sequence changes resulting in a catalytically inactive (non-functional) enzyme, for example missense mutations affecting one of the 15 residues in the enzyme active site, or one of the 8 cysteines essential for proper three-dimensional protein folding, are also class 1

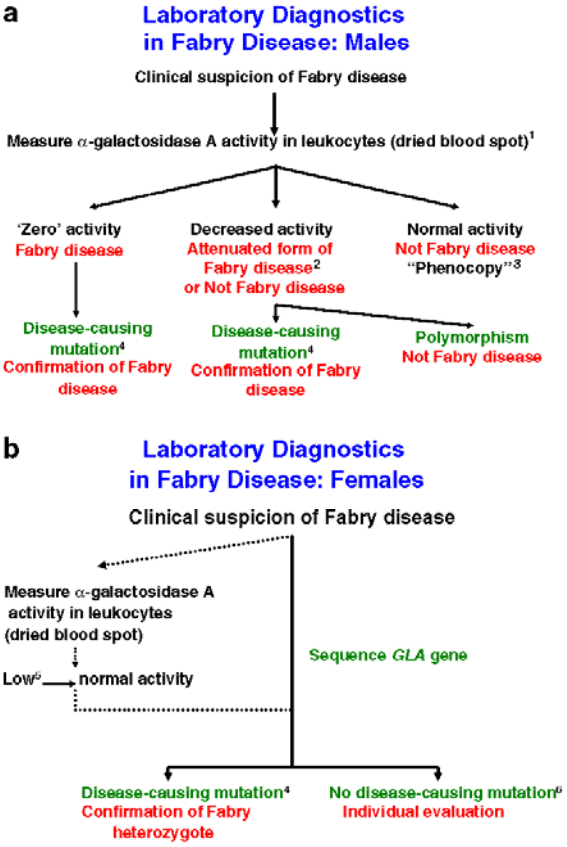

Fig. 1 Algorithm for the laboratory diagnosis of (a) male and (b) female patients with Fabry disease. The flow charts represent summaries of the discussion and conclusions in the text, with extra clarification in points 1-6. 1) Demonstration of a deficiency of α-galactosidase A in leukocytes and plasma from the same blood sample is supporting evidence for a diagnosis of Fabry disease. 2) Variants of Fabry disease with residual α-galactosidase A activity. 3) A patient with some symptoms of Fabry disease not due to deficiency of α-galactosidase A. 4) Class 1 mutation and mutations previously found in affected male or female Fabry patients. 5) Low α-galactosidase A activity can be suggestive of carrier status but not definitive. 6) To decide whether the proband has Fabry disease, all or some of the following investigations should be carried out: (a) re-evaluation of clinical presentation, (b) analysis of family pedigree, (c) measurement of urinary Gb3, and (d) in absence of a Class 1 mutation, any sequence change detected in the *GLA* gene must be expressed *in vitro* to investigate its effect on activity and/or structure of enzyme

mutations. Finally, recurrent disease-causing mutations and the growing number of *GLA* mutations that have been shown to result in non-functional enzyme in *in vitro* expression studies in cells in cultures transduced with the relevant mutant cDNA also belong to this group. It has been suggested that the pathology of some 'simple' disease-causing mutations might occasionally be complex. Indeed, some DNA changes thought to be missense mutations (e.g. p.Ser65Thr, p.Gly183Ser, p.Lys213Asn, or p.Met267Ile) seem to interfere with normal splicing of the *GLA* mRNA (Lai et al. 2003). Similarly, two deep intronic point mutations (c.639+861C>T and c.639+919 G>A) apparently result in α-galactosidase A deficiency by causing complex changes in the pattern of splicing (Ishii et al. 2002, Filoni et al. 2008). About 50% of males with enzymatically proven Fabry disease carry a Class 1 mutation.

Mutations that have been found in males with normal α-galactosidase A activities or with somewhat decreased enzyme activities, which are still, however, well above the pathologic range of values, are called Class 2 mutations and are almost certainly non-pathogenic. These include polymorphisms or sequence changes, e.g. c.937G>T (p.D313Y) described as pseudodeficiency alleles.

Routine mutation analysis of the *GLA* gene consists of sequencing of the coding region and exon-intron boundaries. The interpretation of gene alterations should be performed by an expert and genetic counselling should be offered. In more than 97% of males with pathologic α-galactosidase A activities, a sequence variant (Class 1 mutations or yet unclassified sequence changes) can be detected by routine mutation analysis. The identification of Class 1 mutations is considered a very useful and independent confirmation of the biochemical (and clinical) diagnosis. A small number of mutations, in particular exon-spanning duplications or inversions and deep intronic mutations, may escape detection by using the above method and can only be identified by more sophisticated procedures, such as the analysis of the mRNA or MLPA (multiplex ligation-dependent probe amplification). However, even if no highly probable disease-causing mutation is found in a male patient with an α-galactosidase A deficiency, the diagnosis of Fabry disease remains valid. For mutations not categorized as Class 1 or Class 2, a thorough clinical, biochemical and genetic analysis of the patient and his family may allow designation of the mutation as disease-causing or not. Analysis of evolutionary conservation of the relevant sequence and its absence in a large cohort of unaffected individuals may provide additional arguments for a pathogenic relevance of a change. An easily accessible and quality-controlled gene-specific mutation database would be an invaluable tool both for physicians treating patients, genetic counselors, and scientists involved in DNA diagnostics or research.

Both Class 1 and Class 2 mutations also occur in females. Since enzyme activity measurements do not reliably detect heterozygotes, and many of the clinical features of Fabry disease are frequently observed in the general population, DNA diagnostics is much less efficient in identifying heterozygotes among women with clinical suspicion for Fabry disease than in confirming diagnosis in males with enzymatically proven Fabry disease. Carriers in families with Fabry disease can be identified by pedigree analysis and/or by showing that they have inherited the family-specific mutation. If bidirectional sequencing of the coding region and exon-intron boundaries do not reveal heterozygosity for a Class 1 mutation in a female DNA sample, MLPA may help to pick up the few cases of large DNA rearrangements in females, whereas the analysis of mRNA may be complicated by nonsense-mediated decay. In addition, a thorough clinical re-evaluation of the patient and additional biochemical tests are recommended. A careful analysis of the pedigree by a genetic counselor should also be offered, keeping in mind that nine out of ten patients with Fabry disease should have a positive family history for the trait. In females with typical signs and symptoms of Fabry disease but without positive family history, only the identification of a disease-relevant heterozygous *GLA* mutation allows definite diagnosis of carrier status.

Conclusions (Fig. 1): (i) Thorough analysis of the patient's family and medical history together with a clinical examination are essential prior to laboratory testing. (ii) Diagnostic tests should be done in laboratories with appropriate quality control schemes, experience, and sample load. (iii) Analysis of α-galactosidase A activity is the standard diagnostic test of Fabry disease in males. Molecular analysis of the *GLA* gene is necessary to diagnose heterozygotes.

Acknowledgments The European Consensus on Diagnostics in Fabry Disease was sponsored by an unrestricted education grant generously awarded by The Center for Extramural Clinical Research and Education of Shire Human Genetic Therapies, Inc.

References

Aerts JM, Groener JE, Kuiper S et al. (2008) Elevated globotriaosylsphingosine is a hallmark of Fabry disease. Proc Natl Acad Sci USA 105:2812–2817

Banikazemi M, Bultas J, Waldek S et al. (2007) Agalsidase-beta therapy for advanced Fabry disease: A randomized trial. Ann Intern Med 146:77–86

Clark NE, Garman SC (2009) The 1.9 a structure of human alpha-N-acetylgalactosaminidase: the molecular basis of Schindler and Kanzaki diseases. J Mol Biol 393:435–447

Eng CM, Guffon N, Wilcox WR et al. (2001) Safety and efficacy of recombinant human alpha-galactosidase A–replacement therapy in Fabry's disease. N Engl J Med 345:9–16

Filoni C, Caciotti A, Carraresi L et al. (2008) Unbalanced GLA mRNAs ratio quantified by real-time PCR in Fabry patients' fibroblasts results in Fabry disease. Eur J Hum Genet 16:1311–1317

Gal A (2010) Molecular genetics of Fabry disease and genotype–phenotype correlation. In Elstein et al. eds. *Fabry disease*. Springer Science + Business Media B.V. pp. 3-19

Garman SC (2007) Structure-function relationships in alpha-galactosidase A. Acta Paediatr 96(Suppl 455):6–16

Garman SC, Garboczi DN (2004) The molecular defect leading to Fabry disease: structure of human alpha-galactosidase. J Mol Biol 337:319–335

Gaspar P, Herrera J, Rodrigues D et al. (2010) Frequency of Fabry disease in male and female haemodialysis patients in Spain. BMC Med Genet 11:19–26

Hughes DA, Elliott PM, Shah J et al. (2008) Effects of enzyme replacement therapy on the cardiomyopathy of Anderson-Fabry disease: a randomized, double-blind, placebo-controlled clinical trial of agalsidase-alfa. Heart 94:153–158

Ishii S, Nakao S, Minamikawa-Tachino R, Desnick RJ, Fan JQ (2002) Alternative splicing in the α-galactosidase A gene: increased exon inclusion results in the Fabry cardiac phenotype. Am J Hum Genet 70:994–1002

Lai LW, Whitehair O, Wu M-J, O'Meara M, Lien Y-H H (2003) Analysis of splice-site mutations of the α-galactosidase A gene in Fabry disease. Clin Genet 63:476–482

Li Y, Scott CR, Chamoles NA et al. (2004) Direct multiplex assay of lysosomal enzymes in dried blood spots for newborn screening. Clin Chem 50:1785–1796

Lin HY, Ching KW, HSu JH et al. (2009) High incidence of the cardiac variant of Fabry disease revealed by newborn screening in the Taiwan Chinese population. Circ Cardiovasc Genet 2:450–456

Linthorst GE, Bouwman MG, Wijburg FA, Aerts JM, Poorthuis BJ, Hollak CE (2010) Screening for Fabry disease in high-risk populations: a systematic review. J Med Genet 47:217–222

Rombach SM, Dekker N, Bouwman MG et al. (2010) Plasma globotriaosylsphingosine: diagnostic value and relation to clinical manifestations of Fabry disease. Biochim Biophys Acta May 13. [Epub ahead of print] PubMed PMID: 20471476

Schiffmann R, Kopp JB, Austin HA et al. (2001) Enzyme replacement therapy in Fabry disease: a randomized controlled trial. JAMA 285:2743–2749

Schiffmann R, Ries M, Timmons M, Flaherty JT, Brady RO (2006) Long-term therapy with agalsidase alfa for Fabry disease: safety and effects on renal function in a home infusion setting. Nephrol Dial Transplant 21:345–354

Sessa A, Meroni M, Battini G et al. (2003) Studio multicentrico Italiano sulla malattia di Anderson-Fabry. Evolution of renal pathology in Fabry disease. Acta Paediatr 92 (Suppl 443): 6-8; discussion 5. PubMed PMID: 14989458

Togawa T, Kodama T, Suzuki T et al. (2010) Plasma globotriaosyl-sphingosine as a biomarker of Fabry disease. Mol Genet Metab Apr 1. [Epub ahead of print] PubMed PMID: 20409739

Vedder AC, Strijland A, vd Bergh Weerman MA, Florquin S, Aerts JM, Hollak CE (2006) Manifestations of Fabry disease in placental tissue. J Inherit Metab Dis 29:106–111

Vedder AC, Linthorst GE, van Breemen MJ et al. (2007) The Dutch Fabry cohort: diversity of clinical manifestations and Gb3 levels. J Inherit Metab Dis 30:68–78

Whitfield PD, Calvin J, Hogg S et al. (2005) Monitoring enzyme replacement therapy in Fabry disease - role of urine globotriaosylceramide. J Inherit Metab Dis 28:21–33

Winchester B, Young E (2010) Laboratory diagnosis of Fabry disease. In Elstein et al. eds. Fabry disease. Springer Science + Business Media B.V. pp. 111–132

Young E, Mills K, Morris P et al. (2005) Is globotriaosylceramide a useful biomarker in Fabry disease? Acta Paediatr 94:51–54

Zhang XK, Elbin CS, Turecek F et al. (2010) Multiplex lysosomal enzyme activity assay on dried blood spots using tandem mass spectrometry. Methods in molecular biology 603:339–350

Univerzita Karlova v Praze, 1. lékařská fakulta
Kateřinská 32, Praha 2

Prohlášení zájemce o nahlédnutí
do závěrečné práce absolventa studijního programu
uskutečňovaného na 1. lékařské fakultě Univerzity Karlovy v Praze

Jsem si vědom/a, že závěrečná práce je autorským dílem a že informace získané nahlédnutím do zpřístupněné závěrečné práce nemohou být použity k výdělečným účelům, ani nemohou být vydávány za studijní, vědeckou nebo jinou tvůrčí činnost jiné osoby než autora.

Byl/a jsem seznámen/a se skutečností, že si mohu pořizovat výpisy, opisy nebo kopie závěrečné práce, jsem však povinen/a s nimi nakládat jako s autorským dílem a zachovávat pravidla uvedená v předchozím odstavci.

Příjmení, jméno (hůlkovým písmem)	Číslo dokladu totožnosti vypůjčitele (např. OP, cestovní pas)	Signatura závěrečné práce	Datum	Podpis